University of Southampton

Remote sensing of forest canopy gaps

Robin Geoffrey Jackson

Doctor of Philosophy

DEPARTMENT OF GEOGRAPHY
FACULTY OF SCIENCE

Submitted in August 2000

For my parents

"In nature's infinite book of secrecy, a little I can read"

William Shakespeare. Anthony and Cleopatra [Act *I* scene *ii*]

"When you cannot measure it, your knowledge is of a meagre and unsatisfactory kind"

Lord Kelvin, President of the Royal Society, 1895.

"If you've enjoyed it, tell your friends"

Lurcio the slave (aka Frankie Howard). Up Pompeii!

UNIVERSITY OF SOUTHAMPTON

ABSTRACT

FACULTY OF SCIENCE

GEOGRAPHY

Doctor of Philosophy

REMOTE SENSING OF FOREST CANOPY GAPS

by Robin Geoffrey Jackson

Wind represents a significant problem for forestry in many parts of the world and is a severe threat to commercial forests in the British Isles. The presence of windthrown gaps, primarily formed by the actions of strong winds attributed to the passage of Atlantic depressions, are a common component of upland forests in the British Isles. Despite the importance of such gaps, previous research on windthrown gaps has been largely directed towards analysis of site and crop factors, rather than the formation and progression of windthrown gaps.

This thesis evaluates the potential of fine ($\simeq$ 4 m) spatial resolution remotely sensed data and alternative classification methods to characterise windthrown gaps. The study site was Cwm Berwyn Forest, in central Wales, a planted forest of predominantly Sitka spruce (*Picea sitchensis* (Bong.) Carr.) containing windthrown gaps ranging in size from 50 to 3000 m^2. The remotely sensed data used were acquired by an 11 waveband airborne thematic mapper (ATM) sensor with a spatial resolution of $\simeq$ 4 m. This spatial resolution is finer than the windthrown gaps on the site and comparable to that of future satellite sensors. A thematic map depicting land cover was produced using a conventional maximum-likelihood classification of the ATM data and provided an accurate representation of the land cover (> 90 % of the pixels allocated correctly). This hard classification was also softened to output typicality and posterior class membership probabilities.

The results indicated that the hard classification provided an accurate means of identifying windthrown gaps (> 95 % of known gaps identified) and was capable of identifying a greater number of gaps, than manual interpretation of temporally coincident aerial photographs. Estimates of windthrown gap area, perimeter and shape were derived from the hard and softened classifications. The results indicated the potential to derive more accurate spatial representations of windthrown gaps than a conventional hard classification, by softening the output to derive typicality class membership probabilities. However, the major contribution of the research within this thesis to previous work on windthrown gap formation and progression, is the potential to use rate of change of typicality and posterior class membership probabilities to derive information on various windthrown gap properties, such as exposed soil and living windthrown tree canopies. Rate of class membership probability change was significantly related ($P > 0.01$) to the gap-canopy boundary sharpness. This may enable the direction which windthrown trees fell to be inferred and thus provide an indication of the vulnerability of gap-canopy boundaries to future wind damage. This may allow forest managers to adapt their silvicultural practices to minimise the risk of wind damage formation and progression in upland forests, which represent the bulk of commercial forestry in the British Isles.

TABLE OF CONTENTS

LIST OF FIGURES

Chapter 7: Mapping windthrown gap boundary sharpness from a softened classification

LIST OF TABLES

ACKNOWLEDGEMENTS

I would like to express my sincere thanks and appreciation to the following individuals and institutions who made this research possible.

Firstly, my supervisors, Prof. Giles Foody and Chris Quine for their guidance, patience and frequent encouragement with a cattle prod when required. I will be forever grateful!

Natural Environment Research Council (NERC) and Forest Research, an agency of the Forestry Commission, for Research Studentship GT4/96/258/EO, which funded this work and provided maintenance grants which kept a roof over my head.

NERC Airborne Remote Sensing Facility for the provision of the ATM data from the 1994 airborne remote sensing campaign.

Thanks also go to staff from Forest Research (Northern Research Station) for access and permission to use reference data, in particular, Juan and Sean. In addition, the Forest District Manager for Ceredigion for permission to visit Cwm Berwyn Forest and make field measurements.

Dr. John Sarraille, California State University, provided useful information and advice concerning his FD3 fractal dimension program.

Dr. David Miller from Macauley Landuse Research Institute kindly allowed use of his digital elevation model of Cwm Berwyn Forest and provided general advice.

All the staff and postgraduate students from the Department of Geography, University of Salford, with whom I spent my formative first year (September 1996 to September 1997). In particular, Dr. Nigel Trodd (fellow Arsenal fan) for all things relating to probability density functions; Dr. Mark Danson for his gentle introduction to remote sensing; Helen Ghaly and Andy Stocks for their introduction to the world of computing and the wonder that is UNIX; and finally, fellow postgraduates Neil and Ernest, with whom I experienced the Salford '*nightlife*'.

All the staff from the Department of Geography, University of Southampton, especially Prof. Paul Curran, Dr. Ted Milton and Dr. Pete Atkinson for general advice and words of wisdom; Dr. Jim Milne and Dr. Charles Kerr for their computing advice and valuable technical support; and Tim, John, Roz and Andy from the Cartographic Unit for producing career saving visual props at a moments notice. In addition, I would like to thank my fellow postgraduates (in no particular order!) with whom I have shared victory at darts, enthusiasm, disillusionment, panic and the odd small sherry: Daisy, TP, Tobes, Mark, Chris, Sally and Pedro.

My fellow wardens from South Stoneham and Montefioire Halls of Residence (again, in no particular order!) with whom I served two tours of duty and for sharing the highs and lows of hall life: Katie, WPC Ford, Jo, Nick, TP (again!), Graham, Becky, Jennifer, Tobes (again!), Wangar, Raquel, Sarah, Fi, Simon, Peter, Moody Debs, Chris, Declan, Ria, Botty, Chamois, Iris, Andrea and, especially, Pip 'top banana' (and Ant!) for being great!

In addition, I would also like to acknowledge those long suffering friends who put up with my dire financial position and frequent despair, but whose encouragement meant a great deal: Alan, Anne, Laura, Debs and all the extended Campbell 'family'; Neil; Lisa; Darren; and Dr. Roger Dunham.

Those colleagues in a number of different countries throughout the world, whom I have had the pleasure and privilege of meeting at workshops and conferences during the course of this research, and who have influenced my work for the better.

The staff and students at Plumpton College who have shown solidarity and support with my plight during the writing-up stage. In particular, Kevin, Gerry, Will, Paul, Chris, Aaron, Anita, David, Des, Geoff, Julian and Janie. The quality of my lectures and programme administration might improve now!

Finally, if I have forgotten to thank anyone, please accept my heartfelt apologies, it was unintentional!

LIST OF ABBREVIATIONS

ATM	airborne thematic mapper
AVHRR	advanced high resolution radiometer
AVIRIS	airborne visible-infrared imaging spectrometer
BC	before Christ
BIL	band interleaved by line
CASI	compact airborne spectrographic imager
CCT	computer compatible tape
DBH	diameter at breast height
DEM	digital elevation model
DN	digital number
EMR	electromagnetic radiation
ERS	European remote sensing satellite
ESA	European Space Agency
ETM	enhanced thematic mapper
FASTCo	Forestry and Arboriculture Safety and Training Council
FC	Forestry Commission
FOV	field of view
GCP	ground control point
GIS	geographic information system
GPS	global positioning system
HDDT	high density digital tape
HRV	high resolution visible
IDS	integrated data system
IFOV	instantaneous field of view
IPCC	Intergovernmental Panel on Climate Control
IRS	Indian remote sensing satellite

JL	Japanese larch (*Larix kaempferi* (Lamb.) Carr.)
LIDAR	light detection and ranging
LP	lodgepole pine (*Pinus contorta* var. *Latifolia* Wats.)
LISS	linear imaging self-scanning sensor
MODIS	moderate resolution imaging spectrometer
MSS	multispectral scanner
NASA	National Aeronautic and Space Administration
NDVI	normalised difference vegetation index
NERC	Natural Environment Research Council
NIR	near-infrared radiation
NOAA	National Oceanic and Atmospheric Administration
OS	Ordnance Survey
PAN	panchromatic imager
PAR	photosynthetically active radiation
RADAR	radio detection and ranging
RMSE	root mean square error
SAR	synthetic aperture RADAR
SLAR	side-looking airborne RADAR
SLR	side-looking RADAR
SPOT	*Systeme Probatoire d'Observation de la Terre*
SS	Sitka spruce (*Picea sitchensis* (Bong.) Carr.)
TIMS	thermal infrared multispectral scanner
TM	thematic mapper
TOPEX	topographic exposure
WHC	windthrow hazard classification/class

CHAPTER 1

INTRODUCTION

1.1 BACKGROUND

Since the last Ice Age, around 11000 BC, through a process of colonisation and succession, the British Isles gradually became covered by forests (Rackham, 1986). These forests have subsequently been cleared, largely through settled agriculture, fuelled by a growing population (Miller, 1991). Despite some legislation, often draconian, directed at preserving Britain's forests, there has been a continual erosion of forest cover, particularly in the last 2000 years (Ryle, 1969; Miller, 1991). The poor state of Britain's forest resource came to prominence during the First World War, due to Britain's reliance upon imported wood. This was largely attributed to the necessity of wood for use as pit props for coal mining (Miller, 1991). The Prime Minister at the time, David Lloyd George, commented that Britain had been closer to losing the war due to a lack of wood, than a lack of food (Ryle, 1969).

After the First World War, the Forest Subcommittee of the Reconstruction Committee, examined the forest resource of Britain. The resulting Ackland Report, published in 1917, concluded that Britain required a strategic reserve of wood which would ensure supplies in the eventuality of future wars (Miller, 1991) and suggested that a state forest authority be established to oversee afforestation. Consequently, under the

1919 Forestry Act, state forestry in Britain began with the establishment of the Forestry Commission, which was overseen by a Board of Commissioners (Ryle, 1969; Forestry Commission, 1992; National Audit Office, 1993). These Forestry Commissioners were formally charged with the duty of establishing a strategic reserve of wood, principally through afforestation which has led to a doubling of Britain's forest cover since the Forestry Commission's founding (Miller, 1991).

Afforestation was concentrated on marginal upland regions, where the land was of low agricultural quality, using exotic tree species which were better suited to the environmental conditions (Foot, 1986; Miller, 1991). This land is generally characterised by shallow or poorly drained soils, which can result in rooting problems for trees. The combination of poor soils, exposure and high altitude make trees particularly vulnerable to wind damage (National Audit Office, 1993). Unfortunately, there was no historical evidence to suggest the potential seriousness of wind damage on this land as the environmental conditions were not ideal for native tree species (Quine *et al.*, 1995).

The development and widespread use of mechanised ground preparation in the 1950's led to an increase in the rate of afforestation, particularly on upland sites which had been previously considered unplantable (Schaible, 1992). Unfortunately, the use of early mechanised ground preparation, principally to reduce initial establishment costs, subsequently increased the vulnerability of the eventual forests to wind damage (Schaible, 1987). This has been attributed to development of structural roots being restricted to the direction of the ground cultivation (Schaible, 1987; Nelson and Quine, 1990).

As a consequence of the combination of site factors and silvicultural practices noted above, many forests managed by the Forestry Commission and the commercial private forest sector are vulnerable to significant wind damage. Wind damage can take different forms, for example windsnap, but it is usually the overturning of the stem and root plate, termed windthrow, that is the most common and serious (Quine *et al.*, 1995). Windthrow forms gaps in the forest canopy and these can be viewed positively, particularly with the potential to increase ecological diversity (Quine and Humphrey, 1996). However, windthrow is generally perceived as economically undesirable within forests managed primarily for wood production (Coutts, 1986). The vulnerability of forests to windthrow imposes limitations upon silvicultural practices (Quine *et al.*, 1995). For example, a significant proportion of state managed forests in Britain are managed under a no-thinning regime, specifically due to the risk of windthrow associated with thinning as there is evidence that unthinned stands are more wind stable (Kilpatrick *et al.*, 1981; Schaible and Gawn, 1989).

Silvicultural decisions, such as whether to thin a stand, or which commercial species to plant, are usually taken with reference to the Windthrow Hazard Classification (WHC) (Miller, 1985; Quine *et al.*, 1995). The WHC was originally based upon short term data and changes have subsequently been made due to complaints that it was too pessimistic (Quine, 1994, Quine *et al.*, 1995). Despite these changes, work to date has been largely directed towards site and crop factors, rather than the processes of windthrown gap formation and progression (Quine and Bell, 1998). As a consequence, our understanding of how windthrown gaps influence future wind damage, is limited.

This lack of knowledge is partly due to the spatial and temporal variability of these windthrown gaps. This has limited the value of management tools, such as the WHC, to aid foresters in the management of subsequent ecological and economic implications. In particular, how existing wind damage to a forest stand can influence the risk of future wind damage occurring (Quine, 1994). Acquisition of this information requires monitoring of wind damage formation and progression.

Current monitoring of windthrow has been based upon data acquired by aerial photography, which provides the only practical technique available to acquire information upon windthrown gaps, over the temporal and spatial scales of concern (Quine and Bell, 1998). An alternative may be to use satellite sensor systems, which generally provide a less expensive source of data per unit of area covered, than aerial photography (Richards, 1993; Bolduc *et al.*, 1999; Leblon, 1999). However, the primary limitation with using satellite sensor data for this purpose is that windthrown gaps are usually smaller in size than the spatial resolution of many of the current civilian satellite sensor systems available. This significantly restricts the information concerning windthrown gaps that may be derived and hence limits the value of the remotely sensed data. However, new classification methods and satellite sensors (Aplin *et al.*, 1997; Thomas *et al.*, 1997; McGraw *et al.*, 1998; Celentano, 1999; Lillesand and Kiefer, 2000) may resolve many of the current problems.

1.2 RESEARCH OBJECTIVE

The primary objective of research reported in this thesis is to characterise windthrown gaps using fine (< 5 m) spatial resolution remotely sensed data and alternative classification methods. Particular emphasis will be placed upon the potential range and usefulness of the derived information for the monitoring of the spatial and temporal dynamics of windthrown gaps, that may aid commercial forest management planning for wind stability.

1.3 THESIS STRUCTURE

Chapter 2 provides a review of the literature relevant to investigating windthrown gaps. Emphasis is placed upon the formation of gaps by wind and the subsequent role of windthrown gaps within forest dynamic processes. The benefits and disadvantages of windthrown gaps to managed forest ecosystems are discussed, placing in context, the importance of windthrown gaps within such forest ecosystems. This highlights why the acquisition of spatial and temporal data on windthrown gaps is essential for effective forest management. However, acquiring these data through traditional field surveys is problematic and remote sensing is becoming increasingly used as an alternative. Following a brief introduction to remote sensing, new satellite sensors and classification methods are introduced which may provide the forest management community with the potential to derive spatial information on windthrown gaps from these sources in the near future.

Chapter 3 introduces the Cwm Berwyn Forest wind damage monitoring site upon which the work in this thesis is based. This monitoring site contains a range of windthrown gaps typical in size to those formed throughout upland forests in the British Isles (Quine and Bell, 1998). A summary of the main characteristics of the airborne thematic mapper (ATM) sensor that acquired the remotely sensed data for subsequent research is provided. In addition, the reference data currently used by the Forestry Commission for wind damage monitoring and used in subsequent analyses are introduced.

Chapter 4 describes research methodology used throughout subsequent work. Specifically, it describes the radiometric calibration, geometric correction and classification of the ATM data.

Chapter 5 outlines the initial work which is based upon the analysis of a subset of the ATM data from the monitoring site. A range of spatial resolutions representative of current and new satellite sensors are investigated to evaluate the influence of spatial resolution for future work on windthrown gaps. A conventional hard classification method is examined to determine whether it is possible to accurately identify known windthrown gaps. Estimates of windthrown gap areas derived from this hard classification are compared against those from softened classifications to determine which method provides the most accurate estimate of windthrown gap area.

Chapter 6 builds upon the results from Chapter 5, and investigates whether the conclusions drawn are applicable at the forest-landscape scale and within different stand types. This work is based upon the conventional approach to mapping windthrown gaps, where they are considered as discrete features within forest stands through the allocation

of a hard gap-canopy boundary. The initial work in Chapter 5 is expanded to investigate the ability to accurately estimate windthrown gap perimeter and shape, in addition to windthrown gap area, using hard and softened classification methods.

Chapter 7 considers windthrown gaps as features within a forest stand which are mapped by a soft gap-canopy boundary, rather than a hard boundary. Attention is directed towards whether variation in the gap-canopy boundary, specifically boundary sharpness, can be accurately mapped using data derived from a softened classification. This analysis uses both field survey data and a digital elevation model (DEM) as reference data against which the mapped boundary sharpness is compared. Emphasis is placed upon the possible application of windthrown gap boundary information for forest management planning to reduce windthrow risk.

Chapter 8 provides a general discussion of the results from Chapters 5, 6 and 7, in the context of existing spatial and temporal knowledge of windthrown gaps. The possible operational application of remote sensing methods for assessing wind damage for upland forest management is discussed, with recommendations for further investigations made.

Chapter 9 provides a summary of the thesis and general conclusions.

1.4 SUMMARY

This thesis investigates the use of remote sensing to derive information on windthrown gaps which is difficult to acquire using conventional field survey techniques. The usefulness of remotely sensed data obtained from existing sensor systems and classification methods are compared against new classification methods and remotely sensed data which may be obtained from new sensor systems. Emphasis is placed upon the

potential operational application of remote sensing for the monitoring of wind damage within upland forests in the British Isles. This may enable forest managers to alter or adopt silvicultural strategies to reduce the risk of windthrow and thus improve the long term wind stability of upland forests in the British Isles.

CHAPTER 2

LITERATURE REVIEW

2.1 INTRODUCTION

The aim of this Chapter is to review the literature relevant to the remote sensing of forest canopy gaps, with particular reference to windthrown gaps formed by the action of strong winds. The bulk of this review concerns two broad topics: a) how windthrown gaps are formed and why they are important features within forest ecosystems, b) the potential for remote sensing to derive spatial and temporal information on windthrown gaps and hence improve our understanding of wind damage formation and progression.

2.2 DISTURBANCE AND FOREST DYNAMICS

Forest ecosystems are widely recognised as being structurally and compositionally diverse (Barnes *et al.*, 1998). Much of this diversity is associated with the formation of openings in the canopy which set in motion a vegetation replacement process and over time result in a change to the forest structure (Watt, 1947; Connell and Slayter, 1977; Shugart *et al.*, 1981; Cook, 1996; Dahir and Lorimer, 1996; Coates and Burton, 1997). This vegetation replacement process is intimately linked to the type, frequency and magnitude (in terms of intensity and severity (Quine *et al.*, 1999)) of the disturbance which initially formed the opening in the canopy (Levin and Paine, 1974; Doyle, 1981;

West *et al.*, 1981; Lundquist, 1995; Cook, 1996; Oliver and Larson, 1996; Connell *et al.*, 1997; Hughes and Bechtel, 1997). As a result, disturbance can significantly affect the composition, structure and function of forests (Barnes *et al.*, 1998).

However, disturbance is difficult to define (Rogers, 1996; Quine *et al.*, 1999), although the definition provided by White and Pickett (1985, page 6) is widely used: "any relatively discrete event in time that disrupts ecosystem, community or population structure and changes resources, substrate availability, or the physical environment". A simpler approach for forest management is to define disturbance with reference to the affected organism. For example, disturbance can be considered as a discrete event where at least one canopy tree is killed (Runkle, 1985). Irrespective of the definition used, disturbance is usually a complex interaction between biotic and abiotic factors, can be endogenous or exogenous, and can occur at a variety of temporal and spatial scales (Van Miegroet, 1979; White and Pickett, 1985; Peterken, 1993; Lundquist, 1995; Rogers, 1996; Quine *et al.*, 1999; Clinton and Baker, 2000; Sommerfeld *et al.*, 2000).

2.3 GLOBAL CLIMATE CHANGE

The global climate naturally varies over time and there can often be extremes of climate on occasions which can act as disturbance events. For example, the storm which passed over southeast England on 15/16 October 1987 caused severe damage to both state and private owned forests (Dannatt *et al.*, 1989). In the future, it is possible that global climate change may have a significant effect upon the frequency and magnitude of extreme climatic events, such as the 1987 storm.

The global climate is strongly influenced by the global carbon cycle which results from the flux of carbon between four main carbon stores: fossil carbon, the atmosphere, terrestrial biosphere and the oceans (Schimel, 1995; IPCC, 2000). Often the flux of carbon between these four stores can be influenced by human actions (IPCC, 2000). For example, the process of deforestation transfers carbon dioxide (CO_2) from the terrestrial biosphere to the atmosphere, whilst reforestation transfers CO_2 from the atmosphere to the terrestrial biosphere (Schimel, 1995). In response, it is likely that changes in the global climate will feedback, for example events like the 1987 storm, and result in changes to forests and other forms of vegetation (Henderson-Sellers and McGuffie, 1995; Parton *et al.*, 1995; IPCC, 2000). To evaluate the significance of the contribution to global climate change it is necessary to detect, monitor and periodically measure the effects of disturbances to forests at all temporal and spatial scales (IPCC, 2000).

2.4 CANOPY GAPS

The formation of an opening in a forest canopy by disturbance results in a complex response and recovery process. This process can range from fine resolution gap dynamics (disturbances up to $\simeq$ 0.4 ha (Clinton and Baker, 2000)), which result in uneven-aged stands, through to coarse resolution patch dynamics (disturbances from $\simeq$ 1 ha up to thousands of ha (UN/ECE, 2000a)), usually resulting in whole stand replacement and hence even-aged stands (Quine *et al.*, 1999). It has been suggested that both gap and patch dynamic processes will coexist in upland commercial forests in the British Isles (Quine *et al.*, 1999). However, there is no clear distinction between gap and patch dynamic

processes and the terms are used interchangeably. This ambiguity is evident in the wealth of literature directed at forest dynamic processes (e.g. Watt, 1947; Levin and Paine, 1974; Runkle, 1981; Hibbs, 1982; Lawton and Putz, 1988; Runkle, 1990; Spies *et al.*, 1990; Skinner, 1995; Dahir and Lorimer, 1996; Connell *et al.*, 1997; Hansen and Rotella, 1999; Quine *et al.*, 1999).

In subsequent work, the term 'patch' will not be used and the term 'gap' used to refer to all disturbance formed openings at all temporal and spatial scales (Peterken, 1996; McClure *et al.*, 2000; Sommerfeld *et al.*, 2000). This definition is broader than that suggested by Brokaw (1982a & 1982b) which is widely applied (e.g. Denslow and Gomez Diaz (1990) and Canham *et al.* (1990)).

2.4.1 Canopy gaps formed by wind

Gaps can be formed by a variety of disturbance agents such as fire, snow, fungal pathogens and wind (Quine *et al.*, 1999). The research contained within this thesis investigates windthrown gaps, formed by strong winds, which are a common feature of upland forests in the British Isles.

2.4.1.1 Mode of windthrown gap formation

Wind represents an important disturbance agent and is a significant problem for forest management throughout the world (Matthews, 1989; Everham, 1995; Fridman and Valinger, 1998; Ishizuka *et al.*, 1998; Mitchell, 1998; Hansen and Rotella, 1999; Peltonen, 1999; Mukai and Hasegawa, 2000; UN/ECE, 1999; UN/ECE, 2000a; Clinton and Baker,

2000). For example, wind damage to forests can result in significant financial loss of wood and can complicate conventional silvicultural practices (Coutts, 1986; Price, 1989; Fridman and Valinger, 1998). Annual wind damage to commercial British forests accounts for approximately 15 % of the annual production, although the degree of damage is highly variable from year to year (Quine *et al.*, 1995).

The British Isles have a severe wind climate in places and many of the gaps found throughout upland forests have been formed by strong winds attributed to fronts, depressions and extratropical cyclones (Savill, 1983; Quine, 1991b; Quine *et al.*, 1995; Quine and Bell, 1998; Quine *et al.*, 1999). Wind damage can take many forms such as physical abrasion or windsnap (Quine *et al.*, 1995; Kimmins, 1997; Smith *et al.*, 1997). However, windthrow (Figure 2.1) is the most common and serious form of wind damage to commercial forests in the British Isles (Quine *et al.*, 1995). Windthrow occurs when the stem and the root plate of trees overturn, because the components of anchorage (Figure 2.2) are overcome by the overturning force of the wind (Coutts, 1986; Quine *et al.*, 1995). The combination of soils, exposure and altitude make upland forests in the British Isles particularly vulnerable to windthrow (Section 1.1) (National Audit Office, 1993). In addition, predisposing factors such as poor drainage or restricted root growth can increase the vulnerability of upland forests to damage by strong winds, with the magnitude of the damage influenced by topography (Van Miegroet, 1979; Coutts, 1983; Tabbush, 1988; Coutts and Nicoll, 1989; Nelson and Quine, 1990; Quine, 1991b; Lundquist, 1995; Gardiner *et al.*, 1997; Fridman and Valinger, 1998).

Figure 2.1 Wind damage to a coniferous forest in Normandy, France, which occurred in January 2000. Both windthrown and wind snapped trees can be seen.

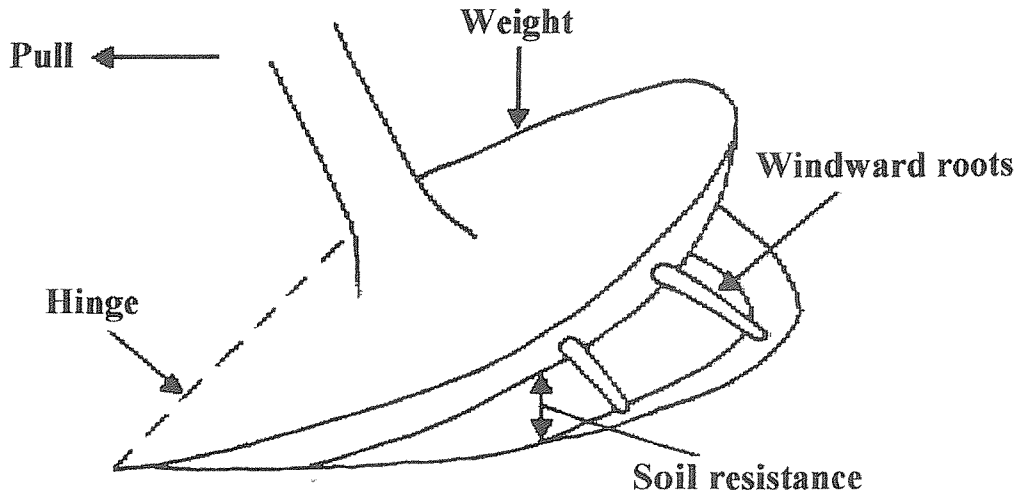

Figure 2.2 Diagram illustrating the four components of anchorage of a shallow rooted tree which resist the horizontal force of the wind acting on the stem (adapted from Coutts (1986)). These components are: resistance to bending at the hinge; resistance by roots under tension at the windward side of the root plate; the weight of the root plate; and soil resistance. The pull on the tree is due to the overturning force exerted by the wind.

2.4.1.2 Ecological implications of windthrown gaps

Disturbance formed gaps are integral to the ecology of forests, generating instability at fine scales, but dynamic stability at coarse scales (Peterken, 1996). Unfortunately, there has been little work undertaken on the ecology of windthrown gaps with commercial forests and parallels must be made with work undertaken on canopy gaps in general.

The formation of a gap within a forest canopy modifies the availability, quantity and distribution of abiotic and biotic conditions and resources within the understorey of a forest. For example, air temperature, spectral quality and quantity of light, available water, available nutrients and root competition (Whitmore, 1978; Van Miegroet, 1979; Canham, 1988a; Canham, 1988b; Lieberman *et al.*, 1989; Poulson and Platt, 1989; Denslow and Gomez-Diaz, 1990; Denslow and Spies, 1990; Chen *et al.*, 1993; Gray and Spies, 1996; Carlson and Groot, 1997; Connell *et al.*, 1997). In this way, disturbance can significantly affect the composition, structure and function of forest ecosystems (Barnes *et al.*, 1998). However, the monitoring of the recovery of the forest to disturbance is not possible without understanding the underlying conditions which might predispose the forest to disturbance, or the processes which mediate the changes following disturbance (Barnes *et al.*, 1998).

Once formed, gaps usually contract through lateral canopy ingrowth, sprouting of epicormic shoots, and regeneration from the seed and seedling banks (Hibbs, 1982; Swaine and Whitmore, 1988; Whitmore, 1989; Runkle, 1990; Everham, 1995; Coates and Burton, 1997; Connell *et al.*, 1997; Nachtergale *et al.*, 1997; Kranabetter and Wylie, 1998;

Matlack and Litvaitis, 1999; Clinton and Baker, 2000; McClure *et al.*, 2000). It is this response, primarily due to the disturbance changing the understorey light environment, that affects the future composition of a forest (Cottam, 1981; Kimmins, 1997). Consequently, over time, gaps become less distinct from the surrounding forest and are increasingly difficult to distinguish.

Gaps can also expand and coalesce, largely due to the initial disturbance increasing the vulnerability of the surrounding forest to further disturbance (Young and Hubbell, 1991; Gray and Spies, 1996; Coates and Burton, 1997). For example, exposed stand interior trees at the gap-canopy boundary of a newly formed windthrown gap have an increased risk of wind damage, although this risk decreases over time as the trees adapt their growth to the new conditions (Quine *et al.*, 1995; Barnes *et al.*, 1998). However, the risk of windthrow progression at windthrown gap-canopy boundaries is influenced by windthrown gap shape and boundary sharpness (Quine and Miller, 1990; Quine *et al.*, 1995; Gardiner and Stacey, 1996; Kimmins, 1997).

Although there is some evidence to suggest that windthrown gaps can negatively affect the ecology of a forest (e.g. Kranabetter and Wylie, 1998), they are generally viewed positively from an ecological perspective. For example, the formation of windthrown gaps can increase the potential regeneration of tree species and ground flora, and increase habitat diversity (Quine and Humphrey, 1996; Drobyshev, 1999; Clinton and Baker, 2000; Vickers and Palmer, 2000). The combination of the gap environment, understorey environment, canopy environment and the transitional boundary environment, usually

results in a higher diversity and density of both flora and fauna species (Hansson, 1983; Greatorex-Davies, 1991; Mayle and Gurnell, 1991; Oliver and Larson, 1996).

The creation of gaps to develop edge vegetation is an accepted silvicultural practice to promote wildlife within forests, although any benefit from an increase in desirable species may be offset by an increase in other species, for example undesirable predator species (Hansson, 1983; Carter and Anderson, 1987; Fuller, 1991; Greatorex-Davies, 1991; King *et al.*, 1998; Steventon *et al.*, 1998). Bird and bat species which have adapted to open areas may increase in number as the direct result of gap formation (Hansson, 1983; Blake and Hoppes, 1986; Grindal and Brigham, 1998; Jung *et al.*, 1999). This is partly due to the increased provision of roosting sites (Briggs, 1998), ease of flight (Grindal and Brigham, 1998), as well as an increase in insect abundance (Blake and Hoppes, 1986; Greatorex-Davies, 1991; Warren, 1991; Briggs, 1998).

Any increase in insect abundance may be due to both the release of understorey flora associated with gap formation and the gap boundary trees being weakened by the disturbance which formed the gap, providing a suitable habitat for insect populations (Carter, 1991; Warren, 1991). Unfortunately, it is an undesirable hazard for commercial forestry that windthrown trees are susceptible to attack by pioneer bark beetles, as the stressed trees are easily colonised (Speight and Wainhouse, 1989; Lundquist, 1995; Gregoire *et al.*, 1997; Safranyik and Linton, 1999). As these windthrown trees become increasingly stressed, they act as focus trees which may provide a breeding habitat and maintain bark beetle pest populations during non-epidemic periods (Speight and Wainhouse, 1989; Peltonen, 1999; Peltonen and Heliovaara, 1999). In addition,

windthrown trees are particularly vulnerable to colonisation by insects which can aid the development of stain and decay fungi (Evans *et al.*, 1989). There are, therefore, indirect and undesirable ecological and forest health implications associated with windthrown gaps within commercial forests (Savill, 1983; Lundquist, 1995; UN/ECE, 1999). As the risk of bark beetle attack to a forest is increased by the presence of windthrown trees (Jakus, 1998), the quantification of wind damage is, therefore, important for forest managers in order to make silvicultural decisions such as the necessity for sanitation felling (Speight and Wainhouse, 1989; UN/ECE, 1999; UN/ECE, 2000b).

2.4.1.3 Commercial implications of windthrown gaps

Natural disturbance, such as by wind, may be useful as a guide to developing a natural approach to forest management (Skorupa and Kasenene, 1984; Quine *et al.*, 1999). Indeed natural disturbance has been important for the development of silvicultural systems and in upland British forests, wind damage has a size range similar to that of conventional harvesting coupes (Runkle, 1985; Kimmins, 1997; Smith *et al.*, 1997; Quine *et al.*, 1999). However, windthrown gaps are usually considered commercially undesirable, primarily as they may result in significant financial losses (Coutts, 1986; Price, 1989; Fridman and Valinger, 1998; Peltonen, 1999). Such is the potential loss, that it is common practice after partial windthrow, but before severe wind damage occurs, for forest managers to undertake anticipatory felling (Foot, 1986; Quine and Miller, 1990).

In the event of severe wind damage, the wood markets may become flooded with damaged wood, reducing prices (Price, 1989; UN/ECE, 1999; Anon., 2000). For example,

storms across Europe on 26 and 28 December 1999 resulted in 165 million m^3 of wood being damaged, the equivalent of six months planned harvesting (UN/ECE, 2000b). In addition to the physical damage, windthrow results in a lower total volume production at the end of an economic rotation (Rollinson, 1986) and subsequent restocking costs are also likely to increase (Price, 1989; Anon., 1999). However, of greatest concern to commercial forest management is the presence of partial windthrow at a stand boundary which opens the stand up and increases the vulnerability of the stand to further wind damage (Quine and Miller, 1990; Quine *et al.*, 1995).

The air turbulence above a forest canopy is influenced by the degree and extent of existing gaps (MacKenzie, 1976; Savill, 1983; Brokaw, 1985; Everham, 1995; Oliver and Larson, 1996; Barnes *et al.*, 1998), as wind is deflected along a gap-canopy boundary (MacKenzie, 1976; Phillips, 1980; Savill, 1983; Price, 1989; Mitchell, 1998). Therefore, the presence of existing windthrown gaps within a forest canopy, contributes to the vulnerability of a forest to wind damage and will increase the risk of future wind damage occurring (Smith *et al.*, 1997).

Forest managers usually attempt to reduce the risk of wind damage by avoiding common silvicultural practices which increase the risk (Matthews, 1989; Price, 1989; Fridman and Valinger, 1998; Quine *et al.*, 1995; Quine and Bell, 1998). These decisions are usually based upon decision support tools such as the WHC (Booth, 1977; Miller, 1985; Quine *et al.*, 1995). To improve these tools, frequent monitoring of wind damage formation and progression is necessary (Quine and Bell, 1998; Sommerfeld *et al.*, 2000).

In addition to increasing the vulnerability of a stand to to windthrow, windthrown gaps also influence the future growth of residual standing trees (Gardiner, 1997). For example, trees in densely stocked stands usually self-prune by shedding branches as shade causes the older branches lower down on the crown to die naturally (Harris, 1978; Haygreen and Bowyer, 1996). However, newly exposed trees on a gap-canopy boundary adapt their growth to take advantage of the extra light resource by developing a side canopy (Matlack and Litvaitis, 1999) (Figure 2.3). This side canopy consists of large branches which become encased in the stem wood, leading to larger knots, thereby reducing overall wood quality.

Gap-canopy boundary trees are also associated with the formation of 'reaction wood', wider annual rings and greater stem taper, which are undesirable physical wood properties (Ward and Gardiner, 1976; Milner, 1980; Kilpatrick *et al.*, 1981; Wilson, 1982; Savill and Sandels, 1983; Brazier *et al.*, 1985; Rollinson, 1986; Wilson and White, 1986; Rollinson, 1988a; Haygreen and Bowyer, 1996). These undesirable wood properties have been shown to be serious, for example, reaction wood is prone to problems such as warping during wood processing (Haygreen and Bowyer, 1996; Gardiner, 1997).

The poor quality of windthrown wood harvested may mean that it is only suitable for sale in low value markets (Ward and Gardiner, 1976; Rollinson, 1986; Rollinson, 1988a; UN/ECE, 1999; Anon., 2000). In addition, wind damage has logistical and harvesting implications as it forms a dangerous work environment (Lonsdale, 1990; Anon., 1999; Health and Safety Executive, 2000; UN/ECE, 1999; UN/ECE, 2000c).

Figure 2.3 Photograph of the edge of a clearfell within a Sitka spruce stand, illustrating the difference in crown architecture between forest stand interior trees (on the left) and forest stand edge trees (on the right).

For example, due to the significant accident rate, it is recommended that anyone harvesting windthrown trees should receive specific training and be certified as competent (Dannatt and Garforth, 1989; Forestry and Arboriculture Safety and Training Council, 1996; Health and Safety Executive, 2000). Unfortunately, the danger of working on windthrown trees has been emphasised with the recent death of a forest contractor working on wind damaged trees in France (Hudson, 2000). As windthrown gaps represent a hazardous work environment, acquiring information on them, such as area of a stand damaged, or the volume of damaged wood, is obtained indirectly by mapping the gap-canopy boundary.

2.5 MAPPING THE GAP-CANOPY BOUNDARY

The conventional approach to mapping gaps considers them to be discrete features distinct from the surrounding canopy (e.g. Blackburn and Milton, 1995; Blackburn and Milton, 1996; Blackburn and Milton, 1997; Lundquist, 1995; Ostertag, 1998), and allocates a hard gap-canopy boundary. This mapping approach is largely done for the sake of convenience (Pukkala *et al.*, 1993). Unfortunately, natural boundaries, such as a gap-canopy boundary, tend to be 'soft' (Bosserman and Ragade, 1982; Wang, 1990; Foody, 1996a; Foody and Trodd, 1990; Ratcliffe, 1991; Peterken, 1996; Wang and Hall, 1996; Kent *et al.*, 1997; Brown, 1998; Sommerfeld *et al.*, 2000).

There are two hard mapping approaches used to differentiate a gap from the canopy. For example, the gap-canopy boundary can be considered as the 'dripline', which is the projected crown edge of trees bordering the 'canopy gap' (Veblen, 1985; Lawton

and Putz, 1988; Worrall and Harrington, 1988; Spies *et al.*, 1990; Lertzman and Krebs, 1991; Perkins *et al.*, 1992; Dahir and Lorimer, 1996; Gray and Spies, 1996; Van Der Meer and Bongers, 1996; Cadenasso *et al.*, 1997; Hughes and Bechtel, 1997; Myers *et al.*, 2000) or the base of the edge trees on the gap side bordering the 'extended gap' (Runkle, 1981; Dahir and Lorimer, 1996) (Figure 2.4).

These alternative hard mapping approaches for allocating a hard gap-canopy boundary are appropriate under different situations. For example, the 'expanded gap' may be more appropriate than the 'canopy gap' for assessing the effects of a gap upon natural regeneration as the increase in light levels extends beyond any projected canopy opening due to a lack of lateral canopy (Runkle, 1990; Brown, 1996; Matlack, 1993).

The high risk of injury whilst working with wind damaged trees, in addition to the time required and cost, means that it is often not practical to derive spatial information on windthrown gaps using conventional ground surveys (Blackburn and Milton, 1996; Quine and Bell, 1998). For example, the immediate response to the catastrophic wind damage attributed to the 1987 storm (Section 2.3), was to survey the affected area in order to estimate the harvesting requirements and predict the likely impact upon wood markets and prices. Due to the cost in both time and money, a ground survey could only sample the area affected by the storm (Dannatt *et al.*, 1989). As an alternative, remote sensing may provide an appropriate technique for the mapping acquisition of spatial and temporal information on windthrown gaps which would aid forest management planning for wind stability.

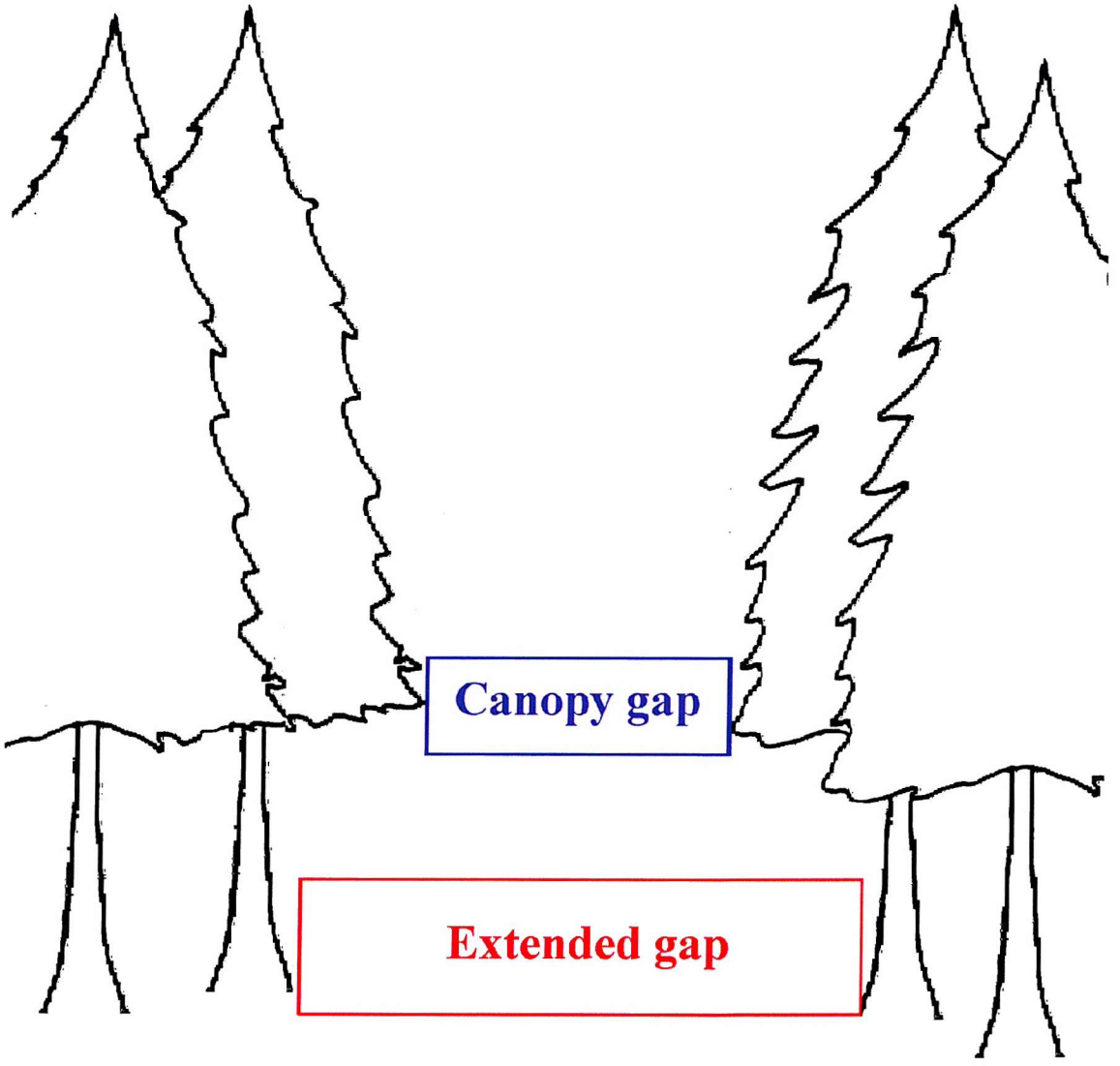

Figure 2.4 Hypothetical gap within the canopy of a forest stand, illustrating the difference between the 'canopy gap' (highlighted by the blue box) and the 'extended gap' (highlighted by the red box) (Runkle, 1990). The 'canopy gap' is bounded by the projected crown edge of trees bordering the opening and the 'extended gap' is bounded by the base of the trees bordering the gap.

2.6 REMOTE SENSING

The term 'remote sensing' is applied to the acquisition of data, using a sensor placed at a distance from a feature of interest (Barrett and Curtis, 1992; Richards, 1993; Campbell, 1996; Mather 1999; Lillesand and Kiefer, 2000). For the purposes of discussion, this broad definition is restricted to the recording of reflected or emitted electromagnetic radiation (EMR) from the Earth's surface which can be analysed to map the landcover mosaic (Curran, 1985; Campbell, 1996; Mather, 1999; Lillesand and Kiefer, 2000).

The selection of remotely sensed data to use for any investigation will be influenced by a number of factors. These can be broadly classified into three categories: data acquisition factors (such as sensor characteristics, the atmosphere and the angles between the illumination source, landcover and sensor); information extraction factors (e.g. classification); and the relationships between the reflecting and emitting elements within the landcover.

2.6.1 Acquisition of remotely sensed data

2.6.1.1 Sensor characteristics

There are a large number of sensors which can acquire remotely sensed data which may be suitable for forest based investigations. These sensors can be broadly classified in a number of different ways. For example, in terms of the portion of the electromagnetic spectrum (EMS) from which the data are acquired (e.g. optical or microwave sensors), the altitude above the forest from which the data are acquired (e.g. airborne or satellite

platforms) (Figure 2.5), or the energy source which illuminates the forest (e.g. passive or active sensors). The following is a brief summary of some of the sensor systems which may be used to acquire remotely sensed data.

2.6.1.1.1 Aerial photography

Aerial photography has long been used as a tool in forestry and uses camera systems that provide instantaneous data records rather than data composed from separately scanned lines (Spurr, 1948; Barrett and Curtis, 1999; Lillesand and Kiefer, 2000). The resulting photographs can be obtained using different film types, such as panchromatic, colour or colour infrared photographic films, or from different camera types, for example panoramic or digital cameras (Campbell, 1996; Barrett and Curtis, 1999; House *et al.*, 1999; Lillesand and Kiefer, 2000). There is also the possibility of acquiring multispectral photographs which are acquired within multiple spectral wavebands (House *et al.*, 1999). The routine and widespread use of aerial photography has resulted from its reliability, flexibility and versatility, for example, the ability to acquire stereopairs of photographs (Campbell, 1996; House *et al.*, 1999; Lillesand and Kiefer, 2000).

2.6.1.1.2 Aerial videography

Aerial videography is the recording of remotely sensed data as video signals (Lillesand and Kiefer, 2000). There are a variety of camera systems which can be used and it is possible to record data within the visible, near-infrared and middle-infrared portions of the EMS (Lillesand and Kiefer, 2000). Aerial videography provides multiple

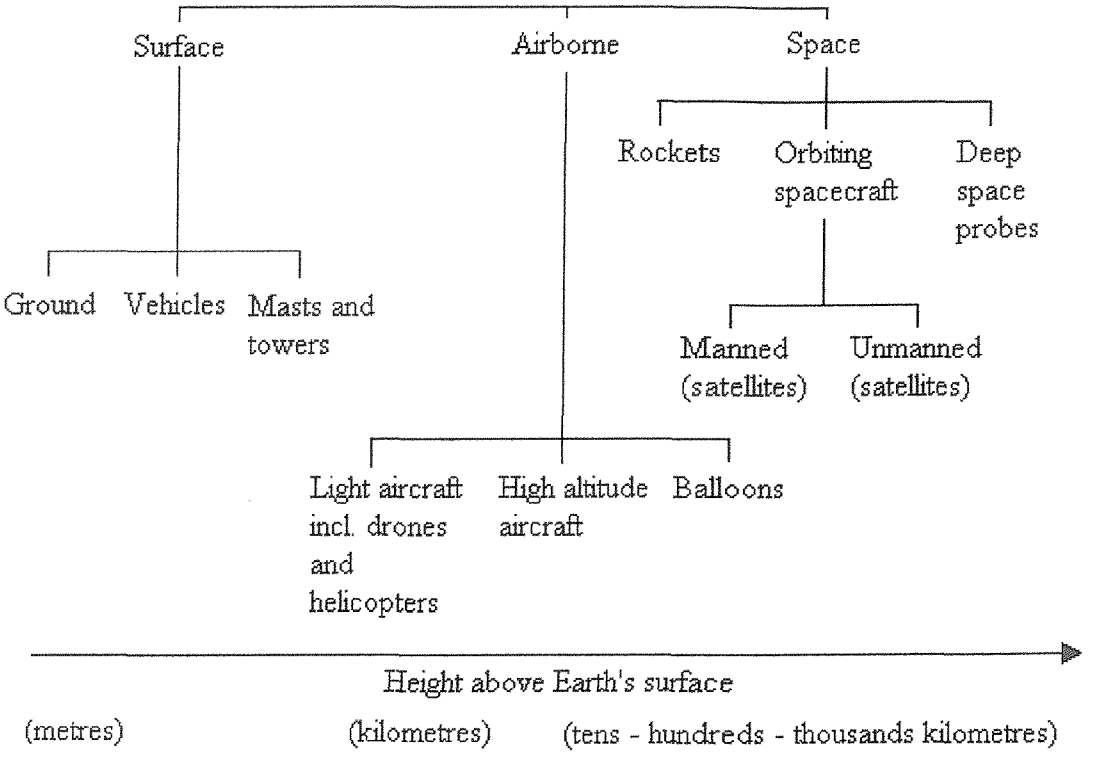

Figure 2.5 Classification of remote sensing platforms by type and altitude (adapted from Barrett and Curtis (1999)).

views of the landcover and hence, provides multiple sensor view angle and sun angle combinations for analysis (Lillesand and Kiefer, 2000). However, the data acquired are usually at a lower spatial resolution compared to aerial photography and is often the main limiting factor (Hosking, 1995; Lillesand and Kiefer, 2000).

2.6.1.1.3 Multispectral remote sensing

These scanning sensor systems are similar to multispectral aerial photography in that they use multiple spectral wavebands, however, they can acquire data from narrower wavebands, many more wavebands and over a greater portion of the electromagnetic spectrum (Lillesand and Kiefer, 2000). Examples of established satellite based multispectral sensors are Landsat's Enhanced Thematic Mapper (ETM), Thematic Mapper (TM) and Multispectral Scanner (MSS) sensors, *Systeme Probatoire d'Observation de la Terre's* (SPOT) High Resolution Visible (HRV) sensor, National Oceanic and Atmospheric Administration's (NOAA) Advanced High Resolution Radiometer (AVHRR), Indian Remote Sensing Satellite's (IRS) Linear Imaging Self Scanning Sensor (LISS) and Panchromatic Imager (PAN). The spatial resolution from these established satellite sensors varies from 1 km to 10 m (AVHRR and HRV (in panchromatic mode) satellite sensors respectively). Typically a spatial resolution of the order of 10 m (SPOT HRV sensor in panchromatic mode) to 30 m (Landsat TM sensor, except in waveband 6) is considered to be a benchmark spatial resolution for commercial remote sensing applications (e.g. Aplin *et al.*, 1997).

There are also a number of relatively new multispectral sensors, which can acquire data with a finer (typically < 5 m) spatial resolution (Aplin *et al.*, 1997). For example, the sensor carried aboard Space Imaging's Ikonos satellite can acquire data at a spatial resolution of 1 m (panchromatic mode) or 4 m (multispectral mode) and the sensors carried aboard EarthWatch's QuickBird satellite can acquire data at a spatial resolution of 1 m (panchromatic sensor) or 4 m (multispectral sensor).

There is also a special type of multispectral sensor system that operates only within the thermal portion of the EMS. An example of this type of sensor is the National Aeronautic and Space Administration's (NASA) Thermal Infrared Multispectral Scanner (TIMS).

2.6.1.1.4 Hyperspectral remote sensing

Hyperspectral remote sensing is concerned with the acquisition of data from a large number of very narrow, contiguous spectral wavebands throughout the visible, near-infrared and mid-infrared portions of the EMS (Lillesand and Kiefer, 2000). Examples of hyperspectral airborne sensors include the Compact Airborne Spectrographic Imager (CASI) and the Airborne Visible-Infrared Imaging Spectrometer (AVIRIS) which both acquire data in 224 contiguous spectral wavebands, and the Moderate Resolution Imaging Spectrometer (MODIS) satellite sensor, which acquires data in 36 contiguous spectral wavebands.

2.6.1.1.5 Microwave remote sensing

There are a number of remote sensor systems that operate within the microwave portion of the EMS. These sensor systems can be ground based, carried upon airborne or satellite platforms and can be either passive or active (Lillesand and Kiefer, 2000). The problem with using the microwave portion of the EMS is that the strength of 'passive' microwaves naturally reflected and/or emitted is weak and highly sensitive microwave radiometers must be used (Campbell, 1996; Lillesand and Kiefer, 2000). Therefore, most remote sensing of the microwave portion of the EMS is usually carried out by active sensing using radio detection and ranging imaging (RADAR) sensor systems (Campbell, 1996; Mather, 1999).

RADAR sensors use artificially generated microwave energy directed towards the object of interest via an antennae. The energy that is recorded by the sensor depends upon a number of factors, such as the wavelength and polarisation of the microwaves, ground relief and surface roughness (Campbell, 1996; Lillesand and Kiefer, 2000). RADAR systems use an antennae which is orientated to the side and termed side-looking radar (SLR) or side-looking airborne radar (SLAR) systems. The resolution of real aperture RADAR systems, is directly proportional to the length of the antennae used to transmit and receive the signal (Campbell, 1996; Mather, 1999).

Synthetic aperture RADAR (SAR) systems were developed to make it possible to increase the resolution of RADAR by achieving an artifically long effective antennae length from a small actual antennae (Campbell, 1996; Mather, 1999). Examples of satellite based SAR systems are carried aboard the European Remote Sensing (ERS) and

Radarsat satellites. ERS-1 and ERS-2, launched in 1991 and 1995 respectively, carry C-band SAR systems operated by the European Space Agency (ESA). Radarsat-1, launched in 1995, is a Canadian remote sensing satellite that also carries a C-band SAR system. In addition, the Radarsat sensor has a variety of operating modes that can provide a variety of swath widths, resolutions and look angles (Campbell, 1996; Mather, 1999; Lillesand and Kiefer, 2000).

RADAR systems have a number of distinct advantages over optical sensor systems. They can acquire data independent of weather and illumination, because they produce their own incident radiation (Ahern *et al.*, 1993; Campbell, 1996; Leblon, 1999; Mather, 1999; Lillesand and Kiefer, 2000). This may make RADAR sensor systems appropriate for monitoring upland commercial forests in the British Isles, since it is often difficult to acquire cloud free remotely sensed data from optical sensors (Puhr and Donoghue, 2000). However, a major restriction to the use of RADAR is the difficulty in identifying forest boundaries which are not facing the direction of RADAR illumination, represented by RADAR shadow (Campbell, 1996; Green, 1998a; Leblon, 1999). In addition, RADAR data do not usually present a familiar representation of the landcover mosaic as the sensors are unable to acquire colour information, unlike optical sensors (Leblon, 1999; Mather, 1999; Lillesand and Kiefer, 2000).

2.6.1.1.6 LIDAR remote sensing

Light detection and ranging (LIDAR) is an active remote sensing method like RADAR, except that it uses pulses of laser light rather than microwaves (Lillesand and

Kiefer, 2000). LIDAR is an airborne sensor system, developed for terrain and surface mapping, that is capable of returning data on the vertical distribution of the ground surface and elements within the landcover (Lillesand and Kiefer, 2000).

2.6.1.2 The atmosphere

All the radiation used for remote sensing passes through the Earth's atmosphere (Campbell, 1996; Lillesand and Kiefer, 2000). The presence of dust, gasses and aerosols within the atmosphere result in radiation absorption and scattering, which can significantly modify the data acquired by a remote sensor (Hame, 1991; Campbell, 1996; Mather, 1999; Lillesand and Kiefer, 2000). Atmospheric absorption, is usually attributed to the presence of ozone (O_3), water vapour (H_2O) and CO_2 (Richards, 1993; Campbell, 1996; Barrett and Curtis, 1999; Lillesand and Kiefer, 2000). CO_2 in particular has a significant role in the global climate and may be associated with forest disturbances (Section 2.2) (Bazzaz, 1990; Hendrey, 1992; Woodward, 1992; Barrett and Curtis, 1999; IPCC, 2000). Atmospheric scattering is strongly influenced by the size and quantity of atmospheric particles, the distance through the atmosphere the radiation must pass (the path length), and radiation wavelength, with scattering increasing as the wavelength becomes shorter (Richards, 1993; Campbell, 1996; Mather, 1999; Lillesand and Kiefer, 2000). This means that the optical portion of the EMS is affected more by the atmosphere than the microwave portion. Changes in atmospheric conditions can alter the atmospheric absorption and scattering which influences the spectral reflectance and illumination of the landcover and ultimately, the radiation recorded by the sensor (Hame, 1991; Mather, 1999).

2.6.1.3 Angles between the illumination source, landcover and sensor

Shadows within remotely sensed data are caused by objects which prevent part of the landcover being directly illuminated (i.e. it only receives diffuse illumination). The ability to see objects within regions of shadow is a benefit of the atmospheric scattering of light (Section 2.6.1.2) (Campbell, 1996). The proportion of shadow within remotely sensed data is a function of the angle of illumination (such as the solar elevation/zenith angle), the sensor view angle, the illumination azimuth angle (the angle between the plane of illumination and the plane of view), as well as the spectral transmittance of the landcover (Barrett and Curtis, 1999; Mather, 1999; Lillesand and Kiefer, 2000). The illumination and view angles are important considerations as there can be significant variability in the reflectance from landcover, in terms of the proportion of the landcover illuminated and viewed respectively. Whether the sensor is viewing into or away from the source of illumination, described by the azimuth angle, will also influence the reflectance recorded.

At the extremes, landcover can act as a specular reflector, reflecting radiation in a single direction, or it can act as a perfectly diffuse reflector, reflecting radiation equally in all directions (Richards, 1993; Campbell, 1996; Mather, 1999). Natural landcover usually exhibits a complex reflectance pattern which is described by the bidirectional reflectance distribution function (BRDF) for all possible combinations of viewing and illumination angles at a given wavelength (Campbell, 1996; Barrett and Curtis, 1999; Mather, 1999; Lillesand and Kiefer, 2000).

2.6.2 Classification of remotely sensed data

Due to the relatively familiar representation of the landcover mosaic, optical remote sensing may be more appropriate for operational forest management use than other methods of remote sensing (Section 2.6.1.1). The remotely sensed data acquired by optical sensors can be stored in pictorial and digital formats. However, it is usually in digital format that the data are most useful, due to the relative ease of classification (Richards, 1993; Campbell, 1996; Lillesand and Kiefer, 2000). Digital remotely sensed data represent the spatial variation in the magnitude of EMR interacting with the Earth's surface (Curran, 1985; Smith *et al.*, 1990; Wang, 1990; Puyou-Lascassies *et al.*, 1994). These data consist of a two-dimensional arrangement of picture elements, or pixels (Richards, 1993; Campbell, 1996; Fisher, 1997; Frohn, 1998; Gerylo *et al.*, 1998; Lillesand and Kiefer, 2000). Each pixel is a spatial sampling unit, associated with the sensor used and bears no direct relation to spatial factors of the Earth's surface.

Pixels represent a sample expressed as an integer value, termed digital number (DN), which denotes the radiance for a specific spectral waveband (Curran, 1985; Mather, 1999). The magnitude of the radiance represented by an individual pixel is a complex function of the atmosphere, the pattern of reflectance as described by the BRDF and the spectral reflectance properties of the components within that pixel (Mather, 1999; Lillesand and Kiefer, 2000).

Classification is used extensively to extract information from remotely sensed data. The aim is to allocate every pixel within the remotely sensed data to classes which have meaning to the end user (Settle and Drake, 1993; Wang and Howarth, 1993; Lillesand and

Kiefer, 2000). For example, remotely sensed data of a town may be crudely classified using classes such as 'road', 'building' and 'grass'. This is based upon the assumption that each class has a distinct reflectance pattern attributed to physical differences and, therefore, each class is statistically distinguishable from the others (Mather, 1999; Lillesand and Kiefer, 2000).

There are two main approaches used to classify remotely sensed data, unsupervised and supervised classifications, and the advantages and disadvantages of each are discussed by Campbell (1996). An unsupervised classification is based purely upon the remotely sensed data and does not require prior knowledge of the landcover represented by the data (Richards, 1993; Campbell, 1996; Lillesand and Kiefer, 2000). This method of classification uses the distribution of pixels in multidimensional feature space to derive statistical information on likely classes and subsequently group the remotely sensed data into classes (Barrett and Curtis, 1999). Supervised image classification uses prior knowledge about the landcover represented by the remotely sensed data to extract information (Richards, 1993; Campbell, 1996; Mather, 1999; Lillesand and Kiefer, 2000). This later method uses reference data to select sample pixels, whose contents are known, to represent thematic classes and subsequently derive statistical information on each class (Campbell, 1996). Classifiers, such as the parallelepiped, minimum-distance or maximum-likelihood, then use this information to allocate each pixel to a class (Campbell, 1996; Mather, 1999; Lillesand and Kiefer, 2000).

However, once a classification has been conducted, its accuracy must be assessed to determine the magnitude and pattern of the error (Mather, 1999; Lillesand and Kiefer,

2000). There are a number of factors which influence classification error, amongst which are the classification algorithm used, the presence of untrained classes within the data and the spatial resolution of the data (Figure 2.6) (Foody, 2000). Conventional unsupervised and supervised classification algorithms, such as the maximum-likelihood, can be described as 'hard', as each pixel is allocated to a discrete mutually exclusive class (Atkinson and Cutler, 1996; Foody, 1996a; Brown, 1998; Foody, 2000). Hard classifications assume that pixels are pure and hence, are well suited for the classification of pure pixels representing landcover classes which the classifier has been trained to recognise (Foody, 1996a; Cadenasso *et al.*, 1997; Foody, 2000).

However, there is often a significant proportion of pixels within remotely sensed data which contain more than one class and are often termed mixture elements, or mixels (Fisher, 1997; Foody, 1998; Gerylo *et al.*, 1998). Most remotely sensed pixels are mixed and these cause problems in analysing remotely sensed data (Smith *et al.*, 1990; Settle and Drake 1993; Kerdiles and Grondona, 1995; Foody, 1996a; Armitage *et al.*, 1997; Foody, 2000). For example, the usefulness of a hard classification for landcover mapping will decrease as the quantity of mixed pixels within the data increases (Foody, 2000). The quantity of these mixed pixels within remotely sensed data is usually a function of the spatial resolution of the sensor used (Figure 2.7), class definitions and the landcover mosaic (Grunblatt, 1987; Nelson, 1989; Wang, 1990; Cross *et al.*, 1991; Settle and Drake, 1993; Wu and Schowengerdt, 1993; Foody and Curran, 1994; Puyou-Lascassies *et al.*, 1994; Kerdiles and Grondona, 1995; Foody, 1996a; Fisher, 1997; Foody, 2000).

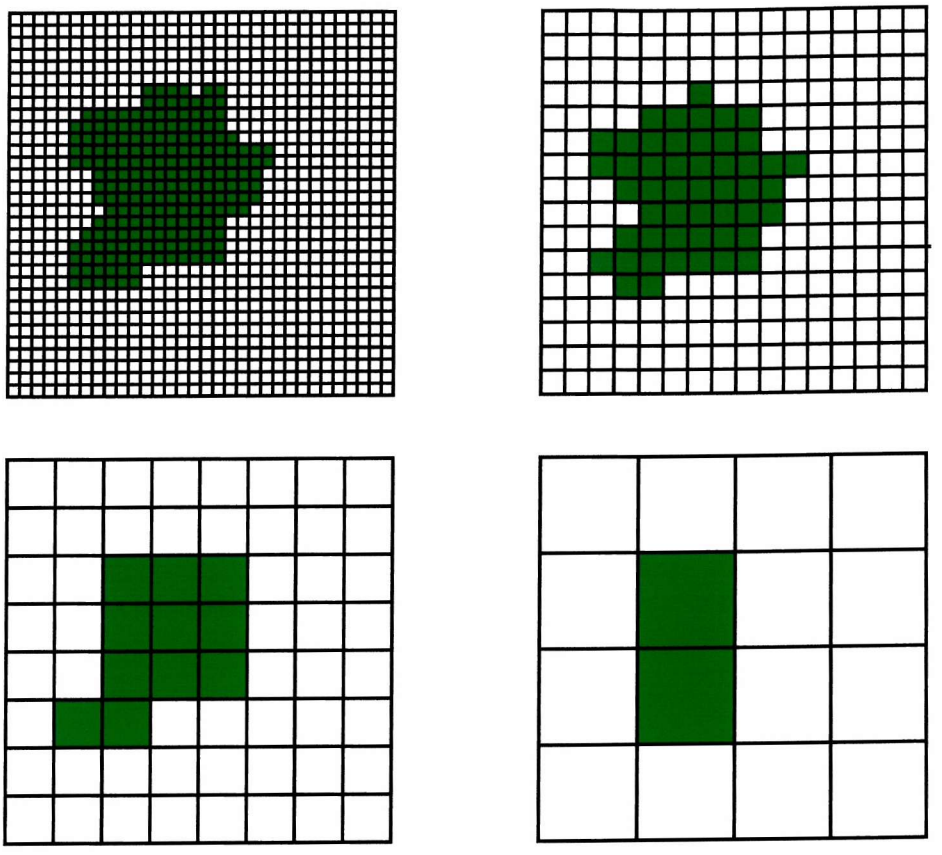

Figure 2.6 The hard classification output of a hypothetical object within remotely sensed data, as a function of the spatial resolution. The spatial resolution of the upper left, upper right, lower left and lower right data are 1 m, 2 m, 4 m and 8 m respectively. As the spatial resolution of the remotely sensed data becomes coarser, the representation of the object derived from a hard classification becomes less accurate.

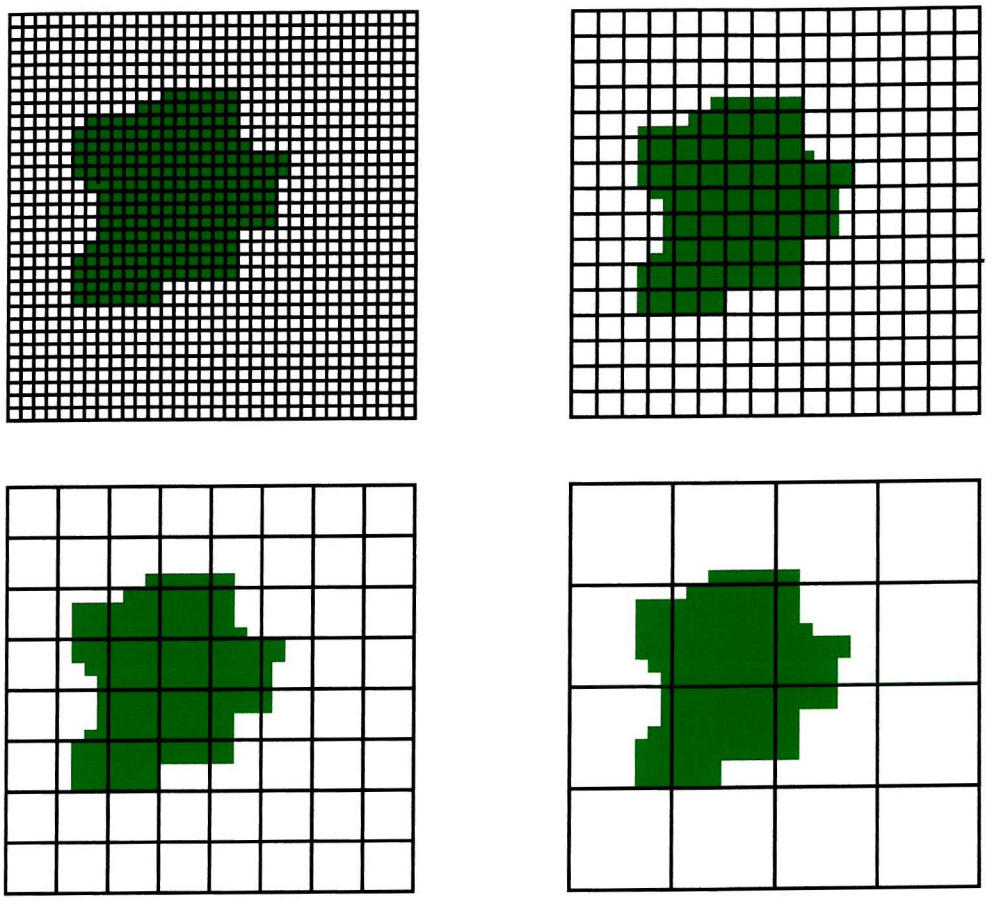

Figure 2.7 A hypothetical homogeneous object within remotely sensed data, as a function of the spatial resolution. The spatial resolution of the upper left, upper right, lower left and lower right data are 1 m, 2 m, 4 m and 8 m respectively. As the spatial resolution of the remotely sensed data becomes coarser, the number of pixels representing the object which are mixed increases.

2.6.3 The remotely sensed response from a forest

The remotely sensed response from a forest is a function of numerous components (Brakke *et al.*, 1989; Baret *et al.*, 1995; Kerdiles and Grondona, 1995; Nilson and Ross, 1997). A pixel representing the response from a forest will usually contain a complex mixture of four main components: sunlit canopy; sunlit gaps; shaded canopy; and shaded gaps (Gerard and North, 1997; Jupp and Walker, 1997; Nilson and Ross, 1997). Due to the high canopy cover maintained in managed British forests, the contribution from the canopy will usually dominate the remotely sensed response from a forest (Stenback and Congalton, 1990; Danson and Curran, 1993).

2.6.3.1 The spectral reflectance from a canopy

The spectral reflectance from a canopy is principally controlled by plant physiology and physiognomy, that are both dependent upon a number of factors, such as species and season (Curran, 1985; Guyot,1990; Barnsley, 1994). Flowers, fruit and woody biomass are important elements within the canopy, although leaves are the dominant element which influence the canopy reflectance. Specifically, it is the pigmentation systems, the physiological structure and the water content which primarily affect the spectral reflectance of leaves and hence the remotely sensed response from a forest canopy (Guyot, 1990).

The pigmentation systems within leaves control the spectral reflectance within visible wavelengths, whilst the structure and water content of leaves determine the spectral reflectance from the near- and middle-infrared wavelengths (Figure 2.8). EMR which is

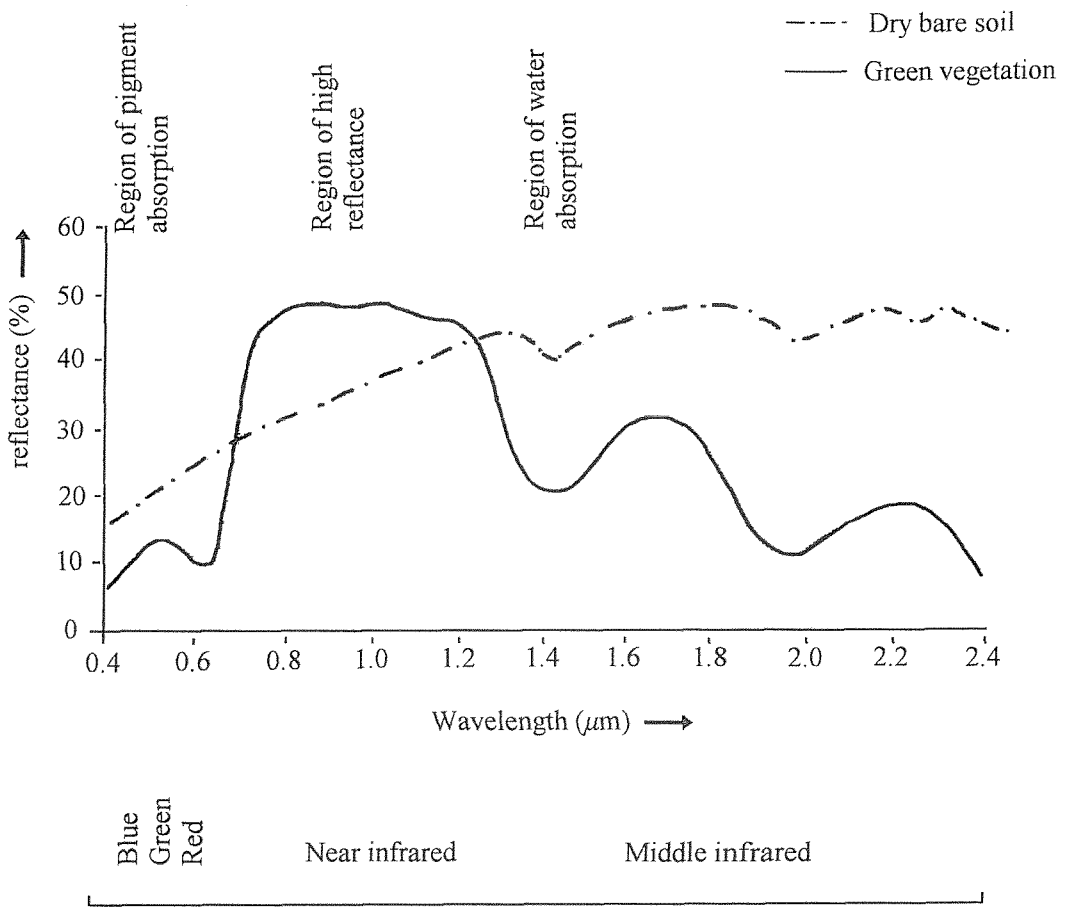

Figure 2.8 Typical reflectance curves for dry bare soil and green vegetation (adapted from Curran (1985) and Lillesand and Kiefer (2000)).

not reflected from the leaf surface is absorbed and transmitted where it is scattered and reflected within the internal leaf structure (Figure 2.9). Leaves contain four primary pigments: chlorophyll a; chlorophyll b; β carotene; and xanthophyll lutein, which absorb photosynthetically active radiation (PAR) for photosynthesis (Campbell, 1990; Salisbury and Ross, 1992). The proportion of these pigment systems, dependent upon the age of the leaf, season and tree species, will affect the spectral reflectance of the canopy. The characteristic reflectance properties of healthy green leaves are (Figure 2.8): low reflectance of red and blue light; medium reflectance of green light; and high reflectance of near-infrared (NIR) radiation. However, as leaves senesce, the spectral reflectance of yellow-green and red light increases as absorption by chloroplasts decreases (Brakke *et al.*, 1989; Guyot, 1990).

The palisade mesophyll on the upper side of the leaves consists of closely packed cells which contain a large quantity of chloroplasts with 5 to 20 % air space, whilst the spongy mesophyll on the under side of the leaves consists of loosely packed cells, with 50 to 80 % air space and fewer chloroplasts (Figure 2.9) (Raven *et al.*, 1986; Brakke *et al.*, 1989; Campbell, 1990). Most of the internal scattering of visible wavelengths within leaves occurs at air-cell interfaces (Brakke *et al.*, 1989; Guyot, 1990; Nilson and Ross, 1997). This may be an evolutionary trait designed to disperse visible light throughout the canopy and hence maximise the light resource available to the leaves for photosynthesis (Brakke *et al.*, 1989). This transmission and reflectance of light within a forest canopy, in conjunction with atmospheric scattering (Section 2.6.1.2) ensures that shadow within a

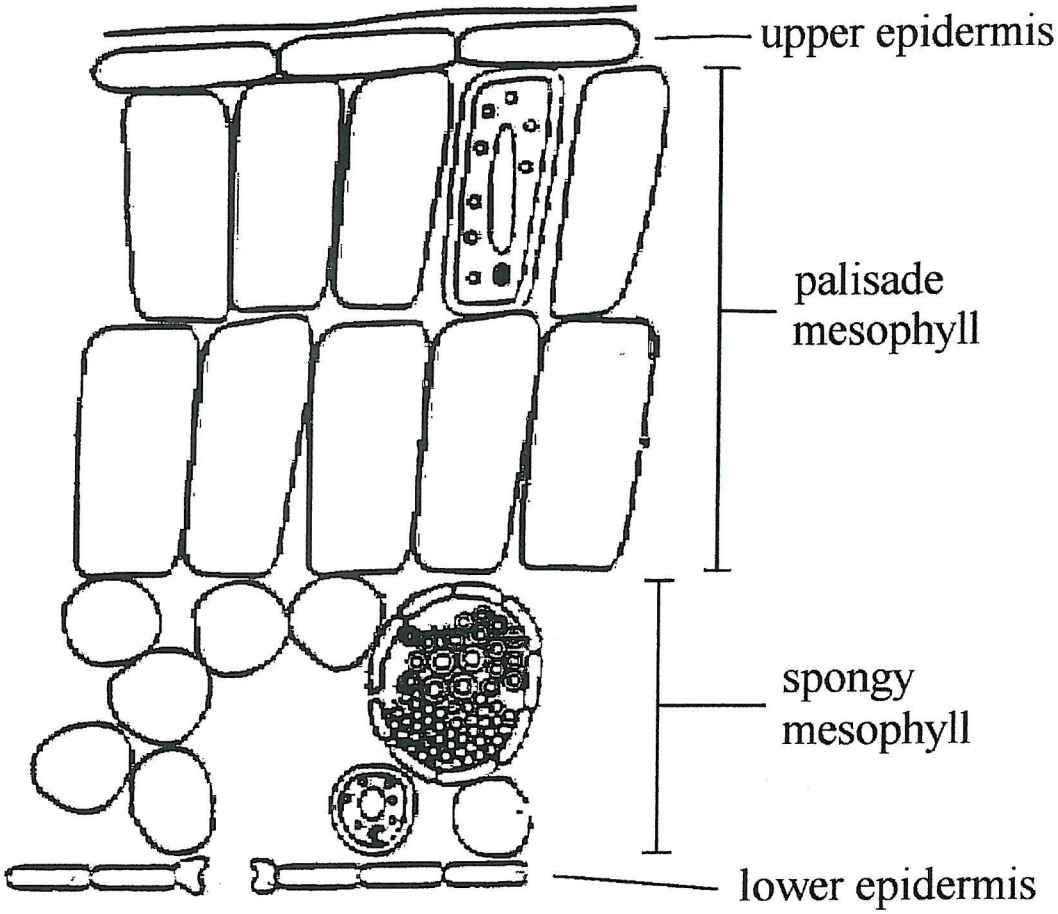

x600 magnification

Figure 2.9 Cross section through a representative broadleaved tree leaf with the epidermal and ground tissue (mesophyll) labelled.

remotely sensed response does not infer absence of solar radiation (Satterlund, 1983; Whitmore, 1990).

2.6.3.2 The spectral reflectance from a gap

The ability to identify a gap within remotely sensed data is based upon the principle that its remotely sensed response will differ significantly from that of the surrounding landcover. The spectral reflectance from a gap will usually be the spectral reflectance from the forest understorey left after the canopy has been removed. Due to conventional silvicultural practices maintaining a high level of canopy cover, understorey vegetation does not usually thrive within upland British forests (Figure 2.10) (Danson and Curran, 1993; Puhr *et al.*, 1997; Green, 1998b; Puhr and Donoghue, 2000). Therefore, the spectral reflectance from a gap formed by the complete removal of trees within Sitka spruce plantations, will be initially influenced by the reflectance of the needle litter and soil. This soil reflectance will depend upon the moisture content, the mineral composition and the particle size. As vegetation gradually colonises and regenerates within a gap, the contribution from the soil and the needle litter to the spectral reflectance of the gap will decrease and it will be more difficult to discriminate between a gap and the surrounding landcover (Walsh *et al.*, 1982; Yatabe and Leckie, 1995).

Figure 2.10 Photograph taken from under a Sitka spruce canopy, looking into a windthrown gap. The lack of ground vegetation in the foreground under the canopy is due to inadequate light.

2.7 REMOTE SENSING OF WINDTHROWN GAPS

Acquiring spatial and temporal information on windthrown gaps using conventional field survey methods is difficult (Section 2.5). Remote sensing may provide an alternative method for acquiring this information because it does not bear the cost of labour and time associated with field survey, although it does require other resources, such as computing facilities.

2.7.1 Previous work on the remote sensing of windthrown gaps

The benefit of RADAR was noted in Section 2.6.1.1.5, however, previous work has indicated that although RADAR has the potential to identify windthrown gaps, its application is restricted by the difficulty in defining boundaries which are not facing the direction of RADAR illumination (Green, 1998a; Leblon, 1999). This problem is largely influenced by gap shape and orientation relative to the illumination (Green, 1998a).

To-date, the mapping of windthrown gaps using remotely sensed data has been based largely upon the manual interpretation of aerial photographs (e.g. Quine and Bell, 1998). However, the use of aerial photographs is not without its problems (Wilson, 1997; Wang *et al.*, 1998). Photographic interpretation is time consuming and subjective (Delaney and Skidmore, 1998; Naesset, 1998). An alternative to aerial photographs is the use of airborne sensor data.

Previous work has investigated the potential to use 2 m spatial resolution data, acquired by a CASI sensor, to delineate gaps within several deciduous woodland types (Blackburn and Milton, 1995; Blackburn and Milton, 1996; Blackburn and Milton, 1997).

The results suggested it was possible to map canopy gaps within the deciduous woodland types, and estimate gap area, perimeter and shape. From these results it was possible to infer the relative ecological implications of the gaps identified. It was concluded that fine spatial resolution remotely sensed data were appropriate for monitoring forest dynamic processes associated with gap formation.

However, the value of aerial photography or airborne sensor data is often limited by factors such as the relatively limited spatial coverage, which may limit the range of useful information which may be derived (Katsch and Vogt, 1999; Scheer and Dursky, 1998; Leblon, 1999). Satellite sensor systems may, however, represent a more appropriate source for the acquisition of data on windthrown gaps. Previous work has involved the use of these satellite sensors for mapping severe wind damage to forests throughout the world (e.g. Gillis *et al.*, 1990; Ramsey *et al.*, 1997; Mukai and Hasegawa, 2000), or studied gaps resulting from forest disturbance in the context of global climate change (e.g. Foody and Curran, 1994; Curran *et al.*, 1995; Schimel, 1995; IPCC, 2000) (Section 2.3). Other work has used satellite sensors to monitor changes in forest stand reflectance associated with relatively small scale gaps formed by thinning the stands, and subsequently identify the presence of these gaps (e.g. Olsson, 1994; Nilson and Olsson, 1995).

These current civilian satellite sensors (e.g. Landsat TM) acquire data at the forest-landscape scale required for the monitoring of wind damage to forests over the range of climatic zones within the British Isles (Quine and Bell, 1998; Quine *et al.*, 1999). The major drawback to the use of these satellite sensing systems is that many windthrown

gaps are smaller or similar in size to the spatial resolution of these sensors (Quine and Bell, 1998). Therefore, many windthrown gaps will be subpixel in size and represented within the remotely sensed data by mixed pixels (Werle *et al.*, 1986). However, it is not easy to account for the presence of mixed pixels using conventional hard classification methods. These hard classification methods (Section 2.6.2) are based upon discrete class allocation and only allow full or zero pixel membership to any class (Wang, 1990; Altman, 1994; Wang and Hall, 1996). This may have important consequence for area estimates derived from the classified data, as well as the spatial representation of classes within the data (Foody, 1996a).

2.7.2 New opportunities for remote sensing of windthrown gaps

New classification methods and new satellite sensor systems may resolve many of the current problems encountered with the use of remotely sensed data.

2.7.2.1 New satellite sensor systems

There are a range of new satellite sensors that can acquire finer (< 5 m) spatial resolution data than established satellite sensors such as Landsat's TM (Aplin *et al.*, 1997; Thomas *et al.*, 1997; McGraw *et al.*, 1998; Celentano, 1999; Lillesand and Kiefer, 2000). Examples of these new sensors include the those carried aboard the Ikonos and QuickBird satellites (Section 2.6.1.1.3). As the spatial resolution of the remotely sensed data available becomes finer, the spatial representation of landcover should become more accurate and the accuracy of areal estimates should increase. An alternative would be to

use the relatively coarse spatial resolution satellite sensor data currently available (e.g. 10m spatial resolution data from Landsat TM), but apply a classification method which provides an alternative representation of class membership within pixels to conventional classification methods.

2.7.2.2 New classification methods

There are a range of alternative methods to a hard classification (Lillesand and Kiefer, 2000), some of which have been used for forest cover mapping when the pixels within the remotely sensed data are mixed (e.g. Foschi, 1994; Williamson, 1994; Hlavka and Spanner, 1995; Huguenin *et al.*, 1997). One alternative is to use soft, or fuzzy classification methods (Foody, 1996a; Foody, 1996b; Foody, 2000) for forest cover mapping (e.g. Maselli *et al.*, 1995). These soft classifications may be more applicable for handling mixed pixels, as they may be used to represent the relative proportion of each component class within a pixel (Wang, 1990; Cross *et al.*, 1991; Settle and Drake, 1993; Puyou-Lascassies *et al.*, 1994; Kerdiles and Grondona, 1995; Foody, 1996a). This may allow a more accurate estimate of component class areas to be derived from a soft classification (Foody, 1996a; Foody, 1996b).

A soft classification allocates partial and multiple class membership to a pixel (Wang, 1990; Heuvelink and Burrough, 1993; Altman, 1994; Foody, 1996b; Brown, 1998). Generally, as the proportion of a class within a pixel increases, the contribution of that class to the spectral reflectance within the pixel increases (Wang, 1990; Shimabukuro and Smith, 1991; Settle and drake, 1993; Puyou-Lascassies *et al.*, 1994; Williamson, 1994;

Kerdiles and Grondona, 1995). However, this is often not straight forward. The relationship between the proportion of a class within a pixel and the contribution of that class to the remotely sensed response may not be linear and a class may exert a disproportionate influence (Smith *et al.*, 1990; Borel and Gerstl, 1994). In addition, it is usually not possible to derive information on the spatial distribution of each class within a pixel (Atkinson, 1997; Huguenin *et al.*, 1997; Foody, 1998).

It is possible to undertake a fully soft classification, in which the training, testing and allocation stages of classification are soft. This requires training with mixed pixels for which the class composition is known and this information is often not available. Alternatively, it is possible to soften the output of a conventional hard classifier. For example, softening the output from a maximum-likelihood classification may provide a more realistic representation of landcover and improved estimates of class area (Foody, 1996b; Foody, 1998).

The maximum-likelihood classification generates information that can be used as a surrogate for the relative proportion of each component class within a pixel (Foody *et al.*, 1992; Foody and Trodd, 1993; Foody, 1996b). This information, from which measures of class membership can be derived, is not fully exploited (Wang, 1990; Maselli, 1994; Foody, 1996b). Softening this conventional hard classification to output class membership may have the benefit to the end user of increasing the accuracy of measurements derived from the output, without the disadvantages of dealing with a larger remotely sensed data volume.

2.8 SUMMARY

Windthrown gaps are a common feature of commercial British forests, and spatial and temporal information is required to develop strategies to manage their effects and further the understanding of the processes involved in wind damage (Quine *et al.*, 1995; Quine, 1998; Quine and Bell, 1998). However, this information is difficult to acquire by traditional field survey methods (Quine and Bell, 1998). Remote sensing has the potential to be used as an operational tool for the provision of information on windthrown gap characteristics. To date, this work has been based upon information on windthrown gaps acquired through the manual interpretation of aerial photographs (Quine and Bell, 1998).

Satellite sensors may provide a more attractive source of remotely sensed data. However, the usefulness of products derived from these data may be constrained by the spatial resolution of the data acquired by established satellite sensors and the limitations of conventional hard classification methods in dealing with mixed pixels. The research in this thesis has investigated fine (< 5 m) spatial resolution remotely sensed data and alternative classification methods for characterising windthrown gaps within commercial upland forests in the British Isles.

CHAPTER 3

STUDY SITE AND REMOTELY SENSED DATA ACQUISITION

3.1 INTRODUCTION

This Chapter describes the forest site for which the remotely sensed data were acquired and summaries the main characteristics of the airborne thematic mapper (ATM) sensor, which was used to acquire the remotely sensed data used in subsequent research. In addition, the operational reference data of known windthrown gaps present within the forest site are also described.

3.2 CWM BERWYN FOREST WIND DAMAGE MONITORING SITE

Cwm Berwyn Forest is located in Central Wales (Figure 3.1). It was established over three planting seasons, between 1960 and 1963, by the Forestry Commission and is a typical upland forest (Davies, 1991). Within Cwm Berwyn Forest a 250 ha wind damage monitoring site was established in 1988 by the Forestry Commission for the study of windthrow prediction (Quine, 1988; Quine and Reynard, 1990). This monitoring site consisted of seven compartments surrounding Llyn Berwyn (Figure 3.2).

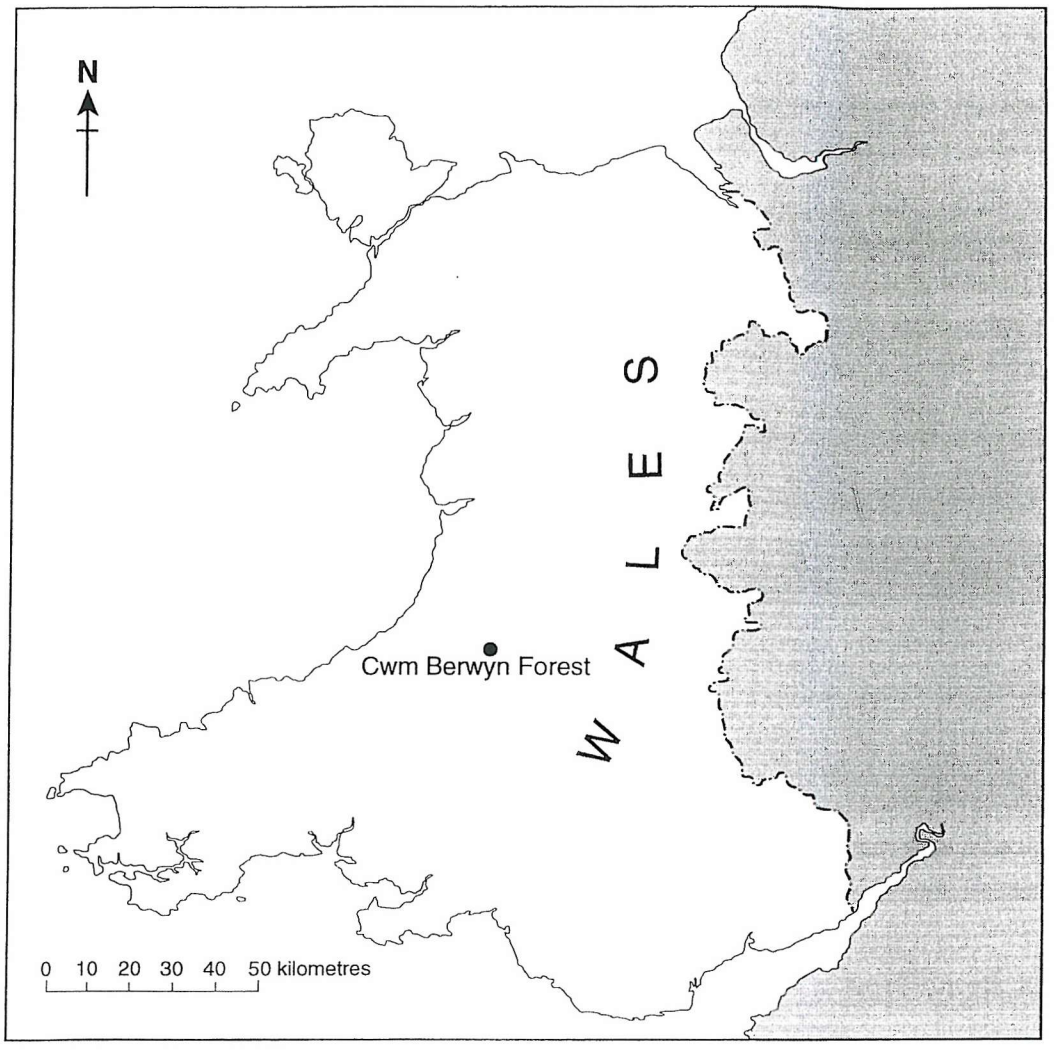

Figure 3.1 Location map of Cwm Berwyn Forest, Wales.

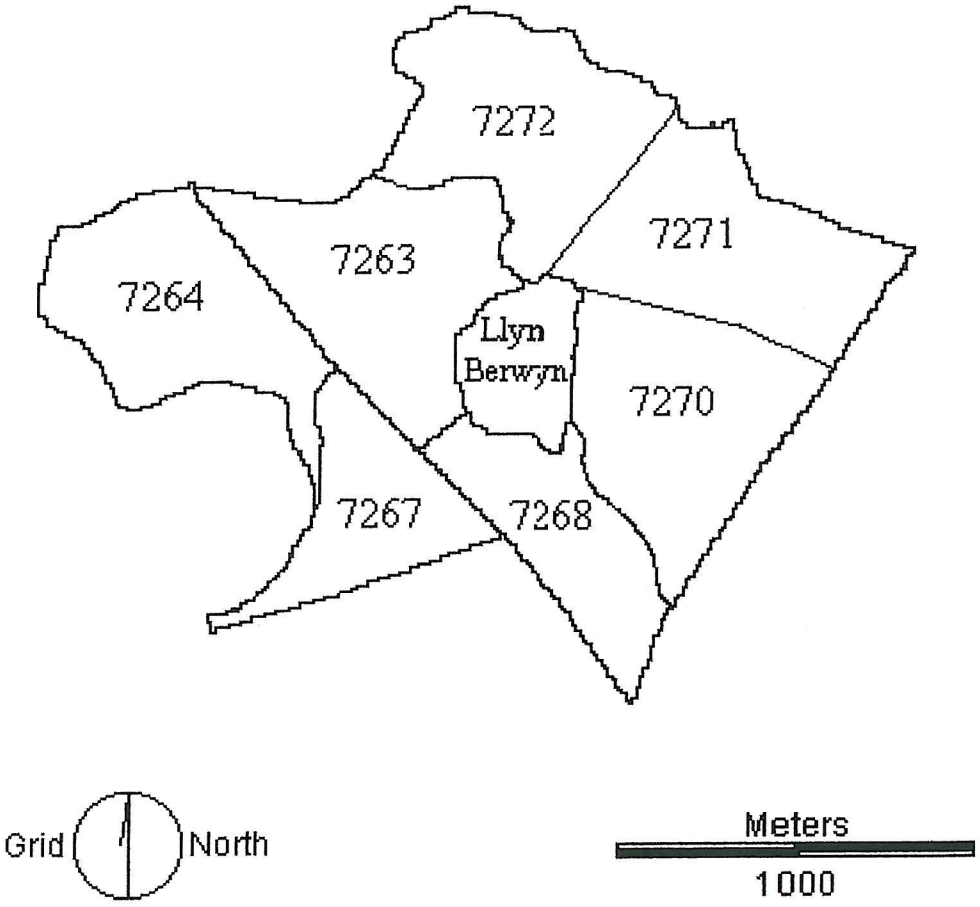

Figure 3.2 Compartments within Cwm Berwyn Forest wind damage monitoring site, surrounding Llyn Berwyn lake.

The Forestry Commission's information on the formation and development of windthrown gaps within this monitoring site has largely been acquired from the manual interpretation of annual 1:10,000 colour aerial photographs, taken since 1988. This information was targeted at the validation and refinement of the WHC, which significantly influences commercial upland forest management practice in the British Isles (Sections 1.1 and 2.4.1.3) (Booth, 1977; Miller, 1985; Quine, 1987; Quine, 1989; Quine *et al.*, 1995).

3.2.1 Site conditions

Ranging in elevation between 300 to 500 m above mean sea level, the monitoring site is characterised by variable topography, as well as variable soil types (Table 3.1). The underlying geology consists primarily of Silurian shales and the soils are dominated by *Molinia* peat bog (Quine, 1991a). The site has approximately 1700 mm rainfall per annum and is exposed, with a topographic exposure (TOPEX) score between 1 and 34 (Miller, 1985; Quine, 1991).

Field survey data acquired in 1988 by the Forestry Commission, in compartment 7271 (Figure 3.2), resulted in a mean WHC score of approximately 29, which indicated WHC 5, although the range across the whole site varied between classes 3 and 6 (see Miller (1985) for a full description of the WHC). This indicated that there was a significant risk of windthrow and that the damage would be frequent (Quine *et al.*, 1995). This WHC score predicted that windthrow would start to occur when the trees reached a critical height of 15.0 m, (Miller, 1985). The 1988 field survey data indicated that the stand height varied from 8.0 to 15.5 m (Quine, 1991a). As a result, in 1988 when the wind

damage monitoring project was established, the trees within the monitoring site had reached a height when the WHC predicted wind damage would commence. Subsequent field surveys have indicated that the observed windthrow concurred with that windthrow predicted by the WHC (Quine, 1991).

Soil type	FC Soil code	Percentage of the monitoring site
Intergrade/Iron pan	4b/4p	18%
Peaty gley	6, 6a, 6p	15%
Surface water gley	7	1%
Juncus peat bog	8	2%
Molinia peat bog	9b	62%
Sphagnum/Calluna/Trichophorum/ Eriophorum peat bog	10	2%

Table 3.1 Soil types of Cwm Berwyn Forest wind damage monitoring site (Quine, 1991a), based upon the soil classification developed for British commercial forestry by Pyatt (1982).

3.2.2 Pre-establishment practice

Due to the poor natural drainage, the majority of the site was ploughed, using a variety of ploughs. These included: a single furrow plough; double furrow plough; and a single mouldboard plough (Davies, 1991). This cultivation is usually undertaken to provide raised planting sites and improve subsequent plant establishment and survival (Tabbush, 1988). After ploughing, the entire monitoring area was initially hand-drained and later plough drained in the wetter areas (Davies, 1991). However, site preparation

undertaken prior to planting can restrict root growth which may also lead to windthrow (Section 1.1) (Coutts, 1983; Schaible, 1987; Tabbush, 1988). Field surveys by the Forestry Commission indicated that the poor alignment of main drains, combined with plough furrows not running perpendicular to the slope, resulted in inadequate drainage and ponding in certain sections of the monitoring site. This appeared to have reduced the stability of the stand to wind damage and hence, increased the risk of windthrow (Quine, 1991a).

3.2.3 Tree species

The monitoring site was established predominantly with stands of Sitka spruce (*Picea sitchensis* (Bong.) Carr.) (SS), with some stands of lodgepole pine (*Pinus contorta* var. *Latifolia* Wats.) (LP) and Japanese larch (*Larix kaempferi* (Lamb.) Carr.) (JL) (Figure 3.3). There were also some mixed stands of Sitka spruce and lodgepole pine (SS/LP), and Japanese larch and Sitka spruce (JL/SS).

Sitka spruce is an exotic tree species, introduced into the United Kingdom in 1831 from Oregon and British Columbia by David Douglas, a Scottish botanist and plant collector (Harris, 1978). Sitka spruce derives its common name from a small seaport in southern Alaska and has a natural range stretching through 22^0 latitude, along a narrow coastal strip from Kodiak Island in Alaska to Caspar in Mendocino County, California (Harris, 1978; Mitchell, 1974; Harris, 1990; Savill, 1991). This range is restricted to humid oceanic conditions, usually occurring below 300 m elevation, and characterised by a high moisture requirement and short growing season (Wood, 1955; Harris, 1978).

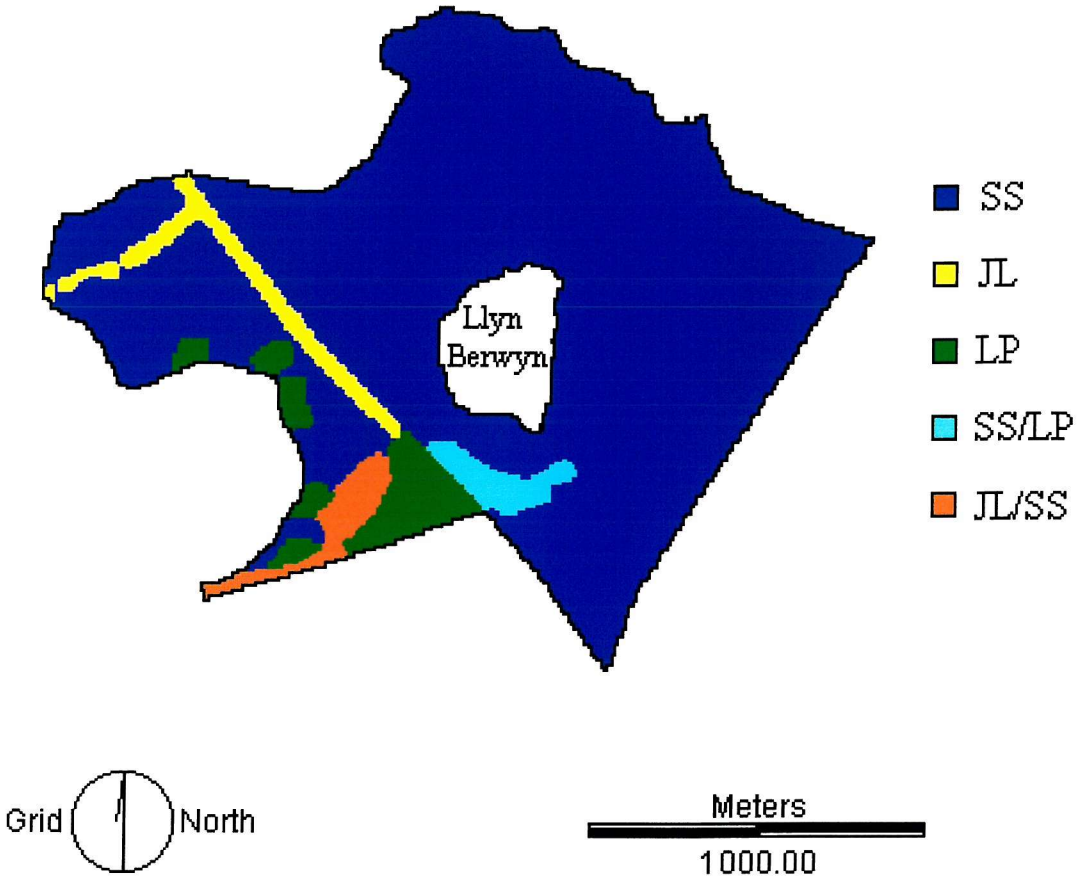

Figure 3.3 Tree species within Cwm Berwyn Forest wind damage monitoring site. Pure stands of Sitka spruce (SS) are represented by dark blue, pure stands of Japanese larch (JL) are represented by yellow, pure stands of lodgepole pine (LP) are represented by dark green, mixed stands of Sitka spruce and lodgepole pine (SS/LP) are represented by light blue and mixed stands of Japanese larch and Sitka spruce (JL/SS) are represented by orange.

Sitka spruce is a very adaptable species, with evidence from early provenance trials indicating that Queen Charlotte Islands provenance is particularly suitable for the UK (Lines, 1978; Savill, 1991). Indeed, the damp soils characteristic of the land upon which upland commercial forests in the British Isles have been established (Section 1.1), such as Cwm Berwyn Forest, are not dissimilar to those found within Sitka spruce's natural range (Day, 1957; Day, 1963).

3.2.4 Post-establishment practice

A major imposition placed upon common silvicultural practice by the wind damage monitoring project, was a restriction on the clearance of wind damaged trees or tidying of any windthrown trees to the nearest windfirm boundary, as newly exposed edges have an increased risk to windthrow (Quine, 1987; Quine *et al.*, 1995). There was no restriction placed upon stand thinning, with approximately 32 ha of the monitoring site thinned during 1986, although two compartments (7270 and 7271) were left as unthinned controls (Figure 3.4). Thinning is perhaps the most useful silvicultural tool available to forest managers and involves the physical removal of a proportion of the trees (Rollinson, 1988b), to provide a variety of financial and economic benefits (Gilliland, 1980; Grayson, 1981; Duthie, 1982). This thinning operation was undertaken about two to three years late which, although financially beneficial, may increase the windthrow risk of the residual standing trees (Grayson, 1981; Harper, 1986; Price, 1989; Moore and Somerville, 1998). The thinning operation within the site was undertaken as a 2:10 systematic motor manual

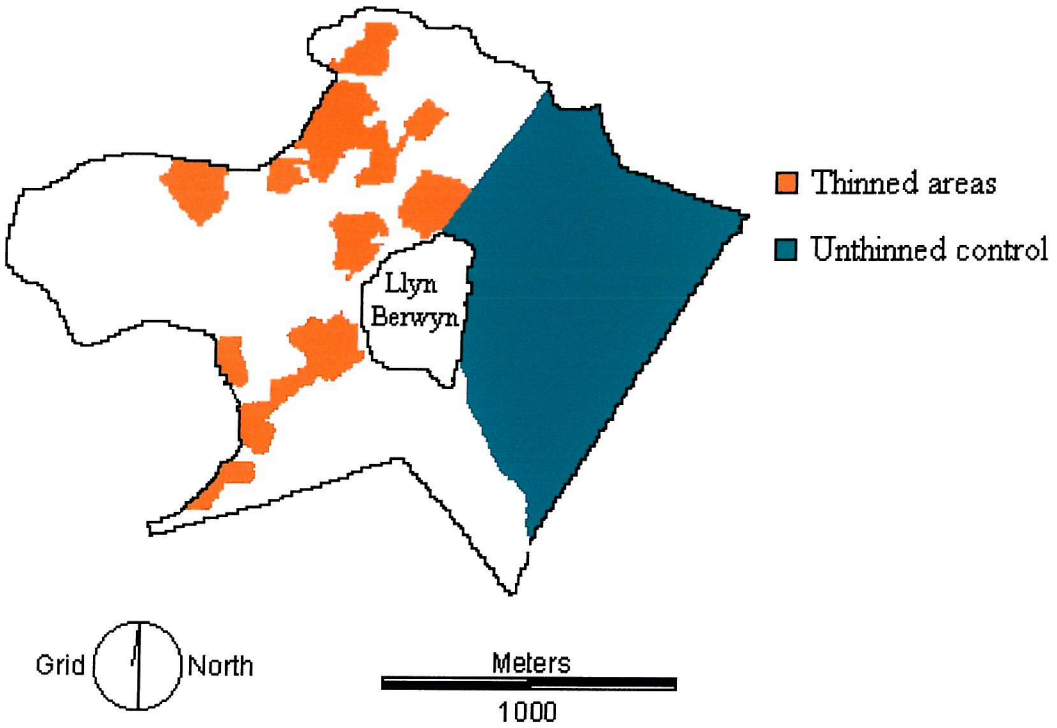

Figure 3.4 Thinned areas and unthinned experimental control within Cwm Berwyn Forest wind damage monitoring site.

line thinning operation, with a feller selected 'tickle' at the edges of the residual rows (Figure 3.5) (Quine, 1997).

3.2.5 Existing windthrown gaps

At the time of the ATM sensor overpass in June 1994, the known windthrown gaps within the monitoring site (Figure 3.6) ranged between 50 to 3000 m^2 in area, representative of typical windthrown gaps found within British forests (Figure 3.7) (Quine and Bell, 1998). The majority of these gaps were located on the boundaries between poor drainage/poor growth areas and well drained/better growth areas. Where the potential for root growth was unrestricted, Sitka spruce root systems will normally penetrate to at least 2 m (Day, 1963). However, the restricted root growth on the site weakened the anchorage component provided by the root systems (Figure 2.2) (Coutts, 1986), causing 'pumping', or movement of the root plate during strong winds. (Quine, 1992). This poor development of the root systems reduces the stability of the trees and increase the vulnerability to windthrow (Section 3.2.2) (Quine *et al.*, 1995; Gardiner, 1997). It has been suggested that such locations may act as windthrown gap initiation sites (Savill, 1983).

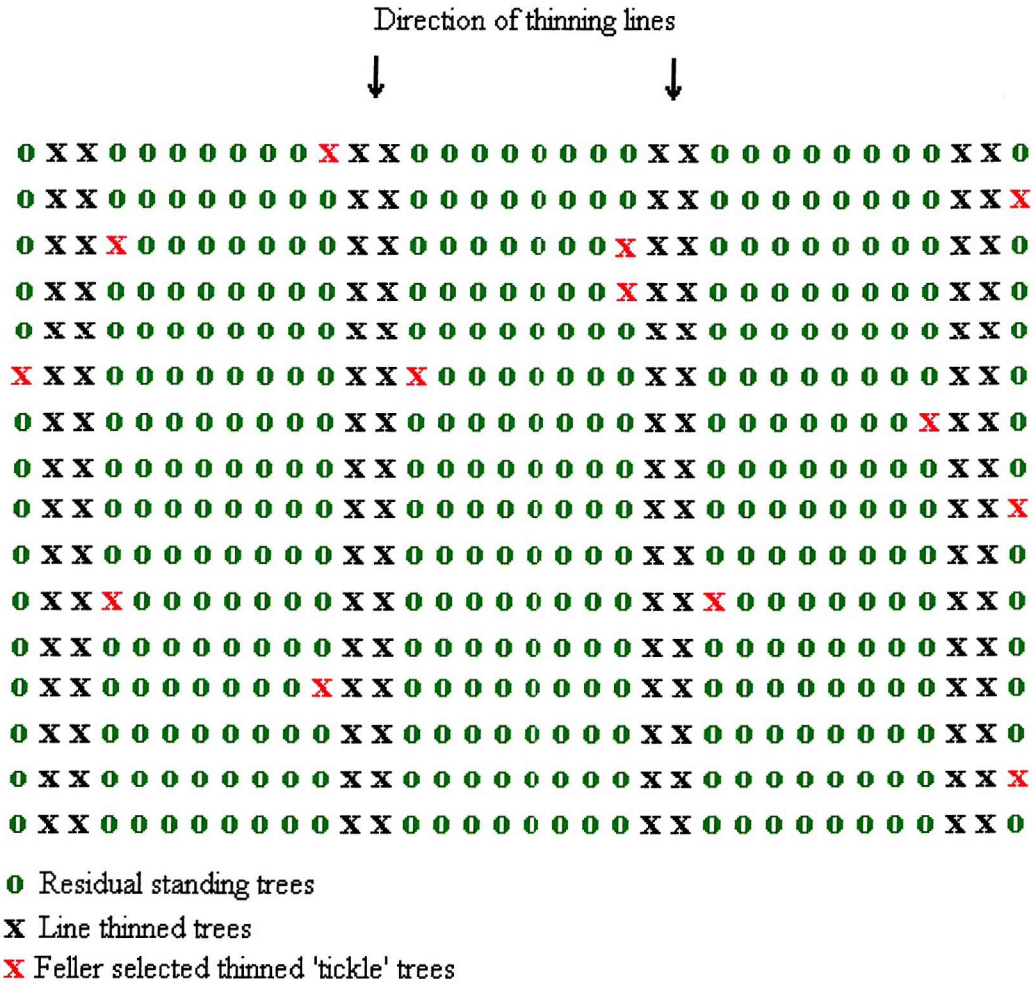

Figure 3.5 A hypothetical stand of trees to illustrate the pattern of line thinning within Cwm Berwyn Forest wind damage monitoring site (Section 3.2.4). This hypothetical stand depicts the residual standing trees remaining after line thinning, the lines of trees systematically removed during thinning (2 rows of trees in every in 10 rows) and the number of additional 'tickle' trees selected by the feller also removed during thinning.

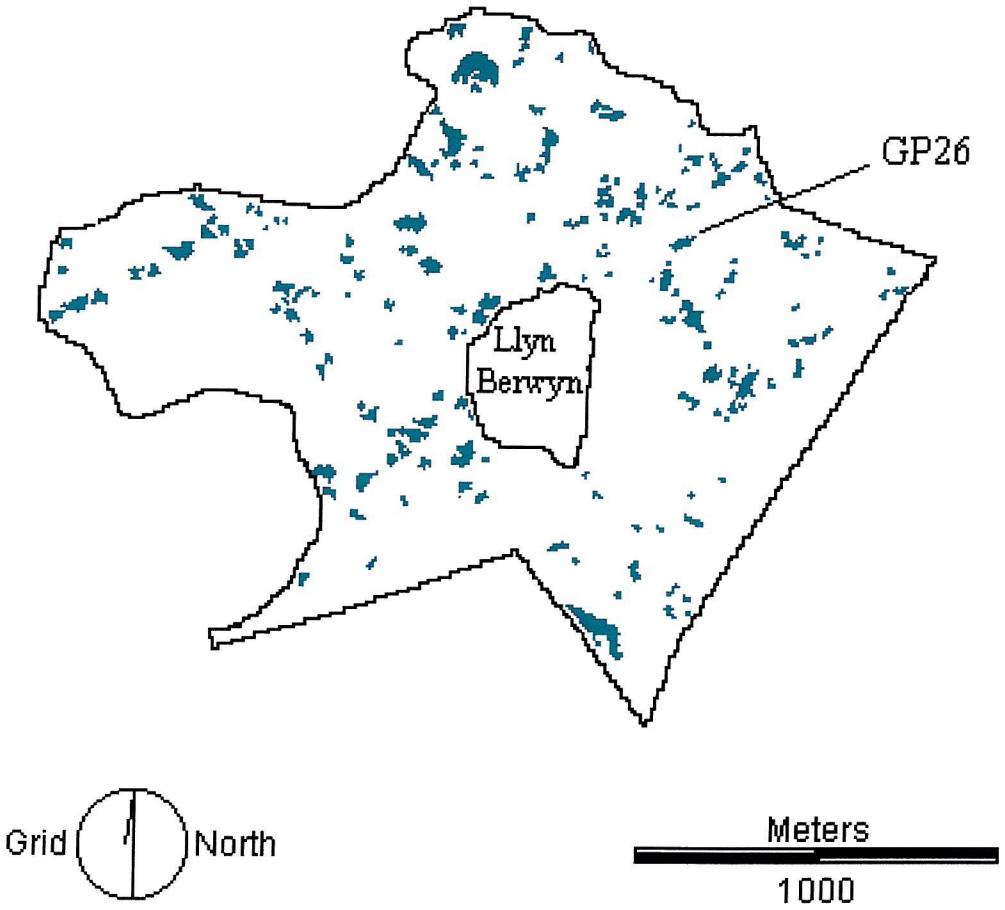

Figure 3.6 Windthrown gaps present within Cwm Berwyn Forest wind damage monitoring site interpreted by the Forestry Commission from aerial photographs acquired in 1994. The sample windthrown gap, GP26, examined in Chapter 7 is indicated.

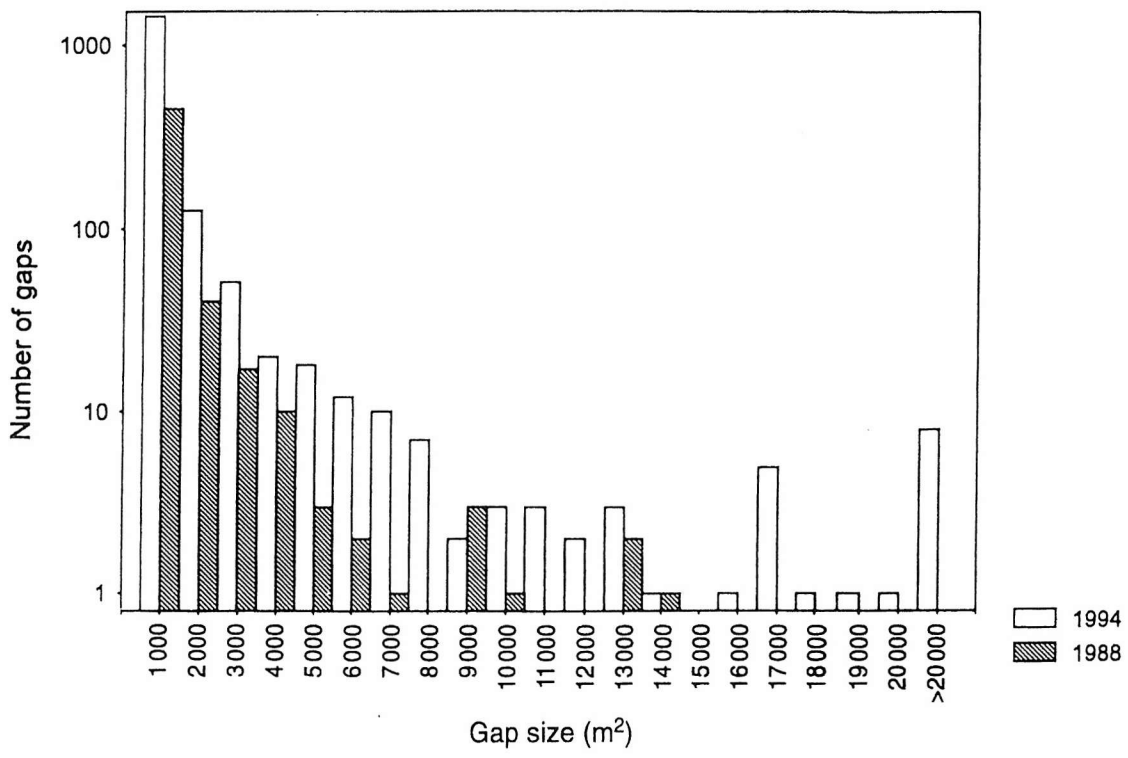

Figure 3.7 Windthrown gap size frequency distribution in 1988 and 1994 for all Forestry Commission wind damage monitoring sites (Quine and Bell, 1998).

3.3 REMOTELY SENSED DATA ACQUISITION

3.3.1 ATM sensor

The remotely sensed data were acquired using an ATM sensor (Wilson, 1997), in April 1994, as part of the 1994 Natural Environment Research Council (NERC) airborne campaign (Table 3.2) (Figure 3.8). The ATM sensor is a passive multispectral line scanner which records data in eleven spectral wavebands from the visible to the thermal infrared sections of the electromagnetic spectrum, including 7 bands which spectrally simulate those used by the Landsat TM sensor (Table 3.3) (Richards, 1993; Wilson, 1995; Wilson, 1997). The ATM sensor also records in a twelfth waveband which is identical to waveband 11, except that it has a gain setting half that of waveband 11 (Hunting Geology and Geophysics, 1985; Wilson, 1988). The gain setting (Appendix 1), is a multiplication factor which is applied to each individual waveband independently, to maximise the sensitivity of the sensor for each flight.

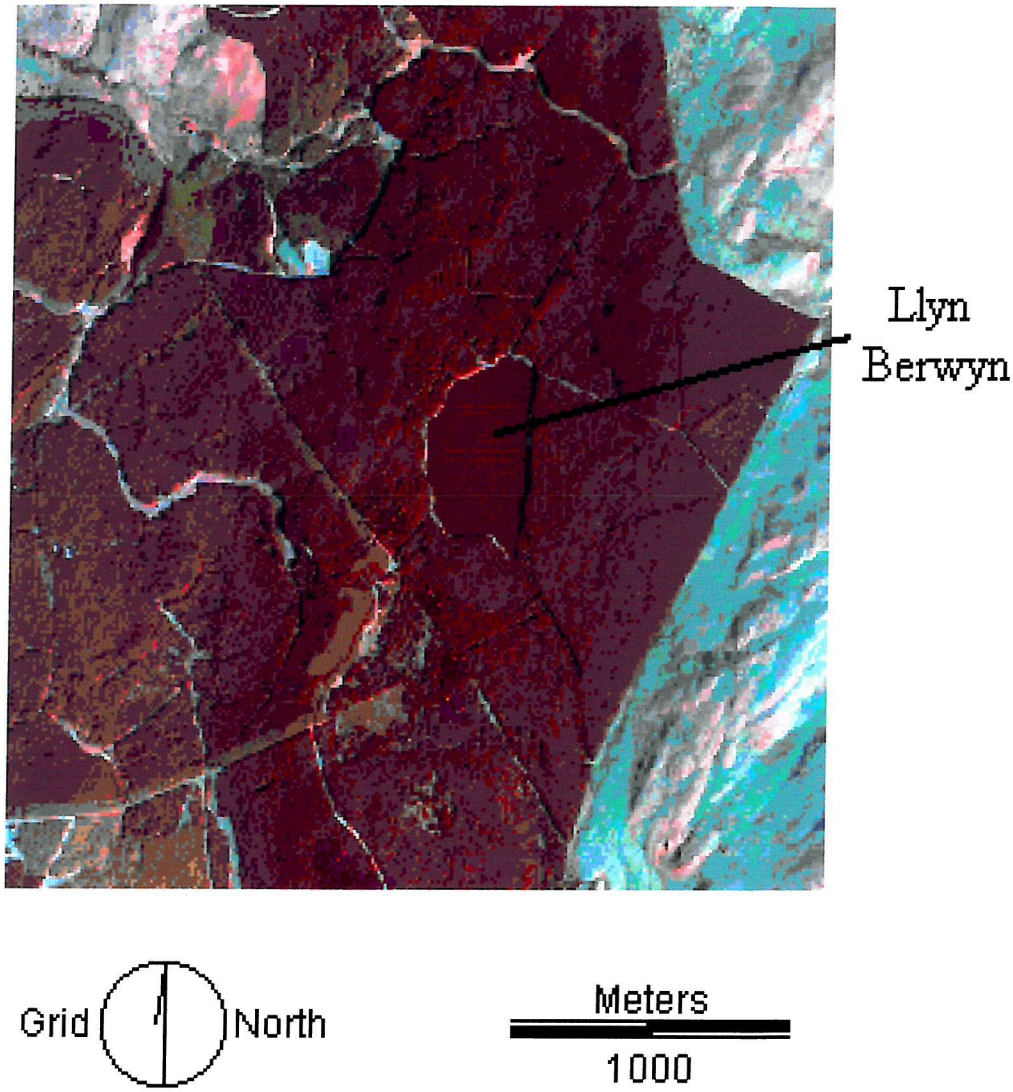

Figure 3.8 Raw ATM data of Cwm Berwyn Forest wind damage monitoring site, displayed as a colour composite of wavebands 3, 5 and 11 (see Table 3.3). The location of Llyn Berwyn lake is indicated. (Note: stripes within the data are the result of the colour repreduction)

Location	Llyn Brianne
Date	18 April 1994
Flight line reference	NERC 93/3 Run 5
Aircraft ground clearance	2000 m
Aircraft speed	150 knots
Image size	3164 rows x 716 columns
Spatial resolution	≃ 4 m
Instantaneous field of view (IFOV)	2.50 mrad
Field of view (FOV)	90^{0}
Dynamic range	8 bit

Table 3.2 Summary of ATM flight line information for the remotely sensed data used in subsequent work.

ATM waveband	Waveband edges (nm)	Description	Landsat TM waveband spectrally simulated
1	420-450	visible blue	
2	450-520	visible blue	1
3	520-600	visible green	2
4	605-625	visible red	
5	630-690	visible red	3
6	695-750	near infrared	
7	760-900	near infrared	4
8	910-1050	near infrared	
9	1550-1750	short-wave infrared	5
10	2080-2350	short-wave infrared	7
11	8500-13000	thermal infrared	6
12	8500-13000	thermal infrared	6

Table 3.3 ATM waveband specification, indicating the waveband range, description and Landsat TM waveband spectrally simulated of each ATM waveband (Hunting Geology and Geophysics, 1985; Wilson, 1988; Wilson, 1995; Wilson, 1997).

3.3.1.1 Data acquisition

The ATM sensor consisted of a scanning mirror which acquired data in a scan line perpendicular to the direction of aircraft flight. As a result, the ATM sensor is also known as an across-track (whiskbroom) multispectral scanning system. The ATM sensor spectrally filtered the collected spectral radiance for each waveband and recorded the electrical signal in an analogue form. These data were pre-amplified and sent to an analogue-to-digital conversion unit, which converted radiance intensity to a DN, subsequently stored as eight-bit (one byte) resolution data with a 0 to 255 DN intensity range (Wilson, 1995). The data were stored during aircraft flight on high density digital tape (HDDT). They were later transferred and stored in standard band interleaved by line (BIL) format on computer compatible tape (CCT), to permit access by conventional computer hardware (Hunting Geology and Geophysics, 1985).

3.3.1.2 Data distortion

The remotely sensed data acquired by the ATM sensor were distorted both laterally and in the direction of aircraft travel. Tangential scale distortion is caused by the sensor scanning mirror rotating at a constant angular velocity whilst the remotely sensed data is recorded at a constant linear rate (Richards, 1993; Campbell, 1996; Lillesand and Kiefer, 2000). This leads to compression of the data towards the edges of each scene and linear features which are not parallel or normal to the scanning direction take on an S-shaped sigmoid curvature (Lillesand and Kiefer, 2000). The ATM sensor electronically corrected for this by varying the digitising scan rate with respect to the scan angle, termed S-bend

correction (Wilson, 1997). However, this leads to over-sampling towards the edges of each scene.

There was also distortion within the data caused by aircraft roll, pitch, yaw and change in velocity (Figure 3.9) (Campbell, 1996; Wilson, 1997; Mather, 1999; Lillesand and Kiefer, 2000). The ATM sensor had a gyroscope device which allowed it to correct for aircraft roll of +/- 15 ^{0} (Wilson, 1995; Wilson, 1997). However, pitch and yaw cannot be electronically compensated for by the ATM sensor, although yaw can be minimised by avoiding data collection during cross-winds and pitch is usually minor enough to be ignored. NERC has subsequently included the ATM sensor within a new sensor package, termed integrated data system (IDS), to provide remotely sensed data with improved geometric characteristics (Wilson, 1997).

3.3.1.3 Spatial resolution

The spatial resolution of a sensor is difficult to define (Mather, 1999). It can be considered to be the smallest object which can be distinguished from its surroundings by a sensor (Lillesand and Kiefer, 2000). The most commonly applied measure of spatial resolution is the instantaneous field of view (IFOV) (Mather, 1999). This is the sensor view angle within which the sensor records reflectance at any instant in time and is based upon the geometric properties of the sensor (Campbell, 1996; Mather, 1999; Lillesand and Kiefer, 2000). This measure is loosely related to the ground resolution element, which is the area on the ground that contributes to the reflectance recorded by the sensor at any instant in time (Lillesand and Kiefer, 2000). The ground resolution element is, therefore,

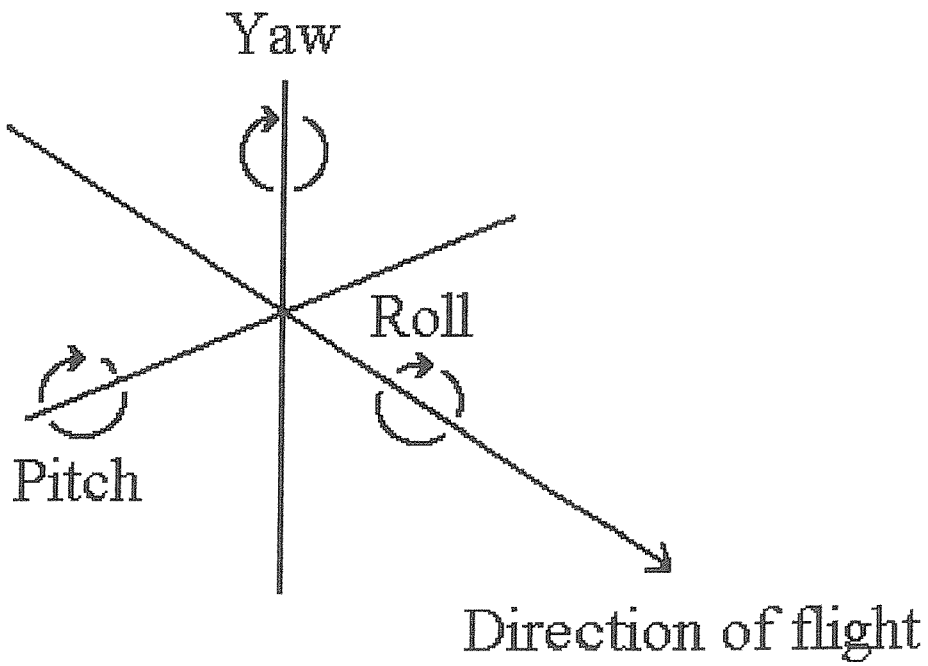

Figure 3.9 Pitch, roll and yaw associated with aircraft flight (adapted from Mather (1999)).

the IFOV projected onto the ground and changes with sensor view angle and the altitude of the platform carrying the sensor (Richards, 1993; Atkinson and Curran, 1995). The ground resolution element at a nadir sensor view is often cited as an alternative measure of a sensors spatial resolution. However, the spatial resolution of a sensor is not the same as the pixel size (Figure 3.10) (Mather, 1999). The reflectance recorded by a sensor is sampled to produce discrete measurements which are represented by pixels (Richards, 1993).

The ATM has an IFOV of 2.50 mrad (Table 3.2) and the remotely sensed data were acquired from a height above ground level of approximately 2000 m. The resulting pixel size of $\simeq$ 4 m is comparable to that that of data acquired from new fine (< 5 m) spatial resolution satellite sensors (Section 2.6.1.1.3) (Aplin *et al.*, 1997; Lillesand and Kiefer, 2000).

3.3.1.4 Radiometric calibration

Radiometric calibration of ATM data is usually undertaken to convert the DN of each pixel to radiance (Equation 3.1) and, for data acquired by most sensors, based upon a linear radiometric response function using reference data for each individual waveband (Appendix 1) (Lillesand and Kiefer, 2000). The ATM sensor was regularly radiometrically calibrated for wavebands 1 to 10 by NERC, using a lamp and a barium sulphate reflectance panel. Waveband 11 was calibrated at the beginning and end of each scan line using two blackbody thermal reference sources contained within the ATM sensor, whose temperatures were adjusted to cover the range of temperature values within the scene.

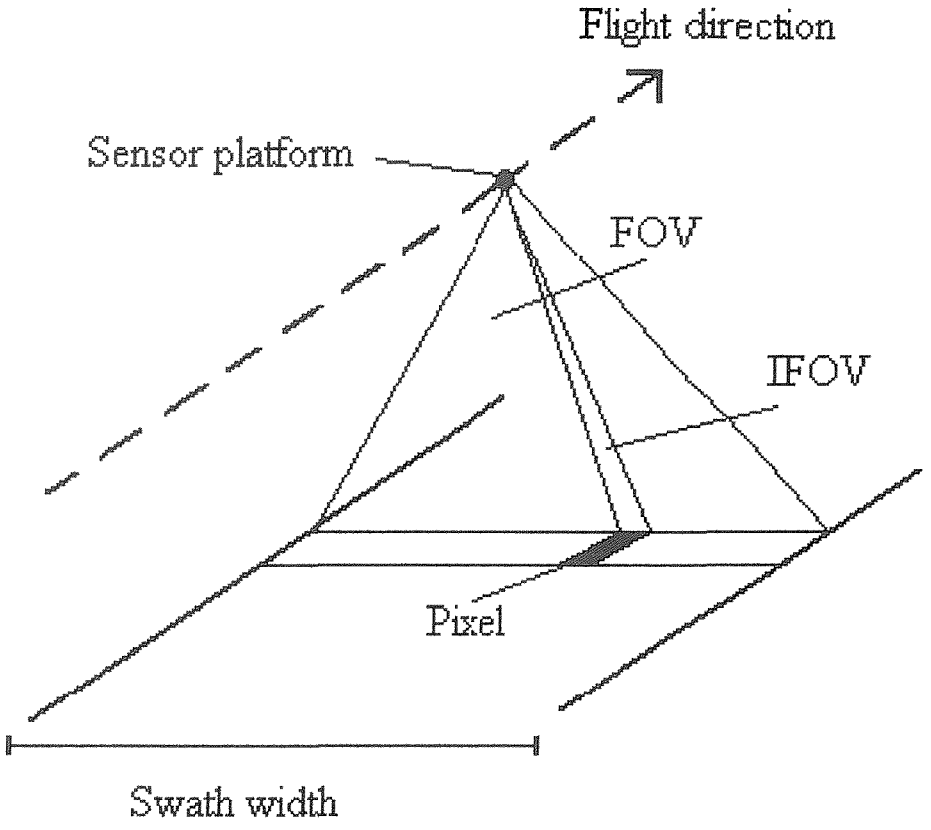

Figure 3.10 Geometry of a pixel (adapted from Richards (1993)). The FOV is the angle over which data are recorded, the IFOV is the angle for a given altitude within which the sensor records data at any instant in time and the swath width is the distance on the ground equivalent to 1 scan line (Richards, 1993; Mather, 1999; Lillesand and Kiefer, 2000).

$$\text{Radiance } (mWm^{-2}sr^{-1}nm^{-1}) = \text{Waveband gain} * (\text{DN} - \text{Waveband base}) \quad 3.1$$

Where: waveband gain = slope of the response function; and waveband base = intercept of the response function (Lillesand and Kiefer, 2000).

3.4 REFERENCE DATA ACQUISITION

To assess the accuracy of landcover mapping using remotely sensed data, reference, or ground data were used (Barrett and Curtis, 1999; Buckland and Elston, 1994; Lillesand and Kiefer, 2000). The reference data used in subsequent analyses comprises data acquired through conventional field surveys and from the manual interpretation of aerial photographs.

3.4.1 Forestry Commission's reference data

The Forestry Commission's Research Division established a database of stand data based upon detailed field survey data collected at sample plots located throughout the monitoring site (Quine, 1989). The objective was to collect stand and site data which could be related to the location and area estimates of wind damage obtained from the manual interpretation of aerial photography collected annually since 1988. The monitoring site was initially stratified into relatively homogeneous sub-populations, before 0.01 ha circular sample plots were marked out. A systematic grid system based upon known site features was used to determine sample plot location, rather than a north-south and east-west alignment. These sample plots were distributed at 100 m intervals, resulting in a sample plot density of one sample plot per ha. These sample plots were permanently

marked using stakes in order to be easily located during future field surveys. The accurate locations of the sample plots were determined using a global positioning system (GPS) and offset survey techniques using compass and tape (Quine *et al.*, 1997). However, this was found to be costly, in terms of time and labour (Quine *et al.*, 1997).

Within each sample plot, stand data such as: yield class; top height; plant spacing within and between furrows; diameter at breast height (dbh); annual top height increment; planting year; and stocking density were recorded (Quine, 1988; Quine, 1989). Data on wind speed and direction were also recorded, based upon measurements collected from tatter flags (Mackie and Gough, 1994) and by automatic wind logging instruments. These data were stored by the Forestry Commission within a raster based geographic information system (GIS). Wind damaged trees encountered during field surveys were recorded and classified by the Forestry Commission according to Quine (1992):

- **Leaning** The lean is due to displacement of the root system and the tree is not significantly supported by neighbouring stems.
- **Hung-up** The lean is due to displacement of the root system, with neighbouring stems providing physical support and prevent the tree falling further.
- **Fallen** Horizontal or near horizontal position where roots have failed, neighbouring stems are not holding the tree up, but branch contact with the ground or another fallen tree may prevent lying completely flat.
- **Snapped** Breakage of stem below lowest green whorl.
- **Broken-top** Breakage of stem above the lowest green whorl.

3.4.2 Forestry Commission's aerial photography data

To complement the field survey data, monitoring of the formation and development of windthrown gaps was based primarily upon the manual interpretation of annual aerial photographs taken at a 1:10000 scale (Figure 3.11). Aerial photography acquired in July 1994 was used to derive reference data on windthrown gaps present within the monitoring site when the ATM data were acquired. The Forestry Commission's interpreted windthrown gaps were plotted onto acetate sheets and then digitised as vector data. These vector data were used as the reference data for subsequent analysis and have been used by the Forestry Commission to generate raster data with a pixel size, or spatial resolution, of 10 m by 10 m within a GIS (Quine and Bell, 1998). This vector-to-raster conversion process using a spatial resolution 10 m was undertaken by the Forestry Commission in order to reduce the volume of the reference data due to limited computer storage facilities. However, this process has the disadvantage of simplifying the boundary and shape of polygon data initially stored as vector data (Bettinger *et al.*, 1996). This 10 m raster data described the windthrown gaps present at the site and has been used by the Forestry Commission as the basis for monitoring the formation and dynamics of windthrown gaps within upland forest ecosystems and for investigating site factors which may influence windthrow.

Visual comparison between the vector data and the 10 m raster data indicated that many of the smallest windthrown gaps were lost during the vector-to-raster conversion process at this 10 m spatial resolution. The Forestry Commission's vector data for each year the wind damage monitoring has been undertaken were used to generate raster data

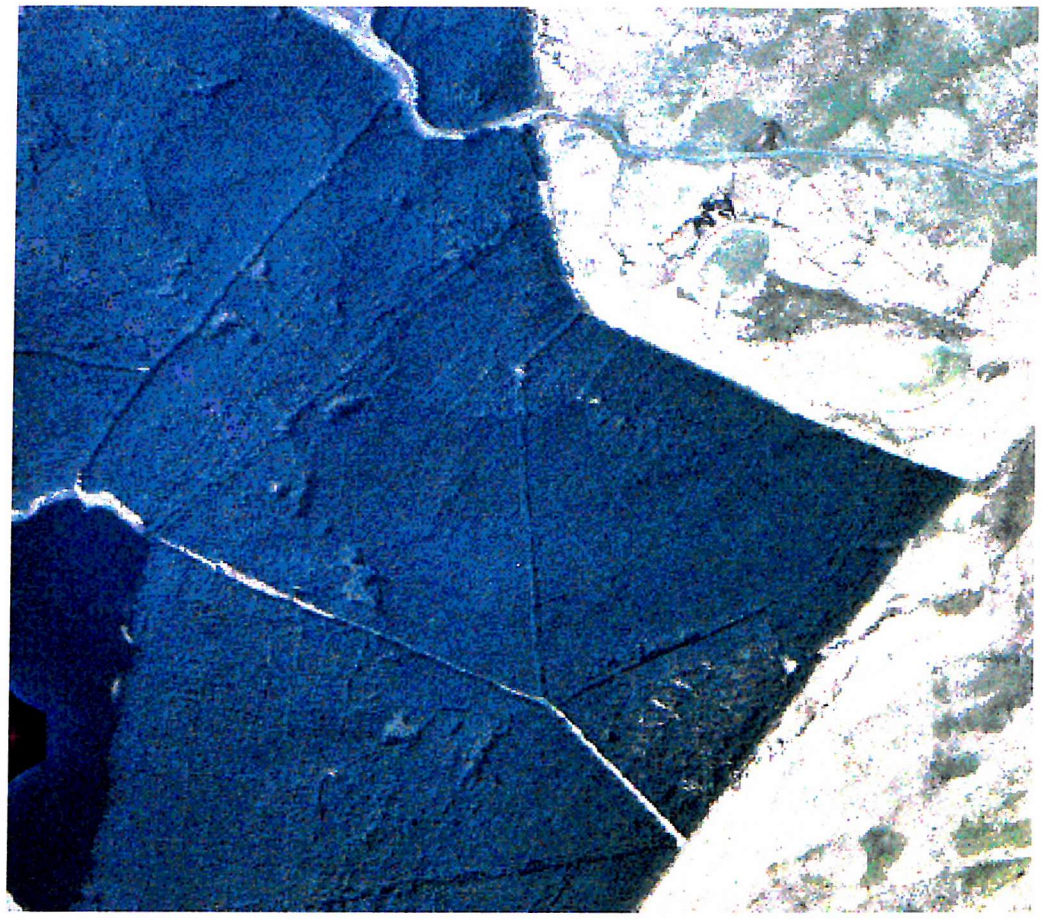

Figure 3.11 Colour aerial photograph of compartment 7271within Cwm Berwyn Forest wind damage monitoring area. Llyn Berwyn lake is located in the lower left corner of the photograph. (Note: the apparent blue colour of the forest canopy is the result of the colour reproduction)

with spatial resolutions of 1 m and 10 m. Figure 3.12 shows the total estimated area of windthrown gaps with respect to the year the aerial photographs were acquired and the spatial resolution. The graph suggests that the use of raster data at either 1 m or 10 m spatial resolution, has little effect upon estimates of total windthrown gap area, although at 1 m spatial resolution, the raster data more accurately represent the vector data. Figure 3.13 shows the total estimated windthrown gap perimeter with respect to the year the aerial photographs were acquired and the spatial resolution. This figure suggests that spatial resolution has a noticeable influence upon the ability to accurately estimate the perimeter of the windthrown gaps. This supports the suggestion made by Bettiner *et al.* (1996), that the boundary and shape of polygons within vector data are simplified by a vector-to-raster conversion process and influenced by the spatial resolution. This may explain why the windthrown gap perimeter estimates derived from the 10 m raster data underestimated the windthrown gap perimeter estimates derived from the 1 m raster data.

Since the Forestry Commission have been primarily concerned with total estimates of windthrown gap areas, raster data with a spatial resolution of 10 m, derived from the vector data, are satisfactory for their purposes. However, work based upon windthrown gap boundaries is likely to require raster data with a spatial resolution finer than 10 m. In addition, the spatial resolution of the ATM data ($\simeq$ 4 m) used throughout subsequent work was much finer than this reference raster data. Therefore, the original vector data used to generate the Forestry Commission's 10 m raster data, were used to produce new raster data with an enhanced spatial resolution of 1 m. These 1m spatial resolution raster data only

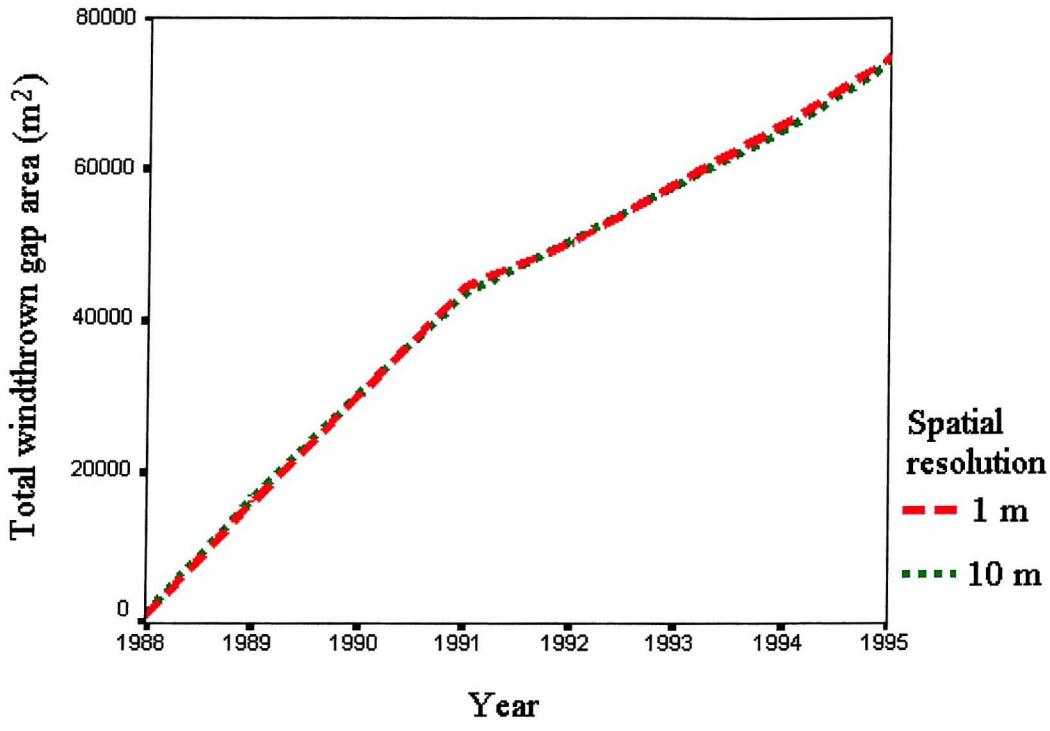

Figure 3.12 Graph representing the total estimated area of windthrown gaps within the Cwm Berwyn wind damage monitoring site for each year aerial photographs were acquired (Note: no aerial photographs were acquired in 1993, so the value for the total area of windthrown gaps in that year has been interpolated). The spatial resolutions (1 m and 10 m) are those used for the vector-to-raster conversion of the Forestry Commission's vector data. The Forestry Commission used a spatial resolution of 10 m, whilst a spatial resolution of 1m was used to generate the reference raster data for subsequent analysis.

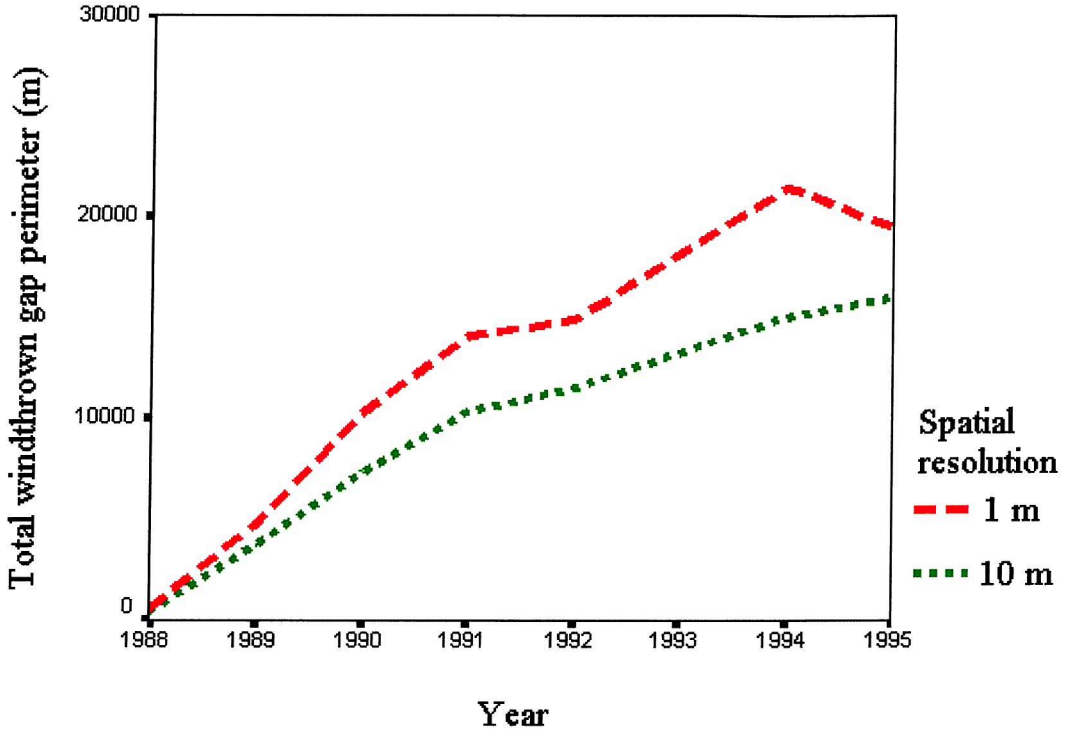

Figure 3.13 Graph representing the total estimated perimeter of windthrown gaps within the Cwm Berwyn wind damage monitoring site for each year aerial photographs were acquired (Note: no aerial photographs were acquired in 1993, so the value for the total perimeter of windthrown gaps in that year has been interpolated). The spatial resolutions (1 m and 10 m) are those used for the vector-to-raster conversion of the Forestry Commission's vector data. The Forestry Commission used a spatial resolution of 10 m, whilst a spatial resolution of 1m was used to generate the reference raster data for subsequent analysis.

were used as the reference data in subsequent analysis. This achieved a balance between data volume and the accuracy of the windthrown gap representation within the reference data.

3.4.3 Assessing the accuracy of the Forestry Commission's data

Analyses were undertaken to determine whether the manual interpretation of the aerial photography provided an accurate representation of the windthrown gaps present within the monitoring site. Estimates of windthrown gap areas derived from the reference data were verified against windthrown gap area estimates acquired from a field survey in September 1997. Despite the three year interval between the acquisition of the reference data and the field survey, a strong relationship would suggest that the reference data provided an accurate representation of the known windthrown gaps present in the monitoring site in 1994. Due to the ease of physical access and because it was part of the no-thinning control, hence the windthrown gaps identified from the interpretation of the aerial photographs could not be confused with thinning racks (Figure 3.4), compartment 7271 (Figure 3.2) was used.

Gap area can be estimated during field surveys in a number of ways. For example, in terms of spherical co-ordinates, from the top of the leading shoot of a tree sapling in the centre of the gap to its boundary, measured as the angle from the vertical and the distance in the eight principal compass directions (Brokaw, 1982b; Brokaw, 1985; Canham, 1988; Canham, 1988b; Canham *et al.*, 1990). However, the most widely used method is to estimate gap area as the area of an octagon, whose corners are located where the eight

principal points of the compass meet the boundary of the gap (Figure 3.14) (Spies *et al.*, 1990; Dahir and Lorimer, 1996).

Due to the physical impracticalities and the unacceptable risk of injury associated with working within windthrown gaps (Section 2.5), windthrown gap area estimates were based upon closed compass traverse survey (Avery and Burkhart, 1994; Bondesson *et al.*, 1998), using successive distance and compass bearing measurements taken of the gap-canopy boundary. Field measurements of the windthrown gaps were based upon the assumption that there was a discrete gap-canopy boundary. As the ATM sensor was looking near vertically down at the gaps, windthrown gap area was defined on the ground as the area directly under the physical canopy opening (Runkle, 1990). Previous research has taken this 'drip line', the projected crown edge of trees bordering the gap on the gap side to represent a 'canopy gap' boundary (Figure 2.4) (Section 2.5) (Runkle, 1981; Spies *et al.*, 1990; Dahir and Lorimer, 1996; Gray and Spies, 1996; Cadenasso *et al.*, 1997; Hughes and Bechtel, 1997). However, determining where this occurred in the gaps made this approach impractical in this field survey. Instead, the stem of the boundary trees on the gap side, the 'expanded gap' boundary (Figure 2.4) (Section 2.5), was used to represent the gap-canopy boundary (Runkle, 1981). This extended gap boundary was used in subsequent field surveys, however, it includes an area underneath the canopy of the gap-canopy boundary trees and, therefore, should slightly overestimate windthrown gap area, compared with the estimates derived from the aerial photographs (Figure 2.4).

Since new gaps have formed since 1994, measurements of gap area were only taken from known windthrown gaps in 1994 (Figure 3.6). Due to the presence of these

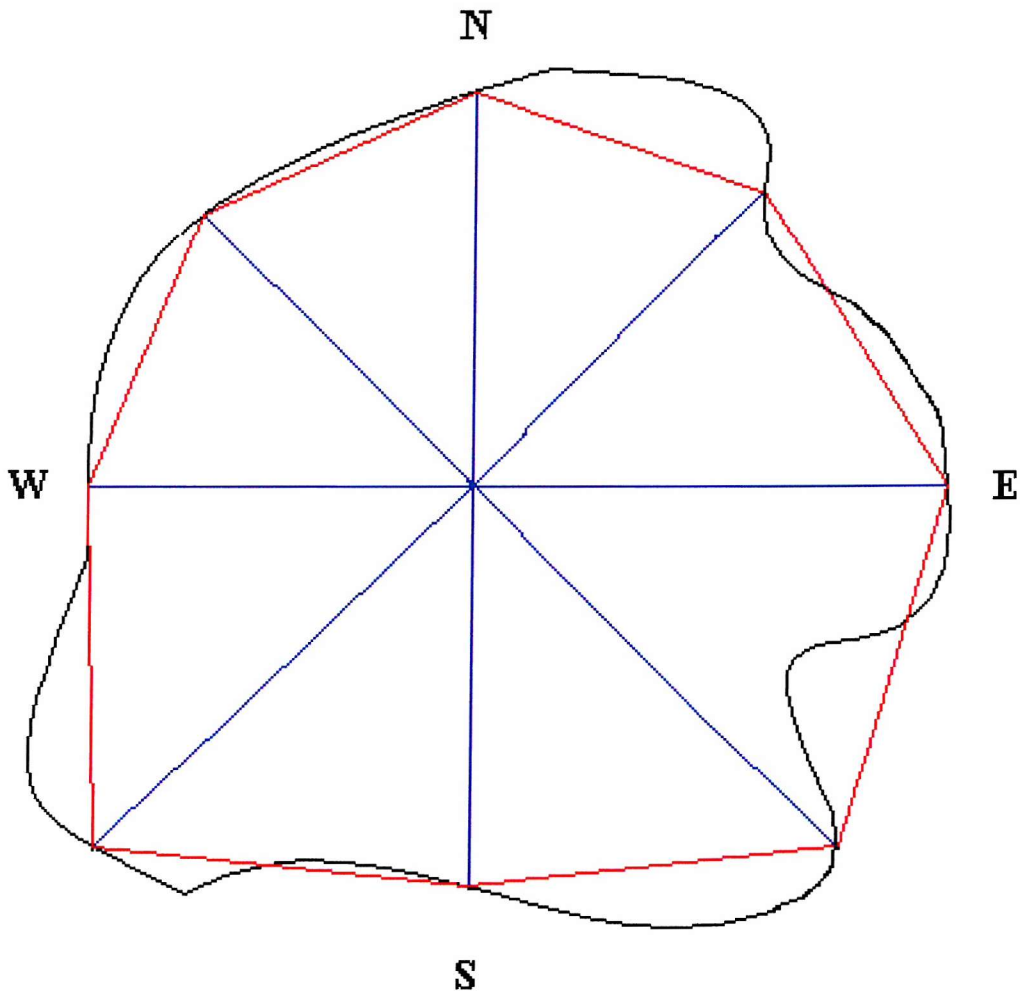

Figure 3.14 A hypothetical boundary of a gap (represented by the black line), illustrating the method for estimating gap area (e.g. Spies *et al.*, 1990; Dahir and Lorimer, 1996), based upon the area of an octagon, whose corners are located where the 8 principal compass points extrapolated from the gap centre (represented by the blue lines) meet the gap edge. The red line depicts the boundary of the octagon.

additional windthrown gaps formed since 1994, it was only possible to accurately locate and survey 26 windthrown gaps in the field. Marking a starting tree on the gap boundary with biodegradable tape, the compass bearing and distance to the next boundary tree was measured, working systematically in the same direction until the starting tree was reached. These bearing and distance measurements were drawn out on graph paper using a 1:100 scale. Estimates of windthrown gap area were derived from these scale drawings using a planimeter. Each gap had three estimates of area derived using this method and the average of the three estimates used. This was undertaken to smooth out any minor errors which may have occurred during boundary tracing.

Comparison of the areal estimates of the windthrown gaps derived from the reference data (Appendix 2) and from field survey indicated a very strong and significant degree of correlation ($r = 0.99$, $P > 0.01$). The field survey estimated gap areas were generally greater than the corresponding areas estimated from the aerial photographs, as was anticipated. This may also have been attributed to gap expansion through progressive wind damage during the three year period between aerial photograph and field survey data acquisition. However, 4 gaps out of the 26 appeared to have decreased in area. These 4 gaps were located in regions of the compartment where the canopy was heterogeneous and possibly led to the photographic interpreter misrepresenting the gap-canopy boundary. These results indicated that the reference data were satisfactory and accepted as providing an accurate representation of the known windthrown gaps present within the monitoring site at the time the ATM data were acquired.

3.5 SUMMARY

The Cwm Berwyn Forest site selected to conduct research is part of a series of sites used by the Forestry Commission to monitor wind damage to forests. The site is representative of forests in the British Isles which are at significant risk from wind damage, particularly in the form of windthrow. The site contains a size range of windthrown gaps, typical of those found throughout forests in the British Isles. The ATM data upon which subsequent research is based, were acquired in 1994. Aerial photographs, acquired four months after the ATM data, were interpreted and derived data stored as 1 m raster data. These were used as the reference data for subsequent analysis.

CHAPTER 4

REMOTELY SENSED DATA CALIBRATION, CORRECTION AND CLASSIFICATION

4.1 INTRODUCTION

This Chapter describes common methodology used in subsequent work. Specifically, it describes how the ATM data were radiometrically calibrated, corrected for geometric distortions and the classification methods used to allocate pixels to classes. Prior to this calibration, correction and classification, the data were initially inspected to identify whether there was any unwanted disturbance, such as banding, which would have necessitated additional data processing.

4.2 RADIOMETRIC CALIBRATION

The ATM data were radiometrically calibrated to convert the DN of each pixel in wavebands 1 to 10 to radiance (Section 3.3.1.4) (Wilson, 1988) using reference data supplied by Natural Environment Research Council (NERC) (Appendix 1). The radiometric calibration of waveband 11 is unlike that of wavebands 1 to 10, as thermal calibration must be undertaken for each individual scan line recorded by the sensor (Hunting Geology and Geophysics Limited, 1985; Wilson, 1988). Difficulties in determining the required procedure resulted in the calibration of waveband 11 not being

undertaken, although waveband 11 was retained for subsequent analysis. As temporal comparison with other data sets was not required and measures of radiance were not to be related with specific properties of features within the data, radiometric calibration was not essential for subsequent analysis (Mather, 1999; Lillesand and Kiefer, 2000).

4.3 ATMOSPHERIC CORRECTION

The remotely sensed data recorded by the ATM sensor are distorted by atmospheric scattering (Section 2.6.1.2) (Richards, 1993; Campbell, 1996). The effects of this atmospheric distortion within the ATM data can be corrected by undertaking an atmospheric correction. However, atmospheric correction of the ATM data was not essential for subsequent analysis as: a) a ratio of pixel values between wavebands was not required, b) measures of radiance were not to be related with specific properties of features within the data and c) temporal comparison between data sets was not required (Mather, 1999). Therefore, atmospheric correction of the ATM data was not undertaken, but if required, atmospheric correction may be achieved by subtracting an estimate of atmospheric path radiance (each estimate is waveband specific as atmospheric scattering is wavelength dependent) for the relevant waveband (Richards, 1993; Huguenin *et al.*, 1997; Mather, 1999; Lillesand and Kiefer, 2000).

One procedure (Richards, 1993; Mather, 1999; Lillesand and Kiefer, 2000) assumes that for each waveband within the ATM data, there are some pixels which have pixel values close to 0 (e.g. regions in shadow). Atmospheric scattering will add a constant value to each of these pixels. Using histograms of each waveband, the lowest

pixel value will approximately represent the atmospheric path radiance for that waveband. This waveband specific value is then subtracted from the appropriate waveband for each pixel.

4.4 GEOMETRIC CORRECTION

The ATM data were corrected to remove geometric distortions (Section 3.3.1.2) (Richards, 1993). Geometrically correcting the ATM data prior to classification, although not essential, made it possible to use the reference data depicting windthrown gap location (Section 3.4.2) to aid in the classification training process (Richards, 1993).

The geometric correction was based on a transformation so that the ATM data had both the scale and projection properties of a map (Mather, 1999). This required easily identifiable ground control points (GCPs), which could be accurately located both on the ATM data and on an Ordnance Survey (OS) map (Campbell, 1996; Mather, 1999). A sample of 30 GCPs is usually satisfactory (Mather, 1999). However, in order to achieve comprehensive coverage and account for the moderate relief of the monitoring site (Section 3.2.1), a total of 49 GCPs were distributed throughout the ATM data (Mather, 1999). The ATM data were geometrically registered to the UK national grid using a second order polynomial transformation (Equation 4.1), due to the moderate relief of the monitoring site (Section 3.2.1) (Mather, 1999). To preserve the statistical properties of the data, they were resampled with a nearest neighbour algorithm, which selects the pixel whose centre is nearest the given location (Richards, 1993; Campbell, 1996; Huguenin *et al.*, 1997; Mather, 1999; Lillesand and Kiefer, 2000).

$$u = a_0 + a_1 g + a_2 h + a_3 gh + a_4 g^2 + a_5 h^2 \quad 4.1a$$

$$v = b_0 + b_1 g + b_2 h + b_3 gh + b_4 g^2 + b_5 h^2 \quad 4.1b$$

Where: (g, h) is the location of the pixel on an OS map; (u, v) is the location of the pixel within the ATM data; and *a* and *b* are coefficients (Richards, 1993).

This geometric transformation resulted in an estimated RMSE of 1.76 pixels. This RMSE was larger than desired, despite the exclusion of potential GCPs with a large RMSE (e.g. Mather, 1999). It was not possible to further reduce this RMSE associated with the geometric transformation. However, since the ATM data are not required to be compared with other data by overlay comparison (e.g. for change detection), this larger than desired RMSE did not appear to represent a significant problem for subsequent analyses.

This RMSE may be a partly due to the effects of tree shadow which made the positioning of the GCPs within the ATM data difficult. In addition, it is common forest management practice not to plant trees right up to the field boundaries which are marked on OS maps, as open space is often left for machinery access, or to increase the visual diversity of the forest landscape (Lucas, 1991). Therefore, the grid reference for GCPs derived from an OS map may not accurately describe the planted forest boundary. In the absence of contrary evidence, the OS map used was assumed to provide an accurate representation of the landcover.

It may be possible to increase the accuracy of the geometric correction by using a GPS to acquire more accurate spatial locations of GCPs. However, in forests such as

Cwm Berwyn, with a high stocking density and a relatively uniform canopy, there are limitations to the use of GPS technology (Quine *et al.*, 1997). These arise primarily from poor sky view and multi-path errors (Lawrence *et al.*, 1995; Courteau, 1996; Quine *et al.*, 1997; Darche and Forgues, 1998; Firth and Brownlie, 1998). It may be possible to use telescopic poles to improve the sky view, or offset survey using directions and distances (Lawrence *et al.*, 1995; Quine *et al.*, 1997). However, under conditions similar to Cwm Berwyn Forest, the use of GPS to accurately locate reference points is slow and costly (Quine *et al.*, 1997), and was not a practical option to possibly reduce the RMSE associated with the geometric correction.

4.5 CLASSIFICATION

Classification of remotely sensed data is used to extract information by allocating each pixel to a particular class based upon a decision rule (e.g. Equation 4.2) (Section 2.6.2) (Richards, 1993; Lillesand and Kiefer, 2000).

4.5.1 Maximum-likelihood classification

The classification method used in subsequent analyses is the per-pixel maximum-likelihood classification. This is the most commonly used supervised image classification method (Section 2.6.2) (Richards, 1993). Assuming equal prior probabilities, this classification method allocates each pixel within the remotely sensed data to the class for which it had the highest posterior probability (or likelihood) of membership ($P(i \mid x)$) (Equation 4.3) (Foody *et al.*, 1992, Richards, 1993). This method

can be described as 'hard', as each pixel is allocated to a discrete, mutually exclusive class (Section 2.6.2) (Trodd *et al.*, 1989; Atkinson and Cutler, 1996; Foody, 2000). The output from this hard classification is a thematic map, representing the landcover class to which each pixel has been allocated.

$$x \in i \text{ if } P(i|x)\,P(i) > P(j|x)\,P(j) \text{ for all } j \neq i \qquad 4.2$$

Where: $P(i|x)$ is the posterior probability of pixel x belonging to class i and is derived from sample data (see Equation 4.3); and $P(i)$ is the prior probability for class i.

$$P(i|x) = P(x|i) \,/\, {}^{C}\Sigma_{j=1}\, P(x|j) \qquad 4.3$$

Where: $P(x|i)$ is the probability density function of pixel x in class i (see Equation 4.4); C is the total number of classes.

$$P(x|i) = 2\pi^{-0.5p}\, |S_i|^{-0.5} \exp\left[-0.5 \left((x - m_i)^t S_i^{-1} (x - m_i) \right) \right] \qquad 4.4$$

Where: S_i is the variance-covariance matrix for class i; $|S_i|$ is the determinant of S_i; $(x - m_i)^t S_i^{-1} (x - m_i)$ is the Mahalanobis squared distance; and p is the number of wavebands.

4.5.2 Softened classification

The allocation of a pixel to only one class through the use of a conventional hard classification, such as maximum-likelihood, is suited for the classification of pure pixels representing landcover classes which the classifier has been trained to recognise (Section 2.6.2) (Foody, 2000). Softening the output from a maximum-likelihood classification may

provide a more realistic representation of landcover (Foody, 1996b; Foody, 1998). The maximum-likelihood classification generates information that can be used to derive surrogate measures of the relative proportion of each component class within each pixel (Trodd *et al.*, 1989; Wang, 1990; Foody and Trodd, 1993). This may be achieved by outputting posterior and/or typicality probabilities which can be used to measure the degree of multiple and partial class membership (Campbell, 1984; Trodd *et al.*, 1989; Wang, 1990; Foody and Trodd, 1990). These probabilities are usually output as probability maps, with each map representing the probability of membership to an individual class.

4.5.2.1 Posterior probability

Assuming each class has an equal prior probability of occurrence (Mather, 1999), the posterior probability of pixel x belonging to a specific class i ($P(i|x)$) (Equation 4.2) is calculated as the probability density function of the pixel to that class (Equation 4.4), relative to the sum of the probability densities to all the classes (Equation 4.3) (Klecka, 1980; Campbell, 1984; Foody *et al.*, 1992; Foody and Trodd, 1993). Posterior probabilities provide a relative measure of class membership strength for each pixel to each class which, over all classes, sums to unity for each pixel (Klecka, 1980; Foody *et al.*, 1992; Foody and Trodd, 1993).

4.5.2.2 Typicality probability

A typicality probability is derived from the Mahalanobis squared distance (D^2) (Cox, 1968; Campbell, 1980; Mather, 1999), used in the maximum-likelihood classification (Equation 4.4). D^2 is a measure of the distance between the centroid of a specific class i and an individual pixel x (Healy, 1968; Klecka, 1980; Foody *et al.*, 1992; Mather, 1999). A typicality probability is calculated by referring the D^2 to the chi-square distribution with p degrees of freedom (where p = the number of wavebands used) (Cox, 1968; Klecka, 1980; Campbell, 1984). A typicality probability represents an absolute measure of an individual pixel belonging to a specific class, independent of all other classes. Hence, the sum of all the typicality probabilities to an individual pixel does not have to sum to unity like posterior probabilities (Klecka, 1980).

4.6 SUMMARY

Subsequent analysis is based upon remotely sensed ATM data which have been radiometrically calibrated and geometrically corrected prior to classification. The output from a hard classification is a thematic map representing the class to which each pixel is allocated and the output from a softened classification are probability maps, each map representing the probability of membership to an individual class.

CHAPTER 5

THE INFLUENCE OF SPATIAL RESOLUTION AND CLASSIFICATION METHOD ON WINDTHROWN GAP AREA ESTIMATES

5.1 INTRODUCTION

To date the main source of remotely sensed data available for the monitoring of wind damage within forests have been aerial photographs acquired from airborne platforms. These photographs represent a useful data source, however, their value is limited by factors, such as platform stability, inherent to all airborne sensor systems (Wilson, 1997). An alternative is to use satellite sensor systems, such as SPOT HRV and Landsat TM. However, these satellite sensors have generally provided remotely sensed data at a spatial resolution that is similar to, or coarser than the size of windthrown gaps (Section 3.2.5), typically between 10 m (SPOT HRV sensor in panchromatic mode) and 30 m (Landsat TM sensor, except in thermal waveband). Several new satellite sensing systems capable of acquiring data with a fine (< 5 m) spatial resolution comparable to current airborne sensors have been developed (Aplin *et al.*, 1997; Lillesand and Kiefer, 2000). These new satellite sensors now provide remotely sensed data that have a spatial resolution appropriate for studying windthrown gaps.

5.2 CHAPTER AIMS

This Chapter aims to use ATM data to simulate and evaluate the spatial resolution available from relatively new satellite sensors, as well as the spatial resolution that is available from conventional satellite sensors such as Landsat TM and SPOT HRV, to provide information on typical windthrown gaps found within British forests. In particular, this Chapter aims to address three questions:

- Is it possible to identify windthrown gaps present within remotely sensed data over a range of spatial resolutions from ≃ 4 m to 30 m?
- Is it possible to accurately estimate the area of windthrown gaps over the range of spatial resolutions from ≃ 4 m to 30 m using a conventional hard classification method?
- Is it possible to increase the accuracy of estimates of windthrown gap area by softening the output from the conventional hard classification method?

5.3 STUDY SITE

Compartment 7271 of the monitoring site was selected (Figure 3.2). This 39 ha compartment was established within a single planting season and, as part of the unthinned control (Figure 3.4), had not undergone any operation which would affect the structure of the canopy at the time the ATM data were acquired. This compartment contained a number of windthrown gaps which were representative of the size range found within the

monitoring site (50 m^2 to 3000 m^2) and, indeed, throughout British forests (Figure 3.7) (Quine and Bell, 1998).

5.4 METHODOLOGY

This Section aims to review the process used to extract information from the ATM data in order to assess the influence of spatial resolution (Section 2.6.2) and classification method upon windthrown gap identification and accuracy of windthrown gap area estimates.

5.4.1 Pre-processing

Pre-processing of ATM data is usually undertaken prior to classification in order to correct for radiometric and geometric distortions in the data and to eliminate unwanted elements of the data (Richards, 1993; Campbell, 1996; Mather, 1999; Lillesand and Kiefer, 2000). The ATM data were not radiometrically calibrated prior to classification in this Chapter as the calibration reference data required (Section 3.3.1.4 and Appendix 1) were not available at the time this work was undertaken. However, this did not represent a significant problem as radiometric calibration of the data was not essential for analysis (Section 4.2). However, geometric correction of the ATM data was undertaken as discussed in Section 4.4 to remove geometric distortions prior to classification (Richards, 1993). This was undertaken to aid in the classification training process (Richards, 1993).

5.4.1.1 Spatial degradation

To evaluate the influence of spatial resolution on the ability to identify windthrown gaps and accurately estimate their areas, the ≃ 4 m ATM data were spatially degraded. This was undertaken using the nearest neighbour resampling algorithm (Section 4.4), to simulate current satellite sensor data with spatial resolutions of 10 m (SPOT HRV in panchromatic mode), 20 m (SPOT HRV in multi-waveband mode) and 30 m (Landsat TM, except in waveband 6 where the spatial resolution is 120 m). This method for simulating current satellite sensor data is crude because it makes no allowance for factors such as point spread function, but it does provide a general means for approximating the spatial resolutions of the remotely sensed data available (Woodcock and Strahler, 1987).

5.4.1.2 Selection of class training data

The ATM data of compartment 7271 were dominated by a relatively homogeneous Sitka spruce canopy interrupted by windthrown gaps and with moorland surrounding the afforested area. The smallest windthrown gaps (≃ 50 m^2) consisted largely of windthrown trees in shadow, whilst the largest windthrown gaps (≃ 2500 m^2) contained some windthrown trees illuminated and some in shadow. The spectral response from sample pixels were selected to represent the 'pure' reflected response for four thematic classes: small windthrown gaps (dominated by leaning trees which were in shadow); large windthrown gaps (dominated by fallen trees some illuminated and some in shadow); (unbroken) canopy; and moorland. Using the reference data depicting the locations of known windthrown gaps (Figure 3.6), it was possible to select sample pixels for each of

these four classes from within the ≃ 4 m ATM data. Mather (1999) suggested that the minimum sample for any class should be 30 times the number of wavebands used for a maximum-likelihood classification, although this will be dependent on the variability of the data. As the ATM sensor used 11 wavebands, the ideal minimum sample for each class was 330 randomly located and independent pixels.

There were a relatively small number of potential pixels which represented the windthrown gaps from which a sample had to be selected. As the windthrown gaps occupied small areas relative to the entire remotely sensed data set, contiguous sample pixels were chosen in order to acquire as large a sample size as possible. These sample pixels will, therefore, be spatially autocorrelated. Ideally, individual random sample pixels should be selected from throughout the area to be classified. Although not used in this Chapter, geostatistical techniques could be used to assess the degree of spatial autocorrelation within the remotely sensed data and this information then used to determine the optimum sampling strategy for selecting sample pixels for each class (Webster *et al.*, 1989; Atkinson, 1996; Curran and Atkinson, 1998).

For the two 'windthrown' classes (i.e. small windthrown gaps dominated by leaning trees which were in shadow and large windthrown gaps dominated by fallen trees which were illuminated and in shadow), 126 and 297 sample pixels were selected respectively. The transformed divergence measure (Richards, 1993; Mather, 1999; Lillesand and Kiefer, 2000) was used as a statistical index of class separability, with calculated values scaled to a range between 0 and 2000. The value of 1600, suggested by Mather (1999), was used as the threshold above which there is good separability between

classes. A transformed divergence value of 0 would indicate that the probability distributions of class are equal (Mather, 1999). A transformed divergence value of 1500 was obtained from the comparison of the probability distributions of small and large windthrown classes. As a result, these 2 windthrown classes were spectrally similar and subsequently amalgamated to form a single windthrown class. The resulting three classes (generated from 423, 1620 and 1287 sample pixels from the windthrown, canopy and moorland classes respectively) were used in subsequent classification and satisfied the recommended minimum sample number (30 pixels per waveband) (Mather, 1999).

As the spatial resolution of the data became coarser, it became increasingly difficult to accurately select sample pixels which represented a 'pure' windthrown class, due to the increasing quantity of mixed pixels within the data (Foody and Curran, 1994; Foody, 1996b; Foody *et al.*, 1996). When it is not possible to determine class responses from pure pixels, it is often necessary to estimate the responses from mixed pixels (Spanner *et al.*, 1989; Hlavka and Spanner, 1995). It is, however, usually not practical to accurately determine the contents of a mixed pixel. As an alternative, the potential to use the original responses generated from the $\simeq$ 4 m ATM data to classify the data at the coarser spatial resolutions was evaluated. Separate sample pixels were selected from each of the 10, 20 and 30 m spatial resolution data sets to represent the canopy class at each spatial resolution.

Using the transformed divergence threshold value of 1600 suggested by Mather (1999), the transformed divergence values (values of 171, 202 and 1300 derived from pairing the canopy response derived from $\simeq$ 4 m ATM data, with responses derived from

10 m, 20 m and 30 m spatial resolution data respectively) indicated that the responses for the canopy at all 4 spatial resolutions were spectrally similar. Therefore, the three thematic class responses (i.e. windthrown, moorland and canopy) generated from the ≃ 4m ATM data were used to classify the data at each spatial resolution.

5.4.1.3 Feature selection

Strong inter-correlations between the 11 wavebands of the ATM sensor (Table 5.1) suggested that information was being duplicated (Campbell, 1996; Mather, 1999) and a feature selection was undertaken to remove those wavebands, which contributed little to class separability. By selecting only the most discriminating wavebands, it was possible to reduce both data volume and computational time required to undertake a classification, without incurring any significant loss of information (Richards, 1993; Campbell, 1996; Mather, 1999; Bruzzone and Serpico, 2000). There are a number of distance measures which can be used as a statistical index of class separability (Richards, 1993; Mather, 1999; Lillesand and Kiefer, 2000) and hence, determine the optimum waveband selection. Transformed Divergence was used to evaluate the separability of each class and hence, select the most discriminating wavebands (Richards, 1993; Mather, 1999).

Waveband	1	2	3	4	5	6	7	8	9	10	11
1	1.000										
2	0.950	1.000									
3	0.893	0.969	1.000								
4	0.859	0.955	0.987	1.000							
5	0.848	0.941	0.980	0.994	1.000						
6	0.835	0.810	0.895	0.860	0.863	1.000					
7	0.796	0.739	0.828	0.786	0.791	0.987	1.000				
8	0.803	0.758	0.845	0.809	0.815	0.979	0.990	1.000			
9	0.818	0.867	0.925	0.925	0.927	0.876	0.827	0.864	1.000		
10	0.667	0.722	0.715	0.706	0.701	0.615	0.577	0.605	0.717	1.000	
11	0.788	0.762	0.794	0.755	0.750	0.842	0.838	0.852	0.828	0.692	1.000

Table 5.1 Correlation matrix for the 11 ATM wavebands, depicting the Pearson correlation coefficient, *r*, for each waveband from a 100 x 100 pixel sub-scene from the ATM data representing moorland vegetation.

Townshend (1984) suggested that an optimal selection of Landsat TM wavebands for discrimination of cover types should be limited to three or four wavebands and include visible, near-infrared and middle- or far-infrared wavebands. Transformed divergence was used to select the four most discriminating ATM wavebands. The results indicated that the use of wavebands 3 (visible green), 5 (visible red), 7 (near-infrared), and 11 (thermal infrared) provided the optimum separability between the three classes. These four wavebands only were used in subsequent work.

5.4.2 Classification

The ATM data were classified using the methodology described in Section 4.5. The maximum-likelihood classification process resulted in a number of classified products: a thematic map depicting the hard classification output; posterior probability maps (one map for each class depicting the posterior probability to that class); and typicality probability maps (one map for each class depicting the typicality probability to that class).

5.4.3 Hard classification accuracy assessment

As a guide to the quality of the maximum-likelihood classification, accuracy assessment was undertaken using an error matrix (Table 5.2). For this 450 pixels independent of the sample pixels used for the generation of the class responses (Section 5.4.1.3) were randomly selected from within the thematic map and the allocated class of each pixel was compared against the class depicted in the reference data. This satisfied the minimum sample number of 50 samples for each class recommended by Congalton (1991) (i.e. 150 pixels in total for the 3 classes assessed). The three class thematic map of the site appeared to provide an accurate representation of the classes (Table 5.2), with an overall classification accuracy of 93.8 % correct class allocation and the Kappa coefficient (0.89) indicated that the classification was 'excellent' (Montserud and Leamans, 1992). This accuracy assessment was only undertaken on the $\simeq$ 4 m ATM hard classified output, as the large number of mixed pixels within the coarser spatial resolution data sets made direct comparison with the reference data set difficult.

		Reference data			
		Windthrown	Canopy	Moorland	Total
Classified data	Windthrown	59	16	0	75
	Canopy	7	231	1	239
	Moorland	0	4	132	136
	Total	66	251	133	450

Producer's Accuracy
Windthrown = (59 / 66) * 100 = 89.4 %
Canopy = (231 / 251) * 100 = 92.0 %
Moorland = (132 / 133)* 100 = 99.3 %

User's Accuracy
Windthrown = (59 / 75) * 100 = 78.7 %
Canopy = (231 / 239) * 100 = 96.6 %
Moorland = (132 / 136) * 100 = 97.1 %

Overall classification accuracy = ((59 + 231 + 132) / 450) * 100 = 93.8 %
Overall Kappa coefficient of agreement = 0.89

Table 5.2 Classification error matrix and accuracy statements (percentage correct allocation and Kappa coefficient of agreement) (Story and Congalton, 1986; Congalton, 1991) for the maximum-likelihood classification of the ≃ 4 m ATM data. The Producer's accuracy, a measure of error of omission, is the probability of a reference pixel being correctly classified. The User's accuracy, a measure of error of commission, is the probability that a classified pixel actually represents that class in the reference data.

Although the probability of a reference windthrown pixel being correctly classified was 89.4 %, the probability that a classified windthrown pixel actually represents a windthrown pixel in the reference data was only 78.7 %. These measures of errors of omission and commission, reported in Table 5.2, suggested that there was confusion in discriminating between the windthrown and canopy classes. The errors of commission are partly due to regions of the compartment with wider than normal tree spacing (≃ 1.8 m), associated with drainage ditches, or poor growth, being identified and allocated to the windthrown class by the classifier (Figure 5.1). It would be possible to reduce these errors by applying a low-pass filter, which would also have the effect of highlighting contiguous blocks of

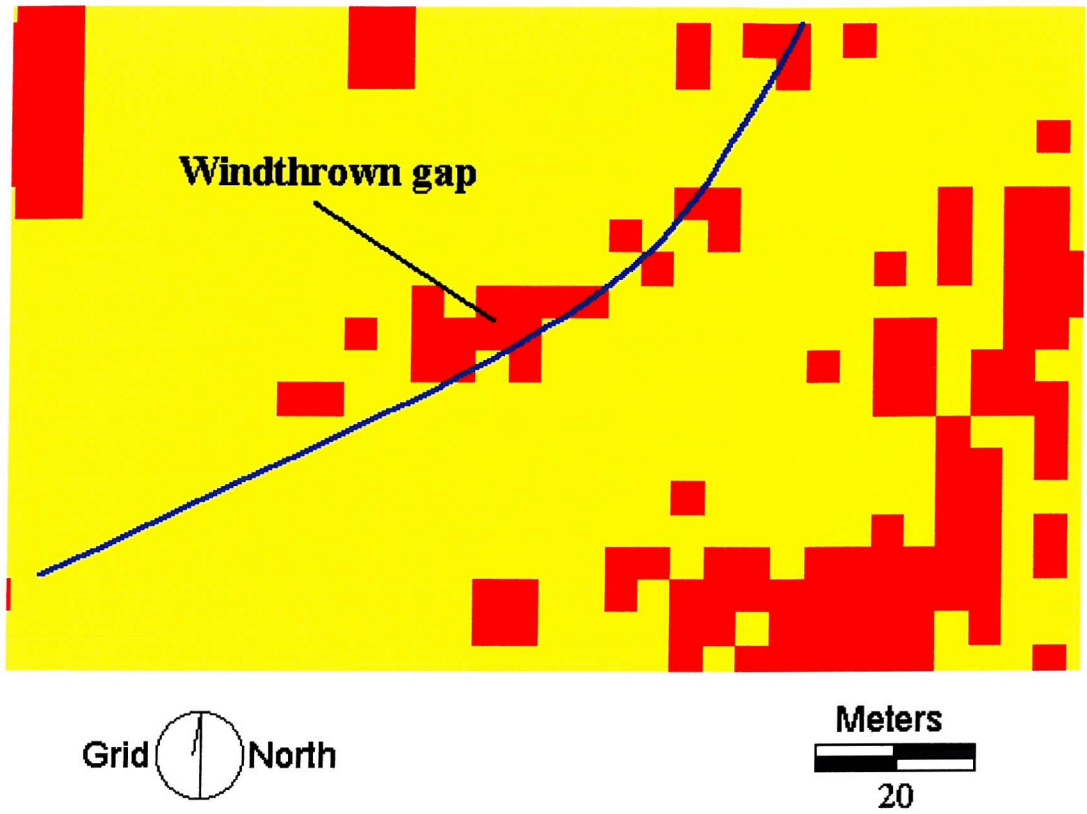

Figure 5.1 Extract from the hard classification of the ≃ 4 m ATM data illustrating classification error. Pixels allocated to the windthrow class are red and pixels allocated to the canopy class are yellow. The blue line represents the approximate position of a drain line, where tree spacing is greater than elsewhere. Note that a number of pixels allocated to the gap class, outwith the windthrown gap indicated, appear to be located in relation to the drain line. This illustrates a possible explanation for the classification errors reported in Table 5.2.

pixels classified as windthrown. However, this would remove single windthrown pixels which represent small windthrown gaps.

5.4.4 Hard classification windthrown gap identification

Within compartment 7271 (Figure 3.2), 54 known windthrown gaps were present. The thematic map, depicting hard classification output, was analysed to evaluate the ability to identify windthrown gaps present, by direct comparison with the reference data. The largest gaps effectively contained moorland and, therefore, the windthrown and moorland classes were amalgamated to form a single 'gap' class for analysis. If a pixel classified as gap (i.e. windthrown or moorland) was located at the centre of the windthrown gap within the reference data, then the hard classification identified that windthrown gap.

5.4.5 Estimation of windthrown gap areas

The ability to estimate accurately windthrown gap area has important ramifications for the management of wind damage within upland forests. For example, estimates of wood volume damaged by winter storms and the subsequent planning of harvesting and restocking operations are routinely made based upon area estimates derived from aerial photographic interpretation. Therefore, the accuracy of windthrown gap area estimates was investigated over a range of spatial resolutions and fine spatial resolution remotely sensed data would appear to be the most appropriate data, in terms of windthrown gap representation.

5.4.5.1 Hard classification windthrown gap area estimation

Initial analysis was undertaken to evaluate the potential of the hard maximum-likelihood classification approach to estimate windthrown gap areas over the range of spatial resolutions. The approximate centre point of each windthrown gap was identified within the reference data. If this was located within a contiguous cluster of pixels that had been allocated by the classification to a gap class (i.e., windthrown or moorland), the area of each pixel within the cluster was summed to estimate total gap area (e.g. Crapper, 1980). For example, a contiguous cluster of 4 pixels allocated as gap within the classified 10 m spatial resolution data would represent an estimated gap area of 400 m^2 (Figure 5.2).

However, within a contiguous cluster of gap pixels representing a large gap, there were pixels allocated to the canopy class. These canopy pixels represented a row of standing trees within the gap (Figure 5.3), but were included within the windthrown gap as a generalisation during the manual interpretation of the aerial photography and recorded as such within the reference data. As these canopy pixels were bounded within the cluster of gap pixels, they were interpreted as contributing to the windthrown gap areal estimate for comparison with the reference data.

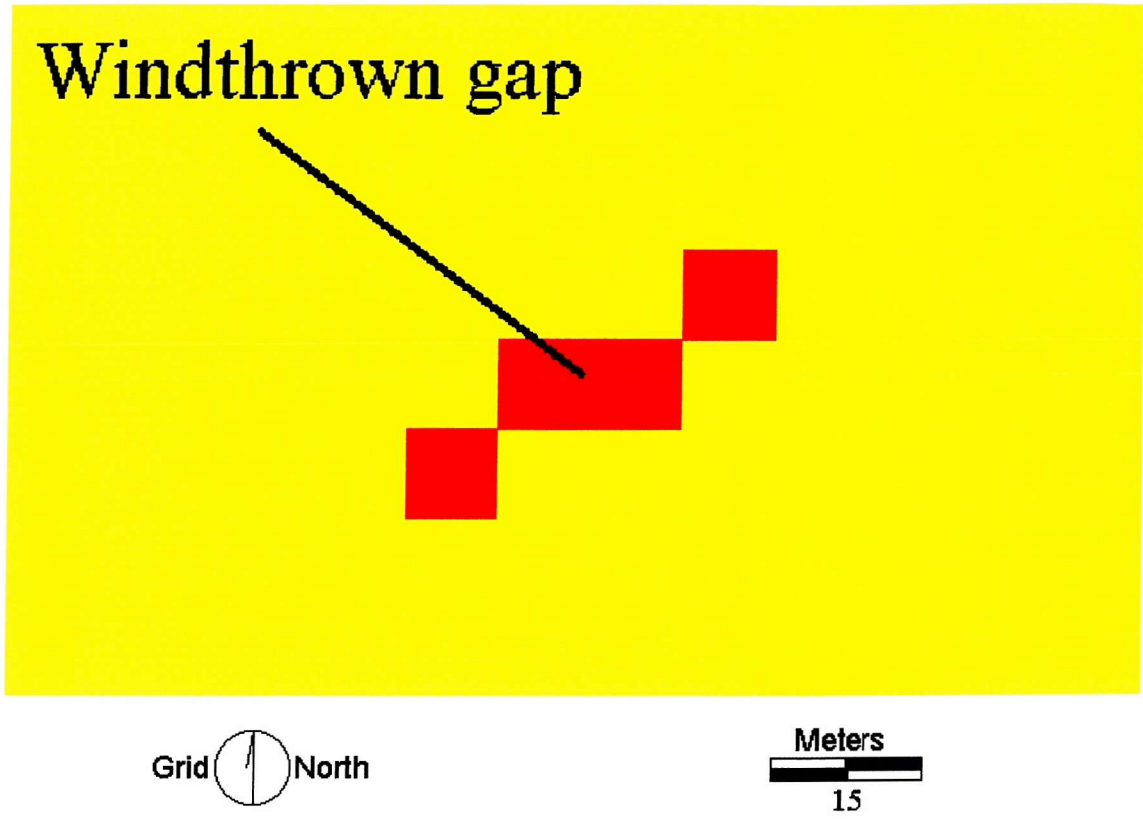

Figure 5.2 Extract from the hard classification of the 10 m spatial resolution data. Pixels allocated to the gap class are red and pixels allocated to the canopy class are yellow. As each pixel has an area = 100 m^2, the total estimated area of the windthrown gap illustrated is = 400 m^2.

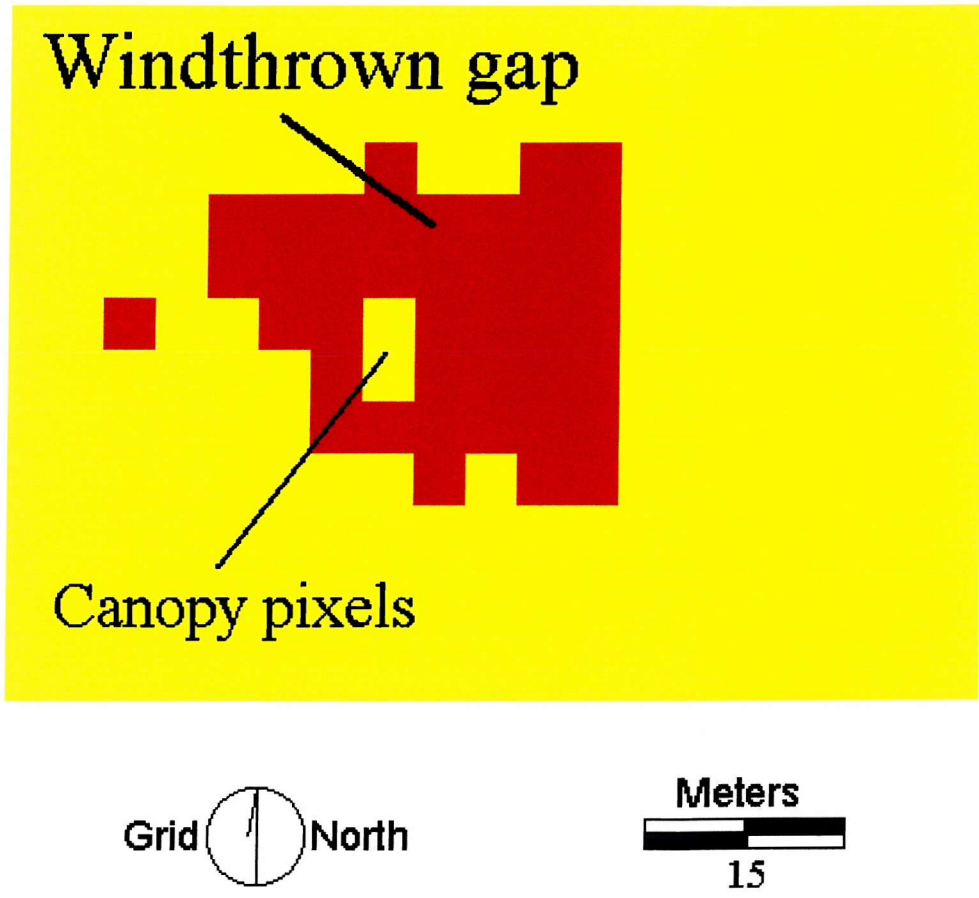

Figure 5.3 Extract from the hard classification of the ≃ 4 m ATM data. Pixels allocated to the gap class are red and pixels allocated to the canopy class are yellow. This diagram illustrates pixels allocated to the canopy class, within a block of gap pixels, and subsequently counted as contributing to the windthrown gap area estimate.

To ensure direct comparability of windthrown gap area estimates and eliminate problems such as discriminating windthrown gaps within regions of poor tree growth (Section 5.4.3), analysis focused upon isolated windthrown gaps which were surrounded by unbroken canopy for at least 12 m (3 pixels) in all directions. This eliminated the need for subjective differentiation of individual gaps from other gaps, or features such as poor tree growth. For example, Figure 5.4 shows a contiguous cluster of gap pixels which the reference data record as 2 windthrown gaps. It is possible to divide the single cluster into two smaller clusters and allocate each to represent an individual windthrown gap. However, an arbitrary division of such a gap represents a source of error affecting the quality of the spatial representation of the individual windthrown gaps.

Restricting analyses to spatially isolated gaps the number of windthrown gaps available for analyses within the ≃ 4 m ATM data was limited to 16 small to medium sized gaps, ranging in reference areal extent from 44 to 560 m^2. These gaps were all larger than the finest spatial resolution data used (≃ 4 m), but also sub-pixel in size compared with the coarsest spatial resolution data (30 m). The number of windthrown gaps available for analysis decreased, as the spatial resolution decreased.

5.4.5.2 Softened classification windthrown gap area estimation

Typicality and posterior probability maps (Section 4.5.2) were analysed to determine whether they provided a more realistic representation of class composition within each pixel and hence, whether it may be possible to derive more accurate estimates of windthrown gap area than from the hard classification. Although it is possible to derive

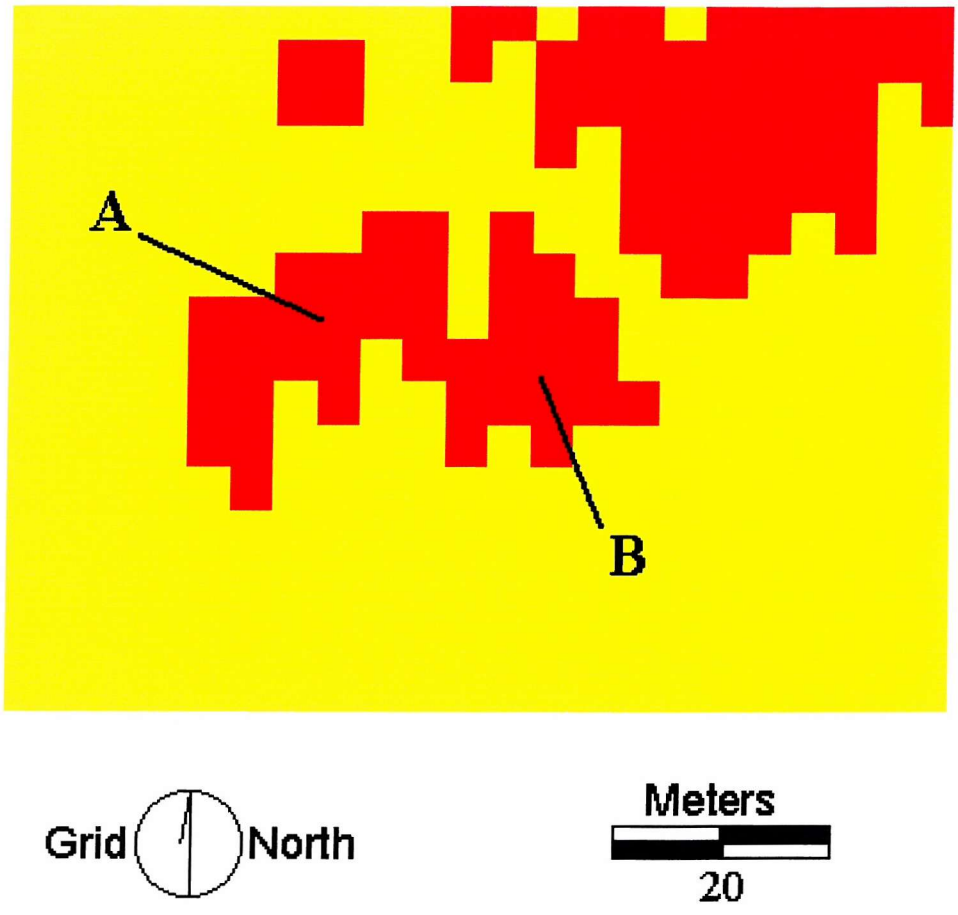

Figure 5.4 Hard classification output of the ≃ 4 m ATM data. Pixels allocated to the gap and canopy classes are red and yellow respectively. The single contiguous block in the centre is represented as 2 windthrown gaps ('A' and 'B') in the reference data. This diagram illustrates the difficulty in objectively distinguishing individual windthrown gaps which are not isolated.

information on the sub-pixel proportions of classes within a pixel, it is not usually possible to determine the spatial distribution of each component class within a pixel (Atkinson, 1997; Hugenin *et al.*, 1997; Foody, 1998). In subsequent analyses, it was assumed that the proportions of each pixel allocated to the gap class would be spatially aggregated. The posterior probability map had a class membership contour fitted at the 0.5 posterior probability to the amalgamated gap class (Foody, 1998). This threshold was selected on the basis that given two component classes within a pixel, the class which had a posterior probability level above 0.5 would be the class that pixel would be allocated to by a maximum-likelihood classification. This 0.5 posterior probability contour was used in subsequent analysis to represent a hard boundary between the gap and canopy classes. Windthrown gap area was estimated as the area bounded by this contour.

Area estimates were also derived by fitting a class membership contour to the typicality probability to the amalgamated gap class map. However, the selection of an appropriate typicality probability contour was less intuitive in comparison to the selection of a posterior probability contour. Therefore, class membership contours at a range of typicality probabilities to the gap class, ranging from 0.99 to 0.69 in steps of 0.05, were analysed to determine an appropriate typicality probability contour (Figure 5.5).

5.5 RESULTS

5.5.1 Hard classification windthrown gap identification

The hard classification of the ≃ 4m ATM data (Figure 5.6) provided an accurate representation of the land cover with an overall classification accuracy of 93.8 %

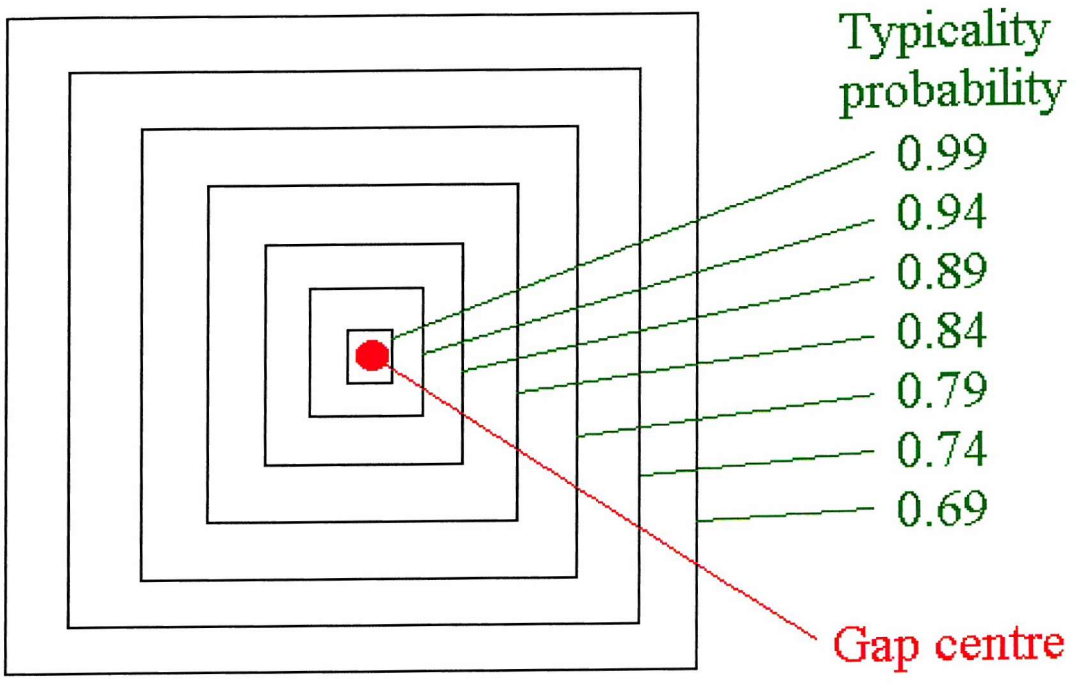

Figure 5.5 Diagram depicting, for a hypothetical gap, the general pattern of typicality class membership probability to gap contours fitted at the probabilities indicated. The centre of the gap is indicated and the contours fitted are increasingly further from the gap centre as the typicality probability to gap decreases.

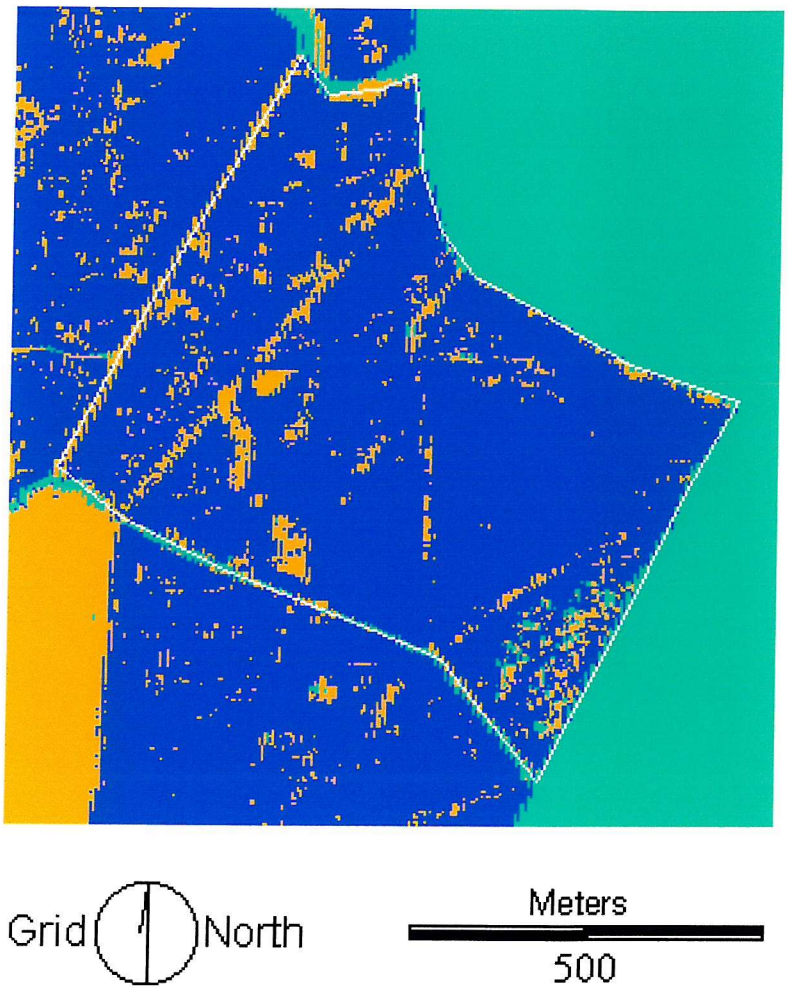

Figure 5.6 Hard classification output of the ≃ 4 m ATM data. Pixels allocated to the windthrow, canopy and moorland class are yellow, blue and green respectively. Compartment 7271 is bounded by the white polygon. (Note: stripes within the output are caused by the colour reproduction)

(Table 5.2). Analyses of the errors of commission to the windthrown class (User's accuracy = 78.7 %) were investigated by field survey in September 1998. A small number of pixels classified as windthrown (27 individual pixels), but represented in the reference data as canopy, were identified during this field survey as individual windthrown trees or small groups of wind damaged trees. This demonstrates error within the reference data which Congalton and Green (1993) suggested may be due to photointerpretation error. However, in terms of the ability to accurately identify known windthrown gaps, the hard classification correctly identified 52 known windthrown gaps out of a possible 54. This resulted in a very good windthrown gap identification accuracy of 96.3 %.

As the spatial resolution of the data became coarser, the quantity of sub-pixel gaps increased (refer to Figure 3.7). At the 10 m spatial resolution, the hard classification identified 37 of the gaps, resulting in an identification accuracy of 68.5 %. With an estimated area of 100 m^2 (i.e. 1 pixel), the smallest windthrown gap identified had a reference area of 98 m^2. At the 20 m resolution, the hard classification identified 20 gaps and hence had an identification accuracy of 37.0 %. The smallest windthrown gap identified had a reference area of 160 m^2, in relation to the hard area estimate of 400 m^2 (i.e. 1 pixel). As the spatial resolution of the data became coarser, at the 30 m resolution only 10 gaps were identified, resulting in an 18.5 % gap identification accuracy. At this spatial resolution, the hard gap area estimate for the smallest windthrown gap was 900 m^2 (i.e. 1 pixel) whilst the reference area estimate was 168 m^2. It was apparent that this windthrown gap exhibited a disproportionate contrast in relation to its size. However,

generally only the largest gaps were identified and the smaller gaps represented subpixel features with the 30 m spatial resolution data.

5.5.2 Estimation of windthrown gap areas

5.5.2.1 Hard classification windthrown gap area estimation

The estimated windthrown gap areas derived from the hard classification of the ≃ 4 m ATM data were compared against the reference areas, with the results summarised in Table 5.3. For the 16 small to medium sized gaps analysed (Section 5.4.5.1), the hard classification tended to underestimate gap area. The RMSE (77.80 m^2) indicated that the accuracy of the gap area estimates derived from the thematic map was poor. However, when compared with the area estimates derived from the 10 m spatial resolution data the Forestry Commission use for wind damage monitoring, which have an RMSE = 64.76 m^2 (Table 5.3), the accuracy of area estimates derived from the thematic map may be acceptable for the operational monitoring of wind damage. In addition, comparison of the areal extent of the gaps derived from the thematic map with that derived from the reference data revealed a very strong and highly significant degree of correlation, $r = 0.85$ ($P > 0.01$). Moreover, the relationship between the gap areas estimated from the thematic map and the reference areas was close to a 1:1 relationship (slope = 0.91) (Figure 5.7).

Visual analysis of the hard classification output suggested that for a number of gaps, there were pixels allocated to the gap class outlying the cluster of gap pixels from which gap areal estimates were derived (Figure 5.8). As only the single contiguous block

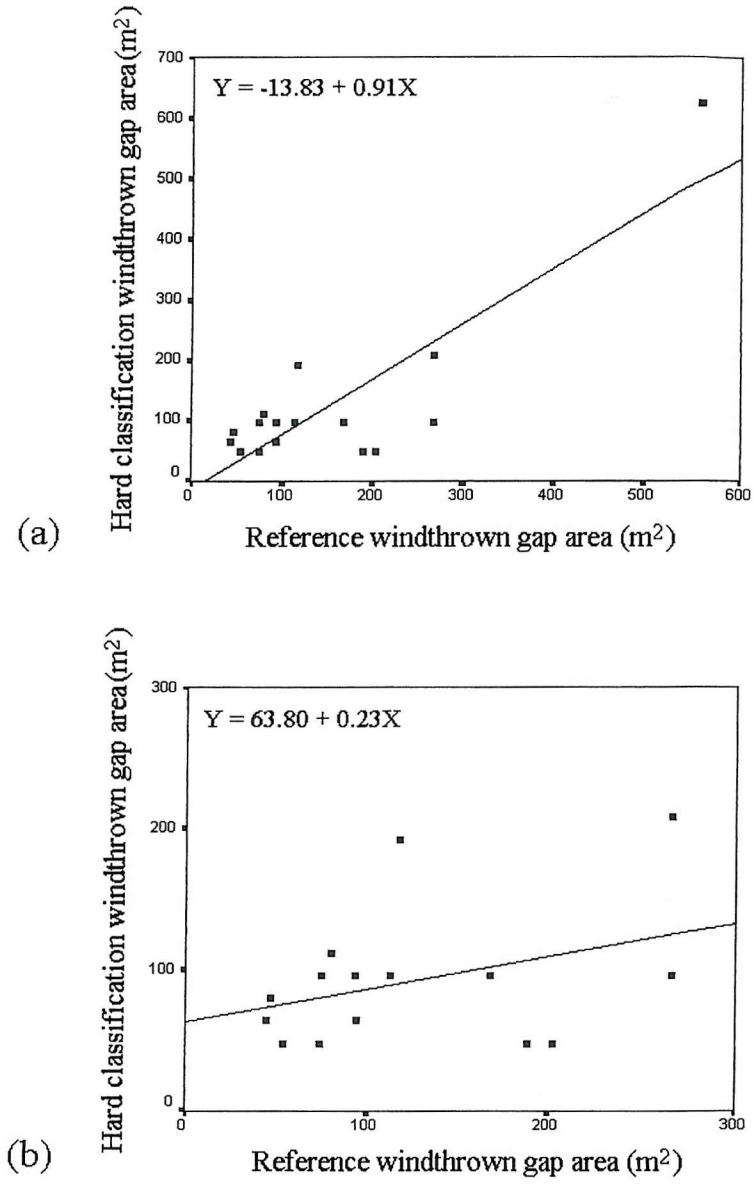

Figure 5.7 Plots of windthrown gap area estimates derived from the hard classification of ≃ 4 m ATM data against reference windthrown gap areas, with linear regression lines fitted. The equations describing the regression lines are also provided. (a) depicts the plot for all 16 windthrown gaps investigated, whilst (b) depicts the plot resulting from the removal of the largest windthrown gap plotted in (a).

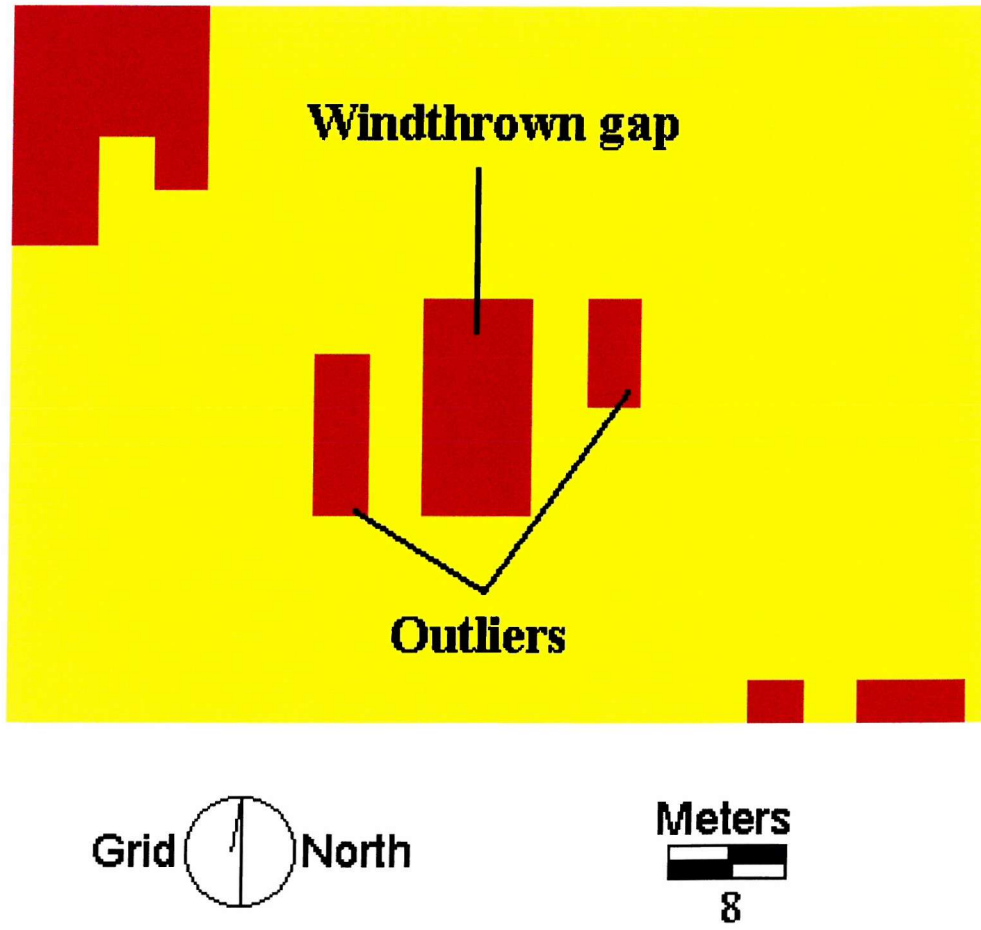

Figure 5.8 Extract from the hard classification of the ≃ 4 m ATM data. Pixels allocated to the gap class are red and pixels allocated to the canopy class are yellow. The contiguous block at the centre corresponds with the spatial location of the windthrown gap in the reference data. The two outlying blocks appear to belong to this windthrown gap, however, their inclusion in the windthrown gap area estimate is subjective.

	RMSE (m^2)	r
Forestry Commission's 10 m data	64.76	0.83
hard classification	77.81	0.85
0.5 posterior contour	82.82	0.85
0.99 typicality contour	153.50	0.84
0.94 typicality contour	121.98	0.86
0.89 typicality contour	101.10	0.87
0.84 typicality contour	79.62	0.89
0.79 typicality contour	70.58	0.89
0.74 typicality contour	70.32	0.89
0.69 typicality contour	88.19	0.86

Table 5.3 Table presenting a summary of the windthrown gap area estimation results (for 16 windthrown gaps) derived from the analysis of the ≃ 4 m ATM data. This table indicates the RMSE and Pearson's correlation coefficient, r, resulting from comparison of each area estimation method against the reference data which has spatial resolution of 1 m (Section 3.4.2). The 'Forestry Commission's 10 m data' represents the original vector representation of the windthrown gaps rasterised to a spatial resolution of 10 m, which is the spatial resolution of the data the Forestry Commission use for wind damage monitoring. 'Hard classification' represents the windthrown gap area estimates derived from the conventional maximum-likelihood classification; '0.5 posterior contour' represents the 0.5 posterior probability to gap contour area estimates; and 'typicality contour' represents the typicality probability contour to gap area estimates at the given probability.

within which the reference gap centre was located was used for the area estimation, the contribution to the gap area estimate from any outlying pixels was initially excluded. The addition of the contribution of these outlying pixels was found to marginally improve the area estimate (RMSE = 76.99 m^2). However, this addition of outlying pixels is highly subjective.

As the spatial resolution of the remotely sensed data decreased from ≃ 4 m to 10 m, the accuracy of area estimates decreased (from RMSE = 77.80 m^2 to RMSE = 140.40 m^2). The relationship between the area estimates at 10 m derived from the hard classification and the reference data (Table 5.4) was poorer than for the fine (≃ 4 m) ATM data.

	RMSE (m^2)	r
hard classification	140.40	0.72
0.5 posterior contour	118.23	0.76
0.99 typicality contour	203.39	0.88
0.94 typicality contour	166.57	0.80
0.89 typicality contour	121.93	0.81
0.84 typicality contour	92.13	0.82
0.79 typicality contour	118.37	0.79
0.74 typicality contour	167.59	0.82
0.69 typicality contour	239.45	0.87

Table 5.4 Table presenting a summary of the windthrown gap area estimation results (for 10 windthrown gaps) derived from the analysis of the 10 m spatial resolution data. This table indicates the RMSE and Pearson's correlation coefficient, *r*, resulting from comparison of each area estimation method against the reference data which has spatial resolution of 1 m (Section 3.4.2). The 'Forestry Commission's data' represents the original vector representation of the windthrown gaps rasterised to a spatial resolution of 10 m, which the Forestry Commission use for wind damage monitoring. ' Hard classification' represents the windthrown gap area estimates derived from a conventional maximum-likelihood classification; '0.5 posterior contour' represents the 0.5 posterior probability to gap contour area estimates; and 'typicality contour' represents the typicality probability contour to gap area estimates at the given probability.

For example, the degree of correlation between the area estimates at 10 m and the reference areas, although significant ($P > 0.05$), was weaker, $r = 0.72$, than that obtained with the ≃ 4 m ATM data ($r = 0.85$). Visual analysis of the classification at each of the coarse spatial resolutions (i.e. 10 m, 20 m and 30 m) suggested that the windthrown gaps were less accurately represented than within the ≃ 4 m ATM data. This can be illustrated with reference to the single gap (from the initial 16 windthrown gaps at ≃ 4 m selected for analysis) that was distinguishable within the hard classification output over all the spatial resolutions used (Table 5.5). The estimated windthrown gap areas were 96, 200, 400 and 900 m^2 at the ≃ 4, 10, 20, and 30 m spatial resolutions respectively. As the reference area was 168 m^2, it was apparent that the accuracy of windthrown gap area estimates declined

markedly at the 20 and 30 m spatial resolutions. Although at the 30 m spatial resolution, the windthrown gap was very much smaller than the pixel size, it had sufficient contrast to the canopy class to be still detectable.

5.5.2.2 Softened classification windthrown gap area estimation

Comparison with the results derived from the hard classification (Table 5.3) indicated that of all the typicality probability contour based area estimates, the 0.79 and 0.74 typicality probability to gap contours appeared to provide the most accurate results. These contours provided more accurate estimates of windthrown gap area (RMSE = 70.58 m^2 and 70.34 m^2 respectively) than estimates derived from the hard classification (RMSE = 77.81 m^2), or the 0.5 posterior probability to gap contour (RMSE = 82.82 m^2). In addition, the RMSEs associated with these typicality probability contour based estimates of windthrown gap areas are close to the RMSE (64.76 m^2) accepted by the Forestry Commission for wind damage monitoring. These 0.79 and 0.74 typicality and 0.5 posterior probability contour area estimates (Figure 5.9) provided a significant degree of correlation with the reference gap areas ($P > 0.01$) and had as strong, or stronger relationship ($r = 0.89$ and $r = 0.85$ respectively) to the reference areas as the hard classification area estimates ($r = 0.85$).

At a spatial resolution of 10 m, the 0.84 and 0.79 typicality probability to gap contours provided more accurate estimates of gap area (RMSE = 92.13 m^2 and 118.37 m^2 respectively) than the hard classification estimate (RMSE = 140.40 m^2) (Table 5.4). The degrees of correlation with respect to the reference data were also both stronger

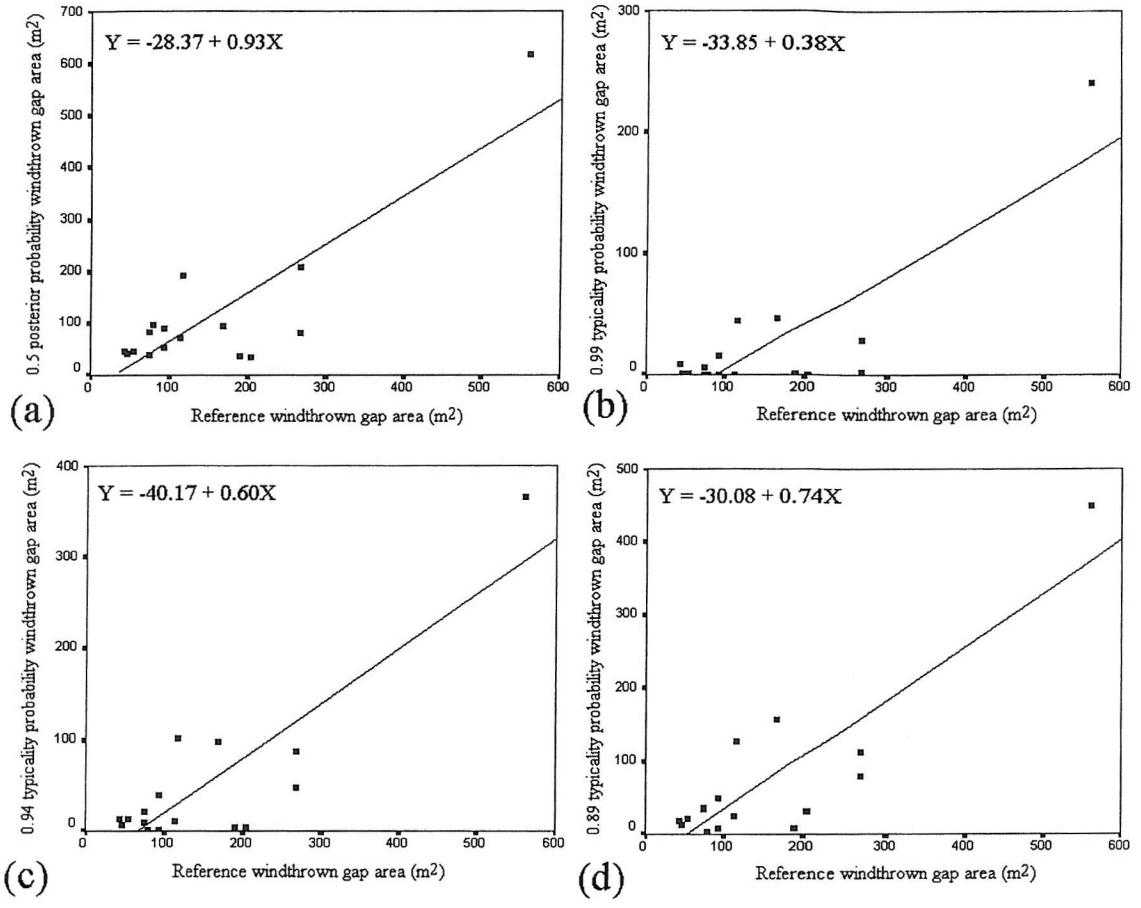

Figure 5.9 Plots of windthrown gap area estimates derived from softening the hard classification of ≃ 4 m ATM data against reference windthrown gap areas, with linear regression lines fitted. The equations describing the regression lines are also provided. The plots represent the windthrown gap area estimates (for all 16 windthrown gaps) derived from: (a) fitting a 0.5 posterior class membership probability contour; (b) fitting a 0.99 typicality class membership probability contour; (c) fitting a 0.94 typicality class membership probability contour; (d) fitting a 0.89 typicality class membership probability contour;

(continued over)

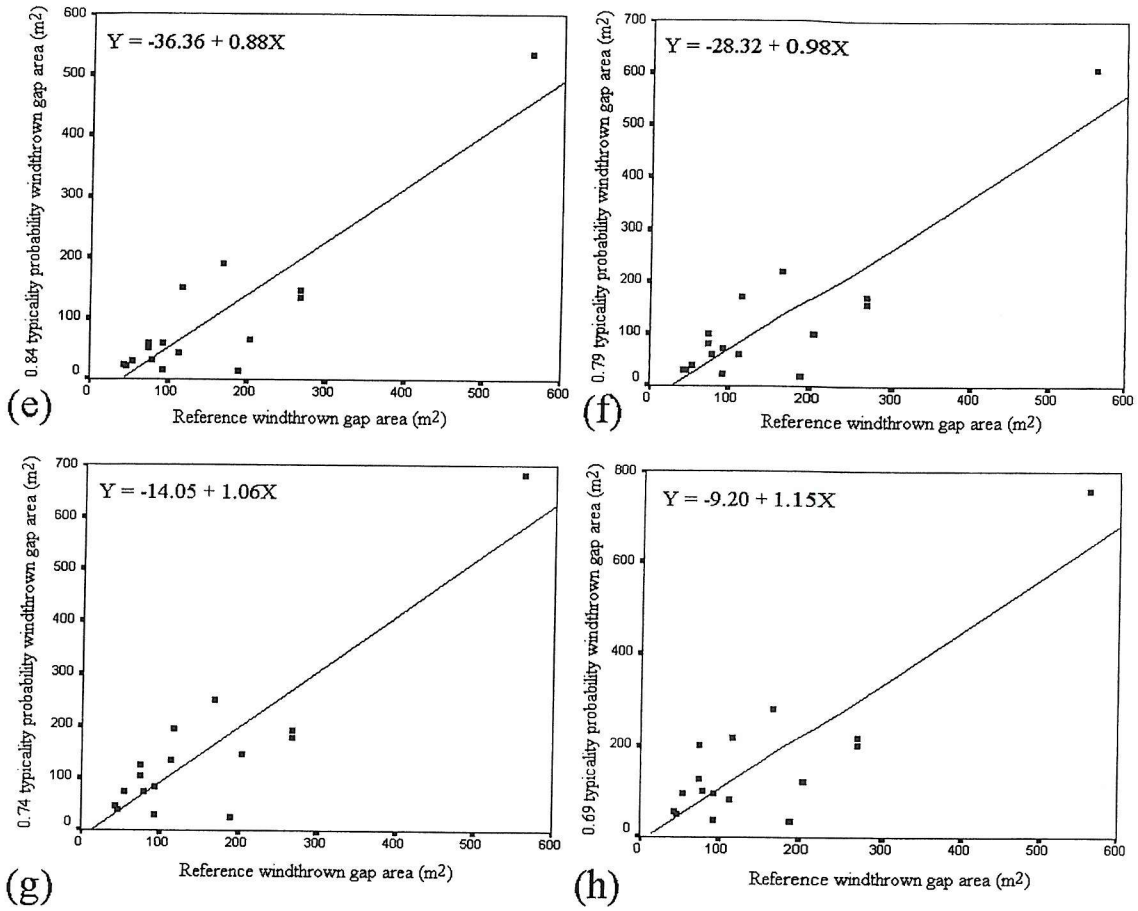

Figure 5.9 (continued) (e) fitting a 0.84 typicality class membership probability contour; (f) fitting a 0.79 typicality class membership probability contour; (g) fitting a 0.74 typicality class membership probability contour; (h) fitting a 0.69 typicality class membership probability contour.

(r = 0.82 and r = 0.79 respectively) than the hard area estimates (r = 0.72). The area estimates derived from the 0.5 posterior probability contour (RMSE = 118.23 m^2) were also more accurate than the hard classification area estimates, although the results were not as good as the area estimates derived from the typicality probability contours noted above.

At spatial resolutions of 20 and 30 m, the softened methods also provided more accurate estimates of windthrown gap area than the hard classification. However, these results are based upon area estimates of one gap (Table 5.5). Despite this, the probability contours fitted to the softened data appeared to provide a visually superior representation of the windthrown gap than the hard (blocky) classification (Figure 5.10) and may indicate a potential to derive further information on gaps, such as perimeter and shape.

5.6 DISCUSSION

The results from this Chapter indicated that a conventional hard classification of remotely sensed data can be used to detect accurately windthrown gaps over the size range which was representative of windthrown gaps found throughout British forests (Figure 3.7). In addition, the hard classification of remotely sensed data with a spatial resolution of $\simeq$ 4 m, identified more windthrown gaps within the compartment than the aerial photograph based estimates. It is possible that the ability to identify gaps from the aerial photographs may have been dependent upon the experience of the interpreter, which may partly explain the classification errors associated with the hard classification (Table 5.2).

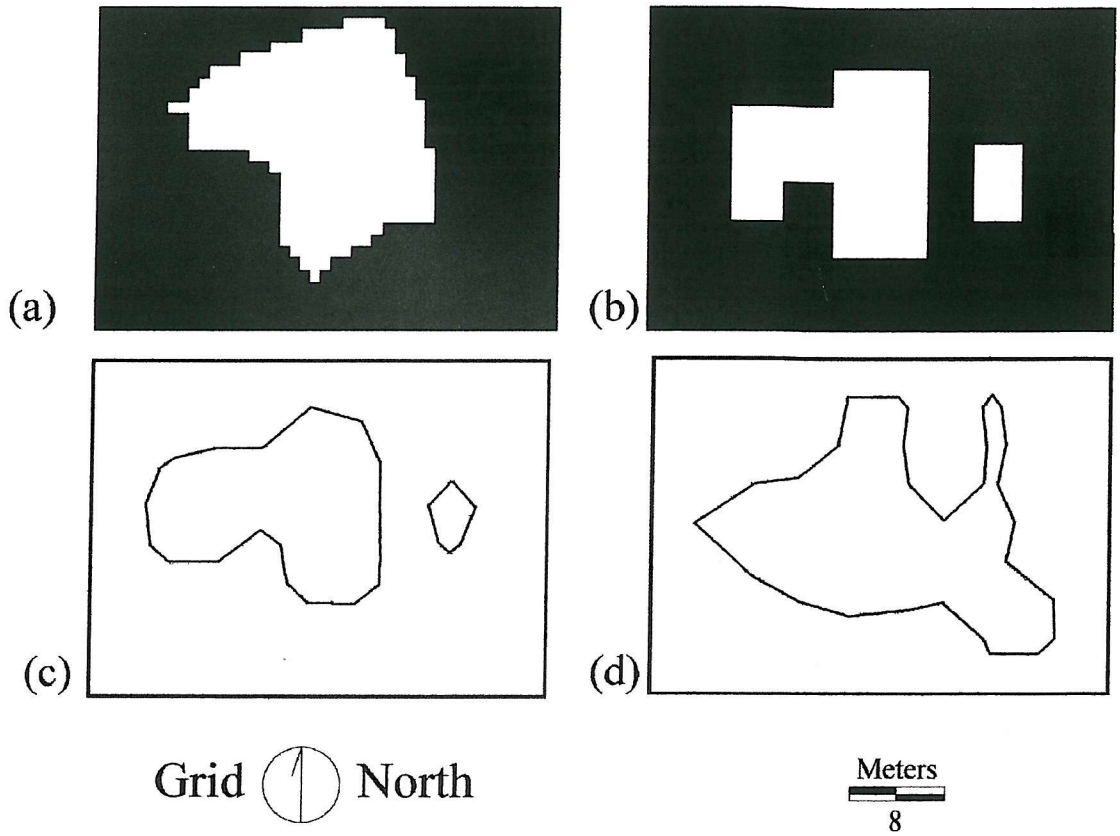

Figure 5.10 Windthrown gap representations derived from: (a) manual interpretation of aerial photographs (gap is white) at a spatial resolution of 1 m; (b) maximum-likelihood classification of ≃ 4 m ATM data (gap is white); (c) 0.5 posterior probability to gap class membership contour; (d) 0.89 typicality probability to gap class membership contour.

Data	Area (m^2)	RMSE (m^2)
Reference data	168.00	
Hard classification		
≃ 4 m	96.00	72.00
10 m	200.00	32.00
20 m	400.00	232.00
30m	900.00	732.00
Softened classification		
Posterior probabilities (0.5)		
≃ 4 m	93.90	74.10
10 m	94.80	73.20
20 m	80.60	87.40
30 m	163.30	4.70
Typicality probabilities (0.79)		
≃ 4 m	220.60	52.60
10 m	319.20	151.20
20 m	67.80	100.20
30m	70.40	97.60

Table 5.5 Estimates of windthrown gap area and RMSE, for the single windthrown gap which was spatially distinct within the classified output at all spatial resolutions (≃ 4 m, 10 m, 20 m and 30 m). The reference data resulted from the vector-to-raster conversion of the Forestry Commission's vector data using a spatial resolution of 1 m.

Quine and Bell (1998) specifically noted that it had been difficult to distinguish small windthrown gaps less than 500 m^2, due to shadow (see Section 2.6.1.3). The vast majority of the errors of commission were accounted for by small windthrown gaps and wide tree spacing associated with drains (Section 5.5.1). Therefore, application of a low-pass filter (Section 5.4.3) would have removed small gaps from the classified data, however, these gaps are important to the overall risk of windthrow to a forest stand (Stacey *et al.*, 1994). As a result, the photographic estimate of windthrown gap numbers appeared to be less accurate in identifying windthrown gaps present within the compartment than the hard classification of the ≃ 4 m ATM data. However, this

identification accuracy is dependent upon the spatial resolution of the data, with accuracy increasing as the spatial resolution becomes finer. This trend is mirrored by the ability to accurately estimate windthrown gap area from the thematic output produced by the conventional hard classification method.

In Section 5.5.2, it was noted that features outwith the windthrown gaps, such as lightly damaged trees, or poor tree growth were allocated to the gap class. Incorporating outlying gap pixels to improve areal estimates is subjective and open to misinterpretation. Nevertheless, the results indicated that remotely sensed data acquired with a spatial resolution of $\simeq$ 4 m, finer than the typical gap size (Quine and Bell, 1998) and comparable to that of new fine spatial resolution satellite sensors, used with conventional classification algorithms do not provide accurate estimates of individual windthrown gap area. However, the accuracy of areal estimates are not that poor when considered against the accuracy accepted by the Forestry Commission for wind damage monitoring.

The accuracy of the windthrown gap areal estimates derived from the hard classification was reduced as the spatial resolution of the remotely sensed data became coarser than the $\simeq$ 4 m data. It is likely that at coarse spatial resolutions, typical windthrown gaps would most likely remain undetected by conventional classification techniques applied to coarse spatial resolution data. Therefore, this combination of classification method and remotely sensed data is not suitable for accurately estimating the areal extent of windthrown gaps found throughout upland forests in British Isles.

As an alternative, the softened classification methods provided more accurate estimates of gap area than the conventional hard classification. The magnitude of this

improvement is inversely related to the spatial resolution of the remotely sensed data used. As the spatial resolution becomes finer, the magnitude of the improvement in area estimates derived from softened classification methods, compared with the conventional hard classification method decreases. Therefore, as the spatial resolution of remotely sensed data becomes finer, there is less advantage to using softened classification methods. However, fitting class membership contours provide a visually more realistic representation of a windthrown gap boundary than the blocky pixel representation. In particular, typicality class membership probabilities appear to provide the softened method with the most potential.

5.7 SUMMARY

Addressing the Chapter aims (Section 5.2), the results indicated that the ability to accurately identify and estimate the area of individual windthrown gaps present within remotely sensed data is a function of the spatial resolution of the sensor data and the size of the windthrown gaps. In addition, softened mapping methods using typicality and posterior class membership probability contours appeared to have the potential to derive more accurate windthrown gap area estimates than a conventional hard classification. These soft mapping methods provided an alternative representation of the gaps and appeared to have potential to derive greater information on the gap-canopy boundary as a spatial feature. Subsequently, investigations will not look further at the effects of spatial resolution upon windthrown gap representations, rather investigate the use of class membership probabilities to spatially characterise windthrown gap boundaries. This will

involve the investigation of mechanisms for quantifying shape in order to objectively compare windthrown gap shapes derived from the reference data, with those derived from the hard and softened classifications.

CHAPTER 6

ESTIMATING SPATIAL CHARACTERISTICS OF WINDTHROWN GAPS DEFINED BY A HARD BOUNDARY

6.1 INTRODUCTION

The value of remotely sensed data is often limited by the imposition of hard decision rules associated with conventional image classification methods (Foody *et al.*, 1992; Foody and Trodd, 1993). As an alternative, softened classifications have been developed which use the strength of class membership (e.g. probabilities) to represent the class composition within each individual pixel. The results from Chapter 5 indicated that it was possible to accurately identify and discriminate windthrown gaps within a uniform canopy of Sitka spruce. In addition, a softened classification based on typicality probabilities appeared to have the potential to provide more accurate windthrown gap area estimates than a conventional hard maximum-likelihood classification.

This Chapter aims to compare hard and softened classification methods for estimating a number of important spatial characteristics of windthrown gaps. For example, gap shape, which can influence the microclimate and environment, particularly in terms of the light environment, has important implications for the regeneration of tree species within gaps (Marquis, 1965; Brokaw, 1985; Howe, 1990; Quine and Humphrey,

1996). Previous work has also indicated that gap shape may influence additional ecological processes, such as migration, foraging, dispersal and pollination within forest ecosystems (Rex and Malanson, 1990; Baskent and Jordan, 1995).

6.2. CHAPTER AIMS

This Chapter uses the entire Cwm Berwyn Forest wind damage monitoring site to evaluate the potential of hard and softened classifications to accurately estimate a number of important spatial characteristics of windthrown gaps within canopies of different tree species. Concentrating upon quantifying and comparing estimates of windthrown gap area, perimeter and shape derived from hard and softened classifications, this Chapter sought to answer four specific questions:

- Is it possible to identify windthrown gaps within the canopy of a tree species other than Sitka spruce using a conventional hard classification?
- Will a softened classification provide a more accurate estimation of windthrown gap area than a conventional hard classification?
- Will a softened classification provide a more accurate representation of windthrown gap perimeter than a conventional hard classification?
- Will a softened classification provide a more accurate representation of windthrown gap shape than a conventional hard classification?

6.3 STUDY SITE

The entire Cwm Berwyn Forest wind damage monitoring area was used as the study site in this Chapter (Figure 3.2). This monitoring area included a number of windthrown gaps within stands of Japanese larch, mixed Sitka spruce and lodgepole pine (Figure 3.3) and stands of Sitka spruce which had been line thinned (Figure 3.4).

6.4 METHODOLOGY

6.4.1 Pre-processing

The ATM data were pre-processed prior to the extraction of information using the methodology described in Chapter 4. In summary, the ATM data were radiometrically calibrated to convert the DN of each pixel in wavebands 1 to 10 to radiance (Section 3.3.1.4) using reference data supplied by NERC (Appendix 1) and geometrically corrected after radiometric calibration resulting in the RMSE of 1.76 pixels reported in Section 4.4.

6.4.2 Spatial autocorrelation

Section 5.4.1.4 noted that individual random sample pixels used to generate class signatures should be selected from throughout the area to be classified and spaced according to the degree of spatial autocorrelation. A variogram was used to examine the pattern of spatial variability within the ATM data and information derived from the variogram used to determine the optimum strategy for selecting sample pixels for each class (Atkinson, 1996; Curran and Atkinson, 1998). A variogram describes the relationship between variance and spatial separation, and was depicted in graphical form

(Figure 6.1) (Burrough and M^{C}Donnell, 1998; Curran and Atkinson, 1998). Figure 6.1 shows the variogram computed from a sample of pixels, 100 pixels by 100 pixels, from waveband 7 of the ATM data. The lag (h) is the distance between a sampled pair of pixels (Figure 6.2) and the semivariance ($\gamma(h)$) (Equation 6.1) is half the expected average squared difference between a sampled pair of pixels at a particular lag (Atkinson, 1996; Burrough and M^{C}Donnell, 1998; Curran and Atkinson, 1998; Curran and Atkinson, 1999).

$$\gamma(h) = \tfrac{1}{2} E[Z(x) - Z(x + h)]^2 \qquad 6.1$$

Where: $\gamma(h)$ = the semivariance; Z = DN of pixel x; h = lag distance between a pair of pixels.

The range of the variogram (Figure 6.1) indicated that the pixels were spatially dependent to a lag of approximately 23 pixels. Therefore, sample pixels selected to generate the classes which will be used in subsequent analysis should be at least 23 pixels apart for them to be independent.

6.4.3 Class definition

In addition to the three thematic classes used in Chapter 5 (i.e. canopy, moorland and windthrown), the remotely sensed response from the entire wind damage monitoring area included a Japanese larch canopy, a mixed Sitka spruce and lodgepole pine canopy, and the lake at the centre of the site. There were only 3 windthrown gaps present within

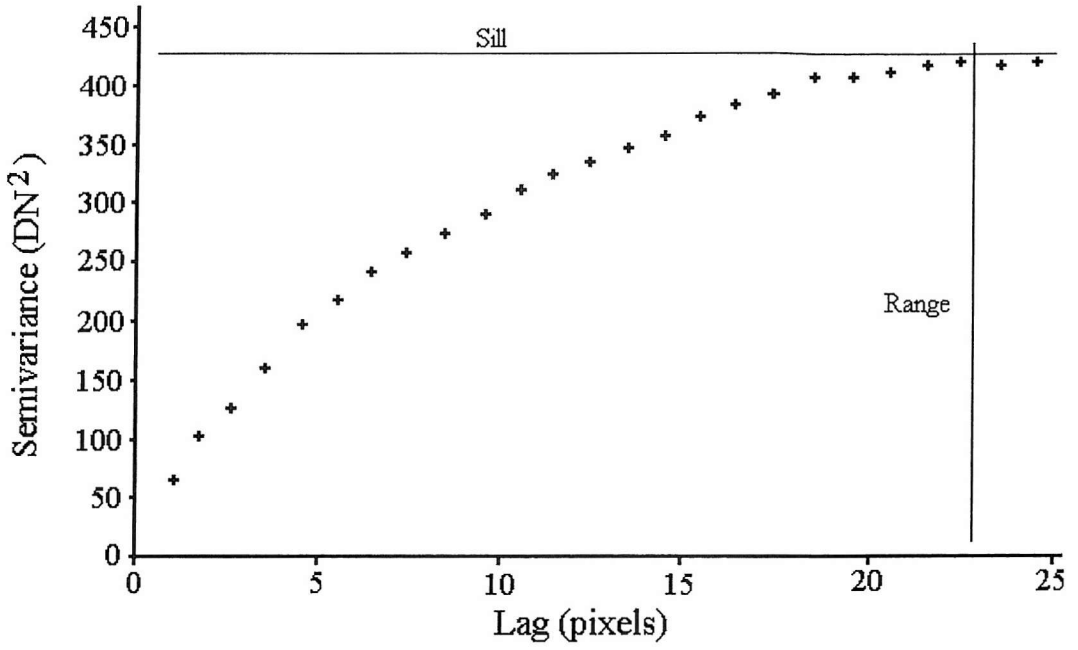

Figure 6.1 Variogram computed for a 100 pixel by 100 pixel extract from waveband 7 of the raw ATM data. The semivariance is the average squared difference between any pair of pixels separated by a given Lag. The lag is the distance between any pair of pixels (Figure 6.2). The Sill represents the maximum value of semivariance and the Range represents the Lag at which the semivariance reaches it's maximum value (Curran and Atkinson, 1998). The Range of the variogram suggests that any pair of pixels within the ATM data separated by a distance of less than approprimately 23 pixels are statistically related.

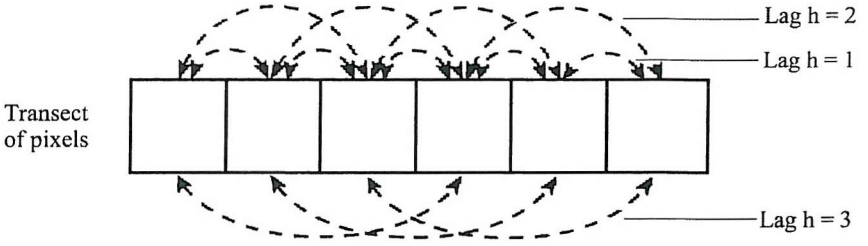

Figure 6.2 Diagram depicting a hypothetical transect of pixels with lags of 1, 2 and 3 illustrated (adapted from Curran and Atkinson (1998)). The lag is the distance between any pair of pixels, h intervals apart.

the stands of mixed spruce and pine and, therefore, it was not practical to establish a spruce and pine class in order to examine these 3 gaps. Class responses were established to represent the 'pure' reflected response for five thematic classes: windthrown; canopy (SS); canopy (JL); water; and moorland. The reference raster data set depicting windthrown gap location was again used to identify sample pixels for the windthrown class. The sample pixels for the windthrown class only consisted of pixels representing wind damage within stands of pure Sitka spruce. No sample pixels were selected to represent wind damage within stands of larch due to the small number of windthrown gaps (32 in total) within the larch stands and the close proximity of these gaps to stands of Sitka spruce.

Despite the spatial autocorrelation illustrated in Figure 6.1, it was not possible for each randomly located sample pixel to be spatially separated by a minimum lag of 23 pixels. As a compromise the randomly located sample pixels had a minimum spatial separation of 10 pixels in order to reduce as far as was possible the potential effects of spatial autocorrelation given the spatial restrictions of the data set. The spectral response from these sample pixels (totalling 137, 192, 111, 174 and 194 pixels from the windthrown, canopy (SS), canopy (JL), water and moorland classes respectively), were used to generate descriptive statistical information on each class, which was used to train the maximum-likelihood classifier to distinguish between the classes (Richards, 1993). The aim had been to select a number of sample pixels, to satisfy the minimum sample for any class (i.e. 30 times the number of wavebands, where the intention was to use four wavebands) suggested by Mather (1999). However, it was not possible to select the

minimum sample for the canopy (JL) class as this class comprised a small canopy component within the monitoring site. However, since the number of sample pixels was close to the minimum number required, this class was retained for subsequent analysis.

6.4.4 Feature selection

As the wavebands of the ATM sensor were strongly inter-correlated (Table 5.1), a feature selection was undertaken to remove those wavebands which contributed little to class separability. The volume of the data set was, therefore, reduced without incurring any significant loss of information (Conese and Maselli, 1993; Richards, 1993; Mather, 1999). Discriminant analysis (Klecka, 1980) was used to select the most discriminating wavebands (e.g. Foody *et al*, 1992; Foody, 1998). This stepwise procedure selected the single waveband which provided the optimum discrimination between all the class signatures (Klecka, 1980). This waveband was then paired with each other waveband to determine the optimal combination of two wavebands for class discrimination. The discriminant analysis continually added the next most discriminating waveband to the combination of wavebands already selected (Klecka, 1980).

Stepwise discriminant analysis suffers from the potential disadvantage of not necessarily selecting the optimum combination of wavebands, as each waveband selected is dependent upon the initial and subsequent wavebands chosen. Hence, stepwise discriminant analysis does not test for every possible waveband combination (Klecka, 1980). Wilk's Lambda was the statistical measure used to determine the combination of wavebands which provided discrimination between class signatures (Klecka, 1980). The

results indicated that wavebands 4 (visible red), 7 (near-infrared), 9 (short-wave infrared) and 11 (thermal infrared) contained most of the discriminating spectral information within the ATM data set. These 4 wavebands corresponded well with the optimal selection of ATM sensor wavebands suggested by Townshend (1984) and only these four wavebands were used in subsequent analysis. Wavebands 7 and 11 had been previously selected in Section 5.4.1.3, suggesting that these two wavebands are particularly useful for discriminating between the classes used in this study. Previous work has indicated that a combination of visible red, near-infrared and short-wave infrared wavebands provide a suitable waveband combination for studying the changes in reflectance from a forest after gaps have been formed by thinning (Olsson, 1994; Nilson and Olsson, 1995).

6.4.5 Classification

A hard classification (Section 4.3.1) was undertaken on the ATM data and the output also softened to derive posterior and typicality probabilities of class membership (Section 4.3.2) (Trodd *et al.*, 1989; Foody and Trodd, 1990).

6.4.5.1 Softened classification

The results from the analysis on the set of 16 windthrown gaps in Chapter 5, independent of the windthrown gaps subsequently analysed in this Chapter, suggested that fitting a class membership contour at the 0.84 and 0.79 typicality probabilities to an amalgamated gap class (i.e., all classes except those representing a canopy class) provided a more realistic visual representation of a windthrown gap than the output from a hard

classification (Figure 5.10). Therefore, only these two typicality probabilities to an amalgamated gap class (i.e. windthrown, moorland and water) were used in subsequent analysis. The 0.5 posterior probability contour to the combined gap class was also used in subsequent analysis, as this is the probability level which has equal membership to both canopy (i.e. canopy (SS) and canopy (JL)) and gap classes.

6.4.5.2 Hard classification accuracy assessment

An accuracy assessment was undertaken to evaluate the overall quality of the hard classification and the results reported in the form of an error matrix (Table 6.1) (Story and Congalton, 1986; Congalton and Green, 1993). This assessment used 1000 pixels, independent of the sample pixels used for the generation of the class signatures. These pixels were selected from within the hard classification output using stratified random sampling (Congalton, 1988) and the allocated class of each pixel was compared against the class depicted in the reference data (Aronoff, 1982; Story and Congalton, 1986; Congalton and Green, 1993). The results indicated that the hard classification provided an accurate representation of the classes within the ATM data, with the Kappa coefficient (0.93) indicating that the classification was 'excellent' (Montserud and Leamans, 1992).

		Reference data					
		Canopy (JL)	Canopy (SS)	Windthrown	Moorland	Water	Total
Classified data	Canopy (JL)	19	2	0	4	0	25
	Canopy (SS)	1	431	9	0	0	441
	Windthrown	1	14	145	7	0	167
	Moorland	1	3	5	281	1	291
	Water	0	0	0	1	75	76
	Total	22	450	159	293	76	1,000

Producer's Accuracy
Canopy (JL) = (19/22)*100 = 86.4%
Canopy (SS) = (431/450)*100 = 95.8%
Windthrown = (145/159)*100 = 91.2%
Moorland = (281/293)*100 = 95.9%
Water = (75/76)*100 = 98.7%

User's Accuracy
Canopy (JL)= (19/25)*100 = 76.0%
Canopy (SS)= (431/441)*100 = 97.7%
Windthrown = (145/167)*100 = 86.8%
Moorland = (281/291)*100 = 96.6%
Water= (75/76)*100 = 98.7%

Overall classification accuracy = ((19+431+145+281+75)/1000)*100 = 95.1%
Overall Kappa coefficient of agreement = 0.93

Table 6.1 Classification error matrix and accuracy statements (percentage correct allocation and Kappa coefficient of agreement) (Story and Congalton, 1986; Congalton, 1991) for the hard classification of the ≃ 4 m ATM data. The Producer's accuracy, a measure of error of omission, is the probability of reference pixel being correctly classified. The User's accuracy, a measure of error of commission, is the probability that a classified pixel actually represents that class in the reference data.

6.4.6 Hard classification windthrown gap identification

Within the monitoring site 183 known windthrown gaps were present within the unthinned Sitka spruce stands (i.e. this included stands in addition to the non-thinning control (Figure 3.4)) and 32 windthrown gaps within the larch stands. The number of these windthrown gaps correctly identified by the hard classification was assessed by comparison with the reference data. As in Section 5.4.4, if a pixel allocated to a class

other than canopy (i.e. windthrown, moorland or water) was located at the centre of the gap within the reference data, then the hard classification was accepted as having identified that windthrown gap.

6.4.7 Estimation of windthrown gap area, perimeter and shape

Estimation of windthrown gap area, perimeter and shape was restricted to those windthrown gaps within unthinned stands of Sitka spruce to ensure a sufficient number of gaps for analysis and avoid confusion with the thinning racks. A set of 36 windthrown gaps, distributed throughout the monitoring site, varying in size and shape were used to compare the accuracy of area, perimeter and shape estimates derived from the hard and softened mapping methods (Section 6.4.5). This set represented all the known windthrown gaps identified by the hard classification that were spatially isolated from other non-canopy features by a minimum separation of 3 pixels (approximately 12 m). As any pixels allocated to the windthrown, moorland or water classes were considered to represent an amalgamated gap class and any pixels allocated to canopy (SS) or canopy (JL) were considered to represent an amalgamated canopy class (e.g. Blackburn and Milton, 1996), the classes considered in the analysis were canopy and gap.

6.4.7.1 Estimation of windthrown gap area and perimeter

Estimates of windthrown gap area were derived from the hard classification output by adding the area of each pixel allocated to the gap class together (Section 5.4.5.1). For this hard classification, a hard windthrown gap boundary was defined by the place of

contact between those pixels allocated to gap and those pixels allocated to canopy (Metzger and Muller, 1996). Estimates of windthrown gap area were derived from the softened classification as the total area constrained within the fitted class membership contour (Section 5.4.5.2). These probability contours represented a hard boundary for the softened classifications. The length of each boundary was used as the estimate of windthrown gap perimeter.

6.4.7.2 Estimation of windthrown gap shape

Shape describes an object as a whole and is, therefore, distinct from that object's perimeter (boundary) or area (size) (Nixon, 1997). Dryden and Mardia (1998) suggested that shape is the geometrical information remaining after location, scale and rotational effects have been accounted for. Unlike area and perimeter, shape is a spatial parameter which is usually difficult to quantify (Hammond and McCullagh, 1974; La Gro, 1991), although there are alternative metrics employed within the field of landscape ecology to quantify shape (e.g. M^{c}Garigal and Marks, 1995).

Despite shape being distinct from area and perimeter (Nixon, 1997), many shape metrics are based largely upon estimates of area and perimeter. These metrics have the advantage of being easy and quick to calculate, although they generally have a poor overall shape discrimination ability (James, 1987). Some shape metrics compare the perimeter or area of an object with that of a regularly shaped object, such as a circle (Hammond and M^{c}Cullagh, 1974; Unwin, 1981). Other metrics are based upon distance measurements taken of axes which transect the object of interest (Boyce and Clark, 1964; Hammond and

M^{c}Cullagh, 1974; Unwin, 1981; Nixon, 1997). These axial shape metrics are similar to the field survey methods identified in Section 3.4.3, whereby gap area is derived by sampling points on the gap boundary (e.g. Spies *et al.*, 1990; Dahir and Lorimer, 1996). However, these metrics would not resolve subtle differences between different representations of windthrown gap shape and, therefore, were not used for shape analysis.

The fractal dimension (Equation 6.2) of an object is an alternative measure of the relationship between area and perimeter and can be used as a measure of that object's shape (Hussain, 1994; Davidson, 1998). Fractal objects are described as self similar which means that as the scale at which the object is examined changes, the shape does not change (Figure 6.3) (Bettinger *et al.*, 1996). There are a number of shape metrics which are a derivative of the fractal dimension (e.g. Patton, 1975; Batchelor, 1978; James, 1987; Jahne, 1995; M^{c}Garigal and Marks, 1995; Nixon, 1997). Other shape metrics claim to derive the actual 'fractal dimension' of an object, however, they have limitations which makes the use of the term 'fractal dimension' inappropriate. For example, they either approximate or ignore k (the constant of proportionality) in calculating the fractal dimension (Frohn, 1998). It is important to note that these fractal dimension metrics do not produce the same results for identical objects and, therefore, it is not possible to directly compare the results for individual objects. Therefore, in order to prevent confusion those shape metrics which claim to derive the fractal dimension of an object (Equation 6.2) will subsequently be referred to according to their method of calculating the fractal dimension.

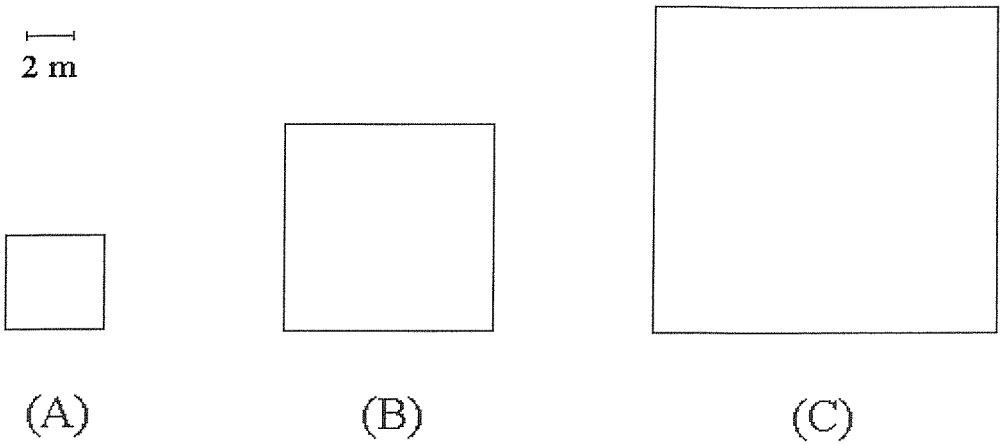

Figure 6.3 Diagram illustrating the principle of self-similarity. The diagram depicts 3 squares, which are of different size, but all have the same shape. Self-similarity dictates that as the scale at which an object is viewed changes, the shape does not change.

$$P = kA^{FD/2} \quad 6.2$$

Where: P = perimeter (m); A = area (m^2); FD = fractal dimension; k = constant of proportionality.

As there are specific problems associated with many of the commonly used shape metrics (for example, many are sensitive to changes in scale (La Gro, 1991)), it was not considered appropriate to use only one shape metric. A number of commonly used shape metrics were used in subsequent analysis to derive estimates of gap shape and allow shape comparison between classification methods. It was not possible to directly compare the numerical results, but possible to examine the trend of the results for each shape metric. Given that the analysis was undertaken on fine ($\simeq$ 4 m) spatial resolution ATM data, any differences in the accuracy of windthrown gap shape representation obtained using the alternative classification methods may be marginal. To investigate this, comparisons were made between the alternative shape representations of the 10 windthrown gaps analysed in Chapter 5 derived from 10 m spatial resolution data.

6.4.7.2.1 Perimeter/area ratio

The perimeter/area ratio (m^{-1}) (PA_R) (Equation 6.3) was used to describe windthrown gap shape, as this is one of the most widely used metrics for shape comparison (e.g. La Gro, 1991; Ripple *et al.*, 1991; Battles *et al.*, 1996; Blackburn and Milton, 1996; Blackburn and Milton, 1997; Jorge and Garcia, 1997; Foody, 1998; Green, 1998).

$$PA_R = P / A \quad (6.3)$$

Where: PA_R = perimeter/area ratio; P = perimeter (m); A = area (m^2).

6.4.7.2.2 Compactness ratio

The compactness ratio (C_R) (Equation 6.4) relates the area of an object to that of a regular object, in this case a circle (Hammond and M^{C}Cullagh, 1974; Unwin, 1981; Chuvieco, 1999). A similar shape metric is based upon the perimeter of an object (e.g. Davis, 1986).

$$C_R = (A / A_C)^{0.5} \quad (6.4)$$

Where: C_R = compactness ratio; A_C = the area of the circle (m^2), which has the same perimeter as the object with area A (m^2).

6.4.7.2.3 Square-pixel metric

The unconstrained form (Sq) (Equation 6.5) of the square-pixel (SqP) metric (Frohn, 1998), based upon the fractal dimension equation (Equation 6.2), was used in subsequent analysis. The values of Sq are not constrained between 0 and 1, but range from 0 to infinity, which Frohn (1998) suggested was a more appropriate form of the metric for investigating landcover.

$$Sq = P / 4 * A^{0.5} \quad 6.5$$

Where: Sq = square-pixel metric; P = perimeter (m); A = area (m^2).

6.4.7.2.4 Landscape dimension

The landscape dimension (L_D) (Equation 6.6) is calculated on the basis of the fractal relationship between area and perimeter (Equation 6.2) for a set of objects (Olsen *et al.*, 1993) and has been used to study the shape of windthrown gaps (Quine and Bell, 1998). L_D can be derived from measures of area and perimeter by regressing the $\log_{10}$ of the perimeter against the $\log_{10}$ of the area. The $\log_{10}$ of k represents the intercept on the Y-axis and L_D is estimated as twice the slope of the regression (Figure 6.4). This shape metric is also widely used, however, k is usually ignored in the calculation (e.g. Milne, 1988; Reinhardt and Ringleb, 1990; Turner, 1990; Gustafson and Parker, 1992; Benson and MacKenzie, 1995; Bettinger *et al.*, 1996; Chuvieco, 1999; Frohn, 1998).

$$L_D = 2 * (\text{Log}_{10}(P) - \text{Log}_{10}(k)) / \text{Log}_{10}(A) \quad 6.6$$

Where: L_D = landscape dimension; P = perimeter (m); A = area (m^2); k = constant of proportionality.

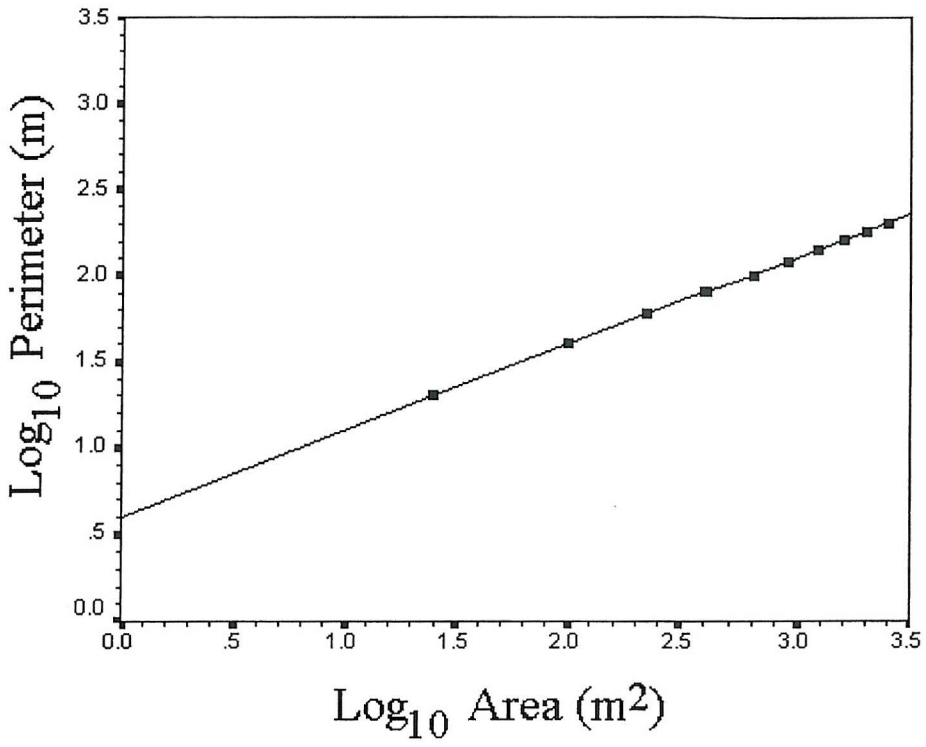

Figure 6.4 Diagram depicting the regression plot used to derive Landscape dimension (Section 6.4.7.3.4), a measure of the shape of a square (adapted from Frohn (1999)). The slope of the regression line is 0.5 and, therefore, the Landscape dimension of a square is 1.0. The intercept on the y-axis is 0.6 and is equal to Log_{10} (k). Therefore, for a square, the constant of proportionality, k, = 4.

6.4.7.2.5 Patch dimension

The patch dimension (P_D) (Equation 6.7) (M^{C}Garigal and Marks, 1995) is derived in the same way from (Equation 6.2) as L_D (Equation 6.6) except that it is applied to individual objects and not a set of objects. In addition, *k* is ignored and assumed to be the same for all objects (e.g. Reinhardt and Ringleb, 1990; Olsen *et al.*, 1993; Baskent and Jordan, 1995; Jorge and Garcia, 1997).

$$P_D = 2\text{Log}_{10}(P) / \text{Log}_{10}(A) \qquad 6.7$$

Where: P_D = patch dimension; P = perimeter (m); A = area (m^2).

6.4.7.2.6 Box counting dimension

The fractal dimension of an object can also be computed using the Box counting method (Barnsley, 1988; Liebovitch and Toth, 1989). The resulting Box counting dimension (BC_D) (Equation 6.8) (Barnsley, 1988; Liebovitch and Toth, 1989; Falconer, 1990), sometimes termed capacity dimension (Liebovitch and Toth, 1989; Falconer, 1990), describes how the shape of an object is resolved, by determining the minimum number of boxes required to cover the entire object (Figure 6.5). The method firstly fits the largest box required to cover the object and then systematically decreases the box size, continually counting the minimum number of boxes required to cover the object until it's shape is fully resolved (Liebovitch and Toth, 1989; Falconer, 1990; Gonzato, 1998; Drake and Weishampel, 2000).

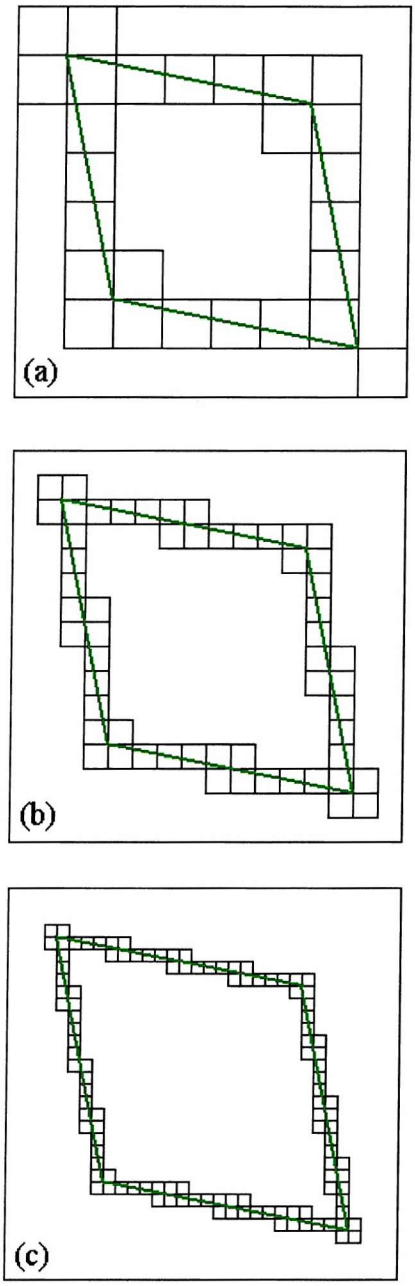

Figure 6.5 A hypothetical object (described by the green line) illustrating the box counting algorithm used to calculate a measure of fractal dimension (adapted from Gonzato (1998)). The algorithm determines the minimum number of boxes required to cover the entire object and systematically decreases the box size (here illustrated as (a) to (b) to (c)), continually counting the minimum number of boxes required to cover the object.

$$BC_D = \lim_{E \to \infty} \log_{10}(N(E)) / \log_{10}(E) \quad 6.8$$

Where: BC_D = Box counting dimension; $N(E)$ = the minimum number of occupied boxes of size E.

6.5 RESULTS

6.5.1 Hard classification windthrown gap identification

There were a total of 183 windthrown gaps, within the unthinned Sitka spruce canopy, identified by the interpretation of the aerial photographs. The hard classification provided a good identification ability, correctly identifying 173 gaps, resulting in an overall gap identification accuracy of 94.5 %, relative to the aerial photographic interpretation. In addition, the hard classification identified an additional 86 gaps within the unthinned region of the monitoring site. This contributed to the error of commission to the windthrown class reported in Table 6.1 and was associated with small gaps not shown in the Forestry Commission's reference data wide tree spacing associated with drains, particularly where drains intersected (Section 5.5.1). Some of these small gaps were identified in the field and or recorded within the Forestry Commission's reference data as 'potential gaps' (Section 3.4.2). As a result, the hard classification provided a more accurate estimate of the number of windthrown gaps present within the wind damage monitoring site than the reference data.

In addition to the windthrown gaps identified within the unthinned Sitka spruce canopy, the classification identified all 32 known windthrown gaps within the larch canopy (gap identification accuracy of 100 %). However, most of these gaps were not

distinct within the thematic map, but joined together and represented as contiguous blocks of pixels primarily allocated to the moorland class. During field surveys, it was observed that these gaps appeared to contain significantly more ground vegetation than the windthrown gaps within the Sitka spruce stands.

6.5.2 Estimation of windthrown gap area, perimeter and shape

6.5.2.1 Windthrown gap area estimates

The RMSE of 144.90 m^2 derived from the hard classification (Table 6.2) indicated that the hard classification provided a poor estimate of windthrown gap area in comparison with the error currently accepted by the Forestry Commission (RMSE 64.76 m^2 (Section 5.5.2)). However, the conventional windthrown gap area estimates from the hard classification were strongly correlated with the Forestry Commission's reference areal estimates (r = 0.96), significant at the 99 % confidence level (Figure 6.6). This hard classification method provided a 'blocky' representation of the windthrown gaps and the softened classifications provided alternative windthrown gap representations (Figure 5.10).

The area estimates derived from fitting a 0.5 posterior probability to gap contour were as strongly correlated with the reference area estimates (r = 0.96, RMSE = 146.05 m^2) as the hard classification estimate of windthrown gap area (r = 0.96) (Figure 6.7). The windthrown gap area estimates derived from fitting 0.84 and 0.79 typicality probability to gap contours were marginally more strongly correlated with the reference gap area estimates (r = 0.97 and 0.97 respectively) than both the hard classification and 0.5

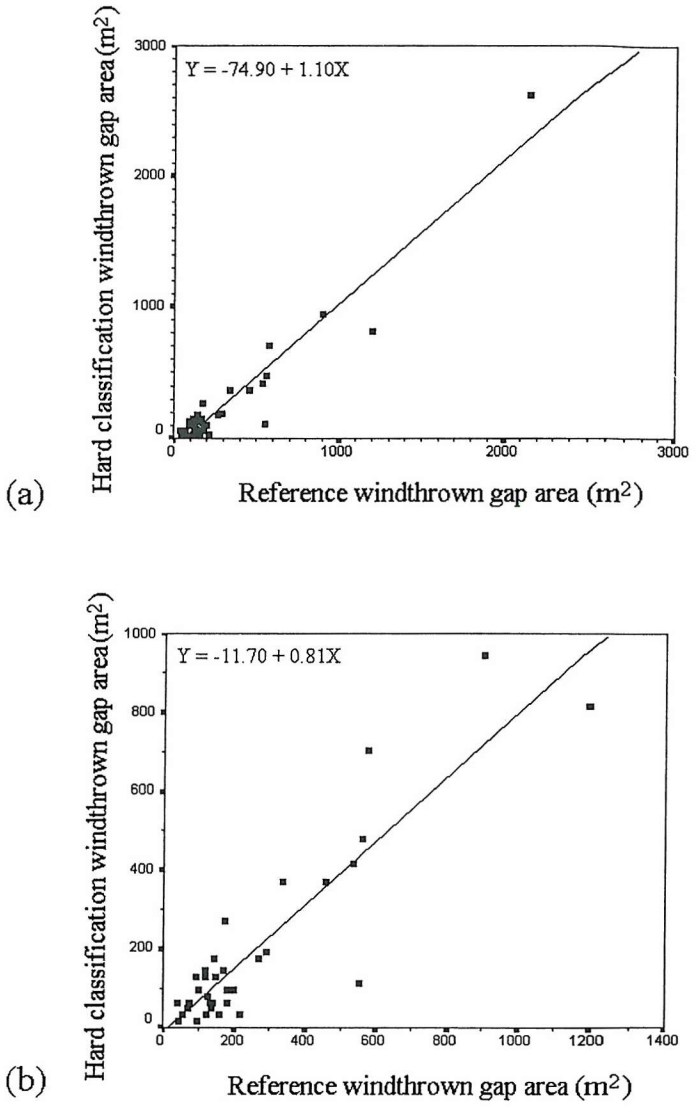

Figure 6.6 Plot of windthrown gap area estimates derived from the hard classification of ≃ 4 m ATM data against reference windthrown gap areas, with linear regression line fitted. The equations describing the regression lines are also provided. (a) depicts the plot for all 36 windthrown gaps investigated, whilst (b) depicts the plot resulting from the removal of the largest windthrown gap plotted in (a).

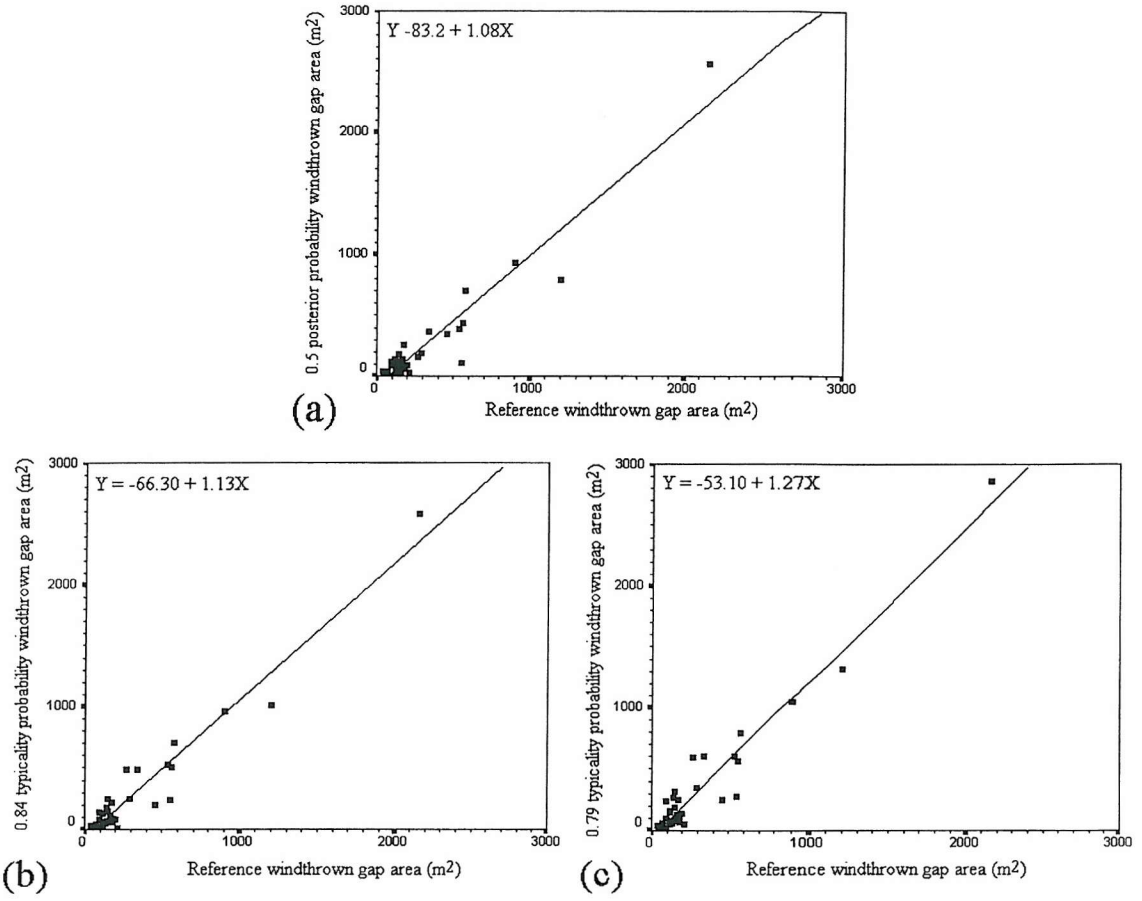

Figure 6.7 Plots of windthrown gap area estimates derived from softening the hard classification of ≃ 4 m ATM data against reference windthrown gap areas, with linear regression lines fitted. The equations describing the regression lines are also provided. The plots represent the windthrown gap area estimates (for all 36 windthrown gaps) derived from: (a) fitting a 0.5 posterior class membership probability contour; (b) fitting a 0.84 typicality class membership probability contour; (c) fitting a 0.79 typicality class membership probability contour.

posterior probability to gap contour (Figure 6.7). However, the 0.84 typicality probability to gap contour provided the most accurate estimation of windthrown gap area of the hard and softened classifications (RMSE = 132.87 m^2). Despite the positive results obtained in Chapter 5, the 0.79 typicality probability to gap contour provided the least accurate estimation of windthrown gap area, as indicated by an RMSE = 170.31 m^2. Therefore, the 0.84 typicality probability to gap contour appeared to provide a more accurate estimate of windthrown gap area, than a hard classification or fitting a 0.5 posterior probability to gap contour. However, it was poor in comparison with the error currently accepted by the Forestry Commission.

6.5.2.2 Windthrown gap perimeter estimates

Both the hard and softened classifications provided estimates of windthrown gap perimeter which were strongly correlated to the reference perimeter estimates ($r > 0.87$), significant at the 99 % confidence level (Table 6.3). The perimeter estimates derived from fitting the 0.5 posterior probability to gap contour were as strongly correlated ($r = 0.87$) (Figure 6.8) to the reference estimates as the hard classification ($r = 0.87$) (Figure 6.9), although it had a larger RMSE than the hard classification (48.10 m and 40.68 m respectively). However, the perimeter estimates derived from fitting both the 0.84 and 0.79 typicality probability to gap contours were more strongly correlated with the reference perimeter estimates than both the hard classification and 0.5 posterior probability to gap contour ($r = 0.90$ and 0.88 respectively) (Figure 6.8). In addition, both typicality

probability contours more accurately represented the perimeter (RMSE = 37.53 m and 38.09 m respectively) than the hard classification.

	RMSE (m^2)	r
Forestry Commission's 10 m data	64.76	0.83
hard classification	144.90	0.96
0.5 posterior contour	146.05	0.96
0.84 typicality contour	132.87	0.97
0.79 typicality contour	170.31	0.97

Table 6.2 Table presenting a summary of the area estimation results (for 36 windthrown gaps) derived from the analysis of the ≃ 4 m ATM data. This table indicates the RMSE and Pearson's correlation coefficient, *r*, resulting from comparison of each area estimation method against the reference data which has spatial resolution of 1 m (Section 3.4.2). The 'Forestry Commission's 10 m data' represents the original vector representation of the 16 windthrown gaps analysed in Chapter 5, rasterised to a spatial resolution of 10 m, which is the spatial resolution of the data the Forestry Commission use for wind damage monitoring. 'Hard classification' represents the windthrown gap area estimates derived from the conventional maximum-likelihood classification; '0.5 posterior contour' represents the 0.5 posterior probability to gap contour area estimates; and 'typicality contour' represents the typicality probability contour to gap area estimates at the given probability (0.84 or 0.79).

	RMSE (m)	r
hard classification	40.68	0.87
0.5 posterior contour	48.10	0.87
0.84 typicality contour	37.53	0.90
0.79 typicality contour	38.09	0.88

Table 6.3 Table presenting a summary of the perimeter estimation results (for 36 windthrown gaps) derived from the analysis of the ≃ 4 m ATM data. This table indicates the RMSE and Pearson's correlation coefficient, *r*, resulting from comparison of each perimeter estimation method against the reference data which has spatial resolution of 1 m (Section 3.4.2). 'Hard classification' represents the windthrown gap perimeter estimates derived from the conventional maximum-likelihood classification; '0.5 posterior contour' represents the 0.5 posterior probability to gap contour perimeter estimates; and 'typicality contour' represents the typicality probability contour to gap perimeter estimates at the given probability (0.84 or 0.79).

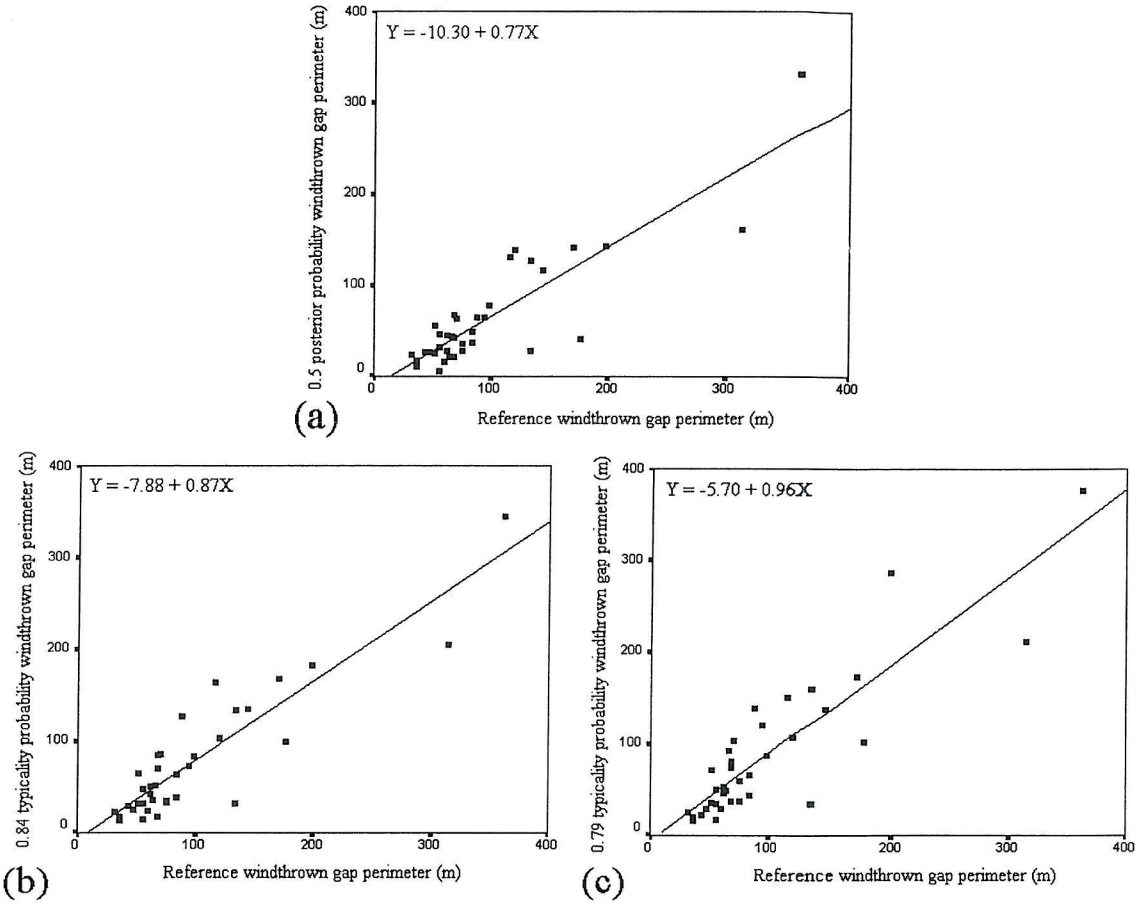

Figure 6.8 Plots of windthrown gap perimeter estimates derived from softening the hard classification of ≃ 4 m ATM data against reference windthrown gap perimeter, with linear regression lines fitted. The equations describing the regression lines are also provided. The plots represent the windthrown gap perimeter estimates (for all 36 windthrown gaps) derived from: (a) fitting a 0.5 posterior class membership probability contour; (b) fitting a 0.84 typicality class membership probability contour; (c) fitting a 0.79 typicality class membership probability contour.

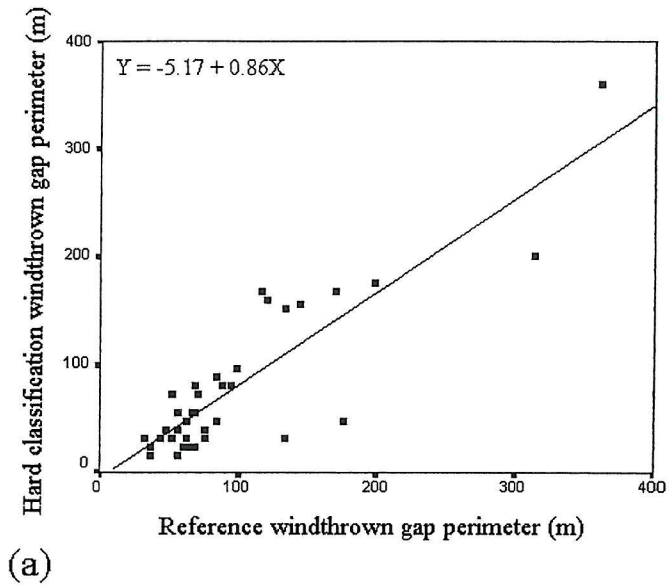

(a)

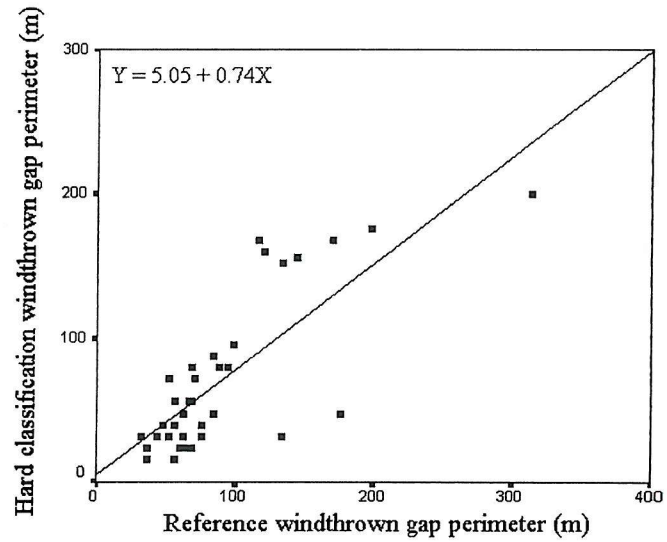

(b)

Figure 6.9 Plot of windthrown gap perimeter estimates derived from the hard classification of ≃ 4 m ATM data against reference windthrown gap perimeters, with linear regression line fitted. The equations describing the regression lines are also provided. (a) depicts the plot for all 36 windthrown gaps investigated, whilst (b) depicts the plot resulting from the removal of the largest windthrown gap plotted in (a).

6.5.2.3 Windthrown gap shape estimates

The results (Table 6.4) based upon windthrown gap shape estimates derived from $\simeq$ 4 m ATM data, indicated that the 0.84 typicality probability to gap contour provided a more accurate representation of windthrown gap shape than the hard classification. This was evident as the results from 4 of the shape metrics suggested it provided more accurate estimates of windthrown gap shape than the hard classification, based upon RMSE of the shape estimates. Only 2 of the shape metrics used (L_D and BC_D) suggested that the 0.79 typicality probability to gap contour and 0.5 posterior probability to gap contour provided more accurate estimates of gap shape than the hard classification. The 2 shape metrics (PA_R and P_D) which suggested the 0.84 typicality probability to gap contour provided a less accurate estimate of gap shape than the hard classification appeared to suffer from systematic inconsistencies. For example, gap representations with the same shape were assigned different shape estimates (Figure 6.10). These inconsistencies affected the results from 8 of the 36 windthrown gaps. These 8 gaps were removed from the analysis and the results from the remaining 28 windthrown gaps (Table 6.4) indicated that although the trend of the results was not affected, the magnitude of the RMSE improved.

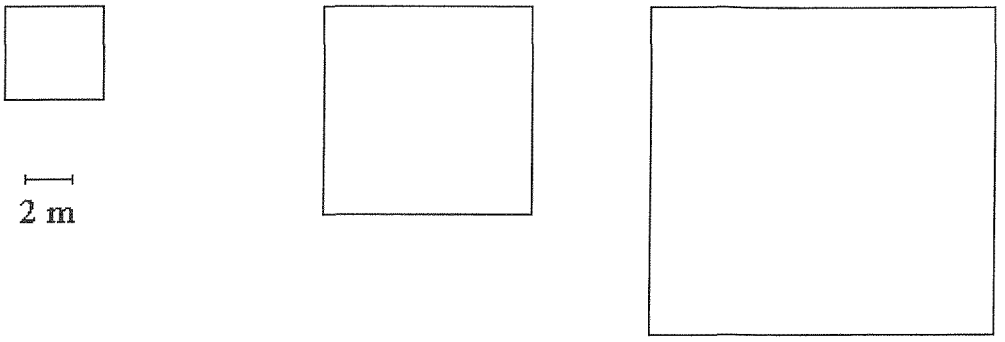

(A)	(B)	(C)
$PA_R = 1.00$	$PA_R = 0.50$	$PA_R = 0.33$
$C_R = 0.89$	$C_R = 0.89$	$C_R = 0.89$
$Sq = 1.00$	$Sq = 1.00$	$Sq = 1.00$
$P_D = 2.00$	$P_D = 1.67$	$P_D = 1.56$
$BC_D = 2.00$	$BC_D = 2.00$	$BC_D = 2.00$

Figure 6.10 Diagram depicting squares of width (A) 4m, (B) 8m and (C) 12m respectively. The estimated shape of each square derived using the alternative shape metrics (Section 6.4.7.2) are illustrated (L_D has not been used as this is calculated for set of objects and not individual objects). The shape estimates indicate that PA_R (Perimeter/area ratio) and P_D (Patch dimension) are sensitive to changes in scale (i.e. the size of the square). However, C_R (Compactness ratio), Sq (Square-pixel metric) and BC_D (Box counting dimension) provide estimates of shape which are insensitive to changes in scale.

	PA_R (m^{-1})	Sq	C_R	L_D	P_D	BC_D
hard	0.175	255.775	0.181	0.128	0.111	0.162
classification	(0.134)	(273.133)	(0.137)	(0.084)	(0.096)	(0.146)
0.5 posterior	0.499	299.252	0.240	0.012	0.141	0.133
contour	(0.151)	(323.404)	(0.208)	(0.032)	(0.115)	(0.127)
0.84 typicality	0.351	227.852	0.173	0.002	0.114	0.118
contour	(0.141)	(238.807)	(0.140)	(0.038)	(0.099)	(0.127)
0.79 typicality	0.184	300.077	0.189	0.085	0.117	0.108
contour	(0.133)	(327.955)	(0.161)	(0.118)	(0.103)	(0.105)

Table 6.4 Table presenting a summary of the RMSE results (for 36 windthrown gaps) for each shape metric from representations of windthrown gap shape derived from the hard and softened classifications of $\simeq$ 4 m data (the results in brackets are based upon the analysis of 28 gaps). 'Hard classification' denotes the hard classification estimates, '0.5 posterior contour' the 0.5 posterior probability to gap contour estimates and 'typicality contour' the typicality probability contour to gap estimates at the given probability (0.84 or 0.79). The results illustrate different shape metrics provide different estimates of windthrown gap shape and, therefore, it is only appropriate to examine the trend of the results within a single shape metric.

The results based upon estimates of windthrown gap shape derived from 10 m spatial resolution remotely sensed data (Table 6.5), indicated that the 0.84 typicality probability to gap contour again provided the most accurate representation of windthrown gap shape, whichever shape metric was used to quantify shape. In addition, 0.79 typicality probability to gap contour and 0.5 posterior probability to gap contour also provided a more accurate representation of windthrown gap shape than the hard classification, for five out of the six shape metrics.

	PA_R (m^{-1})	Sq	C_R	L_D	P_D	BC_D
hard classification	0.270	118.449	0.216	0.122	0.198	0.220
0.5 posterior contour	0.169	59.833	0.124	0.216	0.117	0.095
0.84 typicality contour	0.258	84.366	0.206	0.010	0.175	0.134
0.79 typicality contour	0.252	131.508	0.194	0.026	0.176	0.140

Table 6.5 Table presenting a summary of the RMSE results for each shape metric from representations of windthrown gap shape derived from the hard and softened classifications of 10 m data (for the 10 windthrown gaps studied in Chapter 5). 'Hard classification' denotes the hard classification estimates, '0.5 posterior contour' the 0.5 posterior probability to gap contour estimates and 'typicality contour' the typicality probability contour to gap estimates at the given probability (0.84 or 0.79). The results illustrate different shape metrics provide different estimates of windthrown gap shape and, therefore, it is only appropriate to examine the trend of the results within a single shape metric.

6.6 DISCUSSION

The results indicated that the hard classification appeared to accurately estimate the number of windthrown gaps present within the monitoring site and also identify a number of windthrown gaps that were not represented in the reference data. As with the results from Section 5.5.1, the maximum-likelihood classifier allocated features associated with wider than normal tree spacing, such as drainage ditches, damaged canopy, gaps overlooked during the aerial photographic interpretation, or thinning lines, to the gap class. This supported the earlier conclusions from Section 5.6, that although these pixels were apparently misclassified, they were actually small windthrown or windsnap gaps that had not been identified by the aerial photointerpretation. Quine and Bell (1998) specifically noted that it had been difficult to distinguish small windthrown gaps. Usually, any

differences between the classification output and the reference data are the result of classification error, however, these pixels represent errors associated with the reference data (Congalton and Green, 1993).

These pixels may be removed using a neighbourhood filter, however, as noted in Section 5.6, this would reduce the value of the resulting spatial information which may be derived from the hard classification. It was not possible to distinguish between those gaps associated with wind damage and other canopy irregularities. In particular, there were problems in spatially differentiating individual windthrown gaps within areas which had been thinned, or there was poor tree growth, and the hard classification tended to spatially amalgamate windthrown gaps with these areas.

The results also suggested that although it was possible to identify windthrown gaps within a stand of larch, it was not possible to differentiate individual windthrown gaps due to a number of factors. First, since larch lets more light reach the understory, there is a much less contrast between a gap within a spruce canopy and one within a larch canopy. Secondly, as the larch was planted in a narrow strip, there was considerable interaction with the surrounding spruce canopy. Thirdly, the windthrown larch trees did not maintain their canopies as they are deciduous, unlike the windthrown spruce trees and, therefore, the windthrown signature used in the hard classification did not provide an accurate representation of the remotely sensed response from a windthrown larch gap. Fourthly, the remotely sensed data were collected at a time of the year when the larch had not fully developed an intact canopy and, therefore, it was difficult to distinguish between larch canopy and the understory using ATM data acquired in spring.

The RMSE results of the estimates of windthrown gap areas and perimeters indicated that the hard and softened classifications provided poor estimates of these spatial characteristics. However, the estimates were significantly correlated with the reference data. Crapper (1980) suggested that when estimating areas from remotely sensed data, in particular, when the areas are small or the boundaries are contorted, both circumstances relevant to this study, the relative errors may be very high due to errors of commission or omission at the boundary.

A hard classification generally requires less time to obtain estimates of area and perimeter for a large number of windthrown gaps, than by aerial photographic interpretation. This saving in processing time may outweigh the poor accuracy of the estimates, if estimates are required quickly, or for a large number of gaps at a landscape scale (Quine and Bell, 1998). The increase in area and perimeter estimation accuracy derived from a softened classification, by selecting an appropriate typicality class membership to gap contour, may outweigh the small additional processing time. However, this is dependent upon the use of an appropriate class membership contour. As there may be no obvious appropriate class membership contour, it may be necessary to use a selection of contours, for example in a pilot study (Section 5.4.5.2), and then select the most appropriate contour based upon the results obtained.

The results also indicated that fitting an appropriate typicality probability to gap contour may provide a more accurate representation of the windthrown gap shape than that derived from a conventional hard classification. There was, however, an inconsistency within the estimates of windthrown gap shape that requires clarification. It was apparent

that windthrown gaps with a similar shape could have different estimates of shape (e.g. Figure 6.10). This affected 8 windthrown gaps and these windthrown gaps were removed from the analysis to determine whether they had a significant impact upon the results (Table 6.4). The subsequent results based upon the analysis of the remaining 28 windthrown gaps indicated that the overall trend was not affected. However, this indicated the need for careful interpretation of estimates of shape derived from commonly used shape metrics.

Analysis of estimates of windthrown gap shape derived from classification of ATM data with a spatial resolution of 10 m, indicated the typicality probability contours fitted (0.84 and 0.79) provided more accurate shape estimates than the hard classification (Table 6.5). In addition, the magnitude of the increase in accuracy was greater than for the shape estimation results at a spatial resolution of $\simeq$ 4 m. Therefore, as the spatial resolution of remotely sensed data becomes finer, the magnitude of any increase in shape estimation accuracy obtained from the use of softened classifications is likely to become less significant. However, until inexpensive remotely sensed data with a spatial resolution finer than $\simeq$ 4 m are routinely available for wind damage investigations, softened classifications have the potential to provide improved estimates of windthrown gap shape (Table 6.6). In contrast, as the spatial resolution of the remotely sensed data becomes coarser and the size of the windthrown gap tends to that of a single pixel, the shape of the windthrown gaps will become less complex and hence, estimates of windthrown gap shape less realistic, irrespective of which classification method is used. There is, therefore, likely to be a spatial scale range, relating to the size range of the windthrown gaps under

analysis, within which softened classifications will provide a worthwhile improvement in shape estimation over a hard classification.

Acquiring information on windthrown gap shape is important for understanding how the shape influences the susceptibility of the surrounding forest stand to further wind damage, in terms of the risk of windthrown gap expansion. It is apparent from the results that shape analysis using some commonly used shape metrics can provide inconsistent results (Figure 6.10). Therefore, it may be inappropriate to rely upon an individual shape metric as the basis for objective shape comparison. However, the general trend of the results provided evidence to support the initial visual conclusion that the softened classifications provided a more realistic representation of windthrown gap shape than the conventional hard classification.

It has been suggested that small gaps are simple in shape (Runkle, 1985; Blackburn and Milton, 1996). Certainly, the larger a gap, the greater the possibility for a more irregular boundary, although this will be scale dependent. However, it is not just the overall complexity of the shape which is of interest to forest managers. Rather, it is the combination of shape and orientation in relation to the prevailing wind direction which can influence the risk of windthrown gap expansion through further wind damage (Kimmins, 1997). For example, Figure 6.11 shows the influence of gap shape and orientation on the vulnerability of the residual forest to windthrow. If accurate spatial representations of windthrown gap shape can be derived from softened classifications, then it may be possible to determine a level of risk for gap expansion. However, this risk

Platform	Sensor	Spatial resolution (m)	Number of wavebands	Waveband edges (nm)	Price per km^2 (£)
SPOT	HRV				0.44
	panchromatic mode	10	1	510 - 730	
	multispectral mode	20	3	500 - 590 610 - 680 790 - 890	
Landsat	TM	30 (except in waveband 6)	7	450 - 520 520 - 600 630 - 690 760 - 900 1550 - 1750 2080 - 2350 10400 - 12500	0.02
Ikonos	panchromatic mode	1	1	450 - 900	19.23
	multispectral mode	4	4	450 - 530 520 - 610 640 - 720 770 - 880	

Table 6.6 Technical information and current prices for the purchase of remotely sensed data available from conventional coarse spatial resolution satellite sensors SPOT HRV and Landsat-7 TM, as well as from a new fine spatial resolution satellite sensor carried aboard Ikonos. SPOT HRV data (spatial resolution of 10 m in panchromatic mode, 20 m in multispectral mode) are sold as 60 km by 60 km scenes (total cost £1600). Landsat TM data (spatial resolution of 15 m in panchromatic mode, 30 m in multispectral mode (except thermal waveband)) are sold as 170 km by 170 km scenes (total cost £466). Ikonos sensor data (spatial resolution of 1 m in panchromatic mode, 4 m in multispectral mode) are available as 1 km by 1 km scenes, although the minimum order must be worth £1998 ($3000). The cost of acquiring fine spatial resolution satellite sensor data is significantly higher than the cost of acquiring coarse spatial resolution satellite sensor data per unit area. Financial information was supplied by National Remote Sensing Centre on 30 July 2000, with additional sensor information supplied by Space Imaging, SPOT Image Corporation and NASA (see Appendix 3).

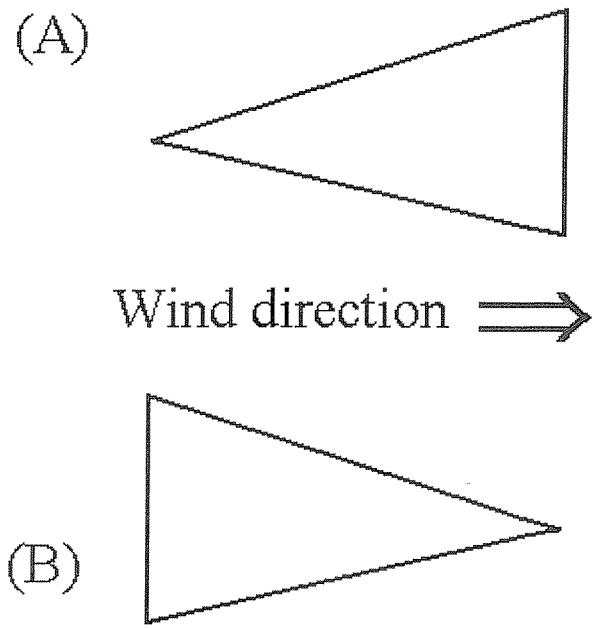

Figure 6.11 Diagram depicting 2 hypothetical gaps, illustrating the influence of gap shape and orientation, with respect to the prevailing wind, on the vulnerability to windthrow (adapted from Kimmins (1997)). Both gap (A) and (B) have the same shape. Gap (B) has the greatest risk of further wind damage, as the wind accelerates within the gap due to the funneling effect of the gap narrowing, whilst within gap (A) there is little or no wind acceleration. However, the risk of further wind damage will also be influenced by the orientation of the prevailing wind with respect to the sharpness of the gap-canopy boundary. For example, a sharp boundary has the highest windthrow risk due to the sudden exposure of stand interior trees, whilst a tapered boundary guides the wind over the gap-canopy boundary and hence, has the lowest windthrow risk.

will be influenced by the nature of the windthrown gap boundary, which may not be sharply delineated (Peterken, 1996). For example, newly exposed trees have a higher likelihood of being windthrown, than trees protected by a bank of trees already windthrown. Therefore, to attempt to determine the risk of windthrown gap expansion it is necessary to derive information on both windthrown gap shape and the sharpness of the windthrown gap boundary. This is a topic which will be considered in further detail in Chapter 7.

6.7 SUMMARY

With reference to the Chapter aims (Section 6.2), the results indicated that for this study, although it was possible to identify windthrown gaps within a stand of a tree species other than Sitka spruce, it was not possible to differentiate individual windthrown gaps. For those individual windthrown gaps accurately identified within a canopy of Sitka spruce, the conventional hard classification provided poor estimates of spatial windthrown gap characteristics, specifically gap area, perimeter and shape. More accurate estimates of these spatial characteristics were obtained by softening the output of the hard classification to produce typicality probabilities. However, this accuracy is dependent upon selecting an appropriate class membership contour.

CHAPTER 7

MAPPING WINDTHROWN GAP BOUNDARY SHARPNESS FROM A SOFTENED CLASSIFICATION

7.1 INTRODUCTION

Allocating a hard boundary is convenient (Pukkala *et al.*, 1993) and provides an operationally acceptable technique for deriving estimates of windthrown gap characteristics, which may be required for forest management planning purposes. For example, whether the volume of wood lost due to wind damage warrants salvage felling. However, the allocation of a hard boundary limits the information available on the variability of windthrown gap-canopy boundary sharpness. The acquisition of this information may be beneficial to forest management, since boundary sharpness can influence the risk of wind damage progression (Quine *et al.*, 1995; Gardiner and Stacey, 1996). For example, trees located on sharp boundaries have a severe wind loading and increased vulnerability to wind damage (Gardiner and Stacey, 1996). A possible alternative to allocating hard boundaries to windthrown gaps, may be to treat the windthrown gap-canopy boundaries as being soft. This requires the estimation of a measure of boundary sharpness.

The results presented in Section 6.5.2 indicated that fitting an appropriate class membership probability contour to a typicality probability map provided a more accurate

representation of windthrown gap area, perimeter and shape, than a conventional maximum-likelihood classification. This windthrown gap representation was based upon allocating a hard gap-canopy boundary (Section 6.4.7.1), whose length was described by perimeter and complexity described by shape. This hard gap-canopy boundary derived from a maximum-likelihood classification was represented as the boundary between two adjoining pixels, one of which was allocated to the gap class (i.e. windthrown, water and moorland) and the other allocated to the canopy class (i.e. spruce canopy and larch canopy). The hard gap-canopy boundary derived from the typicality and posterior probability maps was represented by fitting a class membership probability contour.

7.2 CHAPTER AIMS

This Chapter will use fine ($\simeq$ 4 m) spatial resolution remotely sensed data to investigate the potential of softened classifications to derive information on the sharpness of the gap-canopy boundaries of the set of 36 windthrown gaps previously analysed in Chapter 6. Specifically, there are 2 questions which will be addressed:

- Can accurate maps depicting windthrown gap-canopy boundary sharpness be derived from softened classification outputs?
- Can the sharpness of the windthrown gap-canopy boundary be used to infer the general direction of treefall?

7.3 METHODOLOGY

The potential to use the rate of change in class membership probability to map gap-canopy boundary sharpness was investigated using typicality and posterior probability maps derived by softening the output from a maximum-likelihood classification (Section 4.5.2).

7.3.1 Preliminary study

The probability maps analysed in this Section were derived from the hard classification of the $\simeq 4$ m ATM data in Section 5.4.2. A sample windthrown gap (GP26) (Figure 3.6) was selected for preliminary study and a range of class membership probability contours to the gap class (i.e. windthrown and moorland classes had been amalgamated) were fitted to the typicality and posterior probability maps. Visual interpretation of these fitted contours suggested that the rate of change in class membership probability for this windthrown gap was not uniform along its perimeter.

The pattern of class membership probability change at the boundary of this windthrown gap (GP26) was analysed using transects at a range of compass bearings. These transects dissected the gap centre and were used to sample the rate of change in class membership probability across the gap-canopy boundary and within the gap. A field survey was undertaken in March 1999 to provide reference data on the sharpness of the gap-canopy boundary of this sample windthrown gap (GP26) (Figure 7.1).

However, during the intervening period between the acquisition of field survey data in March 1999 and the ATM sensor data in April 1994, it was possible that the

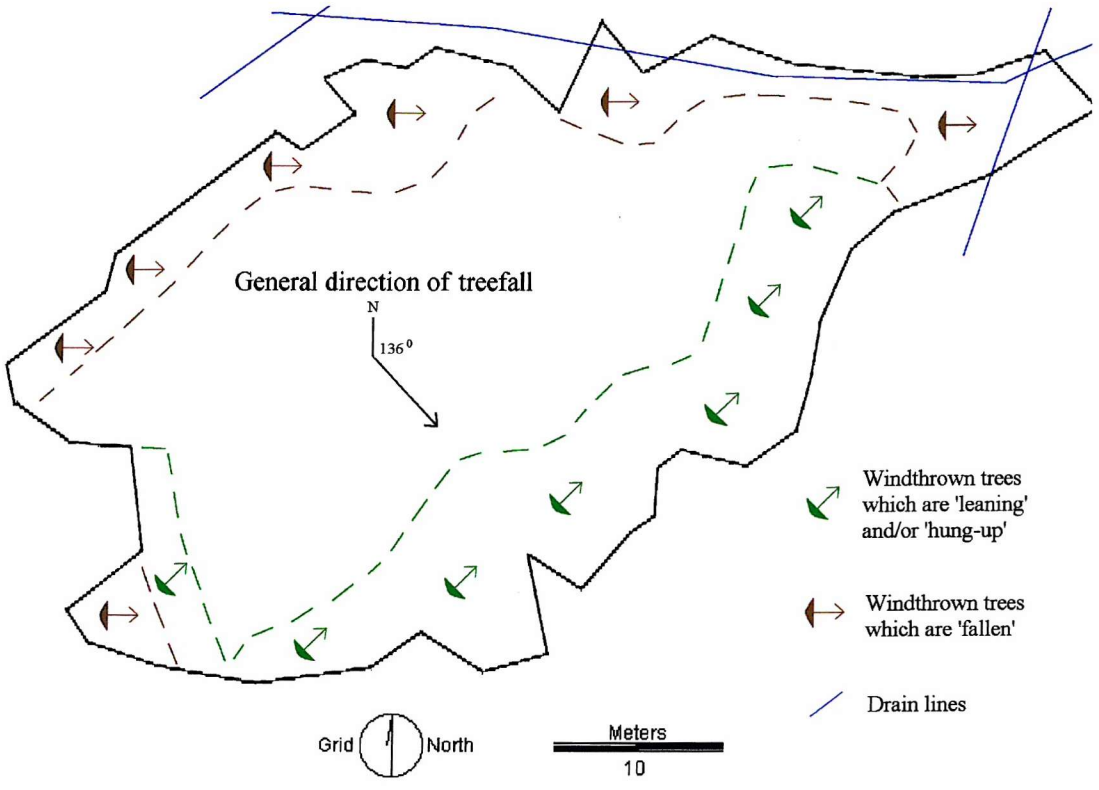

Figure 7.1 Map of the sample windthrown gap (GP26, identified in Figure 3.6), derived from a field survey in March 1999, which illustrates the sharpness of the gap-canopy boundary. The gap-canopy boundary of this gap is represented by the solid black line. The general direction of treefall is also indicated. The gap-canopy boundary represents the 'expanded gap' boundary which is illustrated in Figure 2.4. The region of the gap dominated by windthrown trees which are 'leaning' and/or 'hung-up' (Section 3.4.1) is bounded by the dashed green line. As these trees are supported by standing trees, this region of the gap is characterised as having a gradual gap-canopy boundary. The region of the gap dominated by exposed rootplates, bare soil and understory vegetation resulting from 'fallen' windthrown trees is bounded by the dashed brown line. This region of the gap is characterised as a sharp gap-canopy boundary.

windthrown gaps had expanded through progressive wind damage. It was assumed that the general pattern of boundary sharpness had not changed significantly over this period,. Unfortunately, there was no clear evidence from the field or aerial photographs available to verify this assumption that the field survey data from 1999 provided an operationally accurate representation of gap-canopy boundary sharpness in 1994.

7.3.2 Derivation of boundary sharpness maps from probability maps

The preliminary study on a sample windthrown gap (GP26) using transects to sample the rate of change in class membership probability at the gap-canopy boundary appeared to provide promising results. The rates of change in class membership probability at the gap-canopy boundary were not uniform and appeared to indicate differences in boundary sharpness. The preliminary study was, therefore, expanded to map the boundary sharpness of each individual windthrown gap (a total of 36 windthrown gaps) analysed in Section 6.4.7. The typicality and posterior probability maps to the amalgamated gap class (derived from 3 classes: windthrown, water; and moorland (Section 6.4.3)) derived in Section 6.4.5.2, were used to derive boundary sharpness maps. These boundary sharpness maps represented the rate of change in class membership probability between 2 contours fitted to the probability maps. One contour represented the best representation of windthrown gap area, perimeter and shape, as determined from the results of Chapter 6 (i.e. 0.84 typicality probability to gap and 0.5 posterior probability to gap). The other contour was arbitrarily selected, but spatially constrained within the

contour providing the best windthrown gap representation, so that analysis would concentrate upon the gaps, rather than the surrounding canopy.

Contours were fitted to the typicality probability map at the 0.84 and 0.89 typicality class membership probability to gap and rasterised to a spatial resolution of 0.5 m in order to facilitate subsequent processing to compute measures of boundary sharpness. This was also undertaken by fitting 0.50 and 0.90 posterior class membership probabilities to gap contours to the posterior probability map. The 0.5 m spatial resolution used for this vector-to-raster conversion was selected to provide a compromise between data volume and the accuracy of the rasterised representation of the fitted contours (Van Der Knaap, 1992). Interpolating between these rasterised contours allowed degrees of slope to be computed and these slope measurements were used as measures of boundary sharpness.

It was not the intention to investigate boundary sharpness in detail, rather investigate the general pattern of boundary sharpness. Specifically, to map where the boundary was sharpest and where it was most gradual. This was undertaken by allocating the degrees of slope into quartiles which were then mapped. Since only the sharpest slope and most gradual slope regions of the gap-canopy boundary were of interest, only the quartiles representing these extremes, quartile 1 (most gradual slope) and quartile 4 (sharpest slope), were used in subsequent analysis.

7.3.3 Field survey reference data

A field survey was undertaken in July 1999 to acquire, for each of the 36 windthrown gaps, reference data on the sharpness of the gap-canopy boundaries.

Specifically, this field survey concentrated upon mapping, for each windthrown gap, where the gap-canopy boundary was sharpest and where it was most gradual (this is unlikely to have changed during the time between ATM data acquisition and field survey data acquisition). These extremes were loosely characterised as: 1) a sharp boundary resulting from windthrown trees having fallen away from the boundary and hence, an abrupt change between canopy and gap (Figure 7.2) and; 2) a gradual boundary where leaning and hung-up windthrown trees (described in Section 3.4.1) were supported by standing trees and resulted in a banking structure (Figure 7.2). These mapped data acquired during this field survey were used as field reference maps against which the boundary sharpness maps derived from the probability maps could be compared.

Unfortunately it was not possible to co-register these field reference maps to the boundary sharpness maps. As noted in Section 4.4, there are problems associated with using a GPS to accurately acquire location data, such as for the gap-canopy boundary, largely due to the high stocking density and relatively dense canopy (Quine *et al.*, 1997). It was considered unsafe to venture beyond the gap-canopy boundary into the windthrown gap interior, where interference due to the stand canopy may not have affected the use of a GPS as much. During the field survey, compass bearings had been used to map the gap-boundary structure. This provided a means of geographically referencing the field data, with respect to north. Subsequent analysis, therefore, relied upon overlaying the field reference maps and the boundary sharpness maps in order to obtain the best visual fit between the maps, which were all orientated with respect to north.

Figure 7.2 Photograph of the boundary of the sample windthrown gap (GP26) depicted in Figure 7.1, illustrating the variability of the gap-canopy boundary sharpness. On the left of the photograph is a sharp boundary resulting from windthrown trees having fallen away from the boundary and this is characterised by the exposed rootplates, bare soil and understory vegetation. On the right of the photograph is a gradual boundary resulting from leaning and hung-up windthrown trees being supported by standing trees This results in the banking structure evident, which provides a tapered gap-canopy boundary.

7.3.4 Digital elevation model (DEM)

In addition to the field reference maps depicting boundary sharpness a DEM representing canopy height for Cwm Berwyn Forest (Miller *et al.*, 1997) was used to evaluate the analysis of the ATM data. This DEM, derived by digital photogrammetry from colour aerial photographs acquired in 1957 (prior to afforestation on the site) and 1995, had a horizontal spatial resolution of 1 m and vertical spatial resolution of 0.25 m (Miller *et al.*, 1997). This DEM was co-registered to the boundary sharpness maps derived from the probability maps and used as a soft reference data set to validate these boundary sharpness maps derived from the probability maps.

Analysis was undertaken to determine whether the windthrown gaps had expanded between the acquisition of the ATM data in 1994 and the acquisition of the aerial photographs in 1995 used to generate the DEM. Area estimates for 30 windthrown gaps, randomly selected from throughout the monitoring site, were derived from the Forestry Commission's vector data for 1994 and 1995 (rasterised to a spatial resolution of 1 m). These area estimates were analysed using a Wilcoxon paired-sample test (Zar, 1999). The results indicated that the windthrown gaps within the monitoring site had not significantly increased in area ($P > 0.01$). The DEM was, therefore, assumed to provide an accurate representation of the forest canopy in 1994.

A map depicting canopy height change was derived from the DEM by linear interpolation and degrees of slope subsequently derived. These degrees of slope representing the rate of change in canopy height were allocated into quartiles and mapped.

This canopy height change map was used to validate the boundary sharpness maps derived from the probability maps.

7.3.5 Direction of treefall

In addition to characterising the sharpness of the gap-canopy boundary, the rate of change in class membership probability may provide an indication of the general direction the windthrown trees had fallen. The general directions of treefall for the trees within 34 of the 36 windthrown gaps were acquired during the field survey in July 1999 (the directions of treefall within the remaining 2 gaps were complex and it was not possible to unambiguously identify a general direction of treefall). These treefall data were initially analysed to investigate whether the direction of treefall was the same for each windthrown gap. This may provide a general indication of the prevailing wind direction and hence, a crude means of predicting the likely direction of windthrow progression at stand boundaries.

For each of the 34 windthrown gaps, the compass bearing from the midpoint of each region primarily represented by boundary sharpness quartiles 1 and 4 was estimated and orientated from quartile 4 (sharpest boundary) towards quartile 1 (most gradual boundary) (Figure 7.3). This compass bearing was used as an estimate of direction of treefall for that gap.

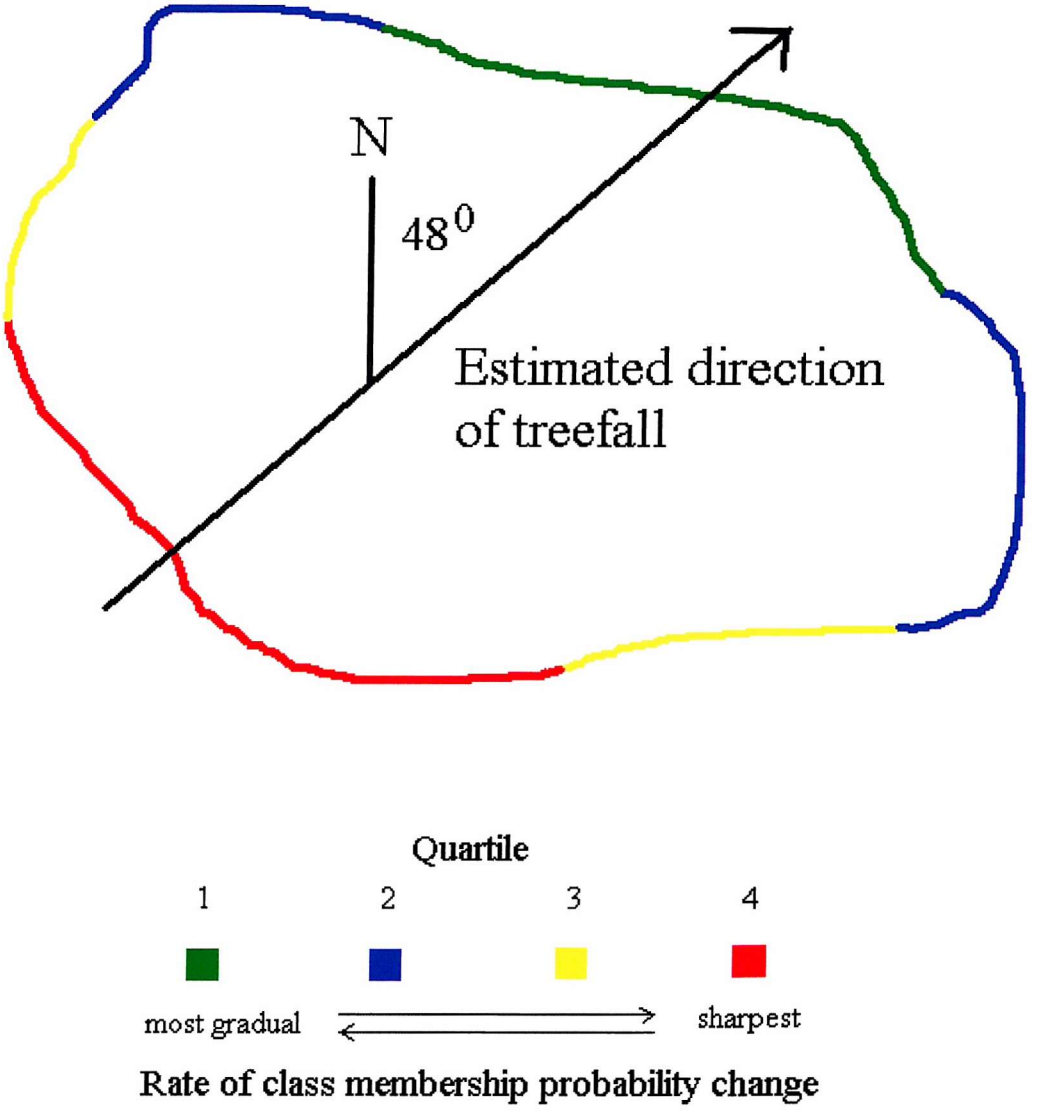

Figure 7.3 Boundary sharpness map for a hypothetical windthrown gap, illustrating the estimated direction of treefall for this gap. The direction of tree fall is taken as the compass bearing from the mid-point of each primary region roughly characterised by boundary sharpness quartiles 1 (most gradual boundary) and 4 (sharpest boundary) and orientated from quartile 4 towards quaartile 1.

7.4 RESULTS

7.4.1 Preliminary study

The rates of change in class membership probabilities along the transects were not uniform and differences were found at the gap-canopy boundary of the sample windthrown gap (GP26). This can be illustrated by depicting the variations in posterior class membership probabilities observed moving eastwards along the west-east transect (Figure 7.4). In the region of the forest stand to the west of the gap, which the hard classification allocated to the canopy class (Figure 7.4(a)), the probability of class membership to both the gap and moorland classes was very low (approximately 0.0), whilst the probability of membership to the canopy class was close to 1.0. At the western gap-canopy boundary the class membership probability to the canopy class decreased sharply and the probability of membership to the gap class increased sharply. There was also an associated small, but noticeable, increase in the probability of membership to the moorland class to 0.05. At the gap centre, the probability of class membership to gap was close to 1.0, whilst the probability of membership to the canopy and moorland classes was close to 0.0.

At the eastern gap-canopy boundary the probability of class membership to gap decreased and the probability of class membership to canopy increased, whilst there was no change in the probability of membership to the moorland class. However, at this boundary the rate of change in membership probabilities was more gradual than at the western boundary. The rate and magnitude of these changes in class membership probabilities appeared to describe structural characteristics of the gap-canopy boundary. The greatest contrast in boundary sharpness was illustrated by the class membership

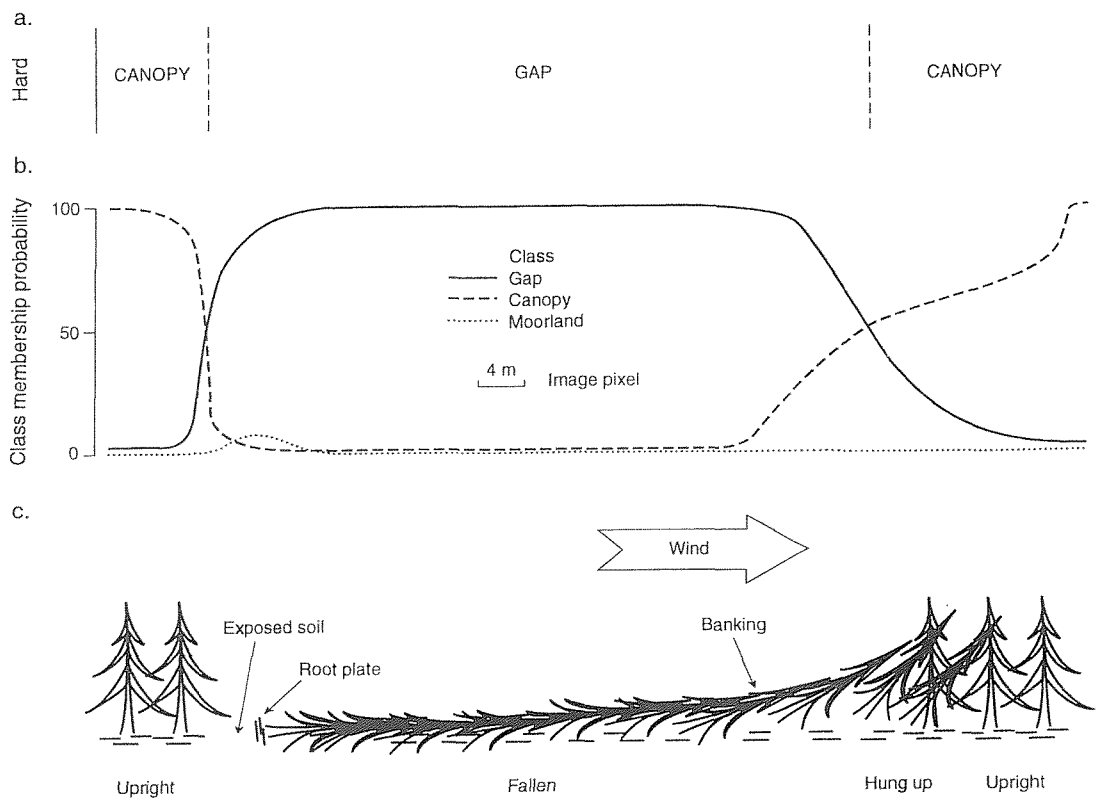

Figure 7.4 A west-east transect (from left to right) through the sample windthrown gap (GP26) depicted in Figure 7.1: (a) represents the output from the hard classification and notes the classes allocated; (b) represents the pattern of posterior class membership probability change to each class (i.e. windthrown, canopy and moorland classes); (c) represents the physical characteristics of the windthrown gap-canopy boundary, with the differences in boundary sharpness evident.

probability change along the west-east transect. However, the other transects (although not illustrated) also indicated that the rates of change in posterior class membership probabilities at the gap-canopy boundary were not uniform. These transects suggested that factors such as shadow, did not present significant problems, as the rates of change in posterior class membership probabilities at the gap-canopy boundary appeared to accurately indicate boundary sharpness. The effects of shadow are largely associated with the southern gap-canopy boundary, as the surrounding trees prevent direct illumination of that region of the gap.

Detailed analysis of the structure and rate of class membership probability change was undertaken for this sample gap (GP26). Figure 7.1 depicts the structure of the gap-canopy boundary, whilst Figure 7.5 and Figure 7.6 depict boundary sharpness, derived from typicality and posterior class membership probabilities to gap respectively. Visual analysis suggested that the most gradual rate of change in typicality and posterior class membership probabilities were associated with a gradual gap-canopy boundary formed from windthrown trees, which were leaning and hung-up on the boundary. In addition, the sharpest rate of class membership probability change was associated with a sharp gap-canopy boundary, where the windthrown trees had fallen away from the boundary.

7.4.2 Verification of boundary sharpness maps using field reference maps

The visual overlaying of the field reference maps and the boundary sharpness maps made it possible to determine the approximate spatial location of the regions where the boundary was sharpest and most gradual, on the boundary sharpness maps, as depicted on

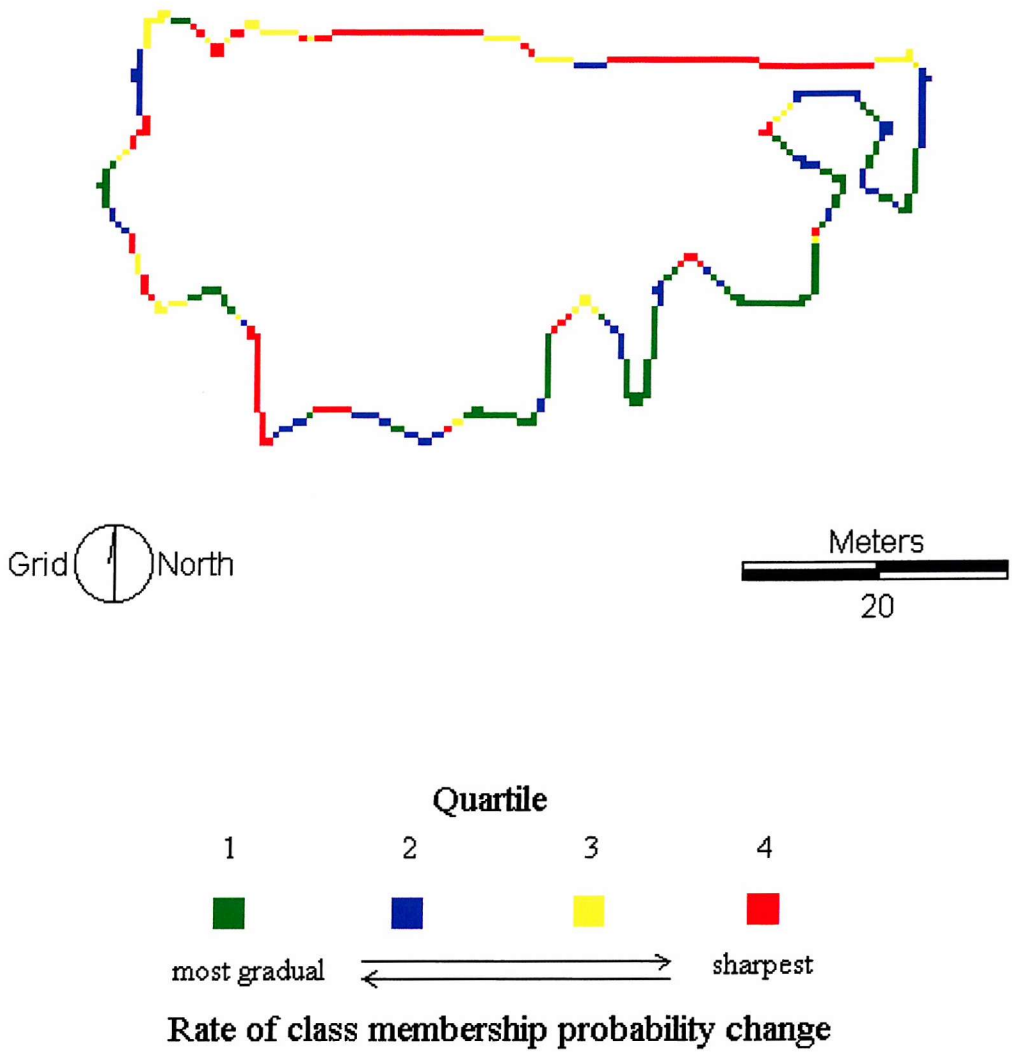

Figure 7.5 Boundary sharpness map for the sample windthrown gap (GP26) depicted in Figure 7.1, derived from typicality class membership probabilities to a gap class (i.e. windthrown and moorland). The pattern of class membership probability change, specifically boundary sharpness is represented by mapped quartiles.

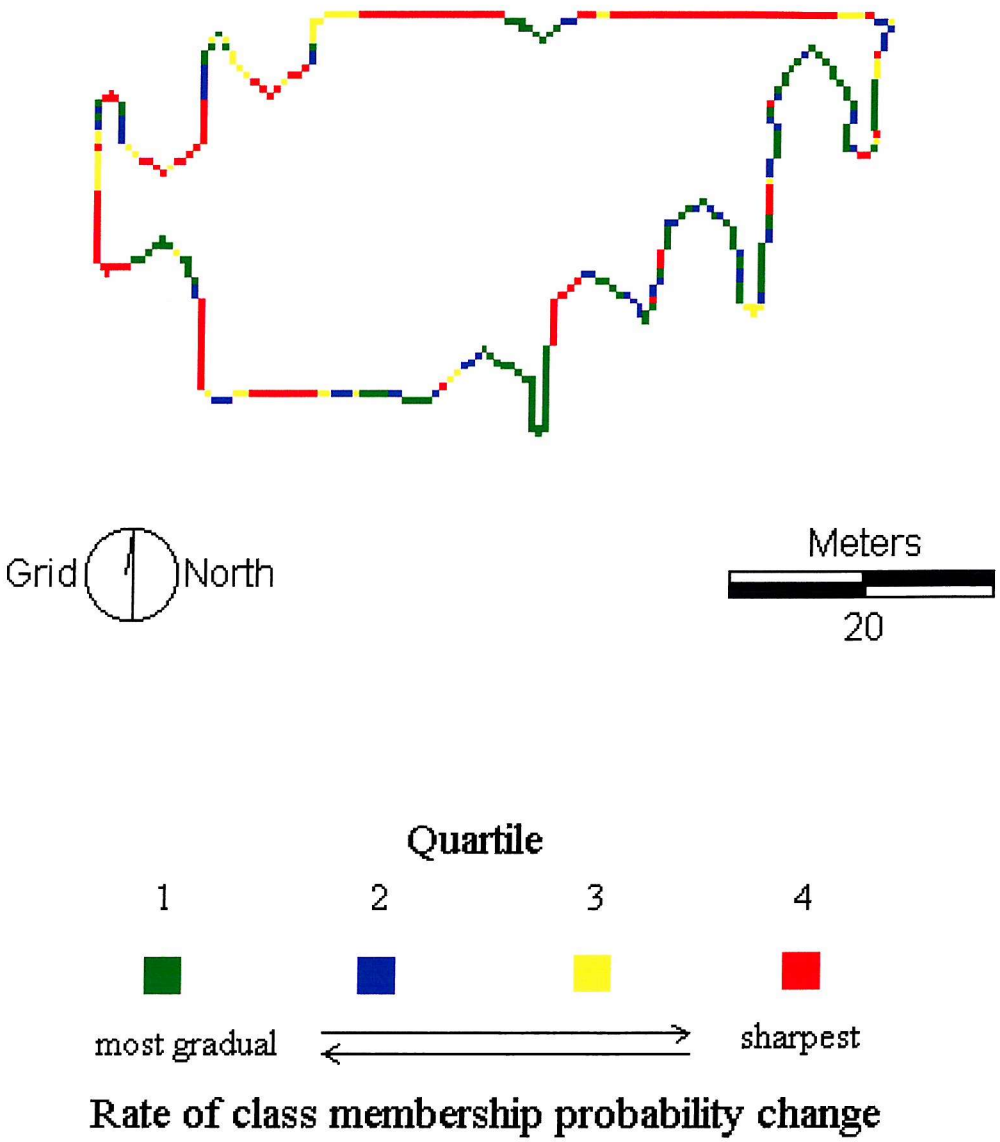

Figure 7.6 Boundary sharpness map for the sample windthrown gap (GP26) depicted in Figure 7.1, derived from posterior class membership probabilities to a gap class (i.e. windthrown and moorland). The pattern of class membership probability change, specifically boundary sharpness is represented by mapped quartiles.

the field reference maps. Analysis of the boundary sharpness for the set of 36 windthrown gaps involved comparing the number of pixels allocated to either quartiles 1 (i.e. most gradual rate of class membership probability change), or 4 (i.e. sharpest rate of class membership probability change) in the boundary sharpness maps, that were located within the corresponding regions depicted on the field reference maps. The magnitude of pixel numbers was analysed in the form of a 2 x 2 contingency table using the chi-square test statistic (Zar, 1999). The results indicated that the sharpest rate of class membership probability change derived from both typicality and posterior probabilities to the gap class was associated with the sharpest gap-canopy boundary ($P < 0.01$), characterised by exposed root plates, moorland vegetation and soil. In addition, the most gradual rate of class membership probability change derived from both typicality and posterior probabilities to the combined gap class was associated with the most gradual boundary ($P < 0.01$), characterised by a tapered boundary formed from windthrown trees which were leaning and hung-up.

Due to the magnitude of the contribution from the largest gaps to the data analysed (i.e. the largest gaps contributed the majority of the pixels for analysis, by virtue of their size), further analysis was undertaken to investigate whether the results were driven by windthrown gap size. It was possible that the results were only significant for the largest windthrown gaps and not significant for the smallest gaps. This analysis of the rate of class membership probability change, performed using the chi-square test statistic, was undertaken separately for the 10 largest (ranging in size from 292 to 2158 m^2) and 10 smallest (ranging in size from 41 to 117 m^2) windthrown gaps. The results suggested that

rate of class membership probability change was significantly related to boundary sharpness ($P < 0.01$), for both these windthrown gap size classes. Therefore, windthrown gap size did not appear to exert a significant influence upon the ability to characterise gap-canopy boundary sharpness using rates of class membership probability change.

7.4.3 Verification of boundary sharpness maps using the DEM

Due to minor image registration discrepancies, it was only possible to analyse the rate of change in canopy height, derived from the DEM, with the rates of typicality and posterior class membership probability to gap change for the 10 largest windthrown gaps (ranging in size from 292 to 2158 m^2). The results derived using the chi-square test statistic (Zar, 1999) indicated that the extreme rates of canopy height change were significantly associated with the extreme rates of typicality class membership probability to gap change ($P < 0.01$) and posterior class membership probability to gap change ($P < 0.01$). The DEM, therefore, provided further validation of the results in Section 7.4.2 which indicated a softened classification may be used to derive accurate information on the sharpness of a windthrown gap-canopy boundary.

7.4.4 Direction of treefall

Wind climate data recorded by the Forestry Commission for the Cwm Berwyn Forest monitoring site, suggest that the prevailing wind is predominantly blowing towards the east (Quine, 2000). Windthrown trees in Cwm Berwyn Forest may be expected to fall away from the direction of this prevailing wind (i.e. towards the east), as the wind load,

which overcomes the components of anchorage (Figure 2.2), is predominantly exerted in that direction. Therefore, the general directions of treefall for the 34 windthrown gaps were analysed using the V test for circular uniformity with a specified mean direction (Zar, 1999). This is a modification of the Rayleigh test for the analysis of circular distributions, when the sampled distribution has an expected mean direction (i.e. trees would be expected to fall in an easterly direction) (Zar, 1999). This test was undertaken to determine whether the directions of treefall are random, which may suggest a variable wind climate. The results indicated that the directions of treefall determined during field survey were not random, but significantly orientated in an easterly direction ($P < 0.01$).

These reference treefall directions were compared with the directions of treefall estimated from the boundary sharpness maps (Section 7.3.5), in order to determine whether boundary sharpness could be used to derive an accurate indication of treefall direction. This analysis was undertaken using the Hotelling test for paired samples of angles (Zar, 1999). The results indicated that the estimated and the reference directions of treefall did not differ significantly ($P > 0.01$). Therefore, estimates of treefall direction derived from extreme rates of class membership probability change may provide an accurate indication of the actual direction of treefall.

7.5 DISCUSSION

To further develop our understanding of the influence an existing windthrown gap exerts on the surrounding forest stand, in terms of the vulnerability to further wind

damage, it is necessary to acquire information on the sharpness of the gap-canopy boundary, in addition to gap shape and orientation. It is not possible to derive information on boundary sharpness from remotely sensed data using a conventional hard classification, or fitting a single class membership probability contour, as these impose a hard boundary to represent the gap-canopy boundary. The results from this Chapter indicated that analysis of the rate of change in either typicality or posterior class membership probability can provide accurate information on the sharpness and characteristics of the gap-canopy boundary of a windthrown gap.

Detailed examination of the west-east transect through the sample windthrown gap (GP26) (Section 7.4.1), indicated that at the gap-canopy boundaries, the probability of membership to both these classes increased and decreased as would be expected (Figure 7.4). The rate of change of class membership probability between the canopy and the gap classes suggested that the eastern gap-canopy boundary was not as sharp as the western boundary. Field observation of the sharpness of the windthrown gap-canopy boundary supported the inferences drawn from these changes in class membership probabilities observed along this transect through this sample windthrown gap (Figure 7.1).

The small rise in moorland class membership probability at the western gap-canopy boundary suggested that bare soil and moorland vegetation were present. This would be expected if this was a region of the boundary where windthrown trees had fallen away from, leaving exposed root plates, stems with the possibility of epicormic growth (Figure 7.2) and a site which vegetation was beginning to colonise and regenerate. The ability to detect this rise in moorland class membership was only feasible when the hard

classification was softened to output class membership probabilities. The hard maximum-likelihood classification, therefore, provided little information on the characteristics of the gap-canopy boundary. Similarly, the small rise in the posterior probability of membership to the moorland class at the sharp boundary (Figure 7.4) appeared to indicate the presence of bare soil, vegetation and exposed root plates. The results from the visual analysis of the 10 largest windthrown gaps suggested that class membership probability to the moorland class is greatest where the gap-canopy boundary is sharpest. Therefore, a rise in probability of membership to the moorland class may provide supporting evidence for the results derived from using rate of class membership probability change and suggest that the sharpest gap-canopy boundary is associated with exposed root plates, bare soil, moorland vegetation and an abrupt transition between the windthrown gap and the surrounding forest stand.

It was not possible to acquire information on boundary sharpness using the output from a hard classification. However, the rates of change of class membership probabilities derived from the softened classifications showed that there was a much more gradual transition between the sample windthrown gap (GP26) and the surrounding canopy, at the eastern boundary. Some pixels allocated to the canopy and gap classes by the hard classification, contained a significant probability of membership to other classes when the class membership probabilities were examined. This suggested that this eastern boundary was not as sharp as the western boundary and was indicative of where windthrown trees had fallen onto standing trees and were leaning and, or hung-up (Figure 7.2). This resulted in a banking structure, with some windthrown trees forced between the standing trees.

These results suggest that it may be possible to accurately map the sharpness of a windthrown gap-canopy boundary using a softened classification. These derived maps may aid the study of windthrow formation and progression, as boundary sharpness may influence the vulnerability of the stand to future wind damage. The most gradual boundary, characterised by the banking structure, represents a smooth or tapered gap-canopy boundary profile (Quine *et al.*, 1995; Gardiner and Stacey, 1996). This gently directs the airflow over the boundary, reducing the wind loading on the stand interior trees which form the gap-canopy boundary (Quine *et al.*, 1995; Gardiner and Stacey, 1996). This affords some degree of wind protection, when compared to a sharp boundary. For example, stand interior trees at newly exposed boundaries are much more vulnerable to wind damage, partly due to the reduction in damping resulting from the removal of neighbouring trees (Quine *et al.*, 1995). However, over time adaptive growth of the root system and the stem will gradually compensate for any initial increased wind loading (Quine *et al.*, 1995).

The sharpness of the gap-canopy boundary, in relation to the prevailing wind direction may provide an indication of the risk for future wind damage at that location. It may also influence air turbulence downwind from the gap (Quine *et al.*, 1995). However, the risk of windthrow progression at a gap-canopy boundary is not only influenced by boundary sharpness, but also influenced by gap shape, in terms of funnelling airflow (Quine and Miller, 1990; Kimmins, 1997). The results in Section 6.5.2.3 suggested that it was possible to derive accurate representations of windthrown gap shape from a softened classification output. The ability to acquire information on the pattern of boundary

sharpness and gap shape, using remote sensing methods, may provide forest management with a means of investigating the influence of existing windthrown gaps on future windthrow formation and progression.

However, it was apparent that the pattern of gap-canopy boundary sharpness, derived from probability maps, was more visually pronounced for the largest gaps. Despite the significant results, the pattern of boundary sharpness of the small gaps was not visually pronounced sufficiently in order to visually differentiate between the sharpest and most gradual boundaries with confidence. This suggests that there is a scale issue to the potential operational use of remote sensing for windthrown gap boundary studies.

7.6 SUMMARY

The results from this Chapter indicated that softened classification methods may be used to derive information on the gap-canopy boundary of windthrown gaps, which may facilitate the development of silvicultural practices to reduce the risk of further windthrow associated with the presence of existing windthrown gaps within upland commercial forests in the British Isles. With reference to the Chapter aims (Section 7.2), the results indicated that the rate of change in class membership probabilities, derived by softening a maximum-likelihood classification to output typicality and posterior class membership probability maps, provided accurate representations of the sharpness of windthrown gap-canopy boundaries.

The potential to map gap-canopy boundary sharpness, may provide an indication of the stability of the boundary to future wind damage (Gardiner and Stacey, 1996). In

particular, the ramping structure, attributed to leaning and hung-up trees, smoothes the profile of the gap-canopy boundary and gently directs the airflow. This reduces the wind loading on the boundary trees, reducing the vulnerability to future wind damage (Quine *et al.*, 1995; Gardiner and Stacey, 1996).

When related to characteristics of the landcover within the windthrown gap, the typicality and posterior probabilities of class membership indicated the presence of exposed soil and upturned root plates. This provided supporting evidence for conclusions drawn from the maps representing boundary sharpness. Using these maps of gap-canopy boundary sharpness it was possible to infer the general direction of treefall.

In conclusion, fine ($\simeq$ 4 m) spatial resolution remotely sensed data from airborne, or satellite sensors may provide an appropriate means of deriving information on the sharpness of windthrown gap boundaries, over the size range of windthrown gaps typically found throughout upland forests in the British Isles.

CHAPTER 8

DISCUSSION AND SUMMARY OF RESULTS

8.1 DISCUSSION OF THE REMOTE SENSING OF WINDTHROWN GAPS

Aerial photographs have long been used as a forest management tool and are routinely used for forest mapping (Spurr, 1948; Howard, 1991; Katsch and Vogt, 1999; Kilpelainen and Tokola, 1999; Leblon, 1999). They represent a familiar source of remotely sensed data which can be relatively easily interpreted to provide data for use by forest managers (Spurr, 1948; Howard, 1991). Currently, research and operational assessment of wind damage to forests within the British Isles, by the Forestry Commission and other forest management organisations, has largely been based upon the manual interpretation of aerial photographs (Dannatt *et al.*, 1989; Quine *et al.*, 1995; Quine and Bell, 1998).

The use of aerial photographs and other airborne data have a number of distinct advantages over other data sources. When compared with conventional data acquisition using field survey techniques, airborne data are usually less labour intensive, less time consuming and hence less expensive (Hyyppa *et al.*, 2000). In addition, airborne data can usually be acquired according to the specific requirements of the user, such as time of acquisition (Richards, 1993). For example, acquiring remotely sensed data at different times of the year may be undertaken to discriminate between tree species (Lillesand and

Kiefer, 2000). However, the advantages of data acquired by airborne sensors are often outweighed by certain disadvantages, such as problems associated with poor platform stability (Wilson, 1997). Satellite sensor platforms are more stable and have a number of other advantages, such as regular revisitation and increased spatial coverage (Defries and Townshend, 1999; Katsch and Vogt, 1999).

8.1.1 Spatial coverage

Airborne data have a relatively limited spatial coverage available, when contrasted against the potential spatial coverage of satellite sensor data (Richards, 1993; Katsch and Vogt, 1999; Leblon, 1999). As a result, airborne sensor data are usually more expensive per unit area than satellite sensor data (Richards, 1993; Bolduc *et al.*, 1999; Leblon, 1999). Cheap satellite sensor data are readily available, although it may not be possible to acquire data for the forest site of interest and, therefore, using airborne sensor data to focus on a specific forest site may be less expensive. Satellite sensor data are, therefore, more appropriate for monitoring wind damage to forests over large areas (Hyyppa *et al.*, 2000; Puhr and Donoghue, 2000). For example, Advanced Very High Resolution Radiometer (AVHRR) data were used to identify hurricane damage to a forested wetland of Louisiana in 1992 (Ramsey *et al.*, 1997). Quine and Bell (1998) stated that it is usually the monitoring of wind damage at the forest-landscape scale (200 - 2000 ha) that is important, therefore, satellite sensor data would appear to be more appropriate than airborne sensor data for monitoring wind damage in British forests.

Quine and Bell (1998) suggested that this forest-landscape level of monitoring is usually associated with the level at which forest managers operate, since this is the level at which they attempt to employ silvicultural techniques to minimise the risk of wind damage. These silvicultural techniques were classified by Quine *et al.* (1995) according to the following forest management stages: establishment (site preparation, initial spacing and planting); tending (manipulation of spacing, edges and drain maintenance); and felling (coupe design and forest design plans).

Although at the forest-landscape scale it is usually monitoring which is important, wind damage is a phenomena which is not restricted to any particular spatial scale. Wind damage to an individual tree within a forest is normally not a significant financial concern and usually considered by forest managers as an acceptable commercial loss, although it may be undesirable. For example, a damaged tree may create a gap in the canopy and hence, increase the risk of further wind damage (Quine *et al.*, 1995), or increase the risk of attack by bark beetles (Lundquist, 1995; Jakus, 1998; Safranyik and Linton, 1999). In addition, there is usually little that forest managers can do to reduce the risk of severe wind damage occurring at or above the forest-landscape scale, such as that resulting from the 1987 storm over southeast England (Section 2.3) (Dannatt *et al.*, 1989). In this situation, management efforts were concentrated upon salvage harvesting to minimise the financial loss (Dannatt and Garforth, 1989). Usually forest managers can not employ silvicultural practices to minimise the risk of wind damage at these extreme spatial scales.

8.1.2 Temporal coverage

The acquisition of remotely sensed data for wind damage monitoring is not, however, wholly dependent upon the ground coverage required, but also the frequency, or revisitation rate, with which the data will be required. If a forest manager needs to estimate how much timber has been damaged following a severe storm, aerial photographs or other airborne data may be entirely appropriate. If the wind damage occurred at the forest-landscape scale, fine ($\simeq$ 5 m) spatial resolution satellite sensor data may be more appropriate on the basis of ground coverage and cost of acquisition. If the wind damage occurred at or above this scale, then coarse ($\geqslant$ 10 m) spatial resolution data available from current satellite sensors (i.e. SPOT HRV and Landsat TM data, although these data have a fine spatial resolution in comparison with AVHRR data) may represent the most appropriate data, on the basis of data volume and spatial coverage. For example, Puhr and Donaghue (2000) suggested that Landsat TM data with a 30 m spatial resolution were appropriate for investigating upland forests in the British Isles at the regional level, although the operational use may be restricted by cloud cover.

8.1.3 Spatial resolution

There is a wide choice of spatial resolutions (Section 3.3.1.3) available from current satellite sensors (Atkinson and Curran, 1995; Atkinson and Curran, 1997). The selection of an appropriate spatial resolution is not easy and will depend upon the information required and the spatial variability of the landcover (Woodcock and Strahler, 1987; Marceau *et al.*, 1994; Curran and Atkinson, 1999). The issue is further complicated

by the scale of the landcover in relation to the spatial resolution of the data (Curran and Atkinson, 1999). Ideally, the spatial resolution selected should be such that the desired information can be acquired from the smallest data set (Atkinson and Curran, 1997).

The relatively coarse spatial resolution data available from existing and widely used satellite sensors (e.g. SPOT HRV and Landsat TM), are not appropriate for small areas (i.e. stand or compartment scale) forest monitoring (Katsch and Vogt, 1999). Given that windthrown gaps within British forests are similar in size to the spatial resolution provided by these current satellite sensors, the information which may be derived from these data may be severely restricted. Specifically, the windthrown gaps within the satellite sensor data will be largely represented by mixed pixels, which cause problems during data analysis (Foody, 2000). The conventional hard classification methods applied to remotely sensed data, to convert them into a thematic map required by the end-user, are most effective when handling data consisting of pure pixels.

One potential solution to this mixed pixel problem is to use remotely sensed data with a finer spatial resolution than data acquired by conventional satellite sensor systems. Usually, the quantity of mixed pixels within remotely sensed data will decrease as the spatial resolution of the sensor becomes finer and may have consequences for classification accuracy (Townshend, 1981). New satellite sensors (e.g. that carried aboard the Ikonos satellite) are able to routinely provide fine ($\simeq$ 5 m) spatial resolution remotely sensed data (Aplin *et al.*, 1997; Thomas *et al*, 1997; McGraw *et al.*, 1998; Celentano, 1999; Lillesand and Kiefer, 2000). However, due to the current cost (Table 6.6), established satellite sensors, such as SPOT HRV, or Landsat TM, will probably represent

the main satellite source of remotely sensed data for forest investigations, and wind damage monitoring in particular, for the foreseeable future.

8.1.4 Classification methods

A possible alternative to using fine (≃ 5 m) spatial resolution remotely sensed data may be to employ unconventional classification methods which may be more appropriate for handling mixed pixels. Conventional hard classification methods have been extensively used for forest studies, both operationally and for research, and as such, have been well tried and tested (e.g. Spanner *et al.*, 1989; Franklin *et al.*, 1994; Blackburn and Milton, 1996; Ardo *et al.*, 1997; Mukai and Hasegawa, 2000). These hard classification methods form the backbone of most image processing software used to manipulate remotely sensed data and are comprehensively described and discussed in image analysis textbooks (e.g. Richards, 1993; Campbell, 1996; Mather, 1999). Only recently have unconventional methods, such as soft and softened classifications, become more widely used. Whichever classification method is applied, it must be familiar to the users of remotely sensed data, such as the Forestry Commission (Franklin *et al.*, 2000). This is in order to minimise confusion between those individuals who may need to use or interpret remotely sensed data and also minimise the cost of training staff or employing trained staff.

Given the stark choice between using relatively coarse (⩾ 10 m) spatial resolution data and unconventional classification methods, or fine (≃ 5 m) spatial resolution data and

conventional hard classification methods, the latter choice would initially appear to be the most appropriate for users unfamiliar with data analysis methods. Although using fine (≃ 5 m) spatial resolution data may reduce the quantity of mixed pixels, the data volume will be larger and hence, will be most costly to store and process. This dilemma between the quantity of mixed pixels and data volume is outlined in Table 8.1. Therefore, it may not be possible to operationally restrict the satellite sensor data for monitoring wind damage in British forests to a specific spatial resolution. The selection will depend upon spatial coverage, temporal coverage, data storage and handling capabilities, data availability and ultimately, cost. However, it is possible to examine the results from the research within this thesis to identify the potential operational capabilities of new fine (≃ 5 m) spatial resolution satellite sensor systems and alternative classification methods for monitoring wind damage within forests.

	Advantages	**Disadvantages**
Fine spatial resolution data e.g. ≃ 5 m	Windthrown gaps mostly represented by pure pixels	Large data volume
		Expensive per unit area
	Easy to focus on specific forest sites	Small spatial coverage
Coarse spatial resolution data e.g. ≃ 30 m	Small data volume	Windthrown gaps mostly represented by mixed pixels
	Inexpensive per unit area	
	Large spatial coverage	Difficult to focus on specific forest sites

Table 8.1 A summary of some of the main advantages and disadvantages associated with using different spatial resolutions of non-photographic remotely sensed data for monitoring windthrown gaps within British forests.

8.1.5 Alternative remote sensing methods

Although beyond the scope of the research within this thesis, it is useful to briefly note the potential operational application of alternative remote sensing methods for the monitoring of wind damage.

8.1.5.1 RADAR remote sensing

RADAR remote sensing has a distinct advantage over optical remote sensing, as it can acquire data independent of weather and illumination conditions, because a RADAR sensor produces it's own long wavelength incident radiation (Section 2.6.1.1.5) (Leblon, 1999). This makes the use of RADAR attractive for monitoring upland British forests, since cloud cover can prove a significant problem for the acquisition of suitable optical sensor data (e.g. Puhr and Donaghue, 2000). Previous research has indicated that RADAR provides a means of accurately identifying windthrown gaps within upland British forests (Section 2.7.1) (Green, 1998a). However, major disadvantages to the use of RADAR are the difficulties associated with complex topographic environments and with defining boundaries which do not face the direction of RADAR illumination (Leblon, 1999). This makes RADAR remote sensing inappropriate for the derivation of estimates of windthrown gap area, perimeter or shape.

8.1.5.2 Forest canopy surface models

The use of a DEM representing the forest canopy as a continuous surface, may provide an appropriate means of monitoring wind damage within upland forests in the

British Isles (Miller *et al.*, 1997). These DEMs can be generated from aerial photographs by digital photogrammetry, or from LIDAR data (Section 2.6.1.1.6). LIDAR has proved useful for canopy surface mapping and is being developed for a number of forestry applications, such as predicting tree heights (Magnussen *et al.*, 1999; Lillesand and Kiefer, 2000).

Although there are a few examples of generated canopy surfaces being used to analyse forest canopy structure (e.g. Mozgeris and Augustaitis, 1999), this work is still largely at a preliminary stage (Miller *et al.*, 1997). This previous work has indicated that the time required for processing DEM data is appropriate for forestry investigations at the forest stand scale (Miller *et al.*, 1997). However, as with other forms of remote sensing, the operational application of DEMs for forestry investigations will depend upon the associated benefits and costs (Miller *et al.*, 1997). Changes in canopy height can be accentuated by the combination of orthophotographs draped over a DEM, which has enabled the identification of wind damage within an upland forest in the British Isles (Miller *et al.*, 1997). However, it is likely to be costly to use canopy surface DEMs for monitoring forested areas at or above the forest-landscape scale, in terms of the initial cost of aerial photograph or LIDAR data acquisition and subsequent data processing required to derive the DEM.

Alternatively, advantage may be made of the spatial coverage of satellite sensor data, as DEMs can be currently generated from stereoscopic SPOT HRV data. Unfortunately, the spatial resolution stereoscopic data available from current satellite sensor systems is usually too coarse for British forestry investigations (Miller *et al.*, 1997).

However, stereoscopic data available from the new fine (≃ 5 m) spatial resolution satellite sensors, may provide an appropriate source of data for wind damage monitoring (Aplin *et al.*, 1997; Miller *et al.*, 1997; Lillesand and Kiefer, 2000).

8.2 DISCUSSION OF RESULTS

The Forestry Commission have used a GIS to develop and refine the existing WHC to provide forest managers throughout the British Isles with ForestGALES, a computer based wind risk model, which can take factors, such as cultivation type, into account (Quine *et al.*, 1995; Quine and Bell, 1998; Dunham, 2000). However, this still requires the basic knowledge of where and when does wind damage occur.

Sitka spruce is the dominant tree species within commercial British forests and in particular, pure stands of Sitka spruce tend to be synonymous with upland forests where wind damage is most prevalent. The results from Sections 5.7 and 6.5 indicated that a conventional hard maximum-likelihood classification, applied to ≃ 4 m spatial resolution data, accurately identified windthrown gaps within forest stands formed entirely of Sitka spruce. As such, this hard classification provided a realistic alternative to manual interpretation of aerial photographs. A hard classification has the benefit of being semi-automated, hence, less reliant upon subjective interpretation and computational time is usually less than the time required for aerial photographic interpretation.

Over the spatial resolution range (≃ 4 m, 10 m, 20 m and 30 m) analysed it was evident that the ability to accurately identify individual windthrown gaps using a hard classification was dependent upon the spatial resolution of the remotely sensed data

(Section 5.7.1). As the spatial resolution of the remotely sensed data becomes coarser, the accuracy with which it was possible to identify individual gaps decreased. However, classification accuracy will be determined by the size of the windthrown gaps with respect to the spatial resolution of the remotely sensed data (Section 8.1.3).

The results in Sections 5.7.1 and 6.5.1 indicated that using the conventional hard classification it was also possible to accurately identify small windthrown gaps which were difficult to identify by manual interpretation of aerial photographs. Since these windthrown gaps may act as initiator sites (Savill, 1983), which expand through progressive wind damage, the output from a hard classification may provide a crude means of predicting those possible sites where future wind damage may occur. However, some features identified by the hard classification as windthrown gaps were associated with wider than normal tree spacing due to the presence of drains. If the location of these drain lines are accurately surveyed and mapped, it may be possible to eliminate these confusing features during a post-classification analysis.

Although it was possible to accurately identify windthrown gaps within Sitka spruce stands, it was not possible to accurately identify windthrown gaps within a stand of larch. The larch was planted in a narrow strip (Figure 3.3) and it was not possible to acquire sufficient sample pixels to train the hard classifier to recognise the spectral reflectance from windthrown gaps within the larch stand. As a potential operational alternative, the identification of windthrown gaps within the larch stand using a hard classification was undertaken using the spectral reflectance from windthrown gaps within stands of Sitka spruce as a surrogate for the spectral reflectance from windthrown gaps

within the larch stand. The resulting hard thematic output suggested that these windthrown gaps within the larch stand were more associated with the spectral response from the moorland than that from the Sitka spruce windthrown gaps.

The Sitka spruce windthrown gap spectral reflectance was dominated by tree stems, canopy foliage and shadow, with a minimal contribution from the underlying soil and leaf litter. Conversely, the ($\simeq$ 4 m) ATM data for larch (a deciduous tree species) were acquired in April, when the larch had not developed a full canopy and, therefore, the spectral reflectance from a windthrown gap within the stand of larch was composed of tree stems and shadow, but dominated by the underlying soil and leaf litter. Since a larch canopy lets more light reach the ground than a Sitka spruce canopy, it would be expected to have a significant quantity of grasses and other natural vegetation present. Hence, it was appropriate that the hard classification output suggested that the larch windthrown gaps were more associated with the spectral reflectance of the moorland, than the Sitka spruce windthrown gaps.

The Cwm Berwyn Forest wind damage monitoring site is typical of the vast majority of upland forested sites in the British Isles. From this perspective it is likely that the hard classification method used in this work could be transferred and successfully applied to other upland forest sites planted with single species, single age class stands. However, the hard classification may not be successful when applied to monitoring wind damage within more complex or natural forest sites, where the canopy is less uniform and there is less of a contrast between the wind damage and the surrounding forest stands.

The results from the analysis of windthrown gaps within the stand of larch indicated that tree species will affect the ability to identify windthrown gaps and the accuracy of subsequent results. Although outside the scope of this thesis, this is an application of remote sensing where future research may prove beneficial, particularly with the emphasis away from forest management systems using non-native tree species.

Much of the previous work on the remote sensing of gaps within forest canopies has been directed at detecting stages in the regeneration of tree species (e.g. Mausel *et al.*, 1993; Curran and Foody, 1994; Hlavka and Spanner, 1995). This is a task the Forestry Commission are currently investigating, with the current interest in silvicultural systems based upon natural regeneration and the potential reliability with which Sitka spruce will regenerate naturally in upland forest sites (Savill, 1991). Whether it would be possible to use remote sensing to specifically detect regeneration within windthrown gaps in British forests requires further research. Some previous work has used forested sites where trees have been completely removed to form the gaps and, hence, the gaps have initially been dominated by the reflectance from the bare understorey (Section 2.6.3.2) (e.g. Hlavka and Spanner, 1995). However, windthrown gaps in British Sitka spruce forests contain a complex mixture of woody stems, epicormic growth and living canopies. It may not be possible to accurately differentiate the growth of epicormic branches or windthrown canopies, from seedling regeneration. If the windthrown trees were removed, for example sanitation felling to prevent insect damage to the residual stand, then the initial contrast between the gap and the surrounding canopy may make subsequent development of regeneration possible to detect. However, as has noted in Section 2.4.1.3, removing

windthrown trees is not usually undertaken unless financially critical, due to the increased risk of further wind damage to the residual stand.

Although windthrown gaps are an example of natural gaps within upland British forests, these forests also contain human made gaps, such as those resulting from thinning operations (Section 2.4.1.3). The type and intensity of the thinning can produce different forms of gaps. For example, line thinning results in evenly spaced linear gaps (e.g. Figure 3.5), whilst selective thinning seldom results in individual gaps formed by the removal of groups of more than 1 or 2 trees. Previous work has suggested that although it is possible to monitor the temporal changes in reflectance from a forest attributed to thinning using Landsat TM data (Olsson, 1990; Olsson, 1994; Nelson and Olsson, 1995), it may be difficult to differentiate between thinned stands and stands subject to other forms of damage (Hame, 1991). In particular, it is unlikely that current operational remote sensing methods will be able to accurately identify windthrown gaps, of a similar size to gaps formed by selective thinning, within a selectively thinned stand in an upland British forest. However, distinguishing windthrown gaps from gaps formed by line thinning and monitoring the subsequent recovery may be possible. Visual analysis of the ($\simeq$ 4 m) hard classified output indicated that it may be possible to identify line thinning as linear features within the thinned areas of Cwm Berwyn Forest. Preliminary investigations suggested that it may be possible to use fitted typicality probability contours to distinguish the wind damage from the thinning lines, although this requires further research.

In addition to identifying when and where wind damage has occurred, forest managers require estimates of how much forest has been damaged. This is essential for

the planning of labour, equipment and subsequent sale of the harvested wood (Dannatt *et al.*, 1989). For example, assessment of the extent of wind damage during the winter of 1994 to upland forests managed by the Department of Agriculture for Northern Ireland Forest Service, in Fermanagh, was required to determine whether the damage was significant to warrant salvage harvesting. This assessment used a crude, but operationally quick and inexpensive remote sensing method. A light aircraft and pilot was hired to fly over the forests (which required approximately 2 hours flight time) and a forest officer took photographs of wind damaged stands from the aircraft using an ordinary 35 mm camera. The developed photographs were then used to roughly sketch on a forest stand map the approximate extent of the wind damage, from which area estimates and subsequently, estimates of timber volume damaged by wind were derived. The whole wind damage assessment took 3 days to complete and cost in the order of £400.

The above technique, although inexpensive and at the time deemed adequate for the simple survey, was relatively unsophisticated and suffered from a number of disadvantages. In particular, as the photographs were unrectified, they were inappropriate for temporal comparison (e.g. monitoring wind damage progression) and due to the poor spatial coverage, inappropriate for monitoring wind damage above the forest-landscape scale. As noted earlier in Section 8.1.1, satellite sensor data can overcome these problems, which may be particularly useful for organisations such as the Forestry Commission, who manage forests throughout Great Britain. Usually it is only the area of wind damaged stands that are operationally required to estimate the volume of wind damaged timber and coarse ($\geqslant$ 10 m) spatial resolution satellite sensor data, such as Landsat TM data, may be

appropriate. It may, therefore, be more advantageous for the Forestry Commission to sacrifice the accuracy with which the areas of individual windthrown gaps can be estimated using fine ($\simeq$ 5 m) spatial resolution satellite sensor data, for a reasonably accurate total area estimate of wind damaged stands using coarse ($\geqslant$ 10 m) spatial resolution data. However, as forests are comprised of stands of different ages and with different growth rates, it may be more appropriate to use fine ($\simeq$ 5 m) spatial resolution satellite sensor data to derive estimates of the volume of wind damaged timber.

The results from Section 6.5.2.1 indicated that the agreement with the reference windthrown gap area estimates was dependent upon the spatial resolution of the remotely sensed data and the strength of this agreement increased as the spatial resolution of the remotely sensed data became finer. However, the accuracy of windthrown gap area estimates will be dependent, amongst other factors, upon the spatial resolution of the remotely sensed data operationally available at an acceptable cost to the end user.

In addition to estimates of windthrown gap areas, it was possible to estimate other spatial characteristics of the gaps, such as perimeter and shape. The amount of boundary (i.e. perimeter) of a windthrown gap facing the direction of the prevailing wind, will influence the vulnerability to further wind damage. In addition, the shape of the gap, for example, in terms of the funnelling effect, will also affect the vulnerability to further wind damage (Kimmins, 1997; Quine *et al.*, 1995). Information on windthrown gap shape and orientation is required to improve the current understanding of how wind damage influences the floral and structural diversity of upland British forests (Quine and Humphrey, 1996).

The results from Section 6.5.2.2 suggested that conclusions drawn concerning the shape of windthrown gaps from conventionally used shape metrics must be interpreted with care. For example, some of these shape metrics are scale sensitive or ignore the constant of proportionality, k, when calculating the fractal dimension. Future work on shape analysis should employ approaches which are more robust to changes in scale. However, suitable metrics are not widely found within the literature and are only beginning to be used for shape analysis within published literature (e.g. Frohn, 1998).

The results in Section 6.5.2.2 have indicated that fine ($\simeq$ 5 m) spatial resolution satellite sensor data may provide an appropriate source of remotely sensed data for future work on windthrown gap shapes. As with windthrown gap area estimates, the accuracy of windthrown gap perimeter and shape estimates are dependent upon the spatial resolution of the remotely sensed data and will increase as the spatial resolution of the remotely sensed data becomes finer. The work contained within this thesis has contributed to wind damage research through the possibility of deriving a more accurate representation of windthrown gap area, perimeter and shape, by softening the output from a hard classification. This may provide a useful technique, particularly if fine ($\simeq$ 5 m) spatial resolution data are not available to the end user.

A major contribution of the research within this thesis are the results which indicated that the rate of posterior and typicality class membership probability change, derived from softening the hard classification provided an accurate representation of the sharpness of the gap-canopy boundary. This mapping of boundary sharpness may provide an indication of the possible stability of a windthrown gap-canopy boundary to expansion

through wind damage progression in the future. For example, a sharp boundary has the highest risk due to the sudden exposure of stand interior trees, whilst the most gradual boundary has the lowest risk due to the gradual transition from gap to canopy attributed to the presence of windthrown trees. This risk of windthrown gap progression will also be influenced by the orientation of the wind with respect to boundary sharpness.

Researchers in the Forestry Commission are currently interested in the possibility of using aerial photographic remote sensing to identify not just windthrown gaps which have expanded, but in which direction they have expanded. It is possible to accurately determine wind damage progression by field survey, using fixed reference points established in the field. However, as noted earlier in Section 2.5, the derivation of data by traditional field survey techniques is expensive, primarily due to the cost of labour and time. In addition, the use of GPS within a forested environment has its own associated problems (Section 4.4) (Lawrence *et al.*, 1995; Courteau, 1996; Quine *et al.*, 1997; Darche and Forgues, 1998; Sigrist *et al.*, 1999).

There are a range of change detection procedures available which can be applied to remotely sensed data (Lillesand and Kiefer, 2000). The advantages associated with the possibility of using satellite or airborne remotely sensed data to monitor windthrown gap progression, such as regular revisitation, spatial coverage and relative ease of data acquisition, is an attractive proposition. However, the temporal comparison between data sets for spatial differences requires accurate image co-registration. This may be difficult, since the boundaries of windthrown gaps are soft, and not well defined like agricultural fields (Turker and Derenyi, 2000).

8.3 FUTURE WORK

The future operational use of remote sensing for the monitoring of wind damage within British forests will be dependent upon a number of factors. Initially, it will be necessary to determine the availability of fine (≃ 5 m) spatial resolution data from new satellite sensors and the associated cost (Table 6.6). In addition, it will be necessary to make the forest management community more familiar with remote sensing and GIS, and continue to integrate alternative classification methods required for the processing of remotely sensed data within computer packages.

In terms of future research, investigations will need to confirm the conclusions drawn from the research within this thesis, that using fine (≃ 5 m) spatial resolution satellite sensor data, rather than simulated data, and alternative classification methods, it is possible to subsequently increase the accuracy of the representation of windthrown gaps and determine whether any increase is cost effective. In particular, consideration should be given to factors such as the angles between the illumination source, landcover and sensor (Section 2.6.1.3) which will affect the reflectance recorded by the sensor. In addition, since conventional satellite sensors, such as SPOT HRV and Landsat TM, have an advantage of acquiring remotely sensed data with an appropriate spatial coverage for forest investigations (Puhr and Donoghue, 2000), research could be directed towards evaluating the accuracy with which it is possible to represent windthrown gaps using alternative methods for handling mixed pixels, such as artificial neural networks (Atkinson and Cutler, 1996; Mather, 1999).

To-date, investigations on wind damage progression have largely ignored information on windthrown gap perimeter, shape and boundary sharpness. This is primarily because this information has been difficult to acquire. The work contained within this thesis indicates that this information may be acquired by remote sensing methods. It may be possible in the near future to relate this information to existing research on site and crop factors which affect the risk of wind damage and hence, increase our understanding of the temporal and spatial dynamics of wind damage to upland forests in the British Isles. In the long term, this will hopefully enable forest managers to evaluate the risk of wind damage associated with the range of conventional silvicultural operations more objectively and develop our upland commercial forests to maximise their potential, for wood production and other benefits.

8.4 SUMMARY

There are a number of examples of forest based work being undertaken in the British Isles using remote sensing as a source of data (e.g. Cameron *et al.*, 2000; Puhr and Donaghue, 2000). To-date, this work has been largely driven by the research community and there have been few operational applications other than using aerial photographs for basic mapping and surveying. The forest industry is becoming increasingly interested in the operational potential of remote sensing for the monitoring of wind damage formation and progression and this should develop as it becomes more familiar with remote sensing and GIS, and applies the methods to operational planning and management. However, the operational use of remotely sensed data will largely be determined by the temporal and

spatial coverage required, as well as what data availability and cost (Katsch and Vogt, 1999; Puhr and Donoghue; 2000). Given that forestry, as with other commercial industries, has limited financial resources, there will be a trade-off between the desirable and undesirable attributes of the remotely sensed data used (McGraw *et al.*, 1998).

Over the size range of typical windthrown gaps found throughout upland forests in the British Isles (Figure 3.6), the spatial resolution of remotely sensed data acquired by conventional satellite sensors, such as SPOT HRV and Landsat TM, does not represent an appropriate spatial resolution for monitoring windthrown gaps. Alternatively, the fine ($\simeq$ 5 m) spatial resolution data that is available from new satellite sensors (Aplin *et al.*, 1997; McGraw *et al.*, 1998; Lillesand and Kiefer, 2000) may provide a more appropriate source of remotely sensed data. In addition, softening a hard classification has the potential to increase the accuracy of windthrown gap representation, particularly windthrown gap area, perimeter and shape. In addition, it also has the potential to provide information on the sharpness of the gap-canopy boundary.

CHAPTER 9

SUMMARY AND GENERAL CONCLUSIONS

9.1 INTRODUCTION

Wind represents a significant problem for forestry throughout the world and is a severe threat to upland forests in the British Isles (Quine *et al.*, 1995). Wind damage to British forests is primarily formed by the actions of strong winds, attributed to the passage of Atlantic depressions. The resulting wind damage is primarily associated with the formation of windthrown gaps in the forest canopy, which are considered common features and represent the most serious form of wind damage to upland forests in the British Isles (Miller, 1985; Quine and Bell, 1998). The risk of windthrow imposes restrictions upon conventional silvicultural practices and the presence of windthrown gaps make forests more susceptible to further wind damage (Quine *et al.*, 1995). Despite the importance of such windthrown gaps, existing work has been largely directed towards site and crop factors, rather than the formation and progression of windthrown gaps (Quine *et al.*, 1995). This is due in part to the spatial and temporal variability of gap formation and progression. Remote sensing may provide an appropriate means for acquiring this spatial and temporal information of windthrown gap formation and progression.

9.2 WIND DAMAGE MONITORING

Information on windthrown gap formation and progression is difficult to acquire through conventional field survey techniques and is costly, in terms of labour and time (Quine and Bell, 1998). Previous work to-date using remote sensing methods, has been based upon information on windthrown gaps acquired through the manual interpretation of aerial photographs (Quine and Bell, 1998). However, there are problems associated with remotely sensed data acquired by an airborne sensor (Section 2.7.1) (Wilson, 1997). Satellite sensor data may, however, represent a more appropriate source of remotely sensed data on windthrown gaps. These satellite sensors acquire data at the forest-landscape level required for monitoring wind damage over the range of forest conditions within the British Isles (Quine and Bell, 1998; Quine *et al*, 1999).

The major drawback to the use of such satellite sensor data is that many gaps are smaller or similar in size to the spatial resolution of current civilian satellite sensor systems (e.g. SPOT HRV and Landsat TM) (Quine and Bell, 1998). However, new classification methods and satellite sensors may resolve many of the current problems encountered with the use of conventional remotely sensed data (Section 2.7.2.1) (Aplin *et al.*, 1997; Lillesand and Kiefer, 2000).

These new satellite sensors are designed to acquire finer ($\simeq$ 5 m) spatial resolution data than current satellite sensors. However, as discussed in Section 8.4.1, using fine spatial resolution remotely sensed data usually represents an increased cost to the user. This increased cost may outweigh any advantages gained.

An alternative to conventional hard classification methods are soft classification methods (Section 2.7.2.2). A fully soft classification method requires training with mixed pixels for which the class composition is known and this information is often not available. Alternatively, it is possible to soften the output of a conventional hard classifier which may provide a more realistic representation of land cover than a conventional hard classification (Foody, 1996b).

9.3 STUDY SITE AND RESEARCH METHODOLOGY

This thesis evaluated the potential of fine ($\simeq$ 5 m) spatial resolution remotely sensed data and alternative classification methods to characterise windthrown gaps. The study site was Cwm Berwyn Forest, in central Wales, a planted forest of predominantly Sitka spruce (*Picea sitchensis* (Bong.) Carr.) containing windthrown gaps ranging in size from 50 to 3000 m^2. The remotely sensed data used were acquired by an 11 waveband ATM sensor with a spatial resolution of $\simeq$ 4 m. This spatial resolution was finer than the windthrown gaps on the site and comparable to that of new satellite sensors. A land cover map of the site was derived using the maximum-likelihood classification. This hard classification was softened to output maps of typicality and posterior class membership probabilities.

9.4 RESULTS

The results from this work demonstrated that a conventional maximum-likelihood classification of fine spatial resolution remotely sensed data can provide an accurate means

of identifying known windthrown gaps (> 95 % of known windthrown gaps identified). In addition, the hard classification identified a number of windthrown gaps present within Cwm Berwyn Forest that were not represented within the reference data derived using aerial photointerpretation by the Forestry Commission. Consequently, the hard classification provided a more accurate means for identifying windthrown gaps than aerial photointerpretation.

The hard classification provided poor estimations of windthrown gap area, perimeter and shape. Softening this hard classification to derive typicality and posterior probabilities of class membership provided more accurate representations of windthrown gap area, perimeter and shape than the hard classification. In addition, the softened classification provided useful information on the sharpness of the gap-canopy boundary, which is an important component of windthrow risk. The rate of class membership probability change was used to accurately map boundary sharpness, as verified against field survey data and a DEM representing canopy height. When related to the actual gap structure, the rate of class membership probabilities indicated, for instance, the presence of exposed soil and living windthrown tree canopies, for which is was possible to accurately infer other information, such as direction of tree fall.

9.5 RESEARCH CONTRIBUTION

The work contained within this thesis contributes to previous research into windthrow formation and progression in upland commercial forests in the British Isles, by indicating the potential of a softened classification to derive more accurate spatial

representations of windthrown gaps than may be derived from a conventional hard classification. However, the major contribution of the research within this thesis is the potential to use the rate of change of typicality and posterior class membership probabilities to derive information on gap-canopy boundary sharpness, from which the presence of exposed soil and living windthrown tree canopies may be inferred.

9.6 CONCLUSIONS

Monitoring wind damage using remote sensing can provide some of the information required to develop silvicultural prescriptions to maximise the potential financial return from managed forests and reduce the windthrow risk associated with certain management operations. The work contained within this thesis suggests that fine ($\simeq$ 5 m) spatial resolution remotely sensed data from satellite sensors may provide an appropriate source of remotely sensed data for monitoring individual windthrown gaps at the forest-landscape in the British Isles. In addition, the work suggests that a more accurate representation of windthrown gaps may be acquired by softening the output from a conventional hard classification. However, this work only indicates the potential usefulness of remote sensing to acquire information on windthrow formation and progression. Any real benefits for the forest management community will only be addressed when non-photographic remote sensing methods prove more useful to monitor wind damage within upland forests in the British Isles than aerial photography.

Appendix 1

ATM SENSOR RADIOMETRIC CALIBRATION DATA

Waveband	Gain setting	Waveband Gain	Waveband Base
1	8	0.752	18.240
2	8	0.189	32.256
3	8	0.216	39.680
4	8	0.422	34.048
5	8	0.216	38.720
6	4	0.410	19.584
7	2	0.435	10.624
8	4	0.300	19.392
9	4	0.084	15.360
10	8	0.012	39.872

Reference data for the radiometric calibration of ATM wavebands 1 to 10 (Wilson, 1998). Waveband gain = slope of the response function; and waveband base = intercept of the response function (Section 3.3.1.4) (Lillesand and Kiefer, 2000). The gain setting is a multiplication factor, applied to each individual waveband independently, to maximise the sensitivity of the ATM sensor for each flight.

Appendix 2

Windthrown gap area and perimeter estimates derived from aerial photography

Gap no.	Area (m2)	Perimeter (m)
1	560	144
2	2158	362
3	168	62
4	174	98
5	180	84
6	93	66
7	292	94
8	574	170
9	200	76
10	145	70
11	133	76
12	536	116
13	554	176
14	1197	198
15	902	314
16	124	56
17	117	84
18	148	68
19	179	134
20	41	32
21	336	134
22	147	68
23	117	52
24	137	52
25	54	36
26	268	88
27	216	68
28	157	64
29	122	60
30	94	56
31	44	36
32	74	48
33	70	44
34	456	120
35	98	56
36	140	62

Note: windthrown gap area and perimeter estimates derived from rasterising the Forestry Commission's vector data to an enhanced spatial resolution of 1 m (Section 3.4.2).

Appendix 3

PUBLICATIONS ARISING FROM THIS WORK

Journal Articles

Jackson, R.G.; Foody, G.M. and Quine, C.P., 2000. Characterising windthrown gaps from fine spatial resolution remotely sensed data. Forest Ecology and Management **135**:253-260.

Conference Proceedings

Jackson, R.G.; Quine, C.P. and Foody, G.M., 1998. Using remote sensing to increase our understanding of windthrown gaps in forests. In: Developing International Connections. Remote Sensing Society, Nottingham. pp121-127.

Foody, G.M.; Jackson, R.G. and Quine, C.P., 1999. Soft classification of forest canopy gaps. In: Earth Observation: From Data to Information. Remote Sensing Society, Nottingham. pp609-613.

Appendix 4

SOURCES FOR SENSOR INFORMATION USED IN THIS WORK

AVHRR http://edcwww.cr.usgs.gov

AVIRIS http://makalu.jpl.nasa.gov/aviris.html

ERS http://www.esa.int

Ikonos http://www.spaceimaging.com

IRS http://www.csre.iitb.ernet.in/isro/

Landsat http://www.nasa.gov/

MODIS http://ltpwww.gsfc.nasa.gov/MODIS/MODIS.html

Quickbird http://www.digitalglobe.com

Radarsat http://www.rsi.ca

SPOT http://www.spotimage.fr

REFERENCES

Ahern, F.J.; Leckie, D.J. and Drieman, J.A., 1993. Seasonal changes in relative C-band backscatter of northern forest cover types. IEEE Transactions on Geoscience and Remote Sensing **31**:668-680.

Altman, D., 1994. Fuzzy set theoretic approaches for handling imprecision in spatial analysis. International Journal of Geographical Information Systems **8**:271-289.

Anon., 1999. Boxing day blows some good after all. Forestry and British Timber May. pp15-17.

Anon., 2000. Millennium windfall. Timber and Wood Products February. pp8-9.

Aplin, P.; Atkinson, P.M. and Curran, P.J., 1997. Fine spatial resolution satellite sensors for the next decade, International Journal of Remote Sensing **18**:3873-3881.

Ardo, J.; Lambert, N.; Henzlik, V. and Rock, B.N., 1997. Satellite-based estimations of coniferous forest cover changes: Krusne Hory, Czech Republic 1972-1989. Ambio **26**:158-166.

Armitage, R.P.; Weaver, R.E. and Kent, M., 1997. Spectral characteristics of boundaries between upland semi-natural plant communities. In RSS97: Observations and Interactions. Remote Sensing Society, Nottingham. pp206-211.

Aronoff, S., 1982. The map accuracy report: a user's view. Photogrammetric Engineering and Remote Sensing **48**:1309-1312.

Atkinson, P.M., 1996. Optimal sampling strategies for raster-based geographical information systems. Global Ecology and Biogeography Letters **5**:271-280.

Atkinson, P.M., 1997. Mapping sub-pixel boundaries from remotely sensed images. In: Innovations in GIS 4 (Ed) Kemp, Z. Taylor and Francis, London. pp166-180.

Atkinson, P.M. and Curran, P.J., 1995. Defining an optimal size of support for remote sensing investigations. IEEE Transactions on Geoscience and Remote Sensing **33**:768-776.

Atkinson, P.M. and Curran, P.J., 1997. Choosing an appropriate spatial resolution for remote sensing investigations. Photogrammetric Engineering and Remote Sensing **63**:1345-1351.

Atkinson, P.M. and Cutler, M.E.J., 1996. Unmixing mixed pixels. GIS Europe June. pp18-19.

Avery, T.E. and Burkhart, H.E., 1994. Forest Measurements (4th Edition). McGraw-Hill, New York.

Baret, F.; Clevers, J.G.P.W. and Steven, M.D., 1995. The robustness of canopy gap fraction estimates from red and near-infrared reflectances: A comparison of approaches. Remote Sensing of Environment **54**:141-151.

Barnes, B.V.; Zak, D.R.; Denton, S.R. and Spurr, S.H., 1998. Forest Ecology. John Wiley & Sons Inc., New York.

Barrett, E.C. and Curtis, L.F., 1999. Introduction to Environmental Remote Sensing (4th Edition). Nelson Thornes, London.

Barnsley, M., 1988. Fractals Everywhere. Academic Press, San Diego.

Barnsley, M.J., 1994. Environmental monitoring using multiple-view-angle (MVA) remotely-sensed data. In: Environmental Remote Sensing from Regional to Global Scales. (Eds) Foody, G. and Curran, P. John Wiley & Sons, Chichester. pp181-201.

Baskent, E.Z. and Jordan, G.A., 1995. Characterising spatial structure of forest landscapes. Canadian Journal of Forest Research **25**:1830-1849.

Batchelor, B.G., 1978. Pattern Recognition: Ideas in Practice. Plenum Press, New York.

Battles, J.J.; Dushoff, J.G. and Fahey, T.J., 1996. Line intersect sampling of forest canopy gaps. Forest Science **42**:131-138.

Bazzaz, F.A., 1990. The response of natural ecosystems to the rising global CO_2 levels. Annual Review of Ecological Systems **21**:167-196.

Benson, B.J. and MacKenzie, M.D., 1995. Effects of sensor spatial resolution on landscape structure parameters. Landscape Ecology **10**:113-120.

Bettinger, P.; Bradshaw, G.A. and Weaver, G.W., 1996. Effects of geographic information system vector-raster-vector data conversion on landscape indices. Canadian Journal of Forest Research **26**:1416-1425.

Blackburn, G.A. and Milton, E.J., 1995. Ecology through spectrometry: the detection and classification of canopy gaps in deciduous woodland. In: *TERRA 2* - Understanding the Terrestrial Environment: Remote Sensing Data Systems and Networks. (Ed) Mather, P.M. John Wiley & Sons, Chichester. pp175-187.

Blackburn, G.A. and Milton, E.J., 1996. Filling the gaps: remote sensing meets woodland ecology. Global Ecology and Biogeography Letters **5**:175-191.

Blackburn, G.A. and Milton, E.J., 1997. An ecological survey of deciduous woodlands using airborne remote sensing and geographical information systems (GIS). International Journal of Remote Sensing **18**:1919-1935.

Blake, J.G. and Hoppes, W.G., 1986. Influence of resource abundance on use of tree-fall gaps by birds in an isolated woodlot. The Auk **103**:328-340.

Bolduc, P.; Lowell, K. and Edwards, G., 1999. Automated estimation of localised forest volume from large-scale aerial photographs and ancillary cartographic information in a boreal forest. International Journal of Remote Sensing **20**:3611-3624.

Bondesson, L.; Stahl, G. and Holm, S., 1998. Standard errors of area estimates obtained by traversing and GPS. Forest Science **44**:405-413.

Booth, T.C., 1977. Windthrow Hazard Classification. Research Information Note 22/77/SILN, Forestry Commission, Edinburgh.

Borel, C.C. and Gerstl, S.A.W., 1994. Nonlinear spectral mixing model for vegetative and soil surfaces. Remote Sensing of Environment **47**:403-416.

Bosserman, R.W. and Ragade, R., 1982. Ecosystem analysis using fuzzy set theory. Ecological Modelling **16**:191-208.

Boyce, R. and Clark, W., 1964. The concept of shape in geography. Geographical Review **54**:561-572.

Brakke, T.W.; Smith, J.A. and Harnden, J.M., 1989. Bidirectional scattering of light from tree leaves. Remote Sensing of Environment **29**:175-183.

Brazier, J.D.; Hands, R. and Seal, D.T., 1985. Structural wood yields from Sitka spruce: the effect of planting spacing. Forestry and British Timber September. pp34, 35 and 37.

Briggs, P.A., 1998. Bats in trees. Arboricultural Journal **22**:25-35.

Brokaw, N.V.L., 1982a. The definition of a treefall gap and its effect on measures of forest dynamics. Biotropica **14**:158-160.

Brokaw, N.V.L., 1982b. Treefalls: Frequency, timing and consequences. In: The Ecology of a Tropical Forest: Seasonal Rhythms and Long-term Changes. (Eds) Leigh, E.G.; Windsor, D.M. and Rand, A.S. Smithsonian Institution Press, Washington DC. pp101-108.

Brokaw, N.V.L., 1985. Treefalls, regrowth, and community structure in tropical forests. In: The Ecology of Natural Disturbance and Patch Dynamics. (Eds) Pickett, S.T.A. and White, P.S. Academic Press, San Diego. pp53-71.

Brown, N., 1996. A gradient of seedling growth from the centre of a tropical rain forest canopy gap. Forest Ecology and Management **82**:239-244.

Brown, D.G., 1998. Classification and boundary vagueness in mapping presettlement forest types. International Journal of Geographical Information Science **12**:105-129.

Bruzzone, L. and Serpico, S.B., 2000. A technique for feature selection in multiclass problems. International Journal of Remote Sensing **21**:549-563.

Buckland, S.T. and Elston, D.A., 1994. Use of groundtruth data to correct land cover estimates from remotely sensed data. International Journal of Remote Sensing **15**:1273-1282.

Burrough, P.A. and McDonnell, R.A., 1998. Principles of Geographical Information Systems. Oxford University Press.

Cadenasso, M.L.; Traynor, M.M. and Pickett, S.T.A., 1997. Functional location of forest edges: gradients of multiple physical factors. Canadian Journal of Forest Research **27**:774-782.

Cameron, A.D.; Miller, D.R.; Ramsey, F.; Nikolaou, I. and Clarke, G.C., 2000. Temporal measurement of the loss of native pinewood in Scotland through the analysis of orthorectified aerial photographs. Journal of Environmental Management **58**:33-43.

Campbell, J.B., 1996. Introduction to Remote Sensing (2nd Edition). Taylor & Francis, London.

Campbell, N.A., 1980. Robust procedures in multivariate analysis I: robust covariance estimation. Applied Statistics **29**:231-237.

Campbell, N.A., 1984. Some aspects of allocation and discrimination. In: Multivariate Statistical Methods in Physical Anthropology. (Eds) Van Vark, G.N. and Howells, W.W. Reidel. pp177-192.

Campbell, N.A., 1990. Biology (2nd Edition). The Benjamin/Cummings Publishing Company, Inc., California.

Canham, C.D., 1988a. Growth and canopy architecture of shade-tolerant trees: Response to canopy gaps. Ecology **69**:786-795.

Canham, C.D., 1988b. An index for understory light levels in and around canopy gaps. Ecology **69**:1634-1638.

Canham, C.D.; Denslow, J.S.; Platt, W.J.; Runkle, J.R.; Spies, T.A. and White, P.S., 1990. Light regimes beneath closed canopies and tree-fall gaps in temperate and tropical forests. Canadian Journal of Forest Research **20**:620-631.

Carlson, D.W. and Groot, A., 1997. Microclimate of clear-cut, forest interior, and small openings in trembling aspen forest. Agricultural and Forest Meteorology **87**:313-329.

Carter, C.I., 1991. Ride orientation and invertebrate activity. In: Edge Management in Woodlands. (Ed) Ferris-Kaan, R. Forestry Commission Occasional Paper 28, Forestry Commission, Edinburgh. pp17-21.

Carter, C.I. and Anderson, M.A., 1987. Enhancement of Lowland Forest Ridesides and Roadsides to Benefit Wild Plants and Butterflies. Research Information Note 126, Forestry Commission Research Division, Surrey.

Celentano, A., 1999. Remote sensing in the 21st century: more precision, more choice, more applications. GEOEurope November. pp28-29.

Chen, S.G.; Impens, I.; Ceulemans, R. and Kockelbergh, F., 1993. Measurements of gap fraction of fractal generated canopies using digitalized image analysis. Agricultural and Forest Meteorology **65**: 245-259.

Chuvieco, E., 1999. Measuring changes in landscape pattern from satellite images short-term effects of fire on spatial diversity. International Journal of Remote Sensing **20**:2331-2346.

Clinton, B.D. and Baker, C.R., 2000. Catastrophic windthrow in the southern Appalachians: characteristics of pits and mounds and initial vegetation responses. Forest Ecology and Management **126**:51-60.

Coates, K.D. and Burton, P.J., 1997. A gap-based approach for development of silvicultural systems to address ecosystem management objectives. Forest Ecology and Management **99**:337-354.

Conese, C. and Maselli, F., 1993. Selection of optimum bands from TM scenes through mutual information analysis. ISPRS Journal of Photogrammetry and Remote Sensing **48**:2-11.

Congalton, R.G., 1988. A comparison of sampling schemes used in generating error matrices for assessing the accuracy of maps generated from remotely sensed data. Photogrammetric Engineering and Remote Sensing **54**:593-600.

Congalton, R.G., 1991. A review of assessing the accuracy of classifications of remotely sensed data. Remote Sensing of Environment **37**:35-46.

Congalton, R.G. and Green, K., 1993. A practical look at the sources of confusion in error matrix generation. Photogrammetric Engineering and Remote Sensing **59**:641-644.

Connell, J.H. and Slayter, R.O., 1977. Mechanisms of succession in natural communities and their role in community stability and organisation. The American Naturalist **111**:1119-1144.

Connell, J.H.; Lowman, M.D. and Noble, I.R., 1997. Subcanopy gaps in temperate and tropical forests. Australian Journal of Ecology **22**:163-168.

Cook, J.E., 1996. Implications of modern successional theory for habitat typing: a review. Forest Science **42**:67-75.

Cottam, G., 1981. Patterns of succession in different forest ecosystems. In: Forest Succession: Concepts and Application. (Eds) West, D.C.; Shugart, H.H. and Botkin, D.B. Springer-Verlag, New York. pp178-184.

Courteau, J., 1996. GPS navigation: the way forward. Canadian Forest Industries October. pp44-48.

Coutts, M.P., 1983. Development of the structural root system of Sitka spruce. Forestry **56**:1-16.

Coutts, M.P., 1986. Components of tree stability in Sitka spruce on peaty gley soil. Forestry **59**:173-198.

Coutts, M.P. and Nicoll, B.C., 1989. Tolerance of Sitka Spruce Roots to Waterlogging. Research Information Note 154, Forestry Commission Research Division, Surrey.

Cox, D.R., 1968. Regression methods: notes on some aspects of regression analysis. Journal of the Royal Statistical Society A **131**:265-279.

Crapper, P.F., 1980. Errors incurred in estimating an area of uniform land cover using Landsat. Photogrammetric Engineering and Remote Sensing **46**:1295-1301.

Cross, A.M.; Settle, J.J.; Drake, N.A. and Paivinen, R.T.M., 1991. Subpixel measurement of tropical forest cover using AVHRR data. International Journal of Remote Sensing **12**: 1119-1129.

Curran, P.J., 1985. Principles of Remote Sensing. Longman, Harlow.

Curran, P.J. and Foody, G.M., 1994. The use of remote sensing to characterise the regenerative states of tropical forests. In: Environmental Remote Sensing at Regional to Global Scales. (Eds) Foody, G.M. and Curran, P.J. John Wiley and Sons, Chichester. pp44-83.

Curran, P.J. and Atkinson, P.M., 1998. Geostatistics and remote sensing. Progress in Physical Geography **22**:61-78.

Curran, P.J. and Atkinson, P.M., 1999. Issues of scale and optimal pixel size. In: Spatial Statistics for Remote Sensing. (Eds) Stein,A.; Van der Meer, F. and Gorte, B. Kluwer Academic Publishers, Netherlands. pp115-133.

Dahir, S.E. and Lorimer, C.G., 1996. Variation in canopy gap formation among developmental stages of northern hardwood stands. Canadian Journal of Forest Research **26**:1875-1892.

Dannatt, N. and Garforth, M.F., 1989. Harvesting and marketing the windblown timber. In: The 1987 Storm: Impacts and Responses. (Ed) Grayson, A.J. Forestry Commission Bulletin 87, HMSO, London. pp24-31.

Dannatt, N.; Dewar, J.; Gibbs, J.N.; Greig, B.J.W.; Patch, D. and Thompson, D.A., 1989. Scale and nature of damage. In: The 1987 Storm: Impacts and Responses. (Ed) Grayson, A.J. Forestry Commission Bulletin 87, HMSO, London. pp9-16.

Danson, F.M. and Curran., P.J., 1993. Factors affecting the remotely sensed response of coniferous forest plantations. Remote Sensing of Environment **43**:55-65.

Darche, M.H. and Forgues, I., 1998. Modes of GPS Positioning: Introduction and Application in Forestry. Wood Harvesting Technical Note TN-277, Forest Engineering Research Institute of Canada, Quebec.

Davidson, C., 1998. Issues in measuring landscape fragmentation. Wildlife Society Bulletin **26**:32-37.

Davies, M.W., 1991. Cwm Berwyn/Diffwys. Unpublished Forestry Commission report, Applied Tree Stability, Silviculture (North), Forest Research, Edinburgh.

Davis, J.C., 1986. Statistics and Data Analysis in Geology (2nd Edition). John Wiley & Sons, Ltd., New York.

Day, W.R., 1957. Sitka Spruce in British Columbia: A Study in Forest Relationships. Forestry Commission Bulletin 28, Forestry Commission, Edinburgh.

Day, W.R., 1963. The development of Sitka spruce on shallow peat. Scottish Forestry **17**:219-236.

Defries, R.S. and Townshend, R.G., 1999. Global land cover characterization from satellite data: from research to operational implementation? Global Ecology and Biogeography **8**:367-379.

Delaney, J.L. and Skidmore, A.K., 1998. Discrepancy or error in forest type classification. Australian Forestry **61**:82-88.

Denslow, J.S. and Gomez Diaz, A.E., 1990. Seed rain to tree-fall gaps in a neotropical rain forest. Canadian Journal of Forest Research **20**:642-648.

Denslow, J.S. and Spies, T., 1990. Canopy gaps in forest ecosystems: an introduction. Canadian Journal of Forest Research **20**:619.

Doyle, T.W., 1981. The role of disturbance in the gap dynamics of a montaine rain forest: An application of a tropical forest successional model. In: Forest Succession: Concepts and Application. (Eds) West, D.C.; Shugart, H.H. and Botkin, D.B. Springer-Verlag, New York. pp56-73.

Drake, J.B. and Weishampel, J.F., 2000. Multifractal analysis of canopy height measures in a longleaf pine savanna. Forest Ecology and Management **128**:121-127.

Drobyshev, I.V., 1999. Regeneration of Norway spruce in canopy gaps in *Sphagnum-Myrtillus* old growth forests. Forest Ecology and Management **115**:71-83.

Dryden, I.L. and Mardia, K.V., 1988. Statistical Shape Analysis. John Wiley & Sons, Chichester.

Dunham, R., 2000. Personnal Communication. Northern Research Station, Forest Research, Edinburgh.

Duthie, A.C., 1982. Thin/non-thin debate. Scottish Forestry **36**:135-137.

Evans, H.F.; Gibbs, J.N. and Thompson, D.A., 1989. Timber degrade. In: The 1987 Storm: Impacts and Responses. (Ed) Grayson, A.J. Forestry Commission Bulletin 87, HMSO, London. pp32-35.

Everham, E.M., 1995. A comparison of methods for quantifying catastropic wind damage to forests. In: Wind and Trees. (Eds) Coutts, M.P. and Grace, J. Cambridge University Press. pp340-357.

Falconer, K., 1990. Fractal Geometry: Mathematical Foundations and Applications. John Wiley & Sons, Chichester.

Firth, J. and Brownlie, R., 1998. An efficiency evaluation of the global positioning system under forest canopies. New Zealand Forestry May. pp19-25.

Fisher, P., 1997. The pixel: a snare and a delusion. International Journal of Remote Sensing **18**:679-685.

Foody, G.M., 1996a. Relating the land-cover composition of mixed pixels to artificial neural network classification output. Photogrammetric Engineering and Remote Sensing **62**:491-499.

Foody, G.M., 1996b. Fuzzy modelling of vegetation from remotely sensed imagery. Ecological Modelling **85**:3-12.

Foody, G.M., 1998. Sharpening fuzzy classification output to refine the representation of sub-pixel land cover distribution. International Journal of Remote Sensing **19**:2593-2599.

Foody, G.M., 2000. Estimation of sub-pixel land cover composition in the presence of untrained classes. Computers and Geosciences **26**:469-478.

Foody, G.M. and Trodd, N.M., 1990. Probability mapping of vegetation continua from airborne thematic mapper data. In: Remote Sensing and Global Change. Remote Sensing Society, Nottingham. pp232-239.

Foody, G.M. and Trodd, N.M., 1993. Non-classificatory analysis and representation of heathland vegetation from remotely sensed imagery. GeoJournal **29**:343-350.

Foody, G.M. and Curran, P.J., 1994. Estimation of tropical forest extent and regenerative stage using remotely sensed data. Journal of Biogeography **21**:223-244.

Foody, G.M.; Campbell, N.A.; Trodd, N.M. and Wood, T.F., 1992. Derivation and applications of probabilistic measures of class membership from the maximum-likelihood classification. Photogrammetric Engineering and Remote Sensing **58**:1335-1341.

Foot, D.L., 1986. Environmental Influences on Forestry Investments in the British Uplands. Research and Development Paper 143, Forestry Commission, Edinburgh.

Forestry and Arboriculture Safety and Training Council, 1996. Chainsaw Clearance of Windblow. Forestry and Arboriculture Safety and Training Council, Edinburgh.

Forestry Commission, 1992. The Forestry Commission of Great Britain. Forestry Commission, Edinburgh.

Foschi, P.G., 1994. A geometric approach to a mixed pixel problem: detecting subpixel woody vegetation. Remote Sensing of Environment **50**:317-327.

Franklin, S.E.; Titus, B.D. and Gillespie, R.T., 1994. Remote sensing of vegetation cover at forest regeneration sites. Global Ecology and Biogeography Letters **4**:40-46.

Franklin, S.E.; Hall, R.J.; Moskal, L.M.; Maudie, A.J. and Lavigne, M.B., 2000. Incorporating texture into classification of forest species composition from airborne multispectral images. International Journal of Remote Sensing **21**:61-79.

Fridman, J. and Valinger, E., 1998. Modelling probability of snow and wind damage using tree, stand and site characteristics from *Pinus sylvestris* sample plots. Scandanavian Journal of Forest Research **13**:348-356.

Frohn, R.C., 1998. Remote Sensing for Landscape Ecology: New Metric Indicators for Monitoring, Modeling, and Assessment of Ecosystems. Lewis Publishers, Boca Raton.

Fuller, R.J., 1991. Effects of woodland edges on songbirds. In: Edge Management in Woodlands. (Ed) Ferris-Kaan, R. Forestry Commission Occasional Paper 28, Forestry Commission, Edinburgh. pp31-34.

Gardiner, B., 1997. Standing up to storms. Biologist **44**:318-321.

Gardiner, B. and Stacey, G., 1996. Designing Forest Edges to Improve Wind Stability. Forestry Commission Technical Paper 16, Forestry Commission, Edinburgh.

Gardiner, B.A.; Stacey, G.R.; Belcher, R.E. and Wood, C.J., 1997. Field and wind tunnel assessments of the implications of respacing and thinning for tree stability. Forestry **70**:233-252.

Gerard, F.F. and North, P.R., 1997. Modeling bi-directional reflectance of forest canopies with gaps. In: RSS97: Observations and Interactions. Remote Sensing Society, Nottingham. pp261-267.

Gerylo, G.; Hall, R.J.; Franklin, S.E.; Roberts, A. and Milton, E.J., 1998. Hierarchical image classification and extraction of forest species composition and crown closure from airborne multispectral images. Canadian Journal of Remote Sensing **24**:219-232.

Gilliland, J., 1980. A re-appraisal of Irish silvicultural practices. Irish Forestry 37:107-111.

Gillis, M.D.; Pick, R.D. and Leckie, D.G., 1990. Satellite imagery assists in the assessment of hail damage for salvage harvest. The Forestry Chronicle October. pp463-468.

Gonzato, G., 1998. A practical implementation of the box counting algorithm. Computers and Geosciences 24:95-100.

Gray, A.N. and Spies, T.A., 1996. Gap size, within-gap position and canopy structure effects on conifer seedling establishment. Journal of Ecology 84:635-645.

Grayson, A., 1981. Current Forestry Commission thinking on thinning. Forestry and British Timber September. pp46-49.

Greatorex-Davies, J.N., 1991. Woodland edge management for invertebrates. In: Edge Management in Woodlands. (Ed) Ferris-Kaan, R. Forestry Commission Occasional Paper 28, Forestry Commission, Edinburgh. pp25-30.

Green, R.M., 1998a. The sensitivity of SAR backscatter to forest windthrow gaps. International Journal of Remote Sensing 19:2419-2425.

Green, R.M., 1998b. Relationships between polarimetric SAR backscatter and forest canopy and sub-canopy biophysical properties. International Journal of Remote Sensing 19:2395-2412.

Gregoire, J.C.; Raty, L.; Drumont, A. and De Windt, N., 1997. Pheromone mass trapping: does it protect windfalls from attack by Ips typographus L. (Coleoptera: Scolytidae)? In: Integrating Cultural Tactics into the Management of Bark Beetle and Reforestation Pests. (Eds) Gregoire, J.C.; Liebhold, A.M.; Stephen, F.M.; Day, K.R. and Salom, S.M. General Technical Report NE-236, USDA Forest Service, Northeastern Forest Experimental Station. pp1-8.

Grindal, S.D. and Brigham, R.M., 1998. Short-term effects of small-scale habitat disturbance on activity by insectivorous bats. Journal of Wildlife Management **62**:996-1003.

Grunblatt, J., 1987. An MTF analysis of Landsat classification error at field boundaries. Photogrammetric Engineering and Remote Sensing **53**:639-643.

Gustafson, E.J. and Parker, G.R., 1992. Relationships between landcover proportion and indices of landscape spatial pattern. Landscape Ecology 7:101-110.

Guyot, G., 1990. Optical properties of vegetation canopies. In: Applications of Remote Sensing in Agriculture. (Eds) Steven, M.D. and Clark, J.A. Butterworths, Kent. pp19-43.

Hame, T., 1991. Spectral interpretation of changes in forest using satellite scanner images. Acta Forestalia Fennica Number **222**.

Hammond, R. and McCullagh, P.S., 1974. Quantitative Techniques in Geography: An Introduction. Clarendon Press, Oxford.

Hansen, A. and Rotella, J., 1999. Abiotic factors. In: Maintaining Biodiversity in Forest Ecosystems. (Ed) Hunter, M.L. Cambridge University Press. pp161-209.

Hansson, L., 1983. Bird numbers across edges between mature conifer forest and clearcuts in Central Sweden. Ornis Scandinavica 14:97-103.

Harper, W., 1986. To thin or not to thin - optimising present and future returns to grower. Forestry and British Timber December. pp22, 24 and 27.

Harris, A.S., 1978. Distribution, genetics, and silvical characteristics of Sitka spruce. In: Proceedings of the IUFRO Joint Meeting of Working Parties: S2-02-05 Douglas Fir Provenences; S2-02-06 Lodgepole Pine Provenences; S2-02-12 Sitka Spruce Provenences; S2-02-05 *Abies* Provenences, Volume 1, Vancouver, Canada. British Columbia Ministry of Forests, Canada. pp95-122.

Harris, A.S., 1990. *Picea sitchensis* (Bong.) Carr., Sitka spruce. In: Silvics of North America: Volume 1, Conifers. (Eds) Burns, R.M. and Honkala, B.H. Agriculture Handbook 654, Forest Service, United States Department of Agriculture, Washington. pp260-267.

Haygreen, J.G. and Bowyer, J.L., 1996. Forest Products and Wood Science: An Introduction (3rd Edition). Iowa State University Press, Ames.

Health and Safety Executive, 2000. Review and Assessment of the Procedures for Dealing with Hung-up and Windblown Trees. HSE Books, Suffolk.

Healy, M.J.R., 1968. Multivariate normal plotting. Applied Statistics 17:157-161.

Henderson-Sellers, A. and McGuffie, K., 1995. Global climate models and 'dynamic' vegetation changes. Global Change Biology 1:63-75.

Hendrey, G.R., 1992. Global greehouse studies: need for a new approach to ecosystem manipulation. Critical Reviews in Plant Science **11**:61-74.

Heuvelink, G.B.M. and Burrough, P.A., 1993. Error propagation in cartographic modelling using Boolean logic and continuous classification. International Journal of Geographical Information Systems 7:231-246.

Hibbs, D.E., 1982. Gap dynamics in a hemlock - hardwood forest. Canadian Journal of Forest Research **12**:522-527.

Hlavka, C.A. and Spanner, M.A., 1995. Unmixing AVHRR imagery to assess clearcuts and forest regrowth in Oregon. IEEE Transactions on Geoscience and Remote Sensing **33**:788-795.

Hosking, G.P., 1995. Evaluation of forest canopy damage using airborne videography. New Zealand Forestry May. pp24-27.

House, J.; Koh, A.; Edwards, E. and Hall, D., 1999. Revolutionising remote sensing. Biologist **46**:123-128.

Howard, J.A., 1991. Remote Sensing of Forest Resources - Theory and Application. Chapman and Hall, London.

Howe, H.F., 1990. Habitat implications of gap geometry in tropical forests. Oikos **59**:141-144.

Hudson, B., 2000. The windblow in Europe: an update report. FCA News July/August. pp39.

Hughes, J.W. and Bechtel, D.A., 1997. Effect of distance from forest edge on regeneration of red spruce and balsam fir in clearcuts. Canadian Journal of Forest Research **27**:2088-2096.

Huguenin, R.L.; Karaska, M.A.; Van Blaricom, D. and Jensen, J.R., 1997. Subpixel classification of bald cypress and tupelo gum trees in thematic mapper imagery. Photogrammetric Engineering and Remote Sensing **63**:717-725.

Hunting Geology and Geophysics, 1985. Airborne Thematic Mapper: Computer Compatible Tape Format. Hunting Geology and Geophysics Limited, Boreham Wood, Hertfordshire.

Hussain, Z., 1991. Digital Image Processing: Practical Applications of Parallel Processing Techniques. Ellis Horwood Ltd., Chichester.

Hyyppa, J.; Hyyppa, H.; Inkinen, M.; Engdahl, M.; Linko, S. and Zhu, Y., 2000. Accuracy comparison of various remote sensing data sources in the retreival of forest stand attributes. Forest Ecology and Management **128**:109-120.

IPCC, 2000. Land use, land-use change, and forestry. Cambridge University Press, Cambridge.

Ishizuka, M.; Toyooka, H.; Osawa, A.; Kushima, H.; Kanazawa, Y. and Sato, A., 1998. Secondary succession following catastrophic windthrow in a boreal forest in Hokkaido, Japa: the timing of tree establishment. Journal of Sustainable Forestry **6**:367-388.

Jakus, R., 1998. Patch level variation on bark beetle attack (Col., Scolytidae) on snapped and uprooted trees in Norway spruce primeval natural forest in endemic condition: effects of host and isolation. Journal of Applied Entomology **122**:409-421.

Jahne, B., 1995. Digital Image Processing: Concepts, Algorithms and Scientific Applications (3rd Edition). Springer-Verlag, Berlin.

James, M., 1987. Pattern Recognition. BSP Professional Books, Oxford.

Jorge, L.A.B. and Garcia, G.J., 1997. A study of habitat fragmentation in Southeastern Brazil using remote sensing and geographic information systems (GIS). Forest Ecology and Management **98**:35-47.

Jung, T.S.; Thompson, I.D.; Titman, R.D. and Applejohn, A.P., 1999. Habitat selection by forest bats in relation to mixed-wood stand types and structure in central Ontario. Journal of Wildlife Management **63**:1306-1319.

Jupp, D.L.B. and Walker, J., 1997. Detecting structural and growth changes in woodlands and forests: the challange for remote sensing and the role of geometric-optical modelling. In: The Use of Remote Sensing in the Modeling of Forest Productivity. (Eds) Gholtz, H.L., Nakane, K. and Shimoda, H. Kluwer Academic Publishers, Dordrecht. pp75-108.

Katsch, C. and Vogt, H., 1999. Remote sensing from space - present and future applications in forestry, nature conservation and landscape management. Southern African Forestry Journal **185**:14-26.

Kent, M.K.; Gill, W.J.; Weaver, R.E and Armitage, R.P., 1997. Landscape and plant community boundaries in biogeography. Progress in Physical Geography **21**:315-353.

Kerdiles, H. and Grondona, M.O., 1995. NOAA-AVHRR NDVI decomposition and subpixel classification using linear mixing in the Argentinean Pampa. International Journal of Remote Sensing **16**:1303-1325.

Kilpatrick, D.J.; Sanderson, J.M. and Savill, P.S., 1981. The influence of five early respacing treatments on the growth of Sitka spruce. Forestry **54**:17-27.

Kilpelainen, P. and Tokola, T., 1999. Gain to be achieved from stand delineation in Landsat TM image-based estimates of stand volume. Forest Ecology and Management **124**:105-111.

Kimmins, J.P., 1997. Forest Ecology: A Foundation for Sustainable Management (2nd Edition). Prentice Hall, New Jersey.

King, D.I.; Griffin, C.R. and DeGraaf, R.M., 1998. Nest predator distribution among clearcut forest, forest edge and forest interior in an extensively forested landscape. Forest Ecology and Management **104**:151-156.

Klecka, W.R., 1980. Discriminant Analysis. Sage, London.

Kranabetter, J.M. and Wylie, T., 1998. Ectomycorrhizal community structure across forest openings on naturally regenerated western hemlock seedlings. Canadian Journal of Forest Research **76**:189-196.

La Gro, J., 1991. Assessing patch shape in landscape mosaics. Photogrammetric Engineering and Remote Sensing **57**:285-293.

Lawrence, M.; Firth, J. and Brownlie, R., 1995. Three forestry applications of the global positioning system in New Zealand. New Zealand Forestry August. pp21-22.

Lawton, R.O. and Putz, F.E., 1988. Natural disturbance and gap-phase regeneration in a wind-exposed tropical cloud forest. Ecology **69**:764-777.

Leblon, B., 1999. Mapping forest clearcuts using radar digital imagery: a review of the Canadian experience. The Forestry Chronicle **75**:675-684.

Lertzman, K.P. and Krebs, C.J., 1991. Gap-phase structure of a subalpine old-growth forest. Canadian Journal of Forest Research **21**:1730-1741.

Levin, S.A. and Paine, R.T., 1974. Disturbance, patch formation, and community structure. Proceedings of the National Academy of Science **71**:2744-2747.

Lieberman, M.; Lieberman, D. and Peralta, R., 1989. Forests are not just Swiss cheese: canopy stereogeometry of non-gaps in tropical forests. Ecology **70**:550-552.

Liebovitch, L.S. and Toth, T., 1989. A fast algorithm to determine fractal dimensions by box counting. Physics Letters A **141**:386-390.

Lillesand, T.M. and Kiefer, R.W., 2000. Remote Sensing and Image Interpretation (4th Edition). John Wiley & Sons, New York.

Lines, R., 1978. The IUFRO experiments with Sitka spruce in Great Britain. In: Proceedings of the IUFRO Joint Meeting of Working Parties: S2-02-05 Douglas Fir Provenences; S2-02-06 Lodgepole Pine Provenences; S2-02-12 Sitka Spruce Provenences; S2-02-05 *Abies* Provenences, Volume 2, Vancouver, Canada. British Columbia Ministry of Forests, Canada. pp211-225.

Lonsdale, D., 1990. Treatment of Storm-Damaged Trees. Arboriculture Research Note 73/90/PAT, Arboricultural Advisory and Information Service, Farnham, Surrey.

Lucas, O.W.R., 1991. The Design of Forest Landscapes. Oxford University Press.

Lundquist, J.E., 1995. Pest interactions and canopy gaps in ponderosa pine stands in the Black Hills, South Dakota, USA. Forest Ecology and Management 74:37-48.

McClure, J.W.; Lee, T.D. and Leak, W.B., 2000. Gap capture in northern hardwoods: patterns of establishment and height growth in four species. Forest Ecology and Management 127:181-189.

McGarigal, K. and Marks, B.J., 1995. Fragstats: Spatial Pattern Analysis Program for Quantifying Landscape Structure. General Technical Report PNW-GTR-351, United States Department of Agriculture, Forest Service, Pacific Northwest Research Station.

McGraw, J.B.; Warner, T.A.; Key, T.L. and Lamar, W.R., 1998. High spatial resolution remote sensing of forest trees. Tree 13:300-301.

MacKenzie, R.F., 1976. Silviculture and management in relation to risk of windthrow in Northern Ireland. Irish Forestry 33:29-38.

Mackie, A.L. and Gough, P.W., 1994. Using Tatter Flags to Assess Exposure in Upland Forestry. Research Information Note 249, Forest Authority Research Division, Surrey.

Magnussen, S.; Gougeon, F.; Leckie, D. and Wulder, M., 1999. Predicting tree heights from a combination of LIDAR canopy heights and digital stem counts. In: Remote Sensing and Forest Monitoring. (Eds) Zawila-Niedzwiecki, T. and Brach, M. EUR19530EN, Office for Official Publications of the European Communities, Luxembourg. pp498-513.

Marceau, D.J.; Gratton, D.J.; Fournier, R.A. and Fortin, J., 1994. Remote sensing and the measurement of geographical entities in a forested environment. 2. The optimal spatial resolution. Remote Sensing of Environment 49:105-117.

Marquis, D.A., 1965. Controlling Light in Small Clearcuttings. U.S. Forest Service Research Paper NE-39, Northeastern Forest Experiment Station.

Maselli, F.; Conese, C. and Petkov, L., 1994. Use of probability entropy for the estimation and graphical representation of the accuracy of maximum likelihood classifications. ISPRS Journal of Photogrammetry and Remote Sensing **49**:13-20.

Maselli, F.; Conese, C.; De Filippis, T. and Norcini, S., 1995. Estimation of forest parameter through fuzzy classification of TM data. IEEE Transactions on Geoscience and Remote Sensing **33**:77-84.

Mather, P.M., 1999. Computer Processing of Remotely-Sensed Images (2nd Edition). John Wiley & Sons, Chichester.

Matlack, G.R., 1993. Microenvironment variation within and among forest edge sites in the eastern United States. Biological Conservation **66**:185-194.

Matlack, G. and Litvaitis, J., 1999. Forest edges. In: Maintaining Biodiversity in Forest Ecosystems. (Ed) Hunter, M.L. Cambridge University Press. pp210-233.

Matthews, J.D., 1989. Silvicultural Systems. Clarendon Press, Oxford.

Mausel, P.; Wu, Y.; Li, Y.; Moran, E.F. and Brondizio, E.S., 1993. Spectral identifiction of successional stages following deforestation in the Amazon. Geocarto International **4**:61-71.

Mayle, B.A. and Gurnell, J., 1991. Edge management and small mammals. In: Edge Management in Woodlands. (Ed) Ferris-Kaan, R. Forestry Commission Occasional Paper 28, Forestry Commission, Edinburgh. pp42-48.

Metzger, J.P. and Muller, E., 1996. Characterizing the complexity of landscape boundaries by remote sensing. Landscape Ecology **11**:65-77.

Miller, K.F., 1985. Windthrow Hazard Classification. Forestry Commission Leaflet 85. HMSO, London.

Miller, H.G., 1991. Forestry Expansion - A Study of Technical, Economic and Ecological Factors. British Forestry in 1990. Forestry Commission Occasional Paper 34, Forestry Commission, Edinburgh.

Miller, D.; Quine, C. and Broadgate, M., 1997. The application of digital photogrammetry for monitoring forest stands. In: Application of Remote Sensing in European Forest Monitoring. (Ed) Kennedy, P.J. European Commission, Brussels. pp57-67.

Milne, B.T., 1988. Measuring the fractal geometry of landscape. Applied Mathematics and Computation **27**:67-79.

Milner, S., 1980. Forest Research: Spacing and Respacing Sitka Spruce. Unpublished Report, Department of Agriculture for Northern Ireland, Forest Service Research Branch, Belfast.

Milton, E.J.; Blackburn, G.A.; Rollin, E.M. and Danson, F.M., 1994. Measurement of the spectral directional reflectance of forest canopies: a review of methods and a practical application. Remote Sensing Reviews **10**:258-308.

Mitchell, S.J., 1998. A diagnostic framework for windthrow risk estimation. The Forestry Chronicle **74**:100-105.

Monserud, R.A. and Leemans, R., 1992. Comparing global vegetation maps with the Kappa statistic. Ecological Modelling **62**:275-293.

Moore, J. and Somerville, A., 1998. Assessing the risk of wind damage to plantation forests in New Zealand. New Zealand Forestry May. pp25-29.

Mozgeris, G. and Augustaitis, A., 1999. Using GIS techniques to obtain a continuous surface of tree crown defoliation. Baltic Forestry **5**:69-74.

Mukai, Y. and Hasegawa, I., 2000. Extraction of damaged areas of windfall trees by typhoons using Landsat TM data. International Journal of Remote Sensing **21**:647-654.

Myers, G.P.; Newton, A.C. and Melgarejo, O., 2000. The influence of canopy gap size on natural regerneration of Brazil nut (Bertholletia excelsa) in Bolivia. Forest Ecology and Management **127**:119-128.

Nachtergale, L.; De Schrijver, A. and Lust, N., 1997. Windthrow, what comes after the storm? Silva Gandavensis **62**:80-89.

Naesset, E., 1998. Positional accuracy of boundaries between clearcuts and mature forest stands delineated by means of aerial photointerpretation. Canadian Journal of Forest Research **28**:368-374.

National Audit Office, 1993. Forestry Commission: Timber Harvesting and Marketing. HMSO, London.

Nelson, R., 1989. Regression and ratio estimators to integrate AVHRR and MSS data. Remote Sensing of Environment **30**:201-216.

Nelson, D.G. and Quine, C.P., 1990. Site Preparation for Restocking. Research Information Note 166, Forestry Commission Research Division, Surrey.

Nilson, T. and Olsson, H., 1995. Effect of thinning cutting on boreal forest reflectance: a comparison of simulations and Landsat TM estimates. International Journal of Remote Sensing **16**:2963-2968.

Nilson, T. and Ross, J., 1997. Modeling radiative transfer through forest canopies: implications for canopy photosynthesis and remote sensing. In: The Use of Remote Sensing in the Modeling of Forest Productivity. (Eds) Gholtz, H.L.; Nakane, K. and Shimoda, H. Kluwer Academic Publishers, Dordrecht. pp23-60.

Nixon, 1997. Feature Extraction in Image Processing and Computer Vision: With Mathcad Implementation. Department of Engineering and Computer Sciences, University of Southampton.

Oliver, C.D. and Larson, B.C., 1996. Forest Stand Dynamics (Update Edition). John Wiley & Sons, New York.

Olsen, E.R.; Ramsey, R.D. and Winn, D.S., 1993. A modified fractal dimension as a measure of landscape diversity. Photogrammetric Engineering and Remote Sensing **59**:1517-1520.

Olsson, H., 1990. Spectral response from thinning cuttings measured by multitemporal satellite data. In: ISPRS Commission VII, Victoria, Canada. pp17-21.

Olsson, H., 1994. Changes in satellite-measured reflectances caused by thinning cuttings in boreal forest. Remote Sensing of Environment **50**:221-230.

Ostertag, R., 1998. Below ground effects of canopy gaps in a tropical wet forest. Ecology **79**:1294-1304.

Patton, D.R., 1975. A diversity index for quantifying habitat "edge". Wildlife Society Bulletin **3**:171-173.

Peltonen, M., 1999. Windthrows and dead-standing trees as bark beetle breeding material at forest-clearcut edge. Scandanavian Journal of Forest Research **14**:505-511.

Peltonen, M. and Heliovaara, K., 1999. Attack density and breeding success of bark beetles (Coleoptera, Scolytidae) at different distances from forest-clearcut edge. Agricultural and Forest Entomology **1**:237-242.

Perkins, T.D; Klein, R.M.; Badger, G.J. and Easter, M.J., 1992. Spruce-fir decline and gap dynamics on Camels Hump, Vermont. Canadian Journal of Forest Research **22**:413-422.

Peterken, G.F., 1993. Woodland Conservation and Management. Chapman & Hall, London.

Peterken, G.F., 1996. Natural Woodland: Ecology and Conservation in Northern Temperate Regions. Cambridge University Press, Cambridge.

Phillips, J.C.L., 1980. Some effects of a no-thinning regime on forest management. Irish Forestry **37**:33-44.

Poulson, T.L. and Platt, W.J., 1989. Gap light regimes influence canopy tree diversity. Ecology **70**:553-555.

Price, C., 1989. The Theory and Application of Forest Economics. Basil Blackwell Ltd., Oxford.

Puhr, C.B. and Donoghue, D.N.M., 2000. Remote sensing of upland conifer plantations using Landsat TM data: a case study from Galloway, south-west Scotland. International Journal of Remote Sensing **21**:633-646.

Puhr, C.B.; Donoghue, D.N.M. and Cox, N.J., 1997. Logit modelling to map canopy closure in conifer plantations: A case study using Landsat TM data from S.W. Scotland. In: RSS97: Observations and Interactions. Remote Sensing Society, Nottingham. pp171-176.

Pukkala, T.; Kuuluvainen, T. and Stenberg, P., 1993. Below-canopy distribution of photosynthetically active radiation and its relation to seedling growth in a Boreal *Pinus sylvestris* stand. Scandanavian Journal of Forest Research **8**:313-325.

Puyou-Lascassies, P.; Flouzat, G.; Gay, M. And Vignolles, C., 1994. Validation of the use of multiple linear regression as a tool for unmixing coarse spatial resolution images. Remote Sensing of Environment **49**:155-166.

Pyatt, G., 1982. Soil Classification. Research Information Note 68/82/SSN, Forestry Commission, Surrey.

Quine, C.P., 1988. Windthrow Prediction - Twyi Forest. Unpublished Forestry Commission report. Applied Tree Stability, Silviculture (North), Forest Research, Edinburgh.

Quine, C.P., 1989. Windthrow Monitoring Areas - Ground Survey. Unpublished Forestry Commission report. Applied Tree Stability, Silviculture (North), Forest Research, Edinburgh.

Quine, C.P., 1991a. Twyi Windthrow Monitoring Area - Cwm Berwyn. Unpublished Forestry Commission report. Applied Tree Stability, Silviculture (North), Forest Research, Edinburgh.

Quine, C.P., 1991b. Recent storm damage to trees and woodlands in southern Britain. In: Research for Practical Arboriculture. (Ed) Hodge, S.J. Forestry Commission Bulletin 97, HMSO, London. pp83-89.

Quine, C.P., 1992. Cwm Berwyn - Return Plot Protocol. Unpublished Forestry Commission report. Applied tree stability, Silviculture (North), Forest Research, Edinburgh.

Quine, C.P., 1994. An Improved Understanding of Windthrow - Moving from Hazard Towards Risk. Research Information Note 257, Forest Authority Research Division, Surrey.

Quine, C.P., 1997. Personnal Communication. Applied tree stability, Silviculture (North), Forest Research, Edinburgh.

Quine, C.P., 2000. Personnal Communication. Applied tree stability, Silviculture (North), Forest Research, Edinburgh.

Quine, C.P. and Bell, P.D., 1998. Monitoring of windthrow occurrence and progression in spruce forests in Britain. Forestry 71:87-97.

Quine, C.P. and Humphrey, J.W., 1996. The potential role of wind in contributing to the floral and structural diversity of planted coniferous forests in Britain. In: The Spatial Dynamics of Biodiversity. (Eds) Simpson, I.A. and Dennis, P. The UK Region of the International Association for Landscape Ecology. pp183-186.

Quine, C.P. and Miller, K.F., 1990. Windthrow - a factor influencing the choice of silvicultural system. In: Silvicultural Systems (Ed) Gordon, P. Institute of Chartered Foresters, Edinburgh. pp71-81.

Quine, C.P. and Reynard, B.R., 1990. A New Series of Windthrow Monitoring Areas in Upland Britain. Forestry Commission Occasional Paper 25, Forestry Commission, Edinburgh.

Quine, C.P; Coutts, M.; Gardiner, B. and Pyatt, G., 1995. Forests and Wind: Management to Minimise Damage. Forestry Commission Bulletin 114, HMSO, London.

Quine, C.P.; Mackie, A. and Bell, P., 1997. In the woods with GPS. Mapping Awareness February. pp28-30.

Quine, C.P.; Humphrey, J.W. and Ferris, R., 1999. Should the wind disturbance patterns observed in natural forests be mimicked in planted forests in the British uplands? Forestry 72:337-358.

Rackham, O., 1986. The History of the Countryside. J.M. Dent Ltd, London.

Ramsey, E.W.; Chappell, D.K. and Baldwin, D.G., 1997. AVHRR imagery used to identify hurricane damage in a forested wetland of Louisiana. Photogrammetric Engineering and Remote Sensing **63**:293-297.

Ratcliffe, P.R., 1991. Edge habitats: An introduction. In: Edge Management in Woodlands. (Ed) Ferris-Kaan, R. Forestry Commission Occasional Paper 28, Forestry Commission, Edinburgh. pp2-4.

Raven, P.H.; Evert, R.F. and Eichhorn, S.E., 1986. Biology of Plants (4th Edition). Worth Publishers, Inc., New York.

Reinhardt, E.D. and Ringleb, R.V., 1990. Analysis of changes in patterns of a forested landscape following wildfire using Landsat data and landscape ecology methodology. In: Resource Technology 90. American Society of Photogrammetry and Remote Sensing. pp83-93.

Rex, K.D. and Malanson, G.P., 1990. The fractal shape of riparian forest patches. Landscape Ecology **4**:249-258.

Richards, J.A., 1993. Remote Sensing Digital Image Analysis (2nd Edition). Springer-Verlag, Berlin.

Ripple, W.J.; Bradshaw, G.A. and Spies, T.A., 1991. Measuring landscape pattern in the Cascade Range of Oregon, USA. Biological Conservation **57**:73-88.

Rogers, P., 1996. Disturbance Ecology and Forest Management: A Review of the Literature. General Technical Report INT-GTR-336, Intermountain Research Station, Forest Service, United States Department of Agriculture, Utah.

Rollinson, T.J.D., 1986. A comparison of selective and systematic respacing of Sitka spruce. Scottish Forestry **40**:19-25.

Rollinson, T.J.D., 1988a. Respacing Sitka spruce. Forestry **61**:1-22.

Rollinson, T.J.D., 1988b. Thinning Control. Forestry Commission Field Book 2, HMSO.

Runkle, J.R., 1981. Gap regeneration in some old-growth forests of the Eastern United States. Ecology **624**:1041-1051.

Runkle, J.R., 1985. Comparison of methods for determining fraction of land area in treefall gaps. Forest Science **31**:15-19.

Runkle, J.R., 1990. Gap dynamics in an Ohio *Acer* - *Fagus* forest and speculations on the geography of disturbance. Canadian Journal of Forest Research **20**:632-641.

Ryle, G., 1969. Forest Service: The First Forty-Five Years of the Forestry Commission of Great Britain. David & Charles, Newton Abbot.

Safranyik, L. and Linton, D.A., 1999. Spruce beetle (Coleoptera: Scolytidae) survival in stumps and windfall. The Canadian Entomologist **131**:107-113.

Salisbury, F.B. and Ross, C.W., 1992. Plant Physiology (4th Edition). Wadsworth Publishing Company, California.

Satterlund, D.R., 1983. Forest shadows: how much shelter in a shelterwood? Forest Ecology and Management **5**:27-37.

Savill, P.S., 1983. Silviculture in windy climates. Forestry Abstracts 44:473-488.

Savill, P.S., 1991. The Silviculture of Trees Used in British Forestry. CAB International, Wallingford.

Savill, P.S. and Sandels, A.J., 1983. The influence of early respacing on the wood density of Sitka spruce. Forestry **56**:109-120.

Schaible, R., 1987. The Influence of Ground Preparation Treatments on Root Development of Sitka Spruce Growing on Mineral Soil. Unpublished report, Department of Agriculture for Northern Ireland, Forest Service, Belfast.

Schaible, R., 1992. Sitka spruce in the 21st century - establishment and nutrition. Irish Forestry **49**:10-26.

Schaible, R. and Gawn, L.J., 1989. Variation in timber strength of fast grown unthinned Sitka spruce in Northern Ireland. Irish Forestry **46**:43-50.

Scheer, L. and Dursky, J., 1998. Assessment of stand productivity employing satellite data. Lesnictvi Forestry **44**:398-405.

Schimel, D.S., 1995. Terrestrial ecosystems and the carbon cycle. Global Change Biology **1**:77-91.

Settle, J.J. and Drake, N.A., 1993. Linear mixing and the estimation of ground cover proportions. International Journal of Remote Sensing **14**:1159-1177.

Shimabukuro, Y.E. and Smith, J.A., 1991. The least-squares mixing models to generate fraction images derived from remote sensing multispectral data. IEEE Transactions on Geoscience and Remote Sensing **29**:16-20.

Shugart, H.H.; West, D.C. and Emanuel, W.R., 1981. Patterns and dynamics of forests: An application of simulation models. In: Forest Succession: Concepts and Application. (Eds) West, D.C.; Shugart, H.H. and Botkin, D.B. Springer-Verlag, New York. pp74-94.

Sigrist, P.; Coppin, P. and Hermy, M., 1999. Impact of forest canopy on quality and accuracy of GPS measurements. International Journal of Remote Sensing **18**:3595-3610.

Skinner, C.N., 1995. Change in spatial characteristics of forest openings in the Klamath Mountains of northwestern California, USA. Landscape Ecology **10**:219-228.

Skorupa, J.P. and Kasenene, J.M., 1984. Tropical forest management: can rates of natural treefalls help guide us? Oryx **18**:96-101.

Smith, D.M.; Larson, B.C.; Kelty, M.J. and Ashton, P.M.S., 1997. The Practice of Silviculture: Applied Forest Ecology. John Wiley & Sons, Inc., New York.

Smith, M.O.; Ustin, S.L.; Adams, J.B. and Gillespie, A.R., 1990. Vegetation in deserts: I. A regional measure of abundance from multispectral images. Remote Sensing of Environment **31**:1-26.

Sommerfeld, R.A.; Lundquist, J.E. and Smith, J., 2000. Characterizing the canopy gap structure of a disturbed forest using the Fourier transform. Forest Ecology and Management **128**:101-108.

Spanner, M.A.; Hlavka, C.A. and Pierce, L.L., 1989. Analysis of forest disturbance using TM and AVHRR data. In: International Geoscience and Remote Sensing Symposium (IGARSS) '89. Vancouver, Canada.

Speight, M.R. and Wainhouse, D., 1989. Ecology and Management of Forest Insects. Clarendon Press, Oxford.

Spies, T. and Turner, M., 1999. Dynamic forest mosaics. In: Maintaining Biodiversity in Forest Ecosystems. (Ed) Hunter, M.L. Cambridge University Press, Cambridge. pp95-160.

Spies, T.A.; Franklin, J.F. and Klopsch, M., 1990. Canopy gaps in Douglas-fir forests of the Cascade Mountains. Canadian Journal of Forest Research **20**:649-658.

Spurr, S.H., 1948. Aerial Photographs in Forestry. The Ronald Press Company, New York.

Stacey, G.R.; Belcher, R.E.; Wood, C.J. and Gardiner, B.A., 1994. Wind flows and forces in a model spruce forest. Boundary-Layer Meteorology **69**:311-334.

Stenback, J.M. and Congalton, R.G., 1990. Using Thematic Mapper imagery to examine forest understory. Photogrammetric Engineering and Remote Sensing **56**: 1285-1290.

Steventon, J.D.; MacKenzie, K.L. and Mahon, T.E., 1998. Response of small mammals and birds to partial cutting and clearcutting in northwest British Columbia. The Forestry Chronicle **74**:703-713.

Story, M. and Congalton, R.G., 1986. Accuracy assessment: a users's perspective. Photogrammetric Engineering and Remote Sensing **52**:397-399.

Swaine, M.D. and Whitmore, T.C., 1988. On the definition of ecological species groups in tropical rain forests. Vegetatio **75**:81-86.

Tabbush, P.M., 1988. Silvicultural Principles for Upland Restocking. Forestry Commission Bulletin 76, HMSO, London.

Thomas, M.; Everard, D.A. and van Wyk, G.F., 1997. An evaluation of two-metre resolution black and white satellite image for woodland remote sensing applications. Southern African Forestry Journal **180**:33-36.

Townshend, J.R.G., 1981. The spatial resolving power of Earth resources satellites. Progress in Physical Geography **5**:32-55.

Townshend, J.R.G., 1984. Agricultural land-cover discrimination using thematic mapper spectral bands. International Journal of Remote Sensing **5**:681-698.

Trodd, N.M., Foody, G.M. and Wood, T.F., 1989. Maximum likelihood and maximum information: mapping heathland with the aid of probabilities derived from remotely-sensed data. In: Remote Sensing for Operational Applications. Remote Sensing Society, Nottingham. pp421-426.

Turker, M. and Derenyi, E., 2000. GIS assisted change detection using remote sensing. Geocarto International **15**:49-54.

Turner, M.G., 1990. Spatial and temporal analysis of landscape patterns. Landscape Ecology **4**:21-30.

Turner, M.G.; O'Neill, R.V.; Gardner, R.H. and Milne, B.T., 1989. Effects of changing spatial scale on the analysis of landscape pattern. Landscape Ecology **3**:153-162.

UN/ECE., 1999. Catastrophic Storms Hit Europe's Forests: Dangers of Aftershocks! UN/ECE News, Press Release ECE/TIM/99/4, United Nations Economic Commission for Europe, Geneva.

UN/ECE., 2000a. Storms of December 1999 Fell 165 Million m^3 of Timber: Equivalent of 6 Months Harvest in Three Days. UN/ECE News, Press Release ECE/TIM/00/2, United Nations Economic Commission for Europe, Geneva.

UN/ECE., 2000b. Aftermath of the December Windstorms in Europe's Forests: Emergency Clean-up Work Initiated, Planning for Future. UN/ECE News, Press Release ECE/TIM/00/1, United Nations Economic Commission for Europe, Geneva.

UN/ECE., 2000c. Safety First! Acute Danger for Workers Clearing Windblown Forests. UN/ECE News, Press Release ECE/TIM/00/3, United Nations Economic Commission for Europe, Geneva.

Unwin, D., 1981. Introductory Spatial Analysis. Methuen & Co. Ltd., London.

Van Miegroet, M., 1979. On forest stability Sylva Gandavensis Number **46**.

Van Der Knaap, W.G.M., 1992. The vector to raster conversion: (mis)use in geographical information systems. International Journal of Geographical Information Systems **6**:159-170.

Van Der Meer, P.J. and Bongers, F., 1996. Patterns of tree-fall and branch-fall in a tropical rain forest in French Guiana. Journal of Ecology 84:19-29.

Veblen, T.T., 1985. Forest development in tree-fall gaps in the temperate rain forests of Chile. National Geographic Review Spring. pp162-183.

Veblen, T.T., 1989. Tree regeneration responses to gaps along a transandean gradient. Ecology **70**:541-543.

Vickers, A.D. and Palmer, S.C.F., 2000. The influence of canopy cover and other factors upon the regeneration of Scots pine and its associated ground flora within Glen Tanar National Nature reserve. Forestry **73**:37-49.

Walsh, S.J.; Vitek, J.D. and Gregory, M.S., 1982. Landsat digital analysis of forest clearcuts and reforestation. In: Remote Sensing for Resource Management. (Eds) Johannsen, C.J. and Sanders, J.L. Soil Conservation Society of America. pp159-171.

Wang, F., 1990. Fuzzy supervised classification of remote sensing images. IEEE Transactions on Geoscience and Remote Sensing **28**:194-201.

Wang, F. and Hall, B.G., 1996. Fuzzy representation of geographical boundaries in GIS. International Journal of Geographical Information Systems **10**:573-590.

Wang, M. And Howarth, P.J., 1993. Modeling errors in remote sensing image classification. Remote Sensing of Environment **45**:261-271.

Wang, G.; Poso, S.; Waite, M. and Holopainen., 1998. The use of digitized aerial photographs and local operation for classification of stand development classes. Silva Fennica **32**:215-225.

Ward, D. and Gardiner, J.J., 1976. The influence of tracheid length and density in Sitka spruce. Irish Forestry **33**:39-56.

Warren, M.S., 1991. Woodland edge management for butterflies. In: Edge Management in Woodlands. (Ed) Ferris-Kaan, R. Forestry Commission Occasional Paper 28, Forestry Commission, Edinburgh. pp22-24.

Watt, A.S., 1947. Pattern and process in the plant community. Journal of Ecology **35**:1-22.

Webster, R.; Curran, P.J. and Munden, J.W., 1989. Spatial correlation in reflected radiation from the ground and its implications for sampling and mapping by ground-based radiometry. Remote Sensing of Environment **29**:67-78.

Werle, D.; Lee, Y.J. and Brown, R.J., (1986). The use of multi-spectral and radar remote sensing data for monitoring forest clearcut and regeneration sites on Vancouver Island. Proceedings of the 10th Canadian Symposium on Remote Sensing. pp319-329.

West, D.C.; Shugart, H.H. and Botkin, D.B., 1981. Introduction. In: Forest Succession: Concepts and Application. (Eds) West, D.C.; Shugart, H.H. and Botkin, D.B. Springer-Verlag, New York. pp1-6.

White, P.S. and Pickett, S.T.A., 1985. Natural disturbance and patch dynamics: an introduction. In: The Ecology of Natural Disturbance and Patch Dynamics, (Eds) Pickett, S.T.A. and White, P.S. Academic Press Inc., London. pp1-13.

Whitmore, T.C., 1978. Gaps in the forest canopy. In: Tropical Trees as Living Systems. (Eds) Tomlinson, P.B. and Zimmermann, M.H. Cambridge University Press, Cambridge. pp639-655.

Whitmore, T.C., 1989. Canopy gaps and the two major groups of forest trees. Ecology **74**:1464-1471.

Whitmore, T.C., 1990. An Introduction to Tropical Rainforests. Oxford University Press, Oxford.

Williamson, H.D., 1994. Estimating sub-pixel components of a semi-arid woodland. International Journal of Remote Sensing **15**:3303-3307.

Wilson, A.K., 1988. Calibration of ATM thermal data: Proceedings of the NERC 1986 Airborne Campaign Workshop. The Institute of Hydrology, Oxford. p219-231.

Wilson, A.K., 1995. NERC Scientific Services Airborne Remote Sensing Facility User Guide Handbook. NSS ARS Facility Handbook Version 1.0, Airborne Remote Sensing Facility, Natural Environmental Research Council, Swindon.

Wilson, A.K., 1997. An integrated data system for airborne remote sensing. International Journal of Remote Sensing **18**:1889-1901.

Wilson, A.K., 1998. Personnal Communication. Airborne Remote Sensing Facility, Natural Environmental Research Council, Swindon.

Wilson, K. and White, D.J.B., 1986. The Anatomy of Wood: Its Diversity and Variability. Stobart & Son Ltd., London.

Wood, R.F., 1955. Studies of North-West American Forests in Relation to Silviculture in Great Britain. Forestry Commission Bulletin 25, Edinburgh.

Woodcock, C.E. and Strahler, A.H., 1987. The factor of scale in remote sensing. Remote Sensing of Environment **21**:311-332.

Woodward, F.I., 1992. Tansley review no. 41: Predicting plant responses to global environmental change. New Phytologist **122**:239-251.

Worrall, J.J. and Harrington, T.C., 1988. Etiology of canopy gaps in spruce-fir forests at Crawford Notch, New Hampshire. Canadian Journal of Forest Research **18**:1463-1469.

Wu, H.P. and Schowengerdt, R.A., 1993. Improved estimation of fraction images using partial image restoration. IEEE Transactions on Geoscience and Remote Sensing **31**:771-778.

Yatabe, S.M. and Leckie, D.G., 1995. Clearcut and forest-type discrimination in satellite SAR imagery. Canadian Journal of Remote Sensing **21**:455-467.

Young, T.P. and Hubbell, S.P., 1991. Crown asymmetry, treefalls, and repeat disturbance of broad-leaved forest gaps. Ecology **72**:1464-1471.

Zar, J.H., 1999. Biostatistical Analysis. Prentice Hall International, Inc., New Jersey.